Author:
Thomas, J. R

Title:
The hydrodynamics of certain wave energy absorbers

THE HYDRODYNAMICS OF CERTAIN WAVE ENERGY ABSORBERS

by

J.R. THOMAS

A dissertation submitted for the degree of Doctor of Philosophy in the Department of Applied Mathematics, University of Bristol.

OCTOBER 1981

ACKNOWLEDGEMENTS

I should like to thank Dr. D.V. Evans for his suggestion of the subject matter of this thesis and for his valuable help and guidance throughout its preparation.

I should also like to thank Dr. G.P. Thomas and Dr. M.A. Srokosz for many useful discussions, Dr. M.J. Simon for his co-operation in a common area of research and the Science Research Council for a maintenance grant.

MEMORANDUM

The work in this dissertation was carried out in the Department of Mathematics, University of Bristol, and has not been submitted for any other degree or diploma of any examining body. All the work presented here is the original work of the author, except that acknowledged in the text.

ABSTRACT

In this thesis, the absorption of energy from sea waves by certain wave energy converters is considered. The problems are studied using linearised water wave theory and it is further assumed that the power extraction mechanism of the converters have linear characteristics.

A brief history of work on wave power is presented in Chapter 1. The majority of this thesis is devoted to the study of oscillating water column or submerged duct devices and these are also described in this Chapter, together with the Bristol cylinder device which is examined in the final Chapter.

The theory of wave energy absorption by two-dimensional or isolated, three-dimensional, oscillating bodies is due to Evans (1976), Newman (1976) and Mei (1976). This theory is used in Chapter 2 to formulate the problem of wave energy absorption by an oscillating water column device.

In Chapter 3 the hydrodynamic interaction of waves with a two-dimensional horizontal duct device is examined using a narrow duct approximation. The three-dimensional problem of wave energy absorption by a vertical, axisymmetric duct device with an upward facing mouth is considered in Chapter 4.

The theory of wave energy absorption by pressure distributions due to Evans (1981b) is used in Chapter 5 to study partially immersed duct devices. Ducts of rectangular and circular cross-section are examined using a shallow draft approximation. Finally, wave energy absorption by a duct of circular cross-section is considered without the shallow draft restriction.

Chapter 6 is concerned with the mean second-order force on bodies in waves. The first part of this Chapter is devoted to a two-

dimensional study of the mean force on the Bristol cylinder device. The second part is a study of the mean force on cylinders of arbitrary cross-section and an approximation of this force for cylinders not abbsorbing power is considered.

CONTENTS

CHAPTER 1

INTRODUCTION

In the wake of the oil crisis in 1973 there has been a great upsurge of interest worldwide in renewable forms of energy. In addition to wave energy, these forms include solar, wind, tidal and geothermal energy. The term renewable refers to the inexhaustible nature of these energy sources. Conventional energy sources such as oil, coal, gas and nuclear fuels are finite, dwindling resources and the pollution of our environment caused by their utilization is a major problem. The renewable forms overcome both these handicaps although their environmental impact needs to be fully evaluated. The desirable qualities of the renewable energy sources must, however, be weighed against the feasibility and economic viability of their use. These considerations will ultimately determine the future of renewable energy.

In the U.K., although the Severn barrage tidal power scheme has recently been receiving much attention, wave energy has been regarded as the most promising form of renewable energy. Why should this be? The U.K., being surrounded by sea, has a relatively high coast length to land area ratio and is particularly well positioned to exploit wave energy. The approaches to the Outer Hebrides are thought to be one of the best sites in the world for wave energy. Early estimates in 1974 suggested that the average power available there was of the order of 80kW per metre of wave crest length but this has since been reduced to a figure of 50kW/m (Crabb, 1980). This still represents a very large resource and, although other possible sites return lower average power levels, wave energy is still potentially capable of providing a significant percentage of Britain's future energy

requirements. The majority of the wave energy arriving at our coast is in the form of swell which is produced by storms in the Atlantic, (the remainder of the energy is contained in locally developed wind waves). A useful aspect of wave energy is the 'integrator' effect of the ocean so that swell is almost continually arriving at our shores from storm areas all over the Atlantic; in contrast, wind and solar power depend on the prevailing conditions at a site. A further attractive feature of wave energy is its good correlation to energy demand; unlike solar power, the energy available from the waves is generally greatest in the winter months when demand is highest.

The concept of harnessing the ocean waves to provide energy is not a recent idea however. In an early paper, Stahl (1892) discusses several types of mechanical wave energy devices consisting mainly of floats or vanes and one or two bear quite a resemblance to currently proposed devices. There were roughly a hundred devices granted British patents before, in 1974, Stephen Salter provided the catalyst for the current wave energy programme now coordinated by the government.

Salter's now well-known 'nodding duck' device, designed from experimental considerations, proved to be capable of absorbing over 80% of the energy incident upon it in regular waves (see Salter, 1974). Its high efficiency coupled with the high value of the predicted power off the Outer Hebrides prompted Salter to suggest that 'a few hundred kilometres of installation could meet the total present electrical energy requirement of the U.K.'. Within two years the British government had begun its current wave energy research programme (Kenward, 1976). Research programmes are now also being pursued in Scandinavia and Japan in collaboration with the U.K. Of the numerous devices which have recently been suggested only about a dozen have received financial aid from the U.K. government.

Detailed descriptions of all the more promising devices can be found in Quarrell (1978), Count (1980) and Stephens & Stapleton (1981).

Much of the early work on wave energy converters concentrated on the performance of a device in absorbing the wave energy. Clearly a high overall efficiency of energy conversion is an essential pre-requisite of any device but it is by no means the only governing factor. Since 1978 a series of costing exercises, aimed at highlighting problem areas of different devices, has been carried out to estimate the cost per kilowatt-hour of producing electricity using different device systems. This involves an overall system assessment including the structural costs, mooring or anchoring system, method of electricity generation and transmission, maintenance, repair and replacement work as well as hydrodynamic performance. The first estimates in 1978 (Clark et al., 1978) ranged from 20 - 40p per KWh for different systems (compared with 2 - 3p for conventional electricity production), with the notable exception of the Lancaster flexible bag (see French, 1978) for which the speculative estimate of 5-10p per KWh was made. Since 1978, efforts by device teams to improve the systems has resulted in a reduction of costs for most devices with the more promising National Engineering Laboratory (N.E.L.), Bristol cylinder and Lancaster flexible bag devices now estimated to be within the 5-10p per KWh range. The next stage of the research programme begins in the Spring of 1982 with the possibility of choosing a particular device to be built as a full-scale prototype to be tested in the open sea.

Of all the various aspects of wave power mentioned above, the hydrodynamic interaction between devices and waves is clearly of major importance. This thesis is concerned with the theoretical treatment of this interaction. The majority of this thesis is devoted to a

number of devices with a common operating principle : the oscillating water-column or submerged duct devices. The essential feature of all these devices is the presence of a column of water which is able to oscillate in response to pressure variations as waves pass. The oscillatory motion of the water column in turn drives the air above it back and forther through a turbine (or, using a system of valves, produces a uni-directional air flow through a turbine).

Such a system had already been successfully developed by Y. Masuda in Japan prior to 1974, to power navigation light buoys. In the U.K. the idea was adopted and has been developed on a larger scale by N.E.L. (see Elliot & Roxburgh, 1981). The original N.E.L. device was envisaged as a moored, floating structure operating in terminator mode (that is, long in the direction parallel to the wave crests) with dimensions of the order of 120m in length and 35 X 35m in cross-section. The device consists of six modules, each of which is a hollow structure with a submerged mouth which faces the incoming waves (see also Chapter 3), and twenty-five devices moored in a line constitute a wave-power station. Inside each module, the air above the water surface is connected to the external atmosphere via a turbine. More recently, in an effort eliminate mooring costs, reduce maintenance costs and improve the survival prospects of the device, N.E.L. have converted the device into a bottom-standing structure. This device would be anchored to the sea-bed in 15 - 20m of water where the major disadvantages are lower incident wave power and probable increased marine fouling.

The submerged duct device proposed by Vickers Limited is also a bottom-standing device. However, this device is completely submerged, consisting of a dome structure with a large mouth at the top, leading to an annular U- shaped duct inside the structure (Chester-Browne, 1978). The appeal of the submerged, bottom-standing device was its

reduced vulnerability to local storms compared to surface devices, for which 'survivability' can be a problem. To extract power, the oscillations of the water column cause overspill into a collecting duct which is then discharged through a water-turbine. The large air-volume inside the dome, needed to avoid high pneumatic stiffness, was however found to add considerably to structural and anchoring costs. These considerations, together with high maintenance costs and a relatively narrow response bandwidth, prompted Vickers Ltd. to develop a modified version. This device is known as a twin oscillating water-column device since it consists of an upward-facing and a downward-facing water column, separated by an air column within the structure. The air-flow passes through a Wells turbine which rotates in the same direction, independent of the air-flow direction. This modified device is a terminator, similar in appearance to the N.E.L. device but it is again completely submerged, situated just below the water surface either fixed on piers or held by moorings. It is also being considered as an attenuator, that is, positioned such that it is long in the direction of wave travel, when it can 'draw in' energy as the waves travel along its length (see Drew, 1981).

A further oscillating water-column device is being developed by Queen's University, Belfast. This consists of a moored, partly submerged, axisymmetric structure, typically spherical in shape, with a downward-facing mouth at the bottom. The air-flow, caused by oscillations of the internal water column, passes through a constricted opening containing a Wells turbine. A similar device, reminiscent of an inverted, drawn-out matchbox in appearance, is currently being investigated by the Central Electricity Generating Board (C.E.G.B).

It is also worth mentioning the Kaimei project which began in 1978 (Butterworth, 1978). This Japanese project, in collaboration with the U.K., U.S.A. and Canada, involves the development and full-

scale testing of a device. It consists of a converted ship, anchored off the coast of Japan, which houses a number of air-chambers in its hull. Different turbine-generator units may be installed and have been tested at sea.

The first part of the final Chapter of this thesis is concerned with the Bristol cylinder device. The operating principle of this device is completely different from those discussed above. The device consists of a hollow, positively-buoyant cylinder of circular cross-section held in position, with its axis horizontal, by two pairs of cables at the ends (see Chapter 7, §3). The cables are attached to hydraulic pumps anchored at the sea-bed, which feed into a common hydraulic transmission system, connecting a number of devices and leading to a water-turbine. The cylinder is a terminator device, of dimensions 48m in length and 12m in diameter (more recently a 72m long cylinder with an extra pair of cables positioned mid-way along its length has been suggested). When subjected to waves, the cylinder rotates about its horizontal axis, absorbing power by the resulting action of its pumps.

The development of the mathematical theory of wave power absorption by devices is described in a valuable review article by Evans (1981a). A brief outline of the theoretical work is given below; a more comprehensive and complete survey may be found in Evans' article.

In 1976, Evans (1976), Newman(1976) and Mei (1976) independently derived a number of results regarding wave power absorption by two-dimensional bodies. These results were arrived at using linearised water wave theory (see Wehausen & Laitone, 1960) which has subsequently been used in the majority of published theoretical work on wave power. A two dimensional or 'infinitely-long' body is important on two accounts, (i) it may be considered as a model for

a terminator, (ii) much of the early experimental work was carried out in narrow wave tanks with devices which spanned the tank so that the two-dimensional theory enabled confirmation and prediction of experimental results.

Evans and Newman showed that the maximum efficiency of power absorption by a body of arbitrary cross-section could be deduced from knowledge of the far-field radiated waves, when the body is forcedto oscillate in its energy absorbing mode in otherwise calm fluid (see also Chapter 3, §1). A result due to Ogilvie (1963), that a cylinder of circular cross-section rotating in a circular orbit produces propagating waves in one direction only, was used by Evans to show that such a body was capable of absorbing all the power in an incident wave. This result has since led to the development of the Bristol cylinder device.

Evans, Newman and Mei derived expressions for the efficiency of power absorption by bodies of arbitrary cross-section moving in a single degree of freedom. It was found that the efficiency depends solely on the added-mass and damping coefficients of the body, hydrodynamic characteristics of the body which may be derived from the radiation problem (see Chapter 2).

Evans and Newman also extended their work to three-dimensional bodies with a vertical axis of symmetry. In this case it was shown that the maximum power such a body could absorb is equal to the power contained in an incident wave of crest length $\ell\lambda/2\pi$, where λ is the wavelength of this incident wave and $\ell=1$ for a heaving buoy, $\ell=2$ for a rolling or swaying body. This surprisingly simple result, also discovered by Budal & Falnes (1975), is independent of the body dimensions.

Evans (1980a,b) and Falnes (1978) independently generalised the theory to include systems or arrays of three-dimensional bodies.

Evans (1981b) has recently developed an analogous theory for arrays of surface pressure distributions. The theory of wave power absorption by pressure distributions is directly relevant to oscillating water-column devices where there exists an internal air-water interface (see Chapter 5).

The general theory of wave power absorption has been extensively applied to a number of proposed devices (see Evans, 1981a). There have been several papers concerning oscillating water-column or submerged duct devices and these are cited in the introductions to Chapters 3-5. In addition to two-dimensional analyses of terminator devices there have been studies of three-dimensional devices, when isolated and in arrays. Although devices such as the Belfast buoy could be positioned in arrays, it is clearly important to understand the hydrodynamics of an isolated device before considering the more complex array problem.

Evans (1980a,b) illustrated the theory of wave power absorption by arrays with some simple examples. By neglecting the diffracted wave due to the interaction of the incident wave and the body when it is held fixed, Evans was able to determine the q-factor (the maximum mean power per device divided by the maximum mean power from an isolated device) for arrays of heaving buoys and arrays of heaving thin-ship devices. These devices are also examined by Thomas & Evans (1981) when the motions of the individual bodies are constrained to be less than some constant multiple of the incident wave amplitude; such a constraint is appropriate and necessary both from physical considerations and for linear theory to be valid. Simon (1981b) has analysed an array of mouth-upward submerged ducts, when the progressive parts of the diffracted waves are retained and the incident, diffracted waves on each device are approximated by plane waves. Simon found the difference in the q-factor results,

between using this method and Evans' simplification mentioned above, surprisingly small.

There has been little theoretical work on non-linear power extraction systems. McCormick (1974) in his study of the Masuda buoy presents a non-linear formulation of its internal air dynamics while Count (1978a) considers non-linear take-off systems with application to the Salter duck. There has likewise been little consideration of non-linear hydrodynamic forces although the mean second-order forces have received some attention (Longuet-Higgins, 1977 and see also Chapter 6) and there has been a study of the effect of breaking waves on submerged cylinders (Brevig et al.,1981).

Experimental studies have been continuing along with the theoretical developments but there has been only a small amount of published experimental work. Count (1978b) has compared his theoretical results for the Salter duck with Salter's experimental results and found good agreement. There has been a series of papers relating to submerged duct devices (Knott & Flower, 1979 and 1980a,b). Experimental results from Knott & Flower (1979) have been compared with the theoretical predictions of Lighthill (1979). There has also been a comparison between theory and experiment for the Bristol cylinder device (Evans et al., 1979) and again reasonably good agreement was found.

As previously mentioned, the majority of this thesis concerns the theoretical study of the hydrodynamic performance of oscillating water-column or submerged duct devices. The governing equations of linearised water wave theory applied to wave energy absorbers are presented in Chapter 2. The formulation is given specifically for an oscillating water-column device which encloses a weightless float attached to a linear spring-damper system to model the power extraction mechanism. Prior to Evans' (1981b) surface pressure distribution theory this has been the usual method of treating such problems.

This formulation is modified in Chpater 5, § 2 to incorporate pressure distribution models.

Chapter 3 examines the two-dimensional, horizontal duct using the narrow duct approximation (see Evans, 1978). It is known that a symmetric, vertical oscillating water-column device has a maximum efficiency of 50% (Evans, 1976) and this study analyses the effect of rotating such a duct so that its mouth faces the incoming waves.

An axisymmetric, mouth-upward duct is examined in Chapter 4. This three-dimensional analysis, formulated for finite fluid depth, enables the limiting case of an oscillating disc on the sea-bed to be taken. This limiting case yields analytic expressions for the various important hydrodynamic quantities which help in understanding the more complicated non-zero length duct problem. A comparison of the added-mass and damping coefficients for the duct is also made with those found by Simon (1981a) who has considered a similar model in infinitely deep fluid.

Chapter 5 is concerned with free-surface intersecting ducts for which the problems may be formulated using Evans' (1981b) pressure distribution theory. Simple illustrations of Evans' theory are presented using a shallow draft approximation. These are followed by an analysis of an axisymmetric, mouth-downward duct which can be solved using the same method employed in the study of the upward-facing duct of Chapter 4. The shallow draft and narrow duct approximations provide two interesting limiting cases with which the exact results may be compared.

Chapter 6 examines a different aspect of bodies in waves, namely, the mean force. Floating or submerged bodies, whether extracting power or not, experience a mean or time-independent, second-order force in addition to the oscillatory, first-order linear force. Fortunately, solution of the linear problem is sufficient to determine

the mean force. This is exploited in Chapter 6 to study the mean forces on the Bristol cylinder device and also on cylinders of arbitrary cross-section. In the latter problem an approximate expression for the mean vertical force is discussed when the body is not absorbing power.

The annual average power spectrum for South Uist (the Outer Hebrides) is given by Crabb (1980). The peak of the spectrum occurs at approximately a wave period of 13.5 sec. (that is, waves of wavelength ~230m as the water depth is 42m), and the majority of the wave energy is contained in the 8-16 second wave period band. This is the current design spectrum for wave energy absorbers. The majority of these absorbers are tuned, resonant devices so that a particular tuning frequency is chosen and for a device to be a 'good' absorber the efficiency of power absorption should be high at this frequency and over the immediate range of frequencies.

The notation used throughout this thesis is intended to be as consistent as possible so that certain quantities, common to a number of problems, such as the wavelength and wavenumber of the incident wave, duct length, fluid depth, etc. are always denoted by the same symbol.

The work presented in Chapter 4 has previously been published in Thomas (1981) while the examples illustrating the surface pressure distribution theory in Chapter 5 have appeared in Evans (1981b).

CHAPTER 2

THE GOVERNING EQUATIONS

2.1 Introduction

All the mathematical analysis presented in this thesis is carried out under the assumptions of classical linearised water-wave theory (see, for example, Wehausen & Laitone, 1960). These assumptions have been adopted in most of the theoretical work on the prediction of the behaviour of wave-power devices. The resulting simplification of the equations of motion make the problems tractable while still enabling reasonably good predictions to be made under the restrictions imposed on the fluid and device motions by the linear theory. The development of the mathematical theory of wave-power absorption is described in a review article by Evans (1981a) in which the governing equations and many of the important results are given. As noted by Evans, the theory for the motion of floating bodies (see Wehausen, 1971 or Newman, 1977) arising from work in the field of ship hydrodynamics has played an important part in this development. The similarity between wave-power structures and ships enables much of this theory and many of the techniques employed in ship hydrodynamics to be used in wave-power problems.

Classical water-wave theory assumes the fluid to be inviscid, incompressible and of uniform density; the fluid motion is assumed to be irrotational, allowing a velocity potential to be defined. It is further assumed that the wave amplitude and body motions are small compared to the wavelength of the incoming waves so that the boundary conditions may be linearised. The validity of classical water-wave theory in the evaluation of wave-forces on offshore structures has been discussed by Garrison (1978) and Standing (1980). In general,

the predicted forces and resulting motion are thought to be a good approximation to the true forces and motion under 'normal operating conditions' although, when wave conditions are severe or the device is undergoing large displacements, linear theory is invalid. There has been very little published experimental work but the experimental results of Knott & Flower (1979) on submerged ducts and Evans et al. (1979) on the Bristol cylinder show good agreement with the predicted results from linear theory.

A linear analysis does restrict the power take-off mechanism of the device to be a linear system, which is unlikely in practice. In particular, the flow of air through a turbine such as would be used for oscillating water-column devices usually obeys a pressure-volume flux law which is approximately quadratic (Fry et al., 1980). Linear theory cannot predict the instabilities which have been found to occur in offshore platforms, such as tethered buoyant platforms (Rainey, 1977) and semi-submersibles (Martin & Kuo, 1979), and similar effects may occur in certain wave-power devices. The instability of semi-submersibles is thought to be caused by second-order time-independent forces. Although these forces are small compared to the first-order oscillatory forces predicted by linear theory, they can be significant, a further example being their effect upon the Bristol cylinder (see Chapter 6). Fortunately, these second-order mean forces can be found using linear wave theory (see, for example, Ogilvie, 1963). Clearly linear theory has its limitations but it is nevertheless extremely useful as a first step in understanding the hydrodynamics of wave-energy absorbers.

2.2 Equations of Motion

The response of a body to regular waves only is considered as linear wave theory enables the response to irregular waves to be

found by linear superposition. Consider a sinusoidal wave train of frequency ω incident upon a wave-power absorbing body immersed in fluid. Suppose the problem is three dimensional and Cartesian co-ordinates (x,y,z) or cylindrical polar co-ordinates (r,θ,z) are chosen such that $z = z_f$ is the undisturbed free surface and z is measured vertically upwards. The fluid motion is assumed to be governed by linear water-wave theory and hence may be described by a velocity potential

$$\Phi(\underline{x},t) = Re\left\{\phi(\underline{x})e^{-i\omega t}\right\}, \qquad (2.2.1)$$

where the time dependence has been removed.

The potential ϕ satisfies Laplace's equation in the fluid

$$\frac{\partial^2\phi}{\partial x^2} + \frac{\partial^2\phi}{\partial y^2} + \frac{\partial^2\phi}{\partial z^2} = 0, \qquad (2.2.2)$$

or

$$\frac{\partial^2\phi}{\partial r^2} + \frac{1}{r}\frac{\partial\phi}{\partial r} + \frac{1}{r^2}\frac{\partial^2\phi}{\partial\theta^2} + \frac{\partial^2\phi}{\partial z^2} = 0. \qquad (2.2.3)$$

The linearised free-surface condition is given by

$$K\phi - \frac{\partial\phi}{\partial z} = 0 \quad , \text{on } z = z_f, \qquad (2.2.4)$$

where $K = \omega^2/g$. In fluid of finite depth the normal velocity of the fluid is zero on the rigid bottom. Only uniform finite depth is considered here, thus

$$\frac{\partial\phi}{\partial z} = 0 \quad , \text{on } z = z_f - d, \qquad (2.2.5)$$

where d is the water depth. If the fluid is infinitely deep the requirement is

$$\nabla\phi \to 0 \quad , \text{as } z \to -\infty. \qquad (2.2.6)$$

It is also necessary to impose a radiation condition as $r \to \infty$; the appropriate condition will be stated for each problem examined.

On the body, the component of the body velocity normal to its surface is required to be equal to the normal velocity of the fluid at that point. For simplicity the body is henceforth considered to be an oscillating-water column device fitted with a piston. The analysis for an arbitrarily shaped rigid body oscillating in one or more modes is similar to the following analysis (see Evans, 1976). Thus

$$\frac{\partial \Phi}{\partial n} = 0 \qquad \text{, on the fixed structure,}$$

$$\frac{\partial \Phi}{\partial n} = \frac{\partial \zeta}{\partial t} \qquad \text{, on the piston,}$$

where $\zeta(t)$ is the piston displacement from its equilibrium position and $\underline{n}$ is the unit normal from the body into the fluid, i.e.

$$\frac{\partial \phi}{\partial n} = 0 \qquad \text{, on the fixed structure,} \qquad (2.2.7a)$$

$$\frac{\partial \phi}{\partial n} = -i\omega\xi \qquad \text{, on the piston,} \qquad (2.2.7b)$$

where $\zeta = Re\{\xi e^{-i\omega t}\}$.

The potential ϕ_o of a wave of amplitude A and frequency ω travelling in a direction making an angle Θ with the positive x - axis can be written

$$\phi_o(x,y,z) = \frac{gA}{\omega} \frac{\cosh k(z+d-z_f)}{\cosh kd} e^{ik(x\cos\Theta + y\sin\Theta)} \quad , \qquad (2.2.8)$$

when the water is of depth d. The wavenumber k is the positive real root of the dispersion relation

$$K = k \tanh kd \quad , \qquad (2.2.9)$$

obtained upon substitution from (2.2.8) into the free-surface boundary condition (2.2.4). Note that this relation in fact has real roots $\pm k$ and also complex roots $\pm ik_n$, $(n=1,2,3,.....)$, $0 < k_n < k_{n+1}$, where the k_n are real positive solutions of

$$K + k_n \tan k_n d = 0 \,. \qquad (2.2.10)$$

The following notation will be used in subsequent chapters

$$N_0 = \tfrac{1}{2}(1 + \sinh 2kd / 2kd) \qquad (2.2.11)$$

$$N_n = \tfrac{1}{2}(1 + \sin 2k_n d / 2k_n d), \text{ for } n \geq 1, \qquad (2.2.12)$$

and

$$k_0 = -ik \,. \qquad (2.2.13)$$

In infinitely deep fluid the corresponding incident wave potential is

$$\phi_0(x,y,z) = \frac{gA}{\omega} e^{iK(x\cos\Theta + y\sin\Theta) + Kz} \,. \qquad (2.2.14)$$

When waves are incident upon the body they will be diffracted, scattering in all directions, and will also set the piston in motion generating further waves. The potential ϕ can hence be decomposed as

$$\phi = \phi_s - i\omega\xi\phi_r \,. \qquad (2.2.15)$$

The complex potential ϕ_s is the solution of the scattering problem in which the piston is held fixed in the presence of incoming waves. The complex potential ϕ_r is the solution of the radiation problem in which the piston is forced to oscillate with unit amplitude in the absence of incoming waves. The boundary condition (2.2.7b) becomes

$$\frac{\partial \phi_s}{\partial n} = 0, \frac{\partial \phi_r}{\partial n} = 1 \quad \text{, on the piston.} \qquad (2.2.16)$$

The power take-off mechanism is assumed to be modelled by a linear spring-damper system attached to the piston. The equation of motion of the piston is then given by

$$m_0 \ddot{\xi} + \beta \dot{\xi} + \alpha \xi = F(t) \,, \qquad (2.2.17)$$

where α, β are the spring and damper constants respectively, m_0 is the mass of the piston and $F(t)$ is the total hydrodynamic force on the piston. This force may be written as

$$F(t) = Re\{X e^{-i\omega t}\} \,,$$

and ,corresponding to the two terms on the right-hand side of (2.2.15), X can be expressed as

$$X = X_s + X_r \quad . \tag{2.2.18}$$

The term X_s is known as the exciting force on the piston. The term X_r may be decomposed into components in phase with the acceleration and velocity of the piston, thus

$$\begin{aligned} X_r &= -M\ddot{\xi} - B\dot{\xi} \ , \\ &= (\omega^2 M + i\omega B)\Xi \ , \end{aligned} \tag{2.2.19}$$

where M and B are real and are called the added-mass and damping coefficients respectively.

The forces may be obtained by integrating the fluid pressure over the piston surface S, giving

$$X_s = -i\omega\rho \int_S \phi_s \, dS \ , \tag{2.2.20}$$

and

$$\omega^2 M + i\omega B = -\rho\omega^2 \int_S \phi_r \, dS \ , \tag{2.2.21}$$

where the pressure p is given by $p = -\rho \partial\Phi/\partial t$ from Bernoulli's equation; ρ is the density of the fluid.

The two-dimensional formulation is almost identical to the above with $\phi(x,y,z)$ replaced by $\phi(x,z)$ if Cartesian coordinates (x,z) are chosen. The only differences are: (i) ϕ satisfies the corresponding two-dimensional Laplace equation, (ii) $\Theta = 0$ or π, depending on whether the waves are incident from $x = -\infty$ or $x = +\infty$ respectively, (iii) the hydrodynamic forces become forces per unit width and hence the integrals in (2.2.20), (2.2.21) become integrals over the body cross-section.

The mean power per unit width of incident wave is given by

$$P_w = \tfrac{1}{2}\rho g A^2 c_g \ , \tag{2.2.22}$$

Where c_g is the group velocity. In finite depth d its value is

$$c_g = \frac{\partial\omega}{\partial k} = \frac{gkd N_0}{\omega \cosh^2 kd} \ , \tag{2.2.23}$$

reducing to the simpler form

$$c_g = g/2\omega \quad , \tag{2.2.24}$$

in infinitely deep fluid.

In two-dimensions, the efficiency of power absorption is defined to be the ratio of the mean power per unit width absorbed by the body to the mean power per unit width of incident wave. In three dimensions, the appropriate measure of device performance is the capture width which is defined as the ratio of the total power absorbed by the body to the mean power per unit width of incident wave.

The mean power absorbed by the body is the mean rate of working by the fluid on the body and, for the piston, is

$$P = \frac{\omega}{2\pi}\int_0^{2\pi/\omega} \dot{j} X \, dt = \tfrac{1}{2}\omega^2 \beta |\xi|^2 \tag{2.2.25}$$

The efficiency (or capture width) is the ratio of the two quantities given by (2.2.22), (2.2.25) and is given by

$$E(\text{or } C_w) = \frac{\omega^2 \beta}{\rho g c_g} \frac{|\xi|^2}{A^2} \tag{2.2.26}$$

A general theory for wave power absorption by oscillating bodies has been independently derived by Evans (1976), Mei (1976) and Newman (1976). In these papers the relations between the radiation and scattering problems (such as the Haskind and Newman relations) have been exploited to derive general expressions for the efficiency, capture width and body displacements which depend solely upon the added-mass and damping coefficients.

In the following two chapters these general expressions are modified to account for finite depth and change of depth, but the method of procedure is essentially as given in Evans (1976). In each case it is found that the efficiency (or capture width) still depends only on the added-mass and damping coefficients; hence it is unnecessary to solve the fully interactive problem and attention is confined to the simpler corresponding radiation problem.

CHAPTER 3

WAVE ENERGY ABSORPTION BY A TWO-DIMENSIONAL SUBMERGED HORIZONTAL DUCT

3.1 Introduction

Two-dimensional models of oscillating water columns or submerged duct devices, being in general more amenable to mathematical analysis than three-dimensional models, are useful as a first step in understanding the hydrodynamics of duct-wave interactions. They are also relevant to proposed wave-energy absorbers such as the National Engineering Laboratory (N.E.L.) device and the modified version of the Vickers device. Both these absorbers are of uniform cross-section and are long in the direction parallel to the wave crests,that is, lie in terminator mode.

In its simplest form the two-dimensional oscillating water column consists of two parallel plates of equal length forming a duct within which the water column oscillates in response to the pressure fluctuations at the duct mouth as waves pass. This motion is then converted into energy of useable form by some power extraction mechanism.

Vertical mouth downward ducts of this type have been studied by Evans (1978) where the power take-off mechanism consisted of a spring damper system attached to a float on the surface of the water column. Lighthill (1979) used conformal mappings to analyse two-dimensional ducts in some detail where the power extraction mechanism was modelled by a complex 'impedance' in the depths of the duct. These papers consider only vertical ducts with plates of equal length although Lighthill examined both the mouth-upward and mouth-downward duct. In either case the maximum efficiency of such a configuration is 50%. This follows from a simple result for the maximum efficiency,

E_{max} due to Evans (1976):

$$E_{max} = |A^+|^2/(|A^+|^2 + |A^-|^2)$$

where A^+, A^- are the (complex) amplitudes of the radiated waves at $x=+\infty$, $-\infty$, respectively in the radiation problem when the piston is forced to oscillate. By introducing some asymmetry to the duct it is clearly possible to ensure $|A^+|/|A^-| > 1$ in which case the maximum efficiency is greater than 50%. (It is desirable to have $|A^+| \gg |A^-|$ so that the maximum efficiency is close to 100%). This is found to be the case experimentally (Meir, 1978 and Robinson & Murray, 1981) and research by N.E.L. and Vickers, both experimental and analytical (numerical), has led to the development of water columns which are strongly asymmetric. The ducts have forward pointing mouths in the direction of the incoming waves in preference to upward or downward facing mouths.

In this chapter the possibility of achieving efficiencies of greater than 50% is investigated by rotating the simple models suggested above such that the mouth of the duct faces the incoming waves. Thus the device consists of two horizontal closely-spaced plates fitted with a light piston attached to a spring-damper system. Following Evans (1978), the assumption that the plates are closely-spaced enables an approximate solution to be derived using matched asymptotic expansions. This approach was originally used by Newman (1974) to study the problem of wave interaction with two closely-spaced vertical plates. The difficulty lies in determining the outer solution of the problem and for this a source potential, derived by Evans (1972) to examine water wave transmission over a shelf, is used..

Due to the water-depth change which occurs as the waves pass over the duct, it is necessary to modify certain general results, (for example, the Newman and Haskind relations) and rederive the efficiency expressions of Evans (1976). This is done in § 3.

These expressions depend solely upon the properties of the radiation problem. In §§4,5 an approximate solution for the potential ϕ_r is described and this is used in §6 to examine the wave energy absorption characteristics of the device.

3.2 Formulation

Consider a wave-power absorbing system consisting of two closely-spaced, horizontal, semi-infinite plates a distance 2a apart, enclosing a light piston situated in the depths of the duct a distance l from the mouth. The system is submerged in water of depth d, with the centre of the duct mouth at a depth h below the undisturbed free-surface and the duct mouth facing the incoming waves. The power is extracted by means of a linear spring-damper attached to the piston.

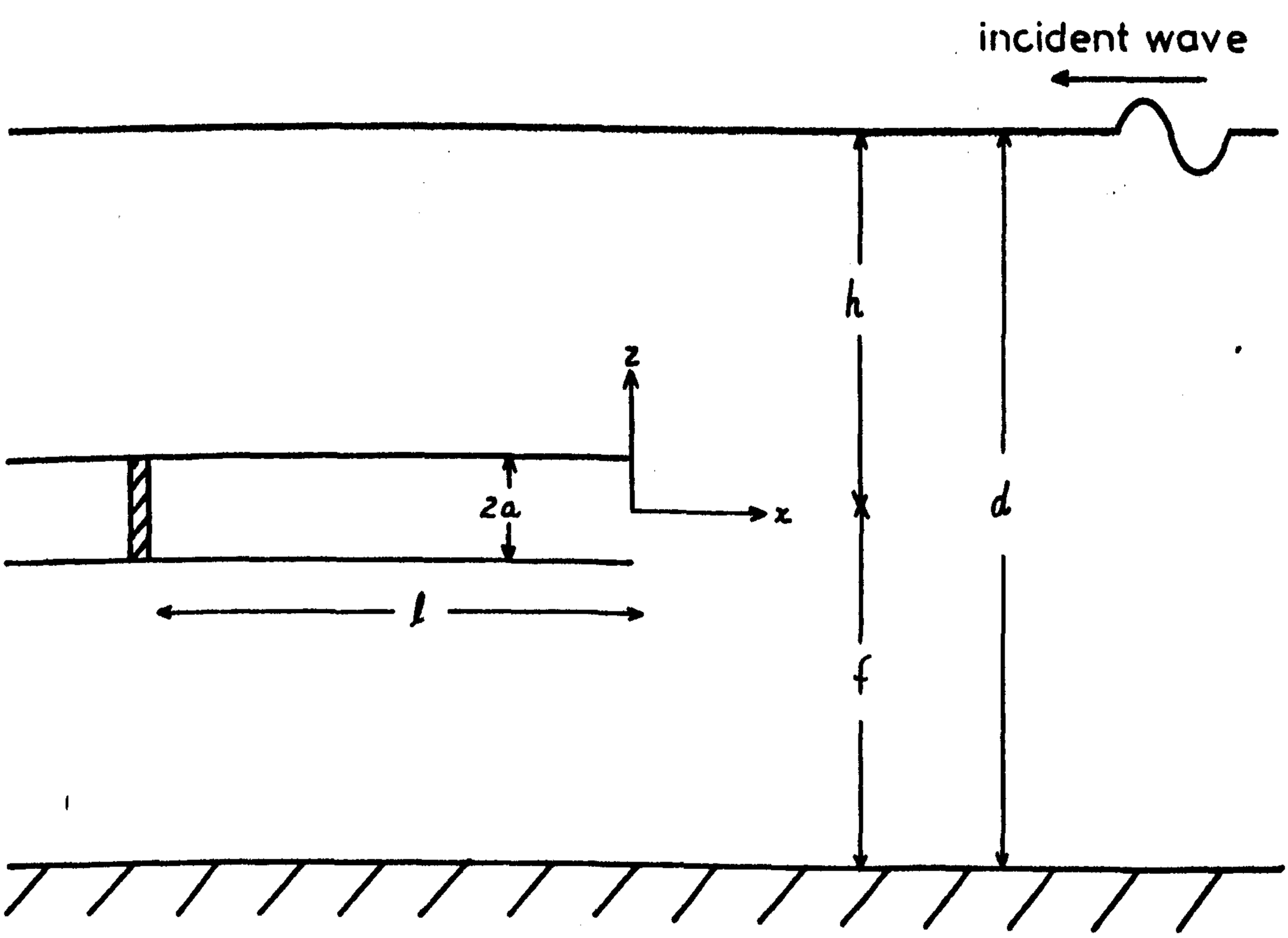

FIGURE (3.1)

When a plane wave of frequency ω and wavenumber k is incident upon the system some portion of the incident wave energy is absorbed by the system while the remainder is partly reflected and partly transmitted. The wave transmitted over the duct will be of the same frequency as the incident wave but of different wavenumber m, due to the change in depth. The frequency ω and wavenumbers k and m are related by the dispersion relations

$$\omega^2 = gk \tanh kd \,, \qquad (3.2.1)$$

$$\omega^2 = gm \tanh mh \,, \qquad (3.2.2)$$

where the assumption $a \ll h$ has been used.

Cartesian coordinates (x,z) are chosen with the positive z-axis vertically upwards and the origin at the centre of the duct mouth as shown in Figure (3.1). The velocity potential $\phi(x,z)$ satisfies (2.2.2), (2.2.4) and (2.2.5) where $z_f = h$ and $d-z_f = f$, while the boundary conditions (2.2.7a,b) on the duct become

$$\partial\phi/\partial z = 0 \,, \qquad \begin{cases} z = a \,, x<0 \,, \\ z = -a \,, x<0 \,, \end{cases} \qquad (3.2.3)$$

$$\partial\phi/\partial x = -i\omega\Xi \,, \qquad x = -l \,, -a<z<a \,. \qquad (3.2.4)$$

Finally, the radiation and scattering potentials are required to satisfy the following radiation conditions

$$\phi_s \sim g\frac{A}{\omega}\left(e^{-ikx} + Re^{ikx}\right)\frac{\cosh k(z+f)}{\cosh kd} \,, \text{as } x \to +\infty \,, \qquad (3.2.5)$$

$$\phi_s \sim g\frac{A}{\omega}\, Te^{-imx}\frac{\cosh mz}{\cosh mh} \,, \text{as } x \longrightarrow -\infty \,, a<z\leq h \,,$$

and

$$\phi_r \sim A^{+}e^{ikx}\frac{\cosh k(z+f)}{\cosh kd} \,, \text{as } x \longrightarrow +\infty \,, \qquad (3.2.6)$$

$$\phi_r \sim A^{-}e^{-imx}\frac{\cosh mz}{\cosh mh} \,, \text{as } x \longrightarrow -\infty \,, a<z\leq h \,,$$

where R and T are the (complex) reflection and transmission coefficients respectively for the scattering problem. Thus the behaviour of ϕ in the far-field is given by

$$\phi \sim g\frac{A}{\omega}\left(e^{-ikx} + R_1 e^{ikx}\right)\frac{\cosh k(z+f)}{\cosh kd}\ , \text{as } x \longrightarrow +\infty,$$

$$\phi \sim g\frac{A}{\omega} T_1 e^{-imx}\frac{\cosh mz}{\cosh mh}\ , \text{as } x \longrightarrow -\infty\ , a < z \leq h, \qquad (3.2.7)$$

where the reflection and transmission coefficients of the total potential are given by

$$R_1 = R - iKA^{+}\Xi/A\ ,\ T_1 = T - iKA^{-}\Xi/A \qquad (3.2.8)$$

Beneath the duct there can be no progressive wave, thus the appropriate condition is

$$\nabla\phi \longrightarrow 0\ ,\ \text{as } x \longrightarrow -\infty\ , -f \leq z < -a. \qquad (3.2.9)$$

The analysis now proceeds under the assumptions that $a \ll h$ and $a \ll l$ while kd and mh are O(1). This corresponds to a narrow duct, when the duct width is small compared to the column length, depth of submergence and wavelengths. This enables the problem to be decomposed into an outer region (Kx, Kz) = O(1) far from the duct mouth, and an inner region $z/a = O(1), -l < x \lesssim 0$ consisting of the area near the mouth and the column of fluid in the duct. These can be matched using the method of matched asymptotic expansions. The technique and its justification is described in greater detail in Newman (1974).

The method of solution outlined above is applied in §§4,5 to determine the radiation potential. However, prior to this, the general expressions derived by Evans (1976) for the maximum efficiency and efficiency of absorbers, together with certain reciprocal relations which exist in linear theory such as the Newman relations (see Newman, 1975), need to be modified in view of the difference in water depth in the far field.

3.3 Modifications to General Theory

The derivation of the modified results involves the use of Green's theorem as in the original derivations. If $\psi_1(x,z)$ and $\psi_2(x,z)$ are harmonic functions in a region bounded by the curve C, then application of Green's theorem to ψ_1 and ψ_2 yields

$$\int_C \left(\psi_1 \frac{\partial \psi_2}{\partial n} - \psi_2 \frac{\partial \psi_1}{\partial n}\right) ds = 0. \qquad (3.3.1)$$

For the formulated problem the boundary C is taken to be the physical boundaries present, together with the vertical planes

$$X_1 : x = X_0, -f \le z \le h \; ; \; X_2 : x = -X_0, 0 < z \le h \; ; \; X_3 : x = -X_0, -f \le y < 0,$$

taking the limit $X_0 \to \infty$. Note that the assumption $a \ll h$ is used to approximate the water depth above the duct as h and a similar approximation is used below the duct.

The equation (3.3.1) is now applied to various linear combinations of ϕ_s, ϕ_r and ϕ_o. In each case, the particular combination and result only are given.

$$\text{(i)}\ \phi_s, \bar{\phi}_s : \quad R\bar{R} + (c_g^- / c_g^+) T\bar{T} = 1, \qquad (3.3.2)$$

where c_g^+, c_g^- are the group velocities in water of depth d and h respectively. This states that wave energy flux is conserved, as one might expect.

$$\text{(ii)}\ \phi_s, \phi_r - \bar{\phi}_r : \quad (A^+ + \bar{A}^+ R) c_g^+ + \bar{A}^- T c_g^- = 0. \qquad (3.3.3)$$

This is the modified form of the Newman relation.

$$\text{(iii)}\ \phi_o, \phi_r : \quad X_s = \rho g A A^+ (2\omega c_g^+ / g). \qquad (3.3.4)$$

This is the corresponding Haskind (1957) result, relating the exciting force to the radiated far-field.

$$\text{(iv)}\ \phi_r, \bar{\phi}_r : \quad B = \tfrac{1}{2}\rho\omega\left[(2\omega c_g^+ / g)|A^+|^2 + (2\omega c_g^- / g)|A^-|^2\right]. \qquad (3.3.5)$$

This final equation demonstrates the relation between the damping coefficient and the radiated far-field.

The efficiency E of the system in absorbing wave energy is simply

$$E = 1 - R_1\bar{R}_1 - (c_g^-/c_g^+)T_1\bar{T}_1 \ ,$$

and, following Evans (1976), the maximum efficiency E_{max} is found to be

$$E_{max} = c_g^+|A^+|^2/(c_g^+|A^+|^2 + c_g^-|A^-|^2) \ , \qquad (3.3.6)$$

which clearly reduces to Evans' result in the particular case of uniform depth throughout. The efficiency can be obtained using the equation of motion of the piston given by (2.2.17), together with (2.2.18), (2.2.19) and (3.3.4)-(3.3.6) to first determine the amplitude ratio of the piston motion

$$\left|\frac{\Xi}{A}\right|^2 = \frac{(2\rho g^2 B/\omega)(2\omega c_g^+/g)E_{max}}{[\alpha-(m_0+M)\omega^2]^2+\omega^2[\beta+B]^2} \ . \qquad (3.3.7)$$

The power in the incident wave (per unit crest length) is $\frac{1}{2}\rho g A^2 c_g^+$, while the power absorbed by the piston (per unit device length) is $\frac{1}{2}\omega^2\beta|\Xi|^2$ (from(2.2.25)). The efficiency of the system is, by definition, the power absorbed by the piston divided by the incident wave power, hence using (3.3.7)

$$E = \frac{4\omega^2\beta B\, E_{max}}{\{\kappa-(m_0+M)\omega^2\}^2+\omega^2[\beta+B]^2} \ . \qquad (3.3.8)$$

This expression is identical to that given by Evans (1976) for infinitely deep fluid, although E_{max} has a different form in this case. All expressions derived in this section reduce to the uniform finite depth throughout results when h = d (i.e. $c_g^+ = c_g^-$) and, thereupon letting $d\to\infty$, the deep water results are obtained.

As stated at the end of Chapter 2, it can be seen from (3.3.6), (3.3.8) that the solution of the radiation problem is sufficient to determine the system efficiency. An approximate solution is now derived for the radiation potential ϕ_r under the assumptions given in § 2.

3.4 The Outer Solution

In the outer region away from the duct mouth the duct appears essentially as a single horizontal plate $z=0, -\infty<x<0$, with a source-type flow at the mouth to account for the mass flux q into the inner region. This flow at the mouth due to the forced oscillations of the piston produces outgoing waves only at $x = \pm\infty$.

Suppose G(x,z) represents a source potential satisfying

$$(\partial^2/\partial x^2 + \partial^2/\partial z^2)G(x,z) = \delta(x)\delta(z), \qquad (3.4.1)$$

$$\partial G/\partial z = 0 \quad , z=0, x<0, \qquad (3.4.2)$$

together with (2.2.4),(2.2.5) and the radiation condition of outgoing waves only, i.e. G(x,z) is the potential at (x,z) due to a pulsating source at (0,0) in the presence of a semi-infinite horizontal plate. Then the outer solution is simply

$$\phi_r = q\,G(x,z). \qquad (3.4.3)$$

The source potential in the presence of a submerged semi-infinite horizontal plate has been derived by Evans (1972), here-after denoted by I, to study the transmission of obliquely incident waves over a shelf. The y- dependence in the problem was removed and thus the Evans source potential G_1 satisfies not (3.4.1), but

$$(\partial^2/\partial x^2 + \partial^2/\partial z^2 - k_1^2)G_1(x,z;\xi,\eta) = \delta(x-\xi)\delta(z-\eta),$$

for some $k_1 > 0$ and where the source is now at arbitrary point (ξ,η). To determine G_1, it is decomposed into the sum of a line-source potential in finite depth and correction potential ϕ_c to satisfy the boundary condition on the plate and the radiation condition at $x=-\infty$. The problem is thus formulated in terms of the unknown potential ϕ_c, and is solved using the Wiener-Hopf method (see Noble, 1958). This method involves taking the Fourier transform of ϕ_c in the x- direction, and it must be assumed that k_1 has a small negative imaginary part in order that the transform exists in a strip of the transform plane. Finally ϕ_c is determined as an inverse Fourier transform and it is shown that letting $Im(k_1) \to 0$ recovers the

required result.

This derivation is also valid for G(x,z) and an outline of assumptions and results only, is given below. The potential G(x,z) may be decomposed as

$$G(x,z) = G_d(x,z) + \phi_c(x,z), \qquad (3.4.4)$$

where $G_d(x,z)$ is the potential of a line-source at the origin in fluid of depth d in the absence of the plate (see, for example, Thorne, 1953). The potential $G_d(x,z)$ may be written

$$G_d(x,z) = \frac{1}{4\pi}\log\left\{\frac{x^2+z^2}{x^2+(z-2h)^2}\right\} - \frac{i\cosh kf\cosh k(z+f)\cos kx}{kd(1+\sinh 2kd/2kd)}$$

$$-\frac{1}{\pi}\int_0^\infty ds\left\{\frac{e^{-sd}\sinh sh\sinh s(h-z)}{s\cosh sd} - \frac{\cosh sf\cosh s(z+f)}{\cosh sd(K\cosh sd - s\sinh sd)}\right\}\cos sx, \qquad (3.4.5)$$

where $\int$ denotes the principal value integral, and this has the limiting form

$$G_d(x,z) \sim -\frac{iN_0^{-1}\cosh kf\cosh kd}{2kd}\,\frac{\cosh k(z+f)}{\cosh kd}e^{\pm ikx}, \text{ as } x \to \pm\infty, \qquad (3.4.6)$$

where N_0 is given by (2.2.11).

The potential ϕ_c is required to be bounded everywhere in the fluid and its first and second partial derivatives bounded everywhere except near (0,0) where

$$\frac{\partial\phi_c}{\partial r} = O\left(\frac{1}{r^p}\right), \quad 0<p<1, \quad r^2 = x^2+z^2.$$

In order that the Fourier transform exists, it is assumed that the wavenumbers k and m have small positive imaginary parts such that

$$\mathrm{Im}\,k = \mathrm{Im}\,m = \tilde{d} > 0. \qquad (3.4.7)$$

This ensures that the Fourier transform

$$\bar{\phi}_c(\gamma,z) = \int_{-\infty}^{\infty}\phi_c(x,z)e^{i\gamma x}dx, \qquad (3.4.8)$$

is regular for γ ($=\sigma+i\tau$) in the strip D:$-\tilde{d}<\tau<\tilde{d}$ of the complex plane. The method of solution is identical to I (with $k_1=0$) and it is found (I, equations (3.41) - (3.43)) that

$$\phi_c(x,z) = \frac{1}{2\pi}\int_C e^{-i\gamma x}\,\bar{\phi}_c(\gamma,z)\,d\gamma\,, \qquad (3.4.9)$$

where C is some path in D from $-\infty$ to ∞, and

$$\bar{\phi}_c(\gamma,z) = \frac{N_-(\gamma)}{L_-(\gamma)}\sinh\gamma f\left\{\frac{\gamma\cosh\gamma(h-z)-K\sinh\gamma(h-z)}{\gamma\sinh\gamma d-K\cosh\gamma d}\right\}, 0<y\leq h, \qquad (3.4.10a)$$

$$= \frac{N_-(\gamma)}{L_-(\gamma)}\left\{\frac{K\cosh\gamma h-\gamma\sinh\gamma h}{\gamma\sinh\gamma d-K\cosh\gamma d}\right\}\cosh\gamma(z+f), -f\leq y<0. \qquad (3.4.10b)$$

The functions N-,L- are regular in D- ($\tau<\tilde{d}$) and are given in Appendix A by (A.2) and (A.14).

(a) <u>The Amplitudes of the Far-Field Radiated Waves</u>

The amplitude of the radiated wave due to G as $x\to+\infty$ is given in I but the expression contains several minor errors. This result is rederived together with the corresponding result as $x\to-\infty$. In the following, the amplitudes of the waves due to G as $x\to\pm\infty$ are given by $B^{\pm}$, using the asymptotic forms given by (3.2.6).

(i) <u>$x\longrightarrow+\infty$</u>

The asymptotic behaviour of ϕ_c can be found from (3.4.9) by closing the path C by a large semicircle in D-. As N-, L- are regular in D-, it can be seen from (3.4.10a) that the only contributions to the integral come from the simple poles of the integrand corresponding to the simple zeros of ($\gamma\sinh\gamma d-K\cosh\gamma d$) within the closed contour, i.e. when $\gamma = -k, -ik_n$, where $\pm ik_n$ $(n=1,2,3,\ldots)$, $0<k_n<k_{n+1}$ are the complex roots of the dispersion relation (3.2.1). The simple poles at $-ik_n$ will clearly only contribute terms which decay exponentially as $x\to+\infty$. Hence the behaviour of ϕ_c as $x\to+\infty$ is determined solely by the simple pole at $\gamma = -k$, and is given by

$$\phi_c \sim -i\operatorname*{Res}_{\gamma=-k}\left[e^{-i\gamma x}\,\bar{\phi}_c(\gamma,z)\right], \text{ as } x\to+\infty.$$

The residue may easily be found, yielding

$$\phi_c \sim \frac{iN_-(-k)N_0^{-1}\sinh kf\cosh kd}{2dL_-(-k)}\cdot\frac{\cosh k(z+f)}{\cosh kd}e^{ikx}\,, \text{as } x\to+\infty, \qquad (3.4.11)$$

and hence the amplitude B_c^+ of the radiated wave due to ϕ_c is given by

$$B_c^+ = \frac{iN_-(-k)N_0^{-1}\sinh kf\cosh kd}{2dL_-(-k)}\,. \qquad (3.4.12)$$

This may be rewritten as

$$B_c^+ = \frac{i N_0^{-2}\cosh kd\cosh kf\sinh^2 kf}{8kd^2}\,\frac{L_+(k)}{L_-(-k)}$$

$$+\ \frac{iN_0^{-1}\sinh kf\cosh kd}{4d^2 L_-(-k)}\sum_{n=1}^{\infty}\frac{N_n^{-1}\sin k_n d\cos k_n d\, L_+(ik_n)}{k_n - ik}\,,$$

using (A.14), and where N_n is given by (2.2.12) and L+ is a function, regular in D+ ($\tau > -\tilde{d}$), given by (A.3). This may be simplified using (A.5), (A.7) to give

$$B_c^+ = \frac{i\cosh kd\, N_0^{-1}}{2kd}\left\{\frac{m-k}{m+k}\,e^{2i\Theta_1}\cosh kf + \frac{k\sinh kf\, L_+(k)}{4fd}\sum_{n=1}^{\infty}\frac{N_n^{-1}\sin 2k_n d\, L_+(ik_n)}{k_n - ik}\right\} \quad (3.4.13)$$

where $\Theta_1 = \arg L_+(k)$. From (3.4.4), (3.4.6) the amplitude B^+ of the radiated wave due to G may be obtained

$$B^+ = -\frac{iN_0^{-1}\cosh kd}{2kd}\left\{\cosh kf\left(1 - \frac{m-k}{m+k}\,e^{2i\Theta_1}\right)\right.$$

$$\left. -\frac{k\sinh kf\, L_+(k)}{4fd}\sum_{n=1}^{\infty}\frac{N_n^{-1}\sin 2k_n d\, L_+(ik_n)}{k_n - ik}\right\}. \quad (3.4.14)$$

(ii) $\underline{x \longrightarrow -\infty}$

Using (A.1), equation (3.4.10a) may be rewritten as

$$\bar{\Phi}_c = \frac{N_-(\gamma)}{\gamma L_+(\gamma)}\left\{\frac{\gamma\cosh\gamma(h-z) - K\sinh\gamma(h-z)}{\gamma\sinh\gamma h - K\cosh\gamma h}\right\}, \quad 0<y\le h. \quad (3.4.15)$$

The path C in (3.4.9) is now closed by a large semicircle in D+. The function L+ is regular in D+, $\gamma = 0$ is a removable singularity, N- has simple poles at $\gamma = k, ik_n$ (see (A.14)) and the only other poles occur when $\gamma = m, im_n$ where $\pm im_n$ $(n=1,2,3,\ldots)$, $0 < m_n < m_{n+1}$ are the complex roots of the dispersion relation (3.2.2). In this case

$$\phi_c \sim i\left(\operatorname*{Res}_{\gamma=k} + \operatorname*{Res}_{\gamma=m}\right)\left\{e^{-i\gamma x}\,\bar{\Phi}_c(\gamma,z)\right\}, \text{ as } x\longrightarrow -\infty.$$

These residues may easily be calculated giving

$$\phi_c \sim i\frac{M_0^{-1}N_-(m)\cosh mh}{2mh\,L_+(m)}\cdot\frac{\cosh mz}{\cosh mh}\,e^{-imx}$$

$$+\frac{iN_0^{-1}\cosh kd\cosh kf}{2kd}\cdot\frac{\cosh k(z+f)}{\cosh kd}\,e^{-ikx}, \quad (3.4.16)$$

where $M_0 = \frac{1}{2}(1+\sinh 2mh/2mh)$.

In determining the amplitude B^- of the radiated wave due to G, the second term of (3.4.16) will clearly cancel with the contribution from G_d given by (3.4.6), thus

$$B^- = \frac{i\cosh mh M_0^{-1}}{2mh} \cdot \frac{N_-(m)}{L_+(m)} . \qquad (3.4.17)$$

Using (A.11) and (A.15) this may be written as

$$B^- = -\frac{iM_0^{-1}\cosh mh}{2mh}\left\{ \frac{M_0^{-1}L_-(-m)}{4m^2 h L_+(m)} - \frac{1}{2hL_+(m)}\sum_{n=1}^{\infty}\frac{M_n^{-1}L_-(-im_n)}{m_n(m_n-im)} + \frac{K\sinh mh - m\cosh mh}{m\sinh md - K\cosh md}\sinh mf \right\},$$

where $M_n = \frac{1}{2}\left(1 + (2m_n h)^{-1}\sin 2m_n h\right)$. This can be reduced to

$$B^- = \frac{iM_0^{-1}\cosh mh}{2mh}\left\{ 1 + \frac{m-k}{m+k}e^{-2i\theta_2} - \frac{L_-(-m)}{2hf}\sum_{n=1}^{\infty}\frac{M_n^{-1}L_-(-im_n)}{m_n(m_n-im)} \right\}, \qquad (3.4.18)$$

where $\theta_2 = \arg L_+(m)$ and use has been made of (3.2.1), (3.2.2) and (A.9).

(b) <u>The Inner Limit of the Outer Solution</u>

To match the outer solution to the inner solution its inner limit as $r = (x^2+z^2)^{\frac{1}{2}} \longrightarrow 0$ is required. This can be determined from (3.4.3) - (3.4.5) and is given by

$$\phi_r(x,z) = \frac{q}{2\pi}\log\left(\frac{r}{2h}\right) - \frac{q}{\pi}\int_0^{\infty}\left\{\frac{e^{-sd}\sinh^2 sh}{s\cosh sd} - \frac{\cosh^2 sf}{\cosh sd(K\cosh sd - s\sinh sd)}\right\}ds$$

$$- \frac{iN_0^{-1}q\cosh^2 kf}{2kd} + q\,\phi_c(0,0) + O\left((r/h)^{\frac{1}{2}}\right), \qquad (3.4.19)$$

where $\phi_c(0,0)$ can be found from (A.16).

3.5 <u>The Inner Solution and Matching</u>

Near the duct mouth the motion simply appears to be an oscillatory flow between two semi-infinite plates, $z = \pm a$, $-\infty < x < 0$.

The solution to this motion is given in an implicit form by Lamb (1932); the appropriate asymptotic forms of this solution can be found in Newman (1974). In the depths of the duct the motion is given by

$$\phi_r \simeq -\frac{\pi x}{e_1 a} + \frac{(1+e_2)}{e_1}, \qquad |x/a| \gg 1, \qquad (3.5.1)$$

where e_1 and e_2 are unknown constants. The constant e_1 may be evaluated using the boundary condition on the piston given by (2.2.16), thus

$$e_1 = -\pi/a . \qquad (3.5.2)$$

The unknowns, e_2 and q may now be determined by matching the inner and outer solutions. The outer limit of the inner solution is given by

$$\phi_r \simeq -\frac{1}{e_1}\log\left(\frac{\pi r}{a}\right) + \frac{e_2}{e_1} + O\left(\frac{a}{r}\log^2\left(\frac{r}{a}\right)\right). \qquad (3.5.3)$$

Upon matching (3.5.3) with the inner limit of the outer solution given by (3.4.19), in the region of overlap $a \ll r \ll h$, it is found that

$$q = -2\pi/e_1 = 2a , \qquad (3.5.4)$$

and, using this result and matching the O(1) terms

$$e_2 = \log\left(\frac{2\pi h}{a}\right) + 2\int_0^\infty \left\{ \frac{e^{-sd}\sinh^2 sh}{s\cosh sd} - \frac{\cosh^2 sf}{\cosh sd(K\cosh sd - s\sinh sd)} \right\} ds$$

$$+ \frac{i\pi N_0^{-1}\cosh^2 kf}{kd} - 2\pi\phi_c(0,0). \qquad (3.5.5)$$

With e_1, e_2 and q given as above, the solution to the problem is complete.

3.6 Wave Power Absorption

The maximum efficiency of the system given by (3.3.6) can be found using (3.4.14), (3.4.18) and (3.4.3). Clearly it does not involve the source strength q and may be written

$$E_{max} = \left(1 + c_g^- |B^-|^2 / c_g^+ |B^+|^2\right)^{-1} \qquad (3.6.1)$$

For each value of h/d the maximum efficiency appears to tend to a finite limit as Kd→0 (see Figure (3.2)). It can be shown analytically that this is indeed the case. As Kd→0, then from (3.2.1), (3.2.2)

$$Kd \sim (kd)^2 ,$$
$$Kh \sim (mh)^2 , \qquad (3.6.2)$$

while the behaviour of the complex roots of the dispersion relations is given by

$$k_n d \sim n\pi + O(Kd), \quad , (n = 1,2,\ldots),$$
$$m_n h \sim n\pi + O(Kh). \qquad (3.6.3)$$

From (A.3), (A.8) and (A.10) it can be seen

$$|L_+(k)| \sim (kd)^{-1},$$

$$|L_+(m)| \sim (mh)^{-1},$$

and

$$\Theta_1 \simeq \Theta_2 \sim \pi/2 \quad , \text{ as } Kd \longrightarrow 0.$$

Thus, using (3.4.14), (3.4.18) it is found

$$B^+ = -\frac{i}{2kd}\left(1 + \frac{m-k}{m+k}\right) + O\left((Kd)^{\frac{1}{2}}\right), \qquad (3.6.4)$$

$$B^- = \frac{-i}{2mh}\left(1 - \frac{m-k}{m+k}\right) + O\left((Kd)^{\frac{1}{2}}\right), \qquad (3.6.5)$$

and, using (2.2.23)

$$c_g^+/c_g^- = \frac{mh}{kd}\left(1 + O(Kd)\right) = \left(\frac{h}{d}\right)^{\frac{1}{2}}\left(1 + O(Kd)\right). \qquad (3.6.6)$$

Thus, from (3.6.1), the limit is given by

$$E_{max} \longrightarrow \left[1 + (h/d)^{\frac{1}{2}}\right]^{-1} \quad , \text{ as } Kd \longrightarrow 0. \qquad (3.6.7)$$

To determine the efficiency of the system it is necessary to find the added-mass and damping coefficients, (see(3.3.8)). These are given by (2.2.21) and it can be shown

$$\omega^2 M + i\omega B = \rho\omega^2\left\{2al + (2a^2/\pi)(1 + e_2)\right\}, \qquad (3.6.8)$$

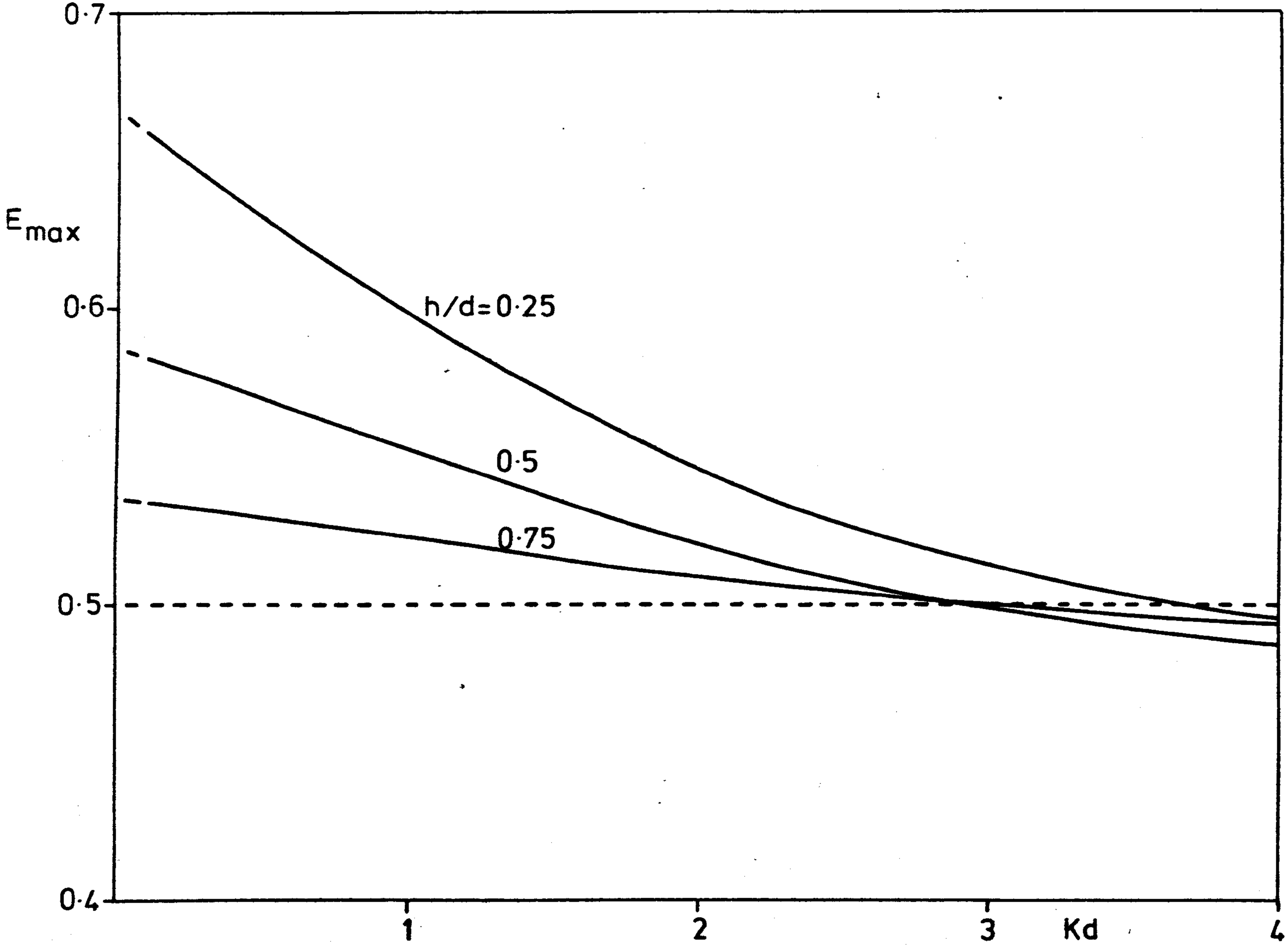

FIG (3·2)

where M and B are the added-mass and damping coefficients respectively, and use has been made of (3.5.1), (3.5.2). Thus

$$M = \rho\{ 2al + (2a^2/\pi)(1 + Re(e_2)) \},$$

$$B = \rho\omega(2a^2/\pi)Im(e_2),$$

or

$$M = M_0\{1 + (a/\pi l)(1 + Re(e_2))\}, \qquad (3.6.9)$$

$$B = M_0\omega(a/\pi l)Im(e_2), \qquad (3.6.10)$$

where M_0 ($= 2al\rho$) is the mass of fluid in the duct.

Thus the added-mass and damping coefficients are both linear in the parameter a/l, and the parameter a/h appears only in the logarithm term in the expression for e_2, which affects only the added-mass coefficient. Apart from this logarithm term, e_2 depends only upon the parameters h/d and Kd (see (3.5.5)).

Curves of the added-mass and damping coefficients as functions of Kd are shown in Figures (3.3) and (3.4). From Figure (3.4) it can be seen that the non-dimensional damping coefficient curves do not tend to a finite value as $Kd \to 0$. As for E_{max}, the limiting behaviour may be found analytically.

The relation (3.3.5) together with (3.6.4), (3.6.5) can be used to give

$$B \simeq M_0\omega \frac{q^2}{2al}\left\{\frac{m^2}{kd(k+m)^2} + \frac{k^2}{mh(k+m)^2}\right\}, \text{ as } Kd \to 0, \qquad (3.6.11)$$

and q is given by (3.5.4), thus

$$B \simeq M_0\omega \frac{2a}{mlh}\left(\frac{k}{m+k}\right)$$

$$\simeq M_0\omega \frac{2a}{l}(kd)^{-\frac{1}{2}}\left(1 + (h/d)^{\frac{1}{2}}\right)^{-1}, \text{ as } Kd \to 0. \qquad (3.6.12)$$

Hence the non-dimensional damping coefficient Λ, given by $B = M_0\omega\Lambda$ behaves as $(Kd)^{-\frac{1}{2}}$ as $Kd \to 0$.

The results for the added-mass and damping coefficients may now be used in (3.3.7), (3.3.8) to determine the amplitude of the piston motion and the efficiency of the system. As explained in Evans (1976), the system may be tuned to a particular frequency, ω_0 by choosing the spring and damper constants, α and β respectively, as

$$\alpha = (m_0 + M(\omega_0))\omega_0^2,$$

$$\beta = B(\omega_0),$$

whence, from (3.3.8)

$$E = E_{max} \text{ at } \omega = \omega_0 .$$

3.7 Results

Curves of maximum efficiency as a function of non-dimensional wavenumber Kd are given in Figure (3.2). Under the assumption that the duct is narrow, the only parameter which affects the maximum efficiency is h/d and, as one might expect, better results are achieved by bringing the duct closer to the free surface. When $Kd \geq 3$ it can be seen that the maximum efficiency actually falls below 50% albeit by a small amount; this may be due to the somewhat artificial model being used. In each case, as $Kd \to 0$ the curves tend smoothly to their limiting value predicted by (3.6.7). This provided one check on the computation and, as a further check, the maximum efficiency was calculated for h/d = 0.95. In this case the duct is very close to the sea-bed and one would expect the maximum efficiency to be very near 0.5 for all values of Kd (if the duct were coincident with the sea-bed, it would be 0.5 by symmetry). It was found that its value decreased from its limit of 0.5063 as $Kd \to 0$ to a value of 0.4990 at Kd=4.

Figure (3.3) illustrates the behaviour of the added-mass coeficient. The solid curves correspond to varying the depth of submergence of the duct.

Near the free surface the behaviour is quite different from when the duct is more deeply submerged although, in each case, the variation in the coefficient value over the whole range is fairly small. The dotted curve gives the added-mass coefficient for h/d = 0.5 but the parameter a/l is decreased while a/d remains constant; this corresponds to increasing the water column length and results in a decrease in the non-dimensional added-mass (the actual added-mass ($= 2alp$) increases). Note that the shape of the curve is very similar to the solid curve for h/d = 0.5, $a/l = 0.1$. This was also found to be the case when the duct width was varied (decreasing duct width and increasing water column length produce similar effects on the non-dimensional added-mass). This arises from the simple way in which the added-mass depends on these parameters (see equation (3.6.9)).

The damping coefficient also displays different behaviour when close to the free surface, as shown in Figure (3.4). Away from the surface, there is a monotonic decrease as Kd increases but, when h/d = 0.25, the damping coefficient remains fairly constant between Kd=1.0 and 2.6. As shown in § 6, the curves behave as $O((Kd)^{-\frac{1}{2}})$ as $Kd \to 0$ and, from (3.6.12), greater values are attained as $Kd \to 0$ when the duct is closer to the sea-bed. Changing the water column length or the duct width alters the damping coefficient in a simple manner (see equation (3.6.10)).

To begin the examination of the efficiency of the system the effect of tuning is considered (Figure(3.5)). The maxima of the curves lie on the appropriate maximum efficiency curve and although the maximum value of the efficiency decreases as the tuning wavenumber K_0d ($= \omega_0^2 d/g$) increases, the bandwidth increases. (Choosing $K_0d = 1.6$, for example, corresponds to tuning to waves of wavelength ~ 147m in water of depth 40m).

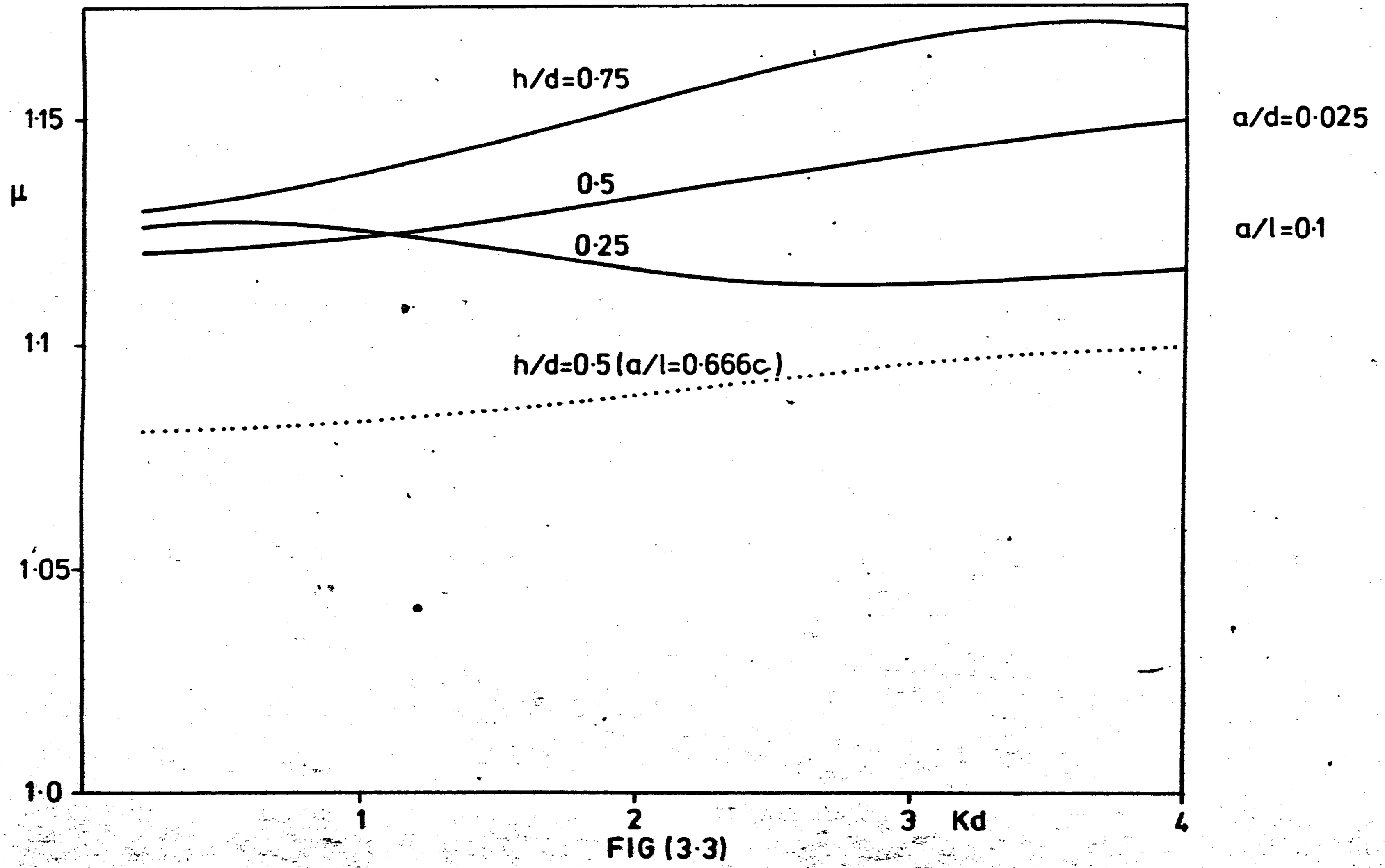

FIG (3·3)

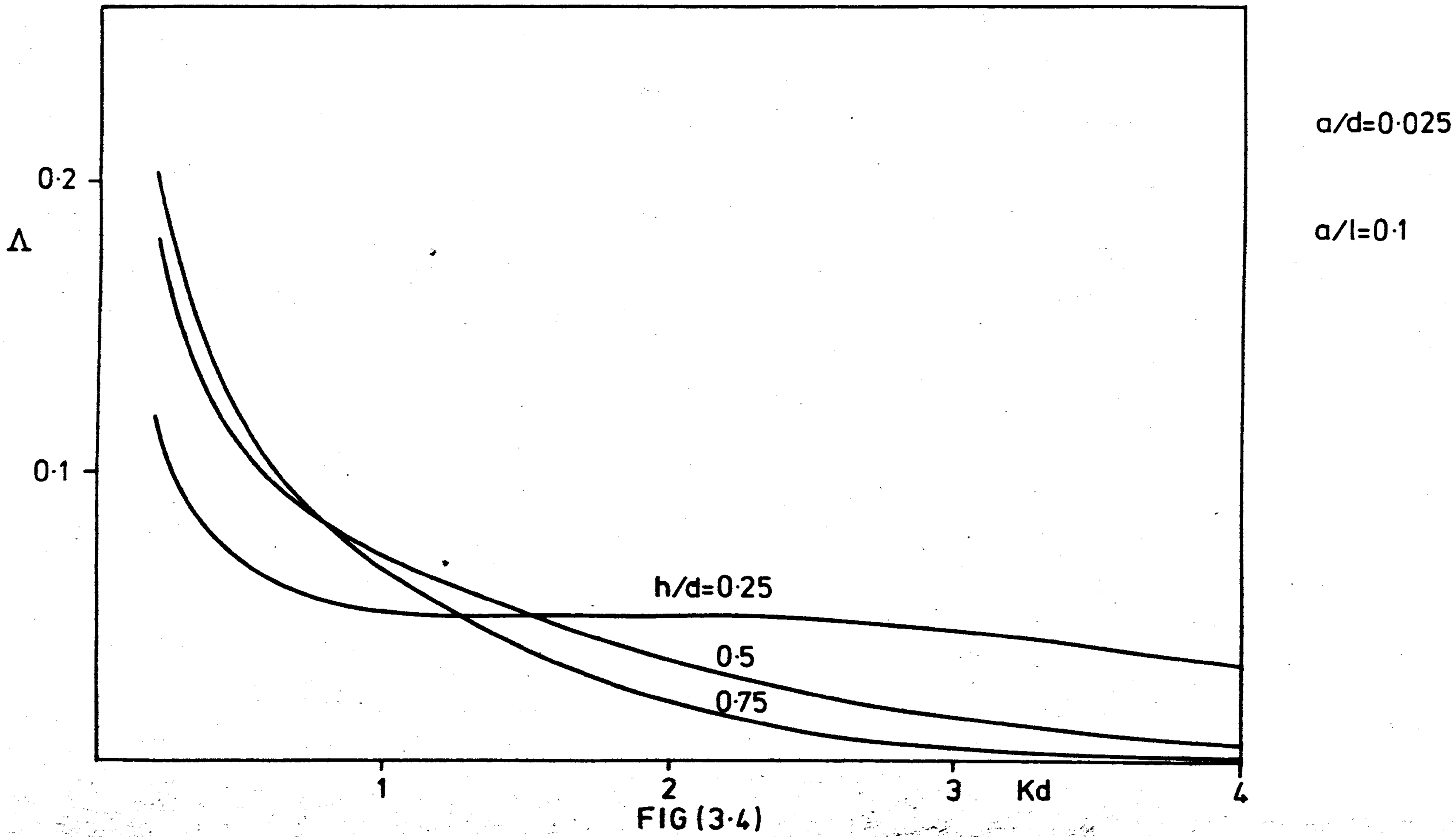

FIG (3·4)

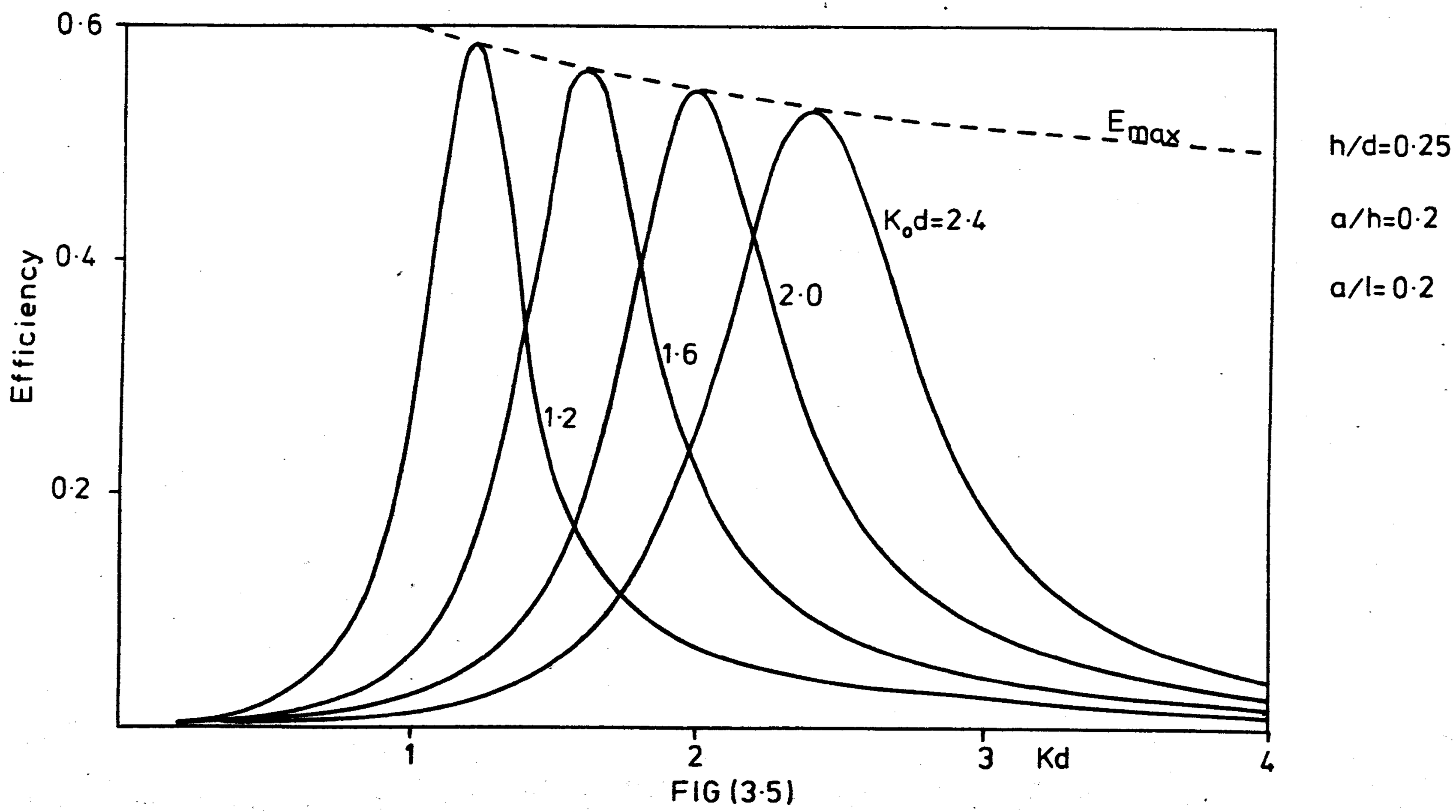
0·6
0·4
0·2
Efficiency
E_{max}
$K_o d = 2·4$
2·0
1·6
1·2
h/d=0·25
a/h=0·2
a/l= 0·2
1
2
3
Kd
4

FIG (3·5)

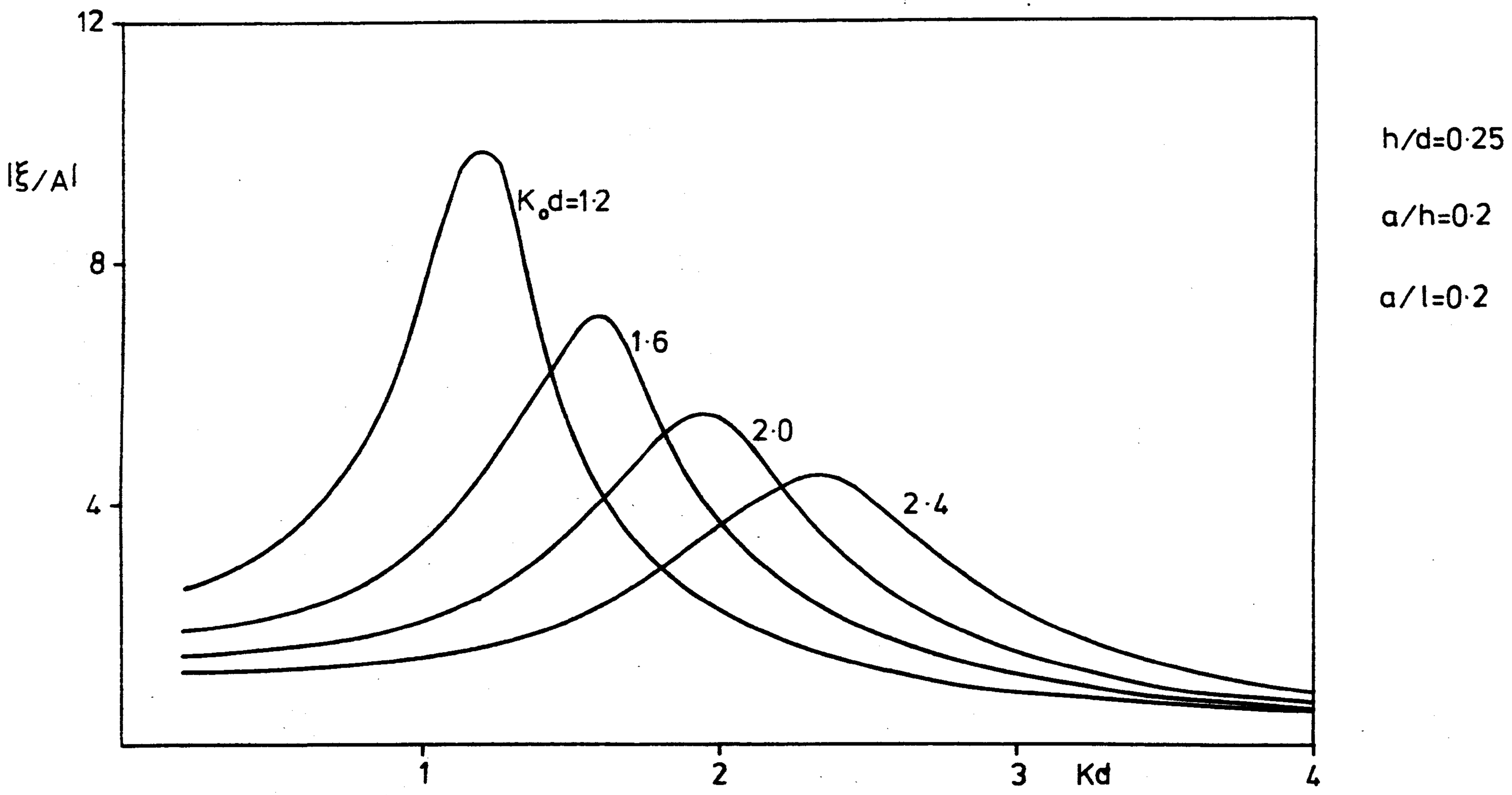

FIG (3·6)

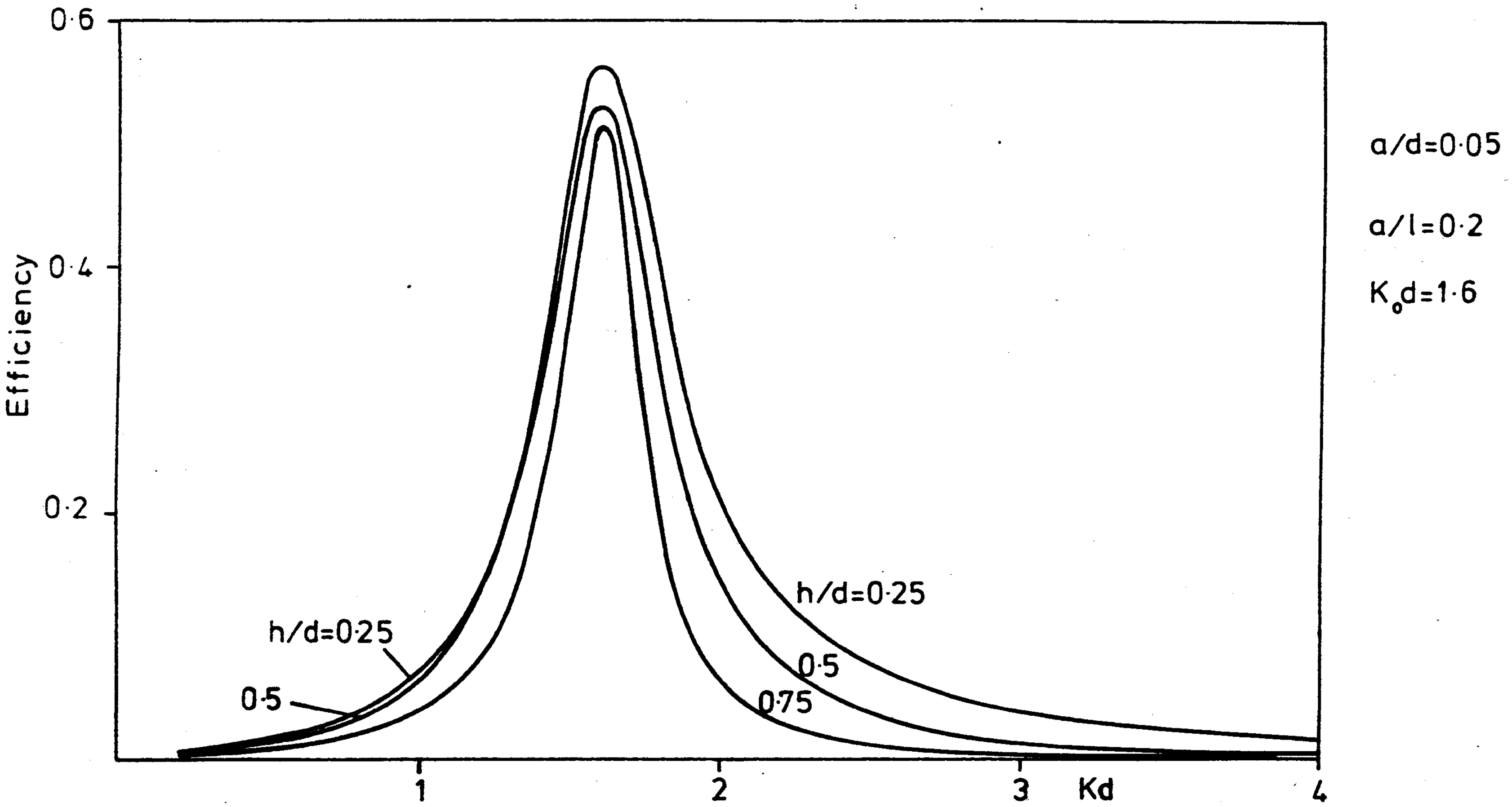
0·6
0·4
0·2
Efficiency
a/d=0·05
a/l=0·2
K₀d=1·6
h/d=0·25
0·5
0·75
h/d=0·25
0·5
1
2
3
Kd
4

FIG (3·7)

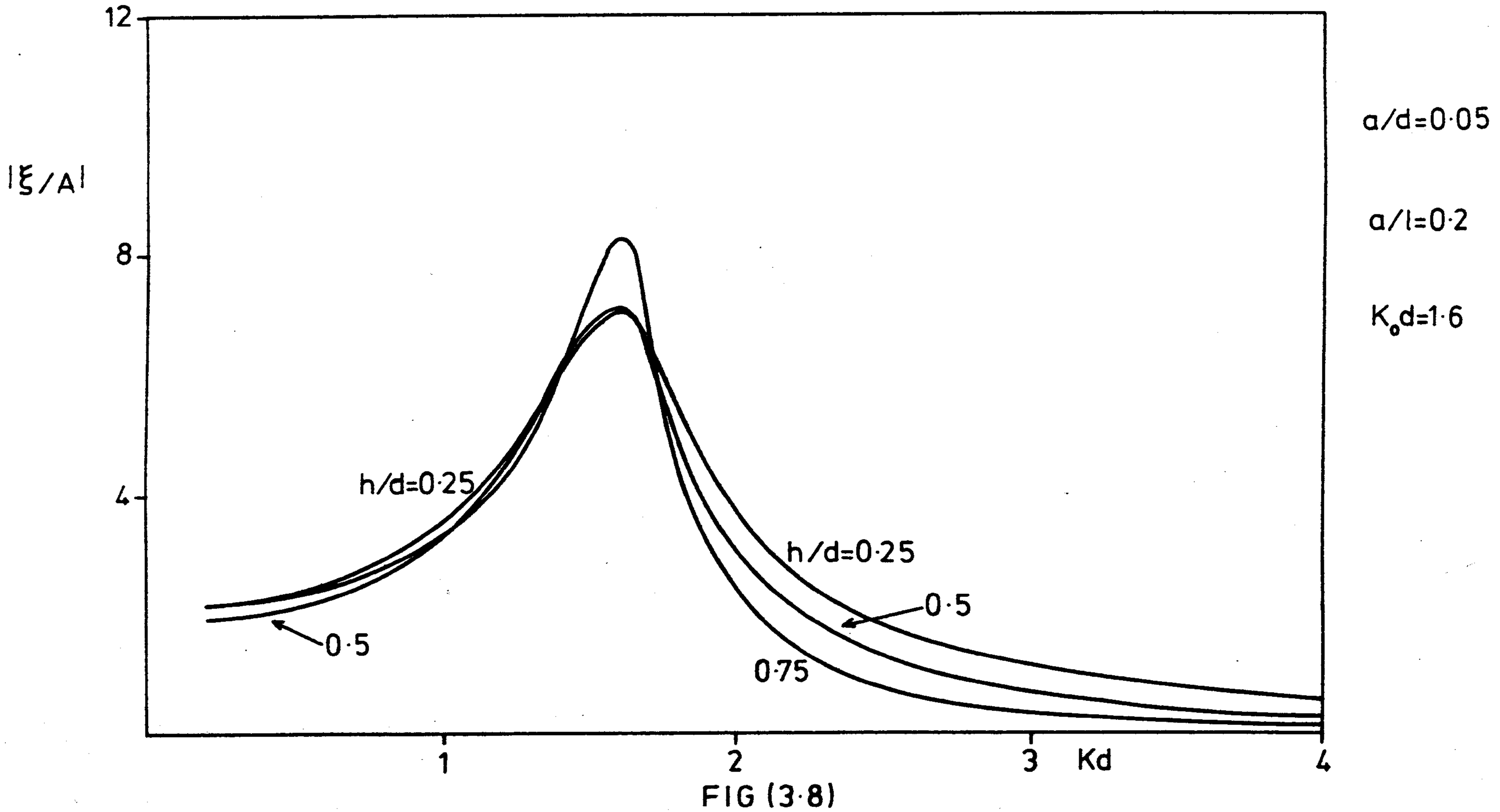

FIG (3·8)

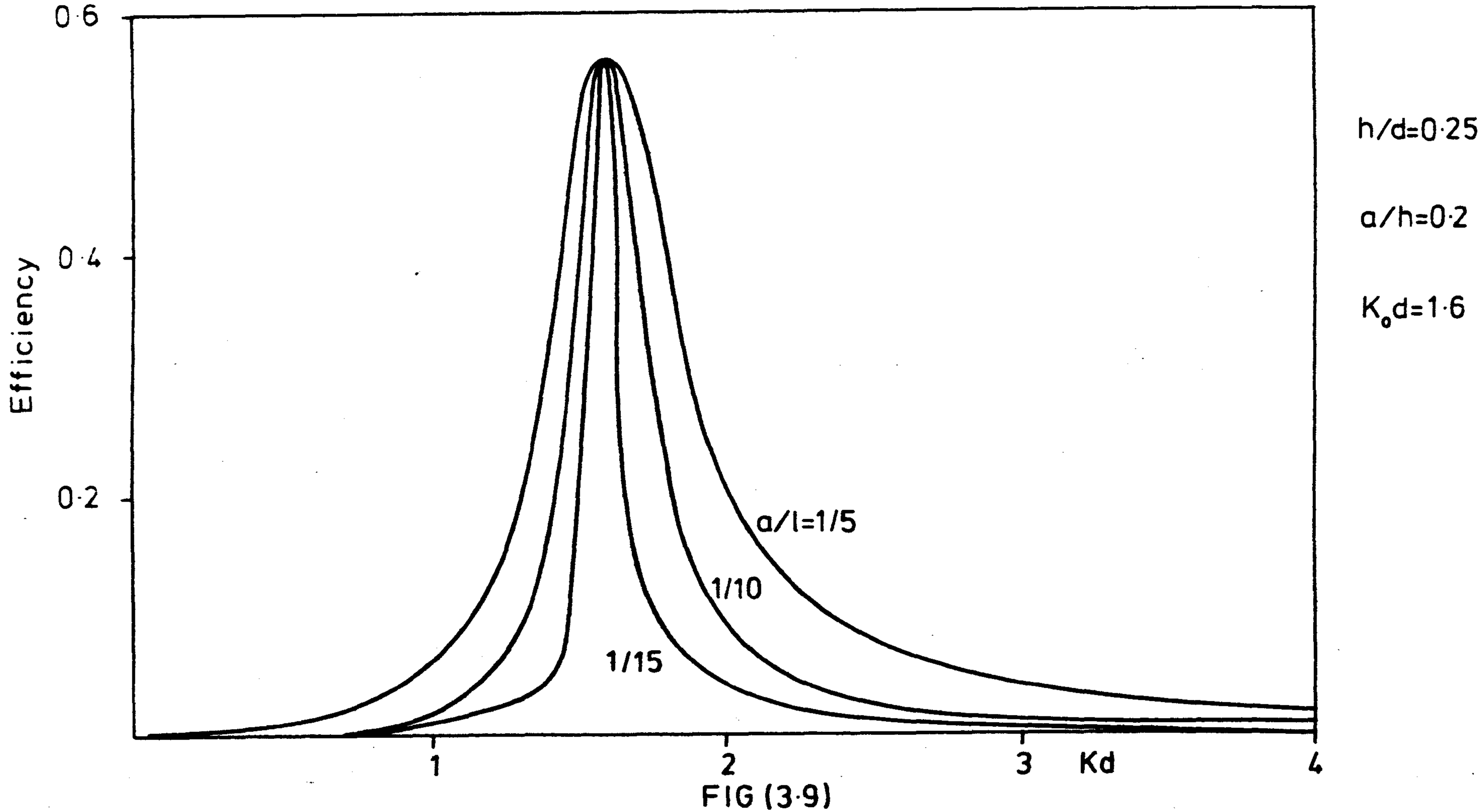

FIG (3·9)

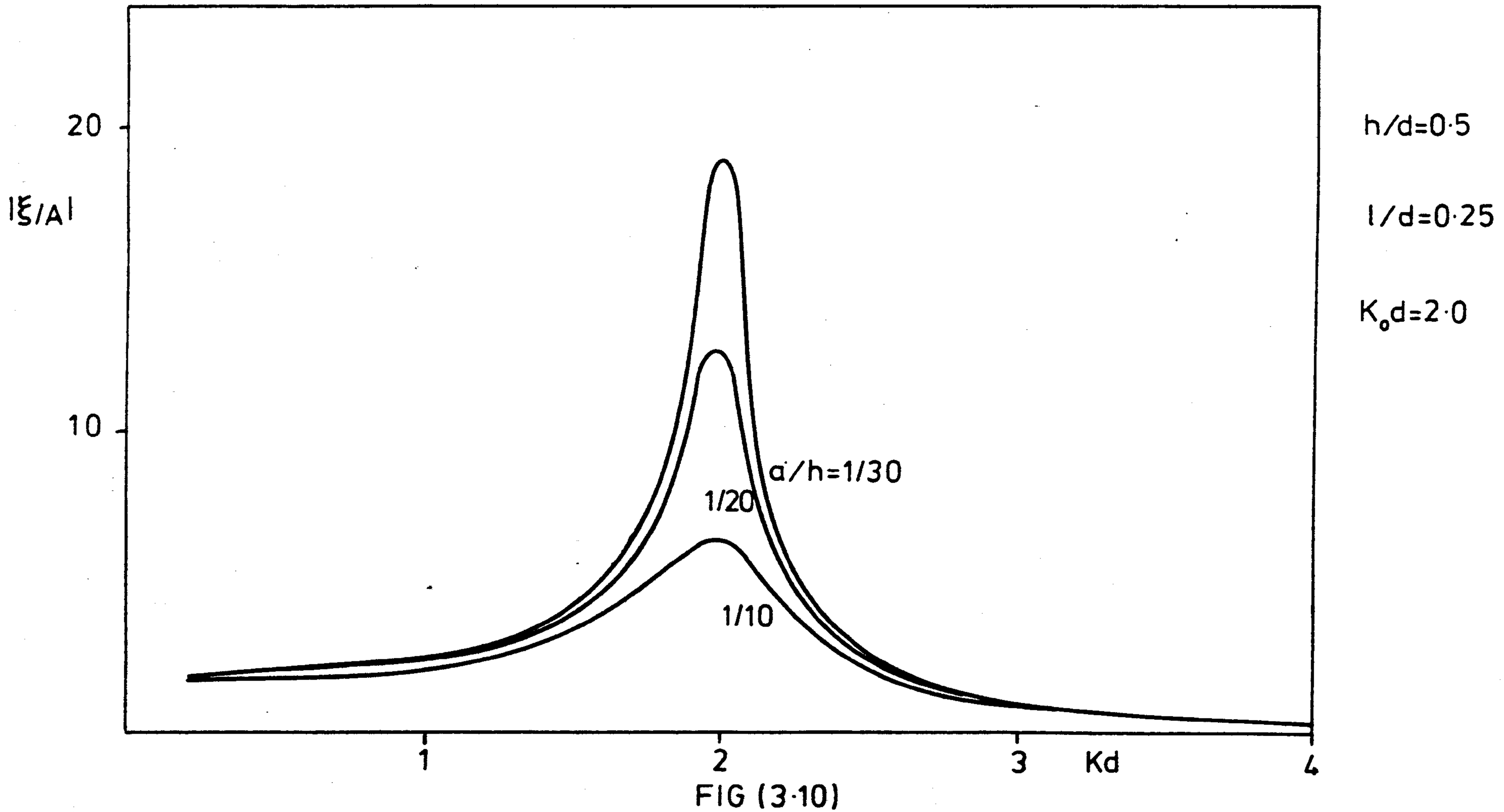

FIG (3·10)

As one might expect, the amplitude ratios given in Figure (3.6) also decrease as K_od increases and for, smaller K_od, are excessively large both from physical considerations and for the linear theory to apply.

Figure (3.7) illustrates the effect of increasing the depth of submergence which both decreases the efficiency and narrows the bandwidth. The corresponding amplitude ratio curves are quite close together even at the tuned wavenumber (see Figure (3.8)); in this case, although the duct is more deeply submerged, it is capturing less energy and so the piston need not undergo much larger oscillations. The efficiency curves when the water column length is varied are shown in Figure (3.9). Increasing the column length narrows the curves considerably (the effect is almost identical when the duct width is narrowed); in both cases the amplitude ratio increases near the tuning wavenumber K_od (Figure (3.10)).

3.8 Discussion

The maximum efficiency and efficiency of a submerged duct facing the incoming waves have been estimated. The mathematical analysis has proceeded under the assumptions: (i) that the duct is narrow; in practice this will probably not be so, but here it does enable the effects of the various parameters on the efficiency to be easily examined, (ii) that the duct length is semi-infinite, an artificial but necessary assumption in applying the mathematical method, and (iii) that linear water-wave theory is applicable.

The maximum efficiency results indicate that it is possible to achieve efficiencies of greater than 50% when the duct faces the incident waves. Better results might be expected if the duct is wider and if, as is common for such devices, a barrier is incorporated above the duct which extends above the free surface.

The results show the effect that duct width and water column length has on the efficiency bandwidths and the amplitude ratios. Bringing the piston closer to the mouth reduces the added-mass but does not affect the damping coefficient and hence the efficiency curve displays a broader bandwidth, while increasing the duct width increases the damping coefficient proportionaly more than the added-mass coefficient and again results in a wider bandwidth. Increasing the depth of submergence of the duct decreases both the maximum value of the efficiency and its bandwidth.

The preceding analysis provides a simple model of a submerged duct oriented to face the incoming waves. Clearly assumption (ii) above is unrealistic but the results do provide some insight into how the various parameters affect the added-mass and damping coefficients and hence, the efficiency.

CHAPTER 4

WAVE ENERGY ABSORPTION BY A THREE-DIMENSIONAL MOUTH-UPWARD DUCT

4.1 Introduction

Unlike the N.E.L. and modified Vickers device, the original oscillating water-column system proposed and investigated by Vickers Limited was axisymmetric with the mouth facing vertically upwards. As explained in Chapter 1, it was designed to be situated on the sea-bed where it would be shielded, to some extent, from local storms which could cause damage to a surface device. Lighthill (1979) points out, in his two-dimensional study of submerged ducts, that two-dimensional models can be informative, giving reliable indications of the behaviour of three-dimensional systems. Nevertheless, a three-dimensional analysis of the original Vickers device is clearly more relevant in understanding the hydrodynamics of the system.

In this Chapter, an upward-facing duct of circular cross-section is considered as an idealised model. It stands on the sea-bed and is fitted with a piston, at sea-bed level for mathematical simplicity, which is attached to a spring-damper system as a means of extracting energy. Evans (1976) has shown that the capture width may be determined from knowledge of the added-mass and damping coefficients, that is from the solution of the radiation problem alone and, further, that the maximum capture width for this device is simply $\lambda/2\pi$, where λ is the wavelength of the incident waves. This result is true for any body with a vertical axis of symmetry which is constrained to move in heave only. Although Evans' expressions were derived for infinitely deep fluid the same results as above are true in finite depth.

The maximum capture width is again $\lambda/2\pi$, where the wavelength is now dependent on the fluid depth; the corresponding finite-depth expressions for the capture width and amplitude ratio are given in § 4. Hence, in this chapter, only the radiation problem is considered. The method of solution is applicable in finite water depth only, and is due to Garrett, who examined the problems of bottomless harbours (1970) and the wave forces on a circular dock (1971).

A similar configuration to the one considered here has been used by Simon (1981a) although he only treats the infinite-depth case and models the power take-off system by an energy extraction coefficient (equivalent to a damper) applied in the depths of the duct. His solution involves the use of an approximate variational technique due to Evans & Morris (1972a,b) to solve the scattering problem together with the application of the Kramers-Kronig relations (Kotik & Mangulis, 1962) to determine the added-mass coefficient from the calculated damping coefficient. A comparison of Simon's results for these coefficients is made with the corresponding results found in finite depth, and is given in § 7.

Added-mass and damping curves as functions of wavenumber are also presented in § 7, for various duct diameters and depths of submergence. For narrow ducts the added-mass coefficient shows little variation over the range considered, being in general slightly larger than the mass of the fluid column in the duct. As the duct length increases, it is shown that the capture width bandwidth actually decreases at first before reaching a minimum and increasing again as the mouth of the duct approaches the surface of the fluid. It appears that the main advantage of the duct is that it reduces the amplitude of the piston motion as the duct length increases.

The limiting case of an oscillating disc on the sea-bed is

considered in §§5,6. This problem is easily solved, yielding analytic expressions for the added-mass and damping coefficients. These expressions give some insight into the behaviour of the coefficients when the duct length is non-zero and they also provide a useful check on the computation necessary for this case.

4.2 Formulation

A submerged vertical duct of length ℓ and circular cross-section of radius a, stands on the sea-bed in water of depth d ($d > \ell$). The duct is fitted with a piston and, as the radiation problem only will be considered, the piston is forced to oscillate with frequency ω and unit amplitude. Cylindrical polar coordinates (r, θ, z) are chosen with z positive upwards and the origin at the mean position of the centre of the piston, (see Figure (4.1)).

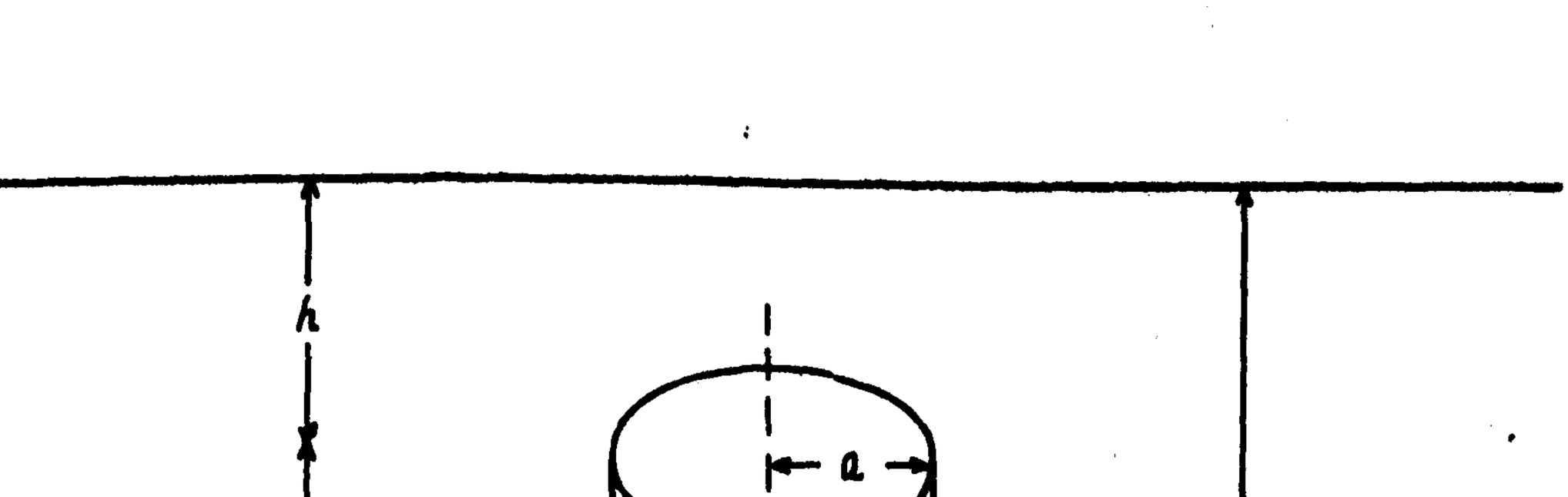

FIGURE (4.1)

Since there is no Θ - dependence in the problem by symmetry, the radiation potential $\phi_r = \phi_r(r,z)$. This potential satisfies (2.2.3), (2.2.4) and (2.2.5) with $z_f=d$, while the boundary conditions (2.2.7a), (2.2.16) become

$$\frac{\partial \phi_r}{\partial r} = 0 \quad , \quad \text{on } r=a \ , 0 \le z \le \ell \ , \tag{4.2.1}$$

$$\frac{\partial \phi_r}{\partial z} = 1 \quad , \quad \text{on } z=0 \ , \ r \le a \ . \tag{4.2.2}$$

The appropriate radition condition is given by

$$\phi_r \sim A_r H_o^{(1)}(kr) \frac{\cosh kz}{\cosh kd} \quad , \text{ as } r \longrightarrow \infty \ , \tag{4.2.3}$$

where A_r is some (complex) constant and k is the wavenumber given by the dispersion relation (2.2.9). Hereafter the subscript r of the potential may be omitted without ambiguity.

Laplace's equation may be solved in the inner ($r \lesssim a$) and outer ($r \gtrsim a$) regions by separation of variables to give

$$\phi = \sum_{n=0}^{\infty} A_n \, I_o(k_n r) Z_n(z) + \left[(z-d) + K^{-1} \right] \ , \ (r \lesssim a), \tag{4.2.4}$$

$$\phi = \sum_{n=0}^{\infty} B_n K_o(k_n r) Z_n(z), \quad (r \gtrsim a), \tag{4.2.5}$$

where A_n, B_n are unknown constants and, using the notation of Miles & Gilbert (1968),

$$Z_o(z) = N_o^{-\frac{1}{2}} \cosh kz, \tag{4.2.6}$$

$$Z_n(z) = N_n^{-\frac{1}{2}} \cos k_n z, \ (n \gtrsim 1). \tag{4.2.7}$$

The quantities k_n, N_o, N_n are given by (2.2.10) - (2.2.13). The $\{ Z_n(z), (n \gtrsim 0) \}$ form a complete orthorgonal set in $[0,d]$ with mean-square values of 1.

Note that

$$K_o(-ikr) = \tfrac{1}{2} \pi \, i H_o^{(1)}(kr),$$

$$I_o(-ikr) = J_o(kr),$$

where J_o is an ordinary Bessel function, I_o and K_o are modified Bessel functions and $H_o^{(1)}$ is the zero-order Hankel function of the first kind.

To satisfy (4.2.2) a particular solution, which is harmonic and also satisfies the free surface condition, is included in the inner region; such solutions are simple to construct and can be found in Black, Mei and Bray (1971) for various configurations and modes of oscillation.

The potential ϕ is now expressed in the inner and outer regions in terms of the radial velocity $\partial\phi/\partial r$ at the cylindrical interface, $r = a$.

Suppose

$$\frac{\partial \phi}{\partial r} = f(z) \quad , \text{at } r=a, \ l < z \leq d \ , \tag{4.2.8}$$

and, from (4.2.1), it is given that

$$\frac{\partial \phi}{\partial r} = 0 \quad , \text{at } r=a, \ 0 \leq z \leq l \ .$$

Hence $\partial\phi/\partial r$ may be expanded over $0 \leq z \leq d$ as

$$\left.\frac{\partial \phi}{\partial r}\right|_{r=a} = \sum_{n=0}^{\infty} \mathcal{F}_n Z_n(z) \ , \tag{4.2.9}$$

where

$$\mathcal{F}_n = \frac{1}{d} \int_l^d f(z) Z_n(z) dz \ . \tag{4.2.10}$$

The representations of ϕ in the inner and outer regions now become

$$\phi = \sum_{n=0}^{\infty} \frac{\mathcal{F}_n I_o(k_n r)}{k_n I_o'(k_n a)} Z_n(z) + \left\{ (z-d) + K^{-1} \right\}, \quad (r \leq a), \tag{4.2.11}$$

$$\phi = \sum_{n=0}^{\infty} \frac{\mathcal{F}_n K_o(k_n r)}{k_n K_o'(k_n a)} Z_n(z) \quad , (r \geq a) \ . \tag{4.2.12}$$

The pressure, and hence ϕ, is continuous at $r = a$, $l < z \leq d$, so matching the solutions in the inner and outer regions yields

$$\sum_{n=0}^{\infty} \mathcal{F}_n \left[\frac{K_o(k_n a)}{k_n K_o'(k_n a)} - \frac{I_o(k_n a)}{k_n I_o'(k_n a)} \right] Z_n(z) = (z-d) + K^{-1} \tag{4.2.13}$$

valid for $\ell < z \leq d$. This may be simplified using the formula

(Abramowitz & Stegun 1970, p.375, equation 9.6.15)

$$-I_o(k_n a)K_o'(k_n a) + I_o'(k_n a)K_o(k_n a) = (k_n a)^{-1} \quad , \text{for } n \geq 0 ,$$

and defining

$$R_n = -\left[k_n^2 a^2 I_o'(k_n a) K_o'(k_n a) \right]^{-1} \quad , \text{for } n \geq 0 . \qquad (4.2.14)$$

The equation (4.2.13) then becomes

$$\sum_{n=0}^{\infty} \mathcal{F}_n R_n Z_n(z) = \frac{1}{a}\left[(d-z) - k^{-1} \right] \quad , \ell < z \leq d . \qquad (4.2.15)$$

4.3 Solution

Miles & Gilbert (1968), studying a similar problem of scattering by a circular dock proceeded to set up an integral equation; however, the approach of Garrett (1970, 1971) is adopted here and an infinite system of simultaneous linear equations for the unknown $\mathcal{F}_n$ is constructed.

From (4.2.1), (4.2.9) it can be seen

$$\sum_{n=0}^{\infty} \mathcal{F}_n Z_n(z) = 0 \quad , 0 \leq z \leq \ell . \qquad (4.3.1)$$

Multiply (4.2.15) and (4.3.1) by $Z_m(z)$, integrate over the region of validity, divide by d and add. Thus

$$\sum_{n=0}^{\infty} E_{mn} \mathcal{F}_n = C_m \quad , \qquad (4.3.2)$$

where

$$E_{mn} = (R_n - 1) D_{mn} + \delta_{mn} \quad , \qquad (4.3.3)$$

$$D_{mn} = \frac{1}{d} \int_{\ell}^{d} Z_m(z) Z_n(z) \, dz \quad , \qquad (4.3.4)$$

and

$$C_m = \frac{1}{ad} \int_{\ell}^{d} \left[(d-z) - k^{-1} \right] Z_m(z) \, dz . \qquad (4.3.5)$$

(See Appendix B for expressions for D_{mn}, C_m).

The above is a complex matrix equation which can be reduced to two real matrix equations by writing

$$\mathcal{F}_n = a_n + i b_n \quad , (n \geq 0) , \qquad (4.3.6)$$

where a_n and b_n are real, and uncoupling the resulting equation. Note that the E_{mn} are real except for n=O (since $R_o = -\left\{ \tfrac{1}{2}\pi i k^2 a^2 J_o'(ka) H_o^{(1)'}(ka) \right\}^{-1}$). Writing

$$E_{mo} = p_m + i q_m \ , \qquad (4.3.7)$$

where p_m and q_m are real (see Appendix B for expressions for p_m, q_m), then, from (4.3.2), the following equations are obtained

$$p_m a_o + \sum_{n=1}^{\infty} E_{mn} a_n = C_m + b_o q_m \ , \qquad (4.3.8)$$

$$p_m b_o + \sum_{n=1}^{\infty} E_{mn} b_n = -a_o q_m \ . \qquad (4.3.9)$$

If r_n, s_n are the solutions of

$$p_m r_o + \sum_{n=1}^{\infty} E_{mn} r_n = C_m \ , \qquad (4.3.10)$$

$$p_m s_o + \sum_{n=1}^{\infty} E_{mn} s_n = q_m \ , \qquad m = 0,1,2,\ldots \qquad (4.3.11)$$

then

$$a_n = r_n + b_o s_n \ , \qquad (4.3.12)$$

$$b_n = -a_o s_n \ , \qquad n = 0,1,2,\ldots \qquad (4.3.13)$$

and, in particular

$$a_o = r_o + b_o s_o \ , \quad b_o = -a_o s_o \ ,$$

thus

$$a_o = r_o/(1+s_o^2) \ , \quad b_o = -r_o s_o/(1+s_o^2) \ .$$

Consequently $\mathcal{F}_n$ is given by

$$\mathcal{F}_n = \left\{ r_n - \frac{r_o s_o s_n}{(1+s_o^2)} \right\} + i \left\{ -\frac{r_o s_n}{(1+s_o^2)} \right\} \ , \ (n \geq 0). \qquad (4.3.14)$$

Hence, upon solving the two real systems of equations (4.3.10), (4.3.11) (the method employed is given in § 7), the $\mathcal{F}_n$ may be evaluated and, from (4.2.11), (4.2.12), a full solution for ϕ obtained.

4.4 Calculation of added-mass and damping coefficients and energy extraction

(a) Added-mass and damping coefficients

These coefficients, defined in Chapter 2, are given by (2.2.21). Using the representation of ϕ in the inner region (equation (4.2.11)) gives

$$\omega^2 M + i\omega B = -\rho\omega^2 \int_{r=0}^{a}\int_{\theta=0}^{2\pi}\left[(K^{-1}-d) + \sum_{n=0}^{\infty}\frac{\mathcal{F}_n I_0(k_n r)}{k_n I_0'(k_n a)} Z_n(0)\right] r\,dr\,d\theta \,, \qquad (4.4.1)$$

$$= -2\pi\rho\omega^2\left\{(K^{-1}-d)\frac{a^2}{2} + \sum_{n=0}^{\infty}\frac{N_n^{-\frac{1}{2}}\mathcal{F}_n}{k_n I_0'(k_n a)}\int_0^a I_0(k_n r)\,r\,dr\right\} \,,$$

$$= -2\pi\rho\omega^2\left\{(K^{-1}-d)\frac{a^2}{2} + a\sum_{n=0}^{\infty}\frac{N_n^{-\frac{1}{2}}\mathcal{F}_n}{k_n^2}\right\} \,. \qquad (4.4.2)$$

Thus

$$M = -2\pi\rho\left\{(K^{-1}-d)\frac{a^2}{2} + a\,\mathrm{Re}\sum_{n=0}^{\infty}\frac{N_n^{-\frac{1}{2}}\mathcal{F}_n}{k_n^2}\right\} \,, \qquad (4.4.3)$$

$$B = -2\pi\rho\omega a\,\mathrm{Im}\sum_{n=0}^{\infty}\frac{N_n^{-\frac{1}{2}}\mathcal{F}_n}{k_n^2} \,. \qquad (4.4.4)$$

(b) Capture width and amplitude ratio

The expressions for the capture width and amplitude ratio given by Evans (1976) are derived for infinitely deep fluid. The corresponding results in finite depth can be found following the method outlined in Chapter 2, § 3. The Haskind relation (Haskind, 1957) is now given by

$$X_s = i\omega\rho\int_{S_o}\left(\phi_o\frac{\partial\phi}{\partial n} - \phi\frac{\partial\phi_o}{\partial n}\right)dS \qquad (4.4.5)$$

(c.f. equation (3.3.4)) where S_o is a control surface which is cylindrical, given by r=R (excluding base and top), X_s is the exciting force and ϕ_o is the incident wave potential given by (2.2.8) as

$$\phi_o = \frac{gA}{\omega}\frac{\cosh kz}{\cosh kd}\,e^{ikx}$$

where, since direction of incidence is of no consequence, $\Theta = 0$ is taken. This may be expanded as

$$\phi_o = \frac{gA}{\omega}\frac{\cosh kz}{\cosh kd}\sum_{m=0}^{\infty}\varepsilon_m i^m J_m(kr)\cos m\theta ,$$

$$= \frac{gA}{\omega}\frac{\cosh kz}{\cosh kd}\sum_{m=0}^{\infty}\frac{\varepsilon_m i^m}{2}\left[H_m^{(1)}(kr)+H_m^{(2)}(kr)\right]\cos m\theta , \qquad (4.4.6)$$

where $\varepsilon_0 = 1$ and $\varepsilon_m = 2$, $(m \geq 1)$, and $H_m^{(1)}$, $H_m^{(2)}$ are m-th. order Hankel functions of the first and second kinds respectively. So, from (4.4.5), and using the asymptotic behaviour of ϕ given by (4.2.3), it is found that as $R \longrightarrow \infty$

$$X_s = -\frac{i\pi\rho g k A A_r}{\cosh^2 kd}\int_0^d \cosh^2 kz\, dz \lim_{R\to\infty} R\left\{H_0^{(1)}(kr)H_1^{(2)}(kr) - H_0^{(2)}(kr)H_1^{(1)}(kr)\right\} , \qquad (4.4.7)$$

as only the θ-independent $(m=0)$ term in (4.4.6) gives a non-zero contribution.

This reduces to

$$X_s = \frac{4\rho g d\, N_0 A A_r}{\cosh^2 kd} ,$$

where use has been made of the asymptotic forms of the Hankel functions for large arguments (Abramowitz & Stegun 1970, p.364, equations 9.2.1 - 9.2.4). This may also be written as

$$X_s = 4\rho\omega c_g k^{-1} A A_r , \qquad (4.4.8)$$

where c_g is the group velocity given by (2.2.23).

Applying Green's theorem to ϕ and $\bar{\phi}$, (the overbar denotes the complex conjugate), it can be shown

$$\frac{2iB}{\rho\omega} = \int_{S_0}\left(\phi\frac{\partial\bar{\phi}}{\partial n} - \bar{\phi}\frac{\partial\phi}{\partial n}\right)ds ,$$

(c.f. equation (3.3.5)) and, using (4.2.3), letting $R\to\infty$ gives

$$B = \frac{4\rho\omega^2}{gk} c_g |A_r|^2 . \qquad (4.4.9)$$

To find the amplitude ratio, the equation of motion of the piston (2.2.17) may be used together with (2.2.18), (2.2.19) and the result (4.4.8) above, to show

$$4\rho\omega c_g k^{-1} A A_r = \left[\left\{\alpha - (m_0+M)\omega^2\right\} - i\omega\left[\beta+B\right]\right]\xi$$

and, using (4.4.9), it is found

$$\left|\frac{\xi}{A}\right|^2 = \frac{4\rho g k^{-1} c_g B}{\left[\alpha-(m_0+M)\omega^2\right]^2+\omega^2\left[\beta+B\right]^2} \quad . \qquad (4.4.10)$$

From (2.2.26) the capture width, C_w is then given as

$$C_w = \frac{4\omega^2 k^{-1}\beta B}{\left[\alpha-(m_0+M)\omega^2\right]^2+\omega^2\left[\beta+B\right]^2} \quad . \qquad (4.4.11)$$

Note that for deep water $\omega^2 = gk$ (from (2.2.9)) and Evans' (1976) result is obtained. The expression (4.4.11) may be written as

$$C_w = k^{-1}\left[1 - \frac{\left[\alpha-(m_0+M)\omega^2\right]^2+\omega^2\left[\beta-B\right]^2}{\left[\alpha-(m_0+M)\omega^2\right]^2+\omega^2\left[\beta+B\right]^2}\right],$$

giving a maximum value

$$C_{w_{max}} = k^{-1} = \lambda/2\pi \quad , \qquad (4.4.12)$$

at $\omega=\omega_0$ when

$$\alpha = \left[m_0+M(\omega_0)\right]\omega_0^2 \quad , \qquad (4.4.13)$$

$$\beta = B(\omega_0) \quad , \qquad (4.4.14)$$

where λ is the wavelength of the incident wave. This result is the same as for the deep water case although λ now depends upon the water depth.

Before computing values of the added-mass and damping coefficients they are non-dimensionalised as

$$M=M_0\mu \quad , B=M_0\omega\Lambda \quad , \qquad (4.4.15)$$

where M_0 = mass of fluid above piston contained in a cylinder of radius a, $M_0 = \pi a^2\rho d$.

This particular M_0 is chosen, instead of the usual mass of the fluid column in the duct, so that the limiting case as the duct length tends to zero may be taken.

If the non-dimensional wavenumber $\upsilon = \omega^2 d/g$ is introduced, then

$$\mu = 1-\upsilon^{-1}-2\left(\frac{d}{a}\right)Re\sum_{n=0}^{\infty} N_n^{-\frac{1}{2}} \mathcal{F}_n/(k_n d)^2 \qquad (4.4.16)$$

$$\Lambda = -2\left(\frac{d}{a}\right)\mathrm{Im}\sum_{n=0}^{\infty} N_n^{-\frac{1}{2}} \mathcal{F}_n/(k_n d)^2 \qquad (4.4.17)$$

Further, assuming the tuning criterion (4.4.13),(4.4.14) can be satisfied, the capture width and amplitude ratio are given by

$$C_W/2a = (2ka)^{-1}\frac{4\upsilon(\upsilon+\Lambda)(\upsilon_0+\Lambda_0)}{(\mu_0\upsilon_0-\mu\upsilon)^2+\upsilon(\upsilon_0+\Lambda_0+\upsilon+\Lambda)^2}\quad , \qquad (4.4.18)$$

$$|\xi/A|^2 = \frac{(2\Lambda/\pi\upsilon)(d/a)^2(\tanh kd + kd\,\mathrm{sech}^2 kd)}{(\mu_0\upsilon_0-\mu\upsilon)^2+\upsilon(\upsilon_0+\Lambda_0+\upsilon+\Lambda)^2}\quad , \qquad (4.4.19)$$

where $\upsilon_0=\omega_0^2 d/g$, $\mu_0=\mu(\omega_0)$, $\Lambda_0=\Lambda(\omega_0)$ and $m_0=0$, i.e. a light piston.

So, for each value of the non-dimensional wavenumber υ, the two real linear systems of equations given by (4.3.10), (4.3.11) may be solved to evaluate $\mathcal{F}_n$ and hence μ and Λ. Once the variation of μ and Λ with υ is known, and a tuning frequency ω_0 is chosen, equations (4.4.18), (4.4.19) may be used to study the capture width and amplitude ratio. The results obtained are presented and discussed in §7, but first the limiting case of an oscillating disc will be examined in some detail.

4.5 Limiting Disc Case

(a) Statement of problem and solution

An interesting limiting case of the resonant duct is that of an oscillating disc on the sea-bed. One approach to the problem is as given above for a non-zero length duct, but the fact that ϕ is now matched at r=a over the whole interval [0,d] produces analytic results for the added-mass and damping coefficients. This provides a better insight into the behaviour of these coefficients, (the similar curves produced in the disc and duct cases indicate that this behaviour is relevant to the duct problem).

The formulation of the problem is clearly identical with that of the duct case, giving now, instead of (4.2.15)

$$\sum_{n=0}^{\infty}\mathcal{F}_n R_n Z_n(z) = \{(d-z)-K^{-1}\}/a\quad , \text{ valid for } 0\le z\le d. \qquad (4.5.1)$$

As before multiply both sides by $(1/d)\,Z_m(z)$ and integrate to obtain

$$\mathcal{F}_m R_m = \frac{1}{ad}\int_0^d \left\{(d-z)-K^{-1}\right\} Z_m(z)\,dz, \qquad (4.5.2)$$

$$= C_m \quad , \text{with } l=0.$$

Thus

$$\mathcal{F}_0 = \frac{C_0}{R_0} \quad , \text{where } C_0 = -\frac{N_0^{-\frac{1}{2}}}{k^2 ad} \quad , \text{(See Appendix B)}, \qquad (4.5.3)$$

$$\mathcal{F}_m = \frac{C_m}{R_m} \, , (m \geq 1) \, , \text{where } C_m = \frac{N_m^{-\frac{1}{2}}}{k_m^2 ad} \quad , \text{(See Appendix B)}. \qquad (4.5.4)$$

Hence

$$\mathcal{F}_0 = -\frac{N_0^{-\frac{1}{2}}}{k^2 ad}\left\{-\tfrac{1}{2}\pi i k^2 a^2 J_0'(ka) H_0^{(1)\prime}(ka)\right\},$$

$$= \tfrac{1}{2} N_0^{-\frac{1}{2}} \pi \left(\frac{a}{d}\right)\left\{-J_1(ka)Y_1(ka) + i\,J_1^2(ka)\right\}, \qquad (4.5.5)$$

and

$$\mathcal{F}_m = \frac{N_m^{-\frac{1}{2}}}{k_m^2 ad}\left\{-k_m^2 a^2 I_0'(k_m a) K_0'(k_m a)\right\},$$

$$= N_m^{-\frac{1}{2}}\left(\frac{a}{d}\right) I_1(k_m a) K_1(k_m a) \, , (m \geq 1). \qquad (4.5.6)$$

(b) **Added-mass and damping coefficients**

Using (4.4.3), (4.4.4) and the fact that the $\mathcal{F}_m$ are real for $m \geq 1$, it is found that

$$M = \pi a^2 \rho\left\{(d-K^{-1}) - \frac{N_0^{-1}\pi}{k^2 d} J_1(ka)Y_1(ka) - \frac{2}{d}\sum_{n=1}^{\infty} N_n^{-1} k_n^{-2} I_1(k_n a) K_1(k_n a)\right\}, \qquad (4.5.7)$$

$$B = \frac{\pi^2 a^2 \rho \omega}{k^2 d} N_0^{-1} J_1^2(ka). \qquad (4.5.8)$$

One important point to note is that for frequencies where ka is equal to a zero of J_1, the damping coefficient is zero and, since this coefficient is proportional to the square of the far-field radiated wave amplitude (see equation (4.4.9)), it is clear that, for an infinite set of frequencies, forced oscillation of the piston produces no propagating waves.

Similar effects have been found numerically by Black, Mei & Bray (1971) when they considered water-wave radiation by rigid oscillating bodies. However, the first zero of $J_1(ka)$ occurs at $ka=3.8317$, i.e.

$$\frac{2\pi d}{\lambda} \simeq 4\left(\frac{d}{a}\right) \quad \text{or} \quad \frac{\lambda}{d} \simeq \frac{2\pi}{4}\left(\frac{a}{d}\right) .$$

So, for a water depth of 40m, for example, then even when the diameter of the disc is equal to the water depth, the first zero will occur at a wavelength of approximately 30m which is outside the region of interest for wave energy devices as the important energy source is contained in waves of wavelengths between 80 and 250m.

After non-dimensionalisation as in § 4, the coefficients are given by

$$\mu = 1 - \upsilon^{-1} - \frac{N_0^{-1}\pi J_1(ka)Y_1(ka)}{(kd)^2} - 2\sum_{n=1}^{\infty} \frac{N_n^{-1} I_1(k_n a)K_1(k_n a)}{(k_n d)^2} , \qquad (4.5.9)$$

$$\Lambda = \frac{N_0^{-1}\pi J_1^2(ka)}{(kd)^2} . \qquad (4.5.10)$$

Using the limiting forms of J_1, Y_1 for small arguments, (Abramowitz & Stegun 1970, p.360, equations 9.1.7, 9.1.9), the behaviour of μ and Λ as $\upsilon \to 0$ is given by

$$\mu \longrightarrow 1 - 4\pi^{-2}\sum_{n=1}^{\infty} n^{-2} I_1(n\pi a/d)K_1(n\pi a/d), \qquad (4.5.11)$$

$$\Lambda \longrightarrow \frac{\pi}{4}(a/d)^2 , \qquad (4.5.12)$$

where use has been made of (3.6.2), (3.6.3). Both μ and Λ tend to finite values as $\upsilon \longrightarrow 0$, the series appearing in μ converging rapidly since $I_1(x)K_1(x) \sim \frac{1}{2}x^{-1}$ as $x \longrightarrow \infty$. The capture width tends to zero as $\upsilon \to 0$ but the amplitude ratio tends to a finite, non-zero value. As $\upsilon \to 0$, then from (4.4.19)

$$|\Xi/A| \longrightarrow (\mu_0 \upsilon_0)^{-1} . \qquad (4.5.13)$$

Thus, the limiting value of the amplitude ratio depends only upon the tuning frequency and the value of the added-mass coefficient at that frequency.

4.6 Alternative methods of solution for the disc

In this section two further methods are given to determine the damping and added-mass coefficients for the oscillating disc. Both will be of use in the following Chapter.

(a) Use of the scattering problem

Newman (1962) has shown that the damping coefficient is related to the exciting force. In the disc case, evaluation of the exciting force is straightforward as there are no diffracted waves. From (4.4.8), (4.4.9) it can be seen

$$B = \frac{k}{4\rho g c_g} \left| \frac{X_s}{A} \right|^2 . \qquad (4.6.1)$$

As there are no diffracted waves, the scattering potential ϕ_s is just the incident wave potential, i.e.

$$\phi_s = \frac{gA}{\omega} \frac{\cosh kz}{\cosh kd} e^{ikx} ,$$

and, using (2.2.20) to determine the exciting force

$$X_s = \frac{-i\rho g A}{\cosh kd} \int_0^a r\,dr \int_0^{2\pi} e^{ikr\cos\theta}\, d\theta ,$$

$$= -\frac{2\pi i \rho g A}{\cosh kd} \int_0^a J_0(kr)\, r\,dr ,$$

$$= -\frac{2\pi i \rho g a A}{k \cosh kd} J_1(ka) . \qquad (4.6.2)$$

Substituting for X_s in (4.6.1) it is found that

$$B = \frac{\pi^2 a \rho g}{c_g k \cosh^2 kd} J_1^2(ka) . \qquad (4.6.3)$$

Using the expression for c_g given by (2.2.23), it can be seen that (4.6.3) agrees with (4.5.8).

(b) Use of Hankel transformation

The radiation problem for the disc can alternatively be solved

by applying the Hankel transformation of order zero, i.e.

$$\tilde{\phi}(\xi,z)=\int_0^\infty r\,J_0(\xi r)\phi(r,z)dr \quad . \tag{4.6.4}$$

For the transform to exist $r^{\frac{1}{2}}\phi(r,z)$ is required to be piecewise continuous and absolutely integrable along the real line, thus it is assumed that $k=k_r+ik_i$ $(k_i > 0)$, i.e. k has a small positive imaginary part, and later the limit $k_i \to 0$ is taken.

The governing equations (2.2.3) - (2.2.5) and (4.2.2) become

$$\left(\partial^2/\partial z^2-\xi^2\right)\tilde{\phi}(\xi,z)=0 \quad , \tag{4.6.5}$$

$$K\tilde{\phi}-\partial\tilde{\phi}/\partial z \;=0 \quad , \text{ on } z=d, \tag{4.6.6}$$

$$\frac{\partial\tilde{\phi}}{\partial z}=\int_0^a r\,J_0(\xi r)dr=\frac{a}{\xi}J_1(\xi a) \quad , \text{ on } z=0. \tag{4.6.7}$$

Solving (4.6.5) with the boundary conditions (4.6.6), (4.6.7) yields

$$\tilde{\phi}(\xi,z)=\frac{a\,J_1(\xi a)}{\xi^2}\left[\frac{\xi\cosh\xi(d-z)-K\sinh\xi(d-z)}{K\cosh\xi d-\xi\sinh\xi d}\right], \tag{4.6.8}$$

and applying the inverse transform

$$\phi(r,z)=\int_0^\infty \xi\,J_0(\xi r)\tilde{\phi}(\xi,z)\,d\xi \quad , \tag{4.6.9}$$

$$\phi(r,z)=\int_0^\infty \frac{a}{\xi}J_0(\xi r)J_1(\xi a)\left\{\frac{\xi\cosh\xi(d-z)-K\sinh\xi(d-z)}{K\cosh\xi d-\xi\sinh\xi d}\right\}d\xi \quad . \tag{4.6.10}$$

The added-mass and damping coefficients are given by (2.2.21), thus

$$\omega^2M+i\omega B=-2\pi\rho\omega^2\left\{\int_0^a r\,dr\int_0^a\frac{a}{\xi}J_0(\xi r)J_1(\xi a)\left(\frac{\xi\cosh\xi d-K\sinh\xi d}{K\cosh\xi d-\xi\sinh\xi d}\right)d\xi\right\},$$

and interchanging the order of integration it is found that

$$\omega^2M+i\omega B=-2\pi\rho\omega^2\left\{\int_0^\infty\frac{a^2}{\xi^2}J_1^2(\xi a)\left(\frac{\xi\cosh\xi d-K\sinh\xi d}{K\cosh\xi d-\xi\sinh\xi d}\right)d\xi\right\}.$$

The poles of the integrand are simple and occur at $\xi = \pm k, \pm ik_n$, $(n=1,2,\ldots)$. If $k_i \to 0$ so that the simple poles at $\xi = \pm k$ approach the real axis, then the path of integration is as shown in Figure (4.2). Thus

$$\omega^2M+i\omega B=-2\pi\rho\omega^2\left[\int_0^\infty d\xi+\pi i\underset{\xi=k}{\text{Res.}}\right]\left\{\frac{a^2}{\xi^2}J_1^2(\xi a)\left(\frac{\xi\cosh\xi d-K\sinh\xi d}{K\cosh\xi d-\xi\sinh\xi d}\right)\right\}. \tag{4.6.11}$$

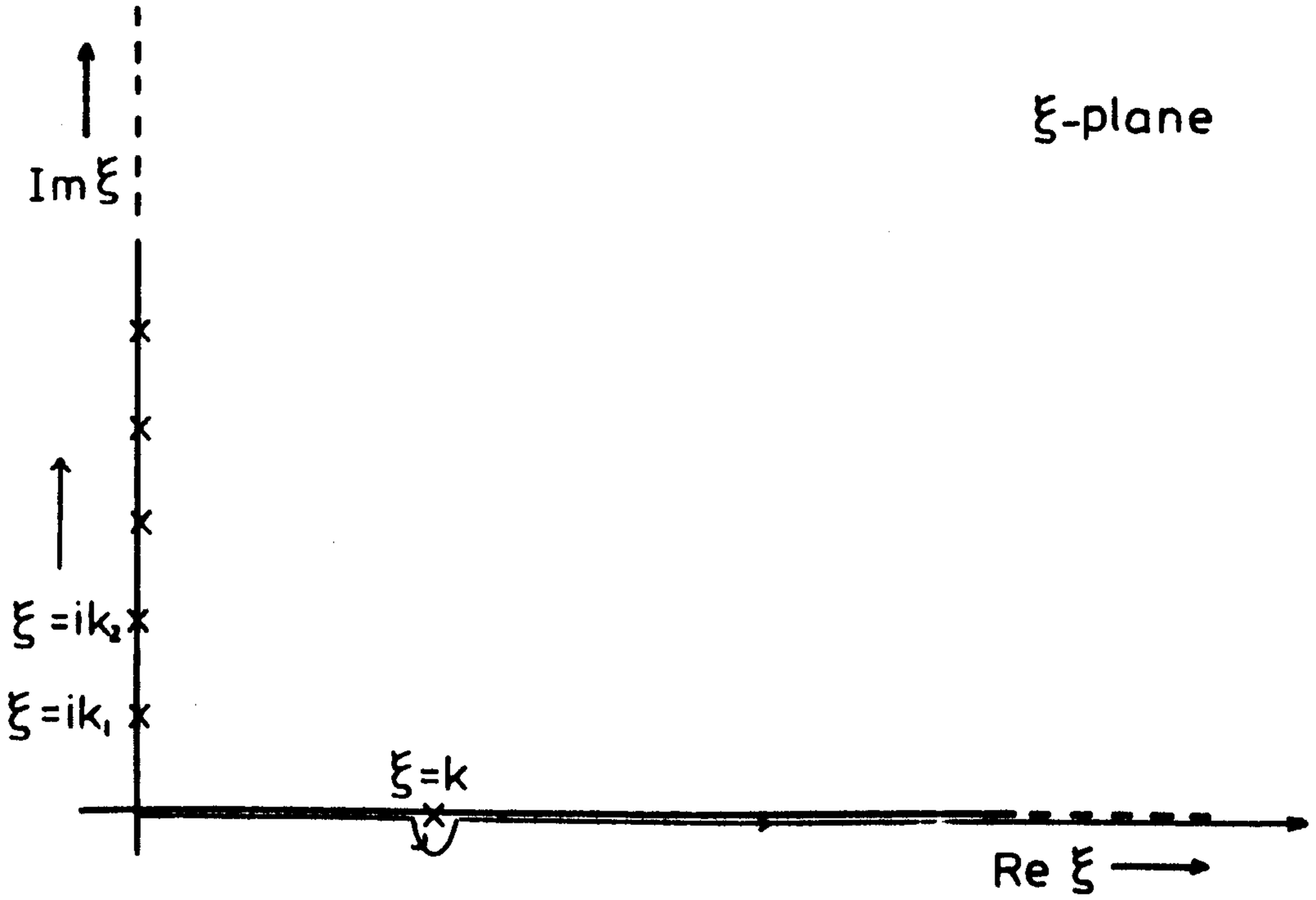

(1) Path of integration

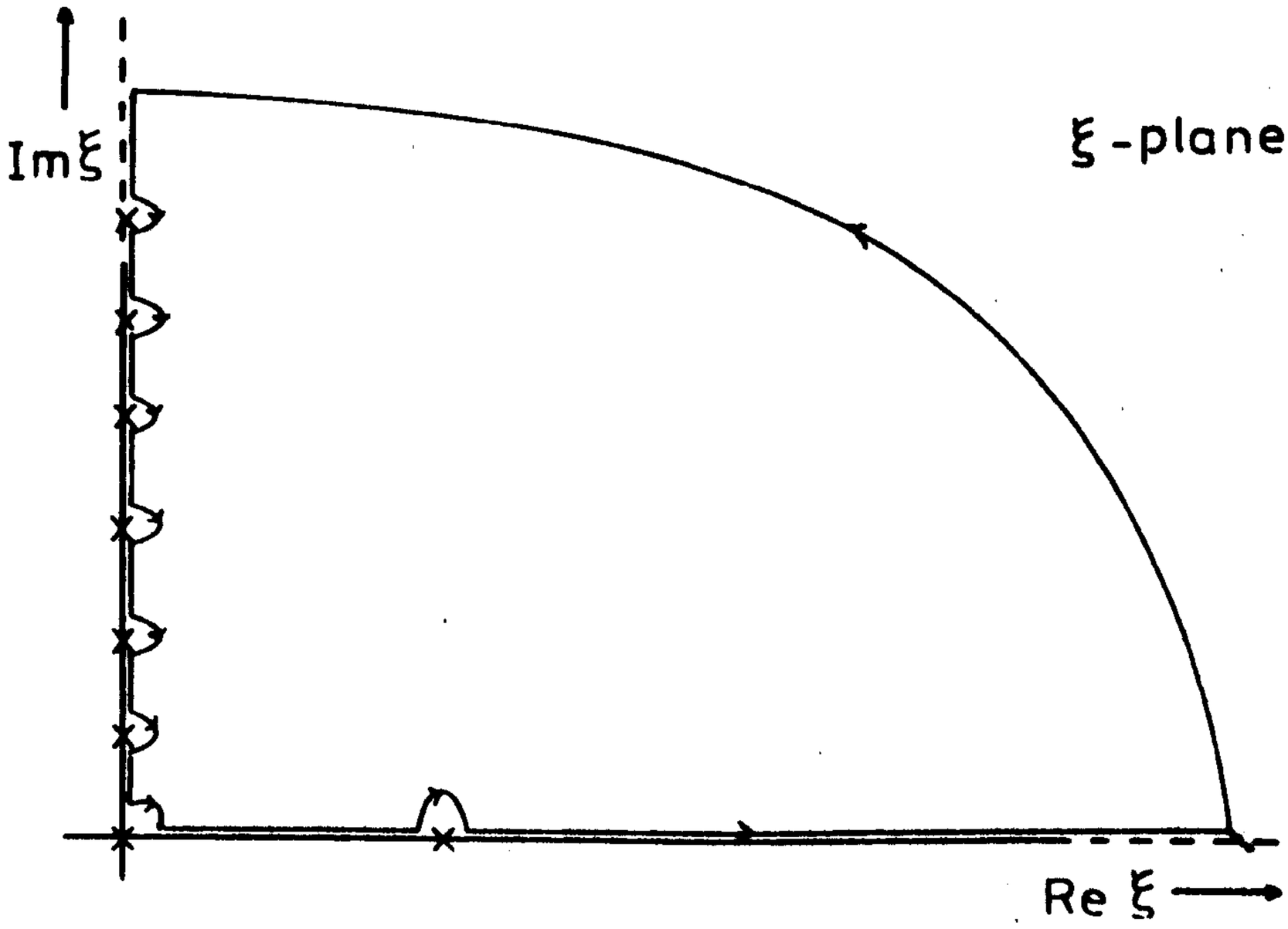

(2) Closed contour

FIG (4·2)

The residue may be easily calculated to give

$$B = \frac{\pi^2 a^2 \rho \omega N_0^{-1}}{k^2 d} J_1^2(ka), \qquad (4.6.12)$$

and

$$M = -2\pi\rho a^2 \int_0^\infty d\xi\, \xi^{-2} J_1^2(\xi a) \frac{(\xi \cosh \xi d - K \sinh \xi d)}{(K \cosh \xi d - \xi \sinh \xi d)}. \qquad (4.6.13)$$

The result (4.6.12) agrees with the expression for B given by (4.5.8), while (4.6.13) may be rewritten as

$$M = -2\pi\rho a^2 Re \oint_0^\infty \frac{d\xi}{\xi^2} J_1(\xi a) H_1^{(1)}(\xi a) \frac{(\xi \cosh \xi d - K \sinh \xi d)}{(K \cosh \xi d - \xi \sinh \xi d)}, \qquad (4.6.14)$$

where $\oint$ denotes the double principal value integral due to the singularity introduced at $\xi = 0$. By closing the path of integration with the contour shown in Figure (4.2) it can be seen that

$$M = -2\pi\rho a^2 Re \left[\pi i \operatorname{Res}_{\xi=k} + \frac{\pi i}{2} \operatorname{Res}_{\xi=0} + \pi i \sum_{n=1}^{\infty} \operatorname{Res}_{\xi=ik_n} \right] \times$$

$$\times \left\{ J_1(\xi a) H_1^{(1)}(\xi a) \frac{(\xi \cosh \xi d - K \sinh \xi d)}{\xi^2 (K \cosh \xi d - \xi \sinh \xi d)} \right\}, \qquad (4.6.15)$$

which, upon evaluation of the residues, becomes

$$M = -2\pi\rho a^2 Re \left[\pi i \left\{ \frac{-N_0^{-1}}{2k^2 d} J_1(ka) H_1^{(1)}(ka) \right\} + \frac{\pi i}{2} \left\{ \frac{-i}{\pi K} (1 - Kd) \right] \right.$$

$$\left. + \pi i \sum_{n=1}^{\infty} \left\{ \frac{N_n^{-1} J_1(ik_n a) H_1^{(1)}(ik_n a)}{2k_n^2 d} \right\} \right], \qquad (4.6.16)$$

i.e.

$$M = \pi a^2 \rho \left[(d - K^{-1}) - \frac{N_0^{-1} \pi}{k^2 d} J_1(ka) Y_1(ka) - \frac{2}{d} \sum_{n=1}^{\infty} \frac{N_n^{-1}}{k_n^2} I_1(k_n a) K_1(k_n a) \right], \qquad (4.6.17)$$

agreeing with the expression for the added-mass coefficient given by (4.5.7).

4.7 Results and Discussion

The results for the disc case will first be given, followed by the duct results.

(a) The disc on the sea-bed

In each case the results for the disc are plotted for values of $^a/d$ = 0.1,0.25, 0.5. Figure (4.3) indicates that, as $^a/d$ decreases, so the added-mass variation decreases over the range of υ and, for $^a/d$=0.1, the added-mass is almost constant over the whole range. The damping curves shown in Figure (4.4) illustrate the decrease of the damping cefficient from its asymptotic value at υ = 0 until it reaches its first zero which will occur at a value of $\upsilon > 2$, when $J_1(ka)=0$.

The disc is now tuned to υ_o =1.0 as explained in § 4, and the results are shown in Figure (4.5). For the disc to be a 'good' absorber the inequality $C_w/2a > 1$ should hold over some appreciable range of values of υ . Physically this means that the disc is capturing all the energy in a wave of crest length greater than the disc diameter. Now $C_{w_{max}}/2a = (2ka)^{-1}$ so it would seem that, at the tuned wavenumber, $kd < \frac{1}{2}$ (d/a) should be satisfied. However, as explained in Srokosz (1979), $C_w/2a$ does not attain its maximum value at υ_o , but at a value $\upsilon < \upsilon_o$. This can most easily be seen when a/d=0.5 in Figure (4.5), and occurs because, although $C_w/2a < (2ka)^{-1}$ for $\upsilon \neq \upsilon_o$, $C_w/2a$ is still able to rise above its value at υ_o and lie below the curve given by $C_{w_{max}}/2a = (2ka)^{-1}$.

While the curve for a/d = 0.25 in particular, seems promising, the amplitude ratio curves shown in Figure (4.6) indicate that the disc oscillations are too large to satisfy the assumption of small amplitude motion required by the linear theory. The magnitude of these oscillations can be reduced by tuning to smaller wavelengths (larger wavenumbers) or increasing the disc diameter. However, it does not seem possible to combine these to make the disc a 'good' absorber while ensuring the motion remains within the bounds of linear theory. So, as expected, the disc is not a 'good' absorber and, indeed, the

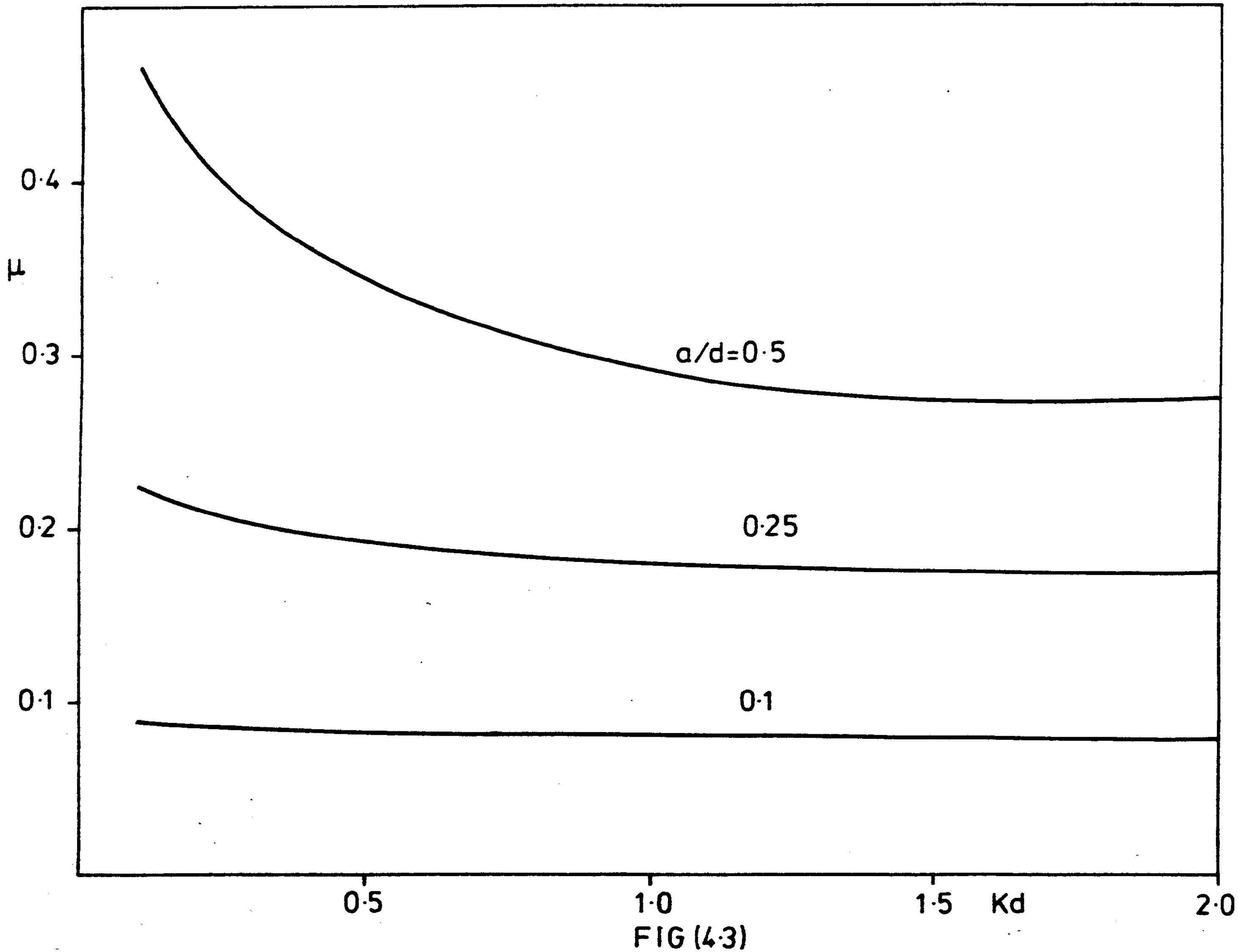

FIG (4·3)

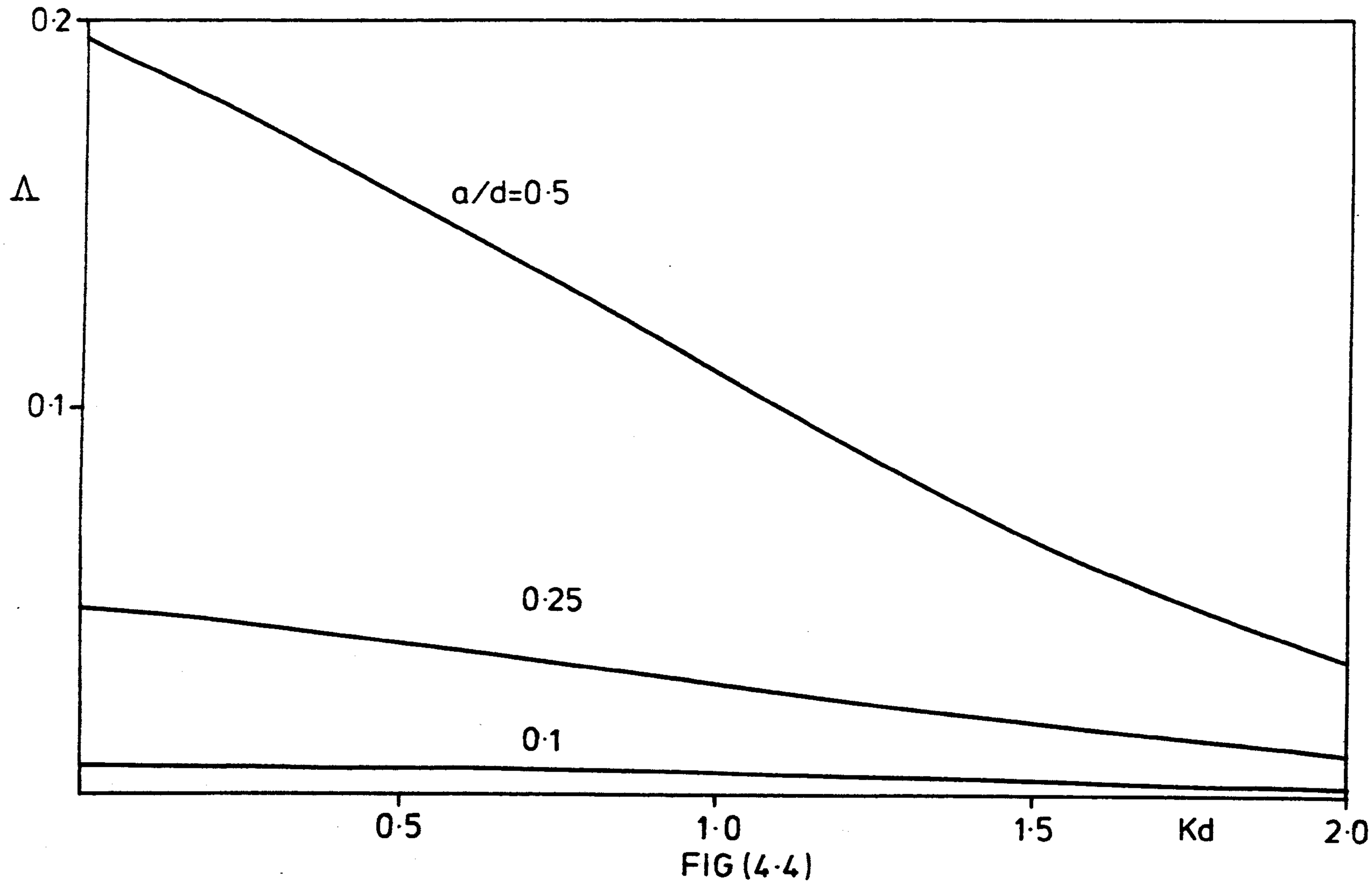

FIG (4·4)

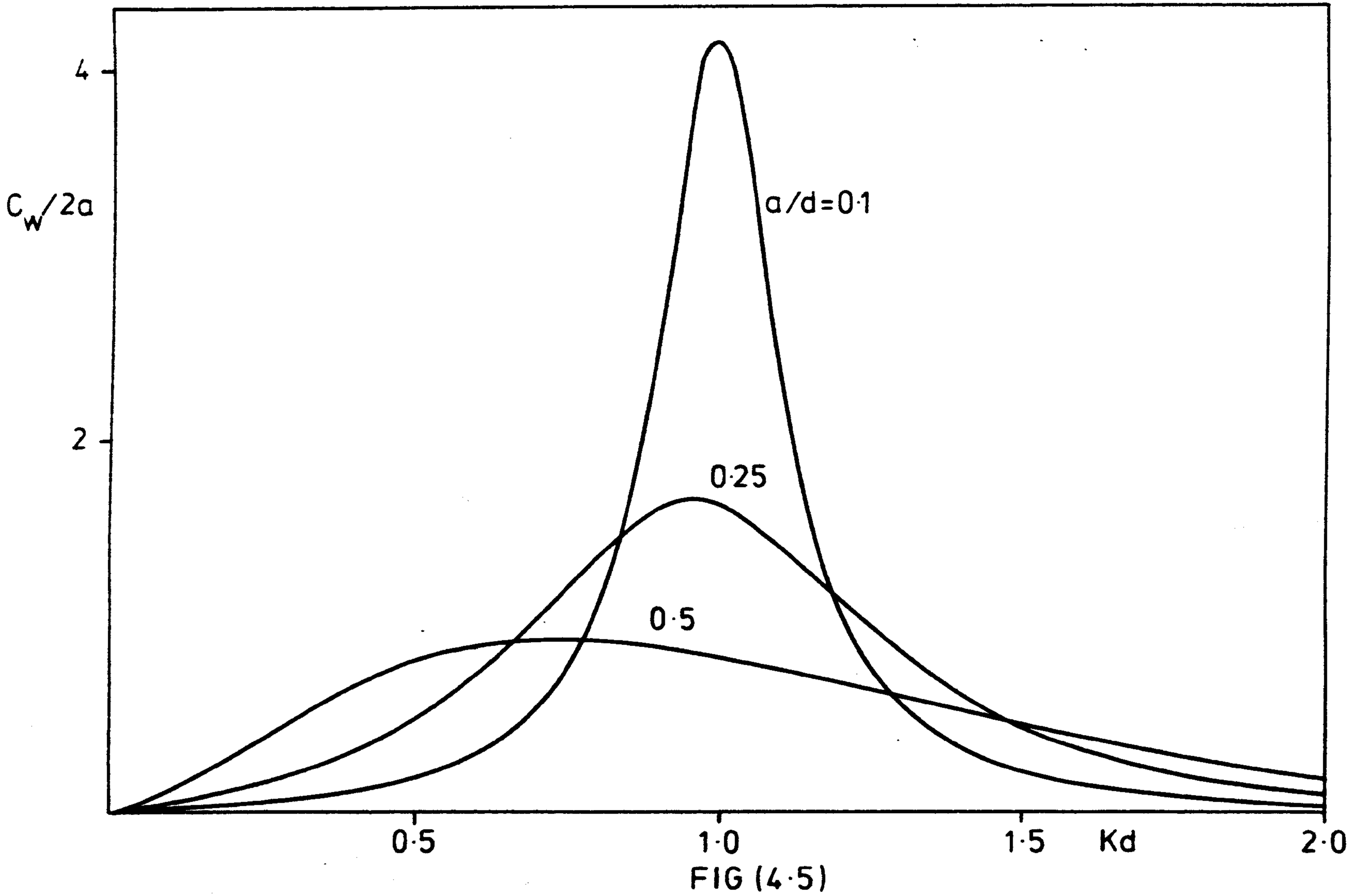

FIG (4·5)

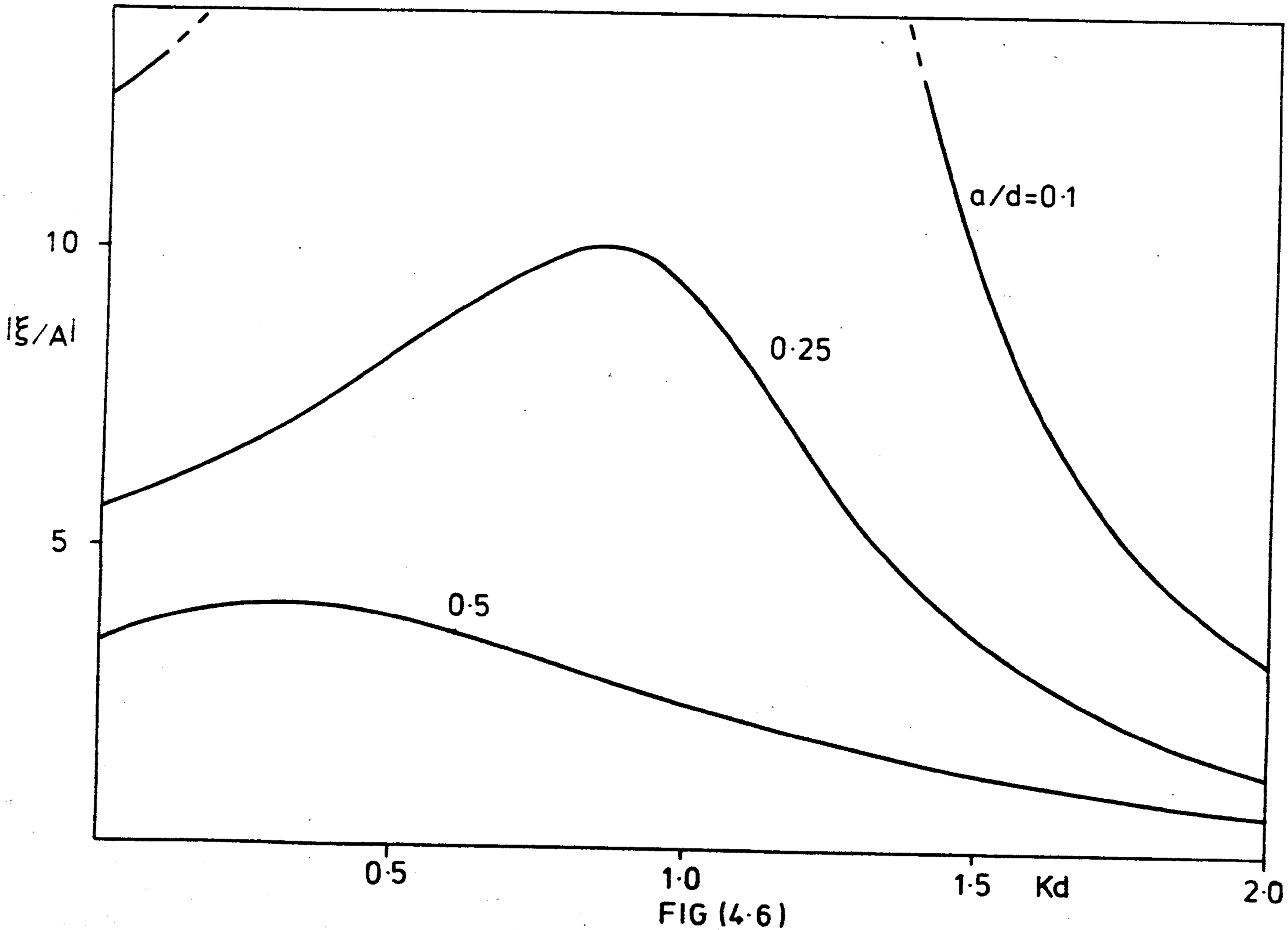

FIG (4·6)

main purpose of its study was to provide a check for the duct results and to provide analytic expressions for the added-mass and damping coefficients, which in many cases behave similarly to the corresponding coefficients for the duct.

(b) <u>The mouth-upward duct</u>

Figure (4.7) gives the added-mass curves (shown as dashed lines) for fixed a/d=0.1 when ℓ/d = 0.4,0.6,0.8. As for the disc with a/d = 0.1, the added-mass remains almost constant over the range of ν and, in each case, the values of the added-mass are slightly larger than the mass of water in the duct. This is because, as a/d becomes smaller, the piston is effectively having to move the column of water in the duct and hence the added-mass will approach the mass of water in the duct. (An end correction L may also be expected, as in the case of an open pipe in an infinite fluid with no free surfaces present, where L=0.6133a. However, this value of L does not apply here due to the presence of the free surface and the sea-bed; no simple formula apparently exists). The added-mass curves for fixed ℓ/d =0.5 are also shown in Figure (4.7). As for the disc, the larger variation in the added-mass occurs for larger a/d.

The damping curves given in Figure (4.8) show some difference from those for the disc case for larger values of ℓ/d, when the damping now rises to a maximum before decreasing to the first zero. (The zeros of the damping are found to occur at the same values that were obtained for the corresponding disc case; the reason for this can more easily be seen in the following chapter when the mouth-downward duct is discussed).

The damping curves for fixed ℓ/d =0.5 are shown in Figure (4.9). The damping coefficient in each case, although seeming to approach the same value as for the disc of the same a/d as $\nu \to 0$, does not fall

---------- a/d=0·1; ———————— l/d=0·5.

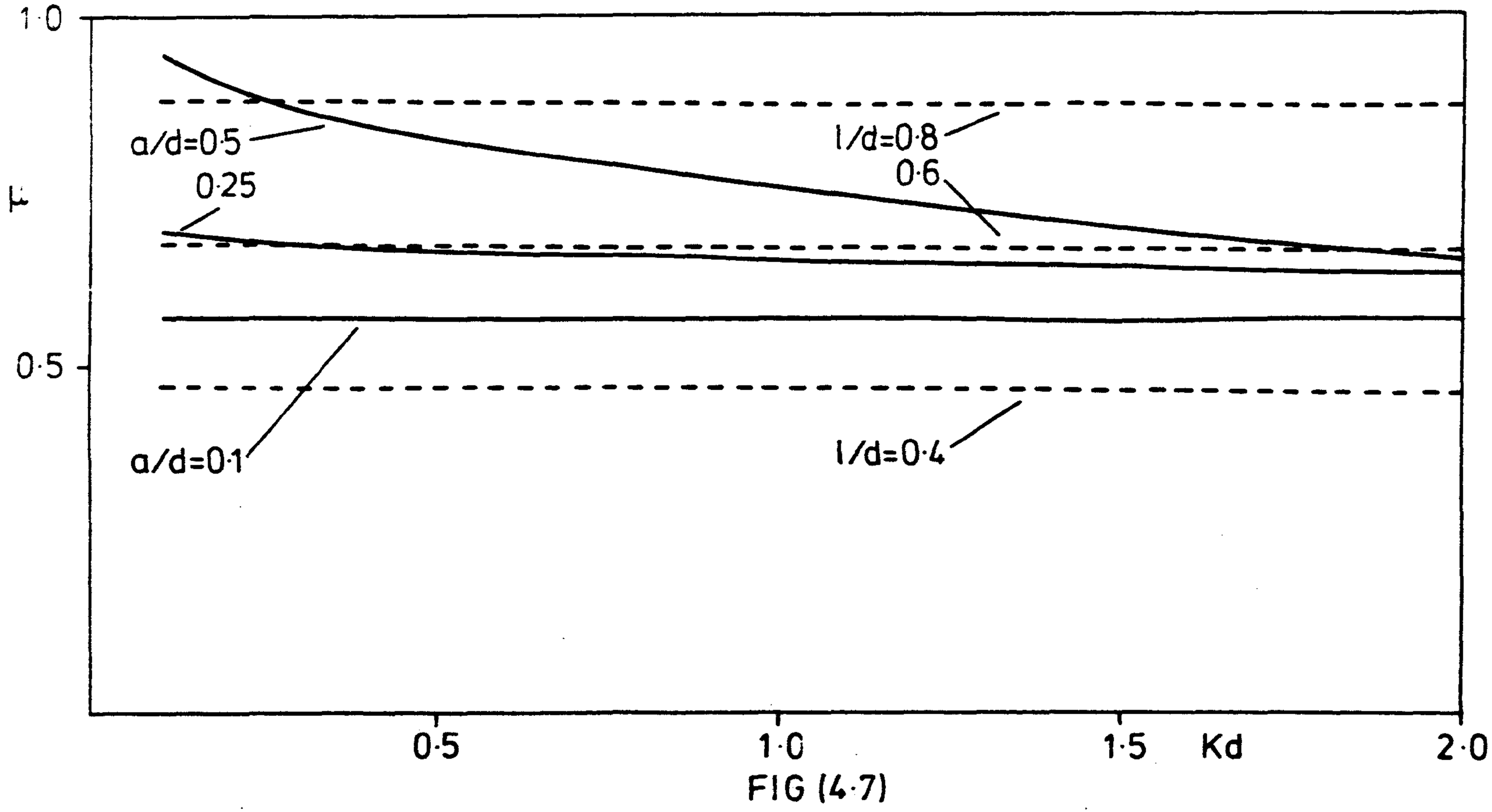

FIG (4·7)

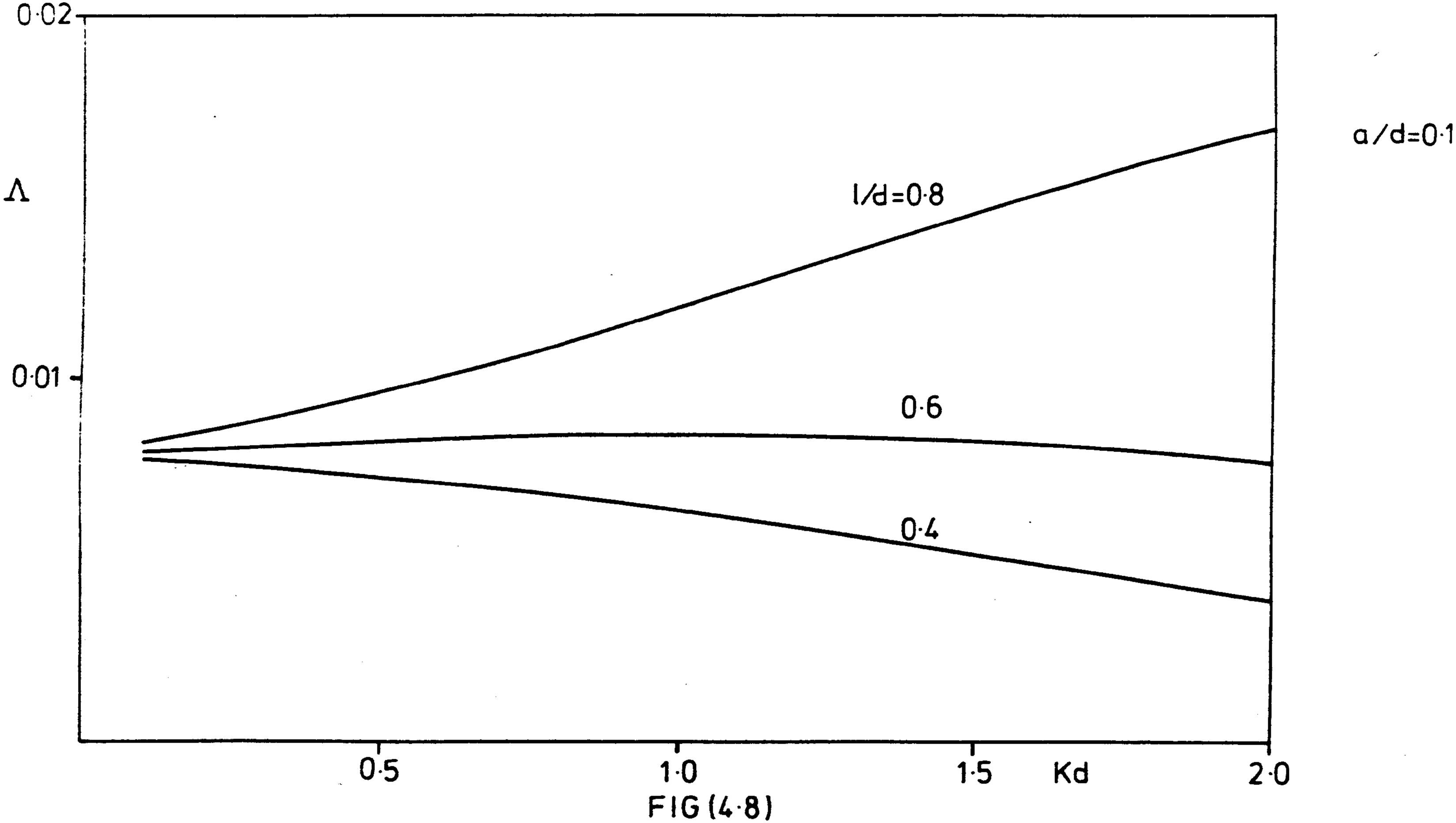

FIG (4·8)

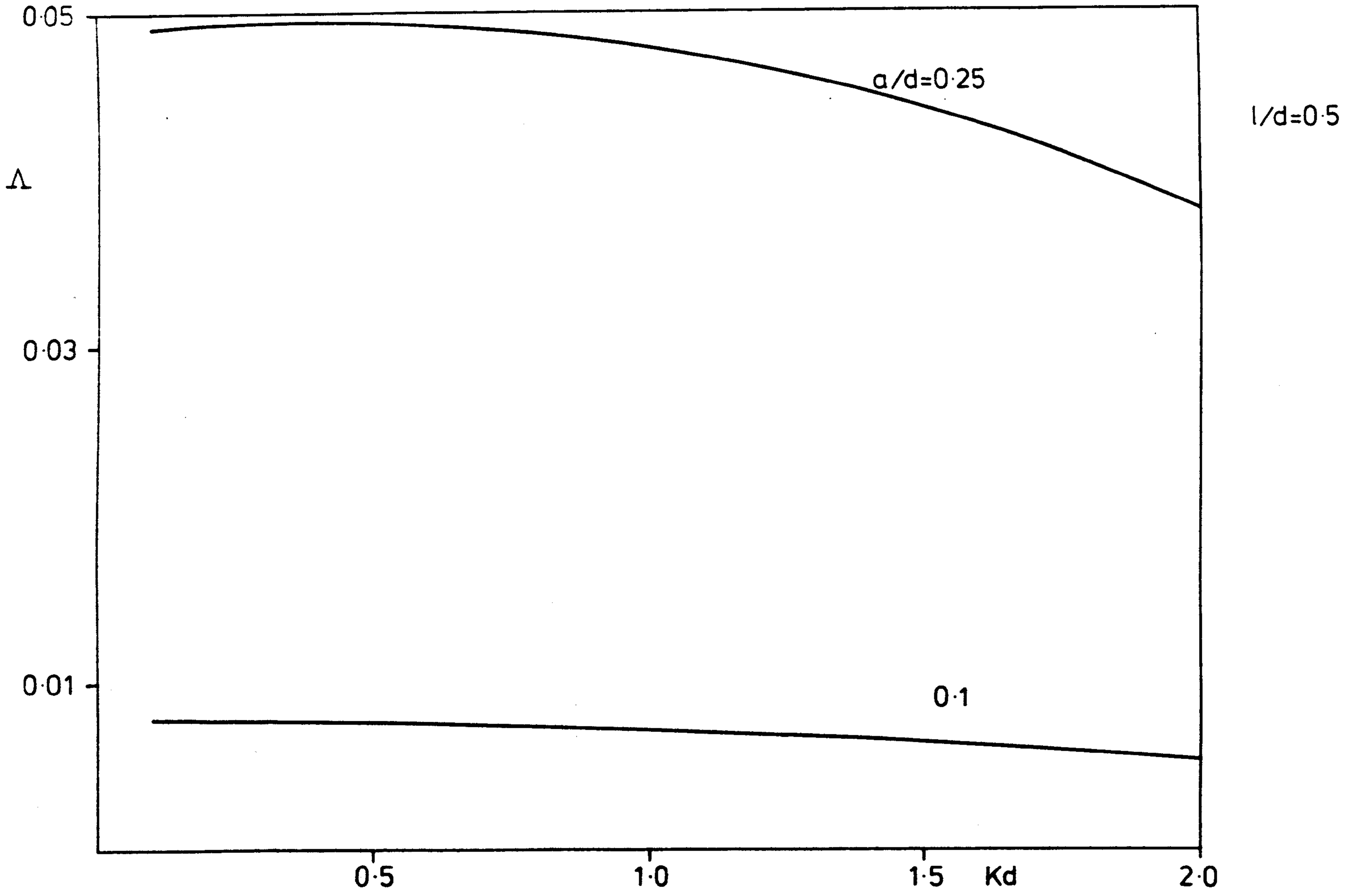

FIG (4·9)

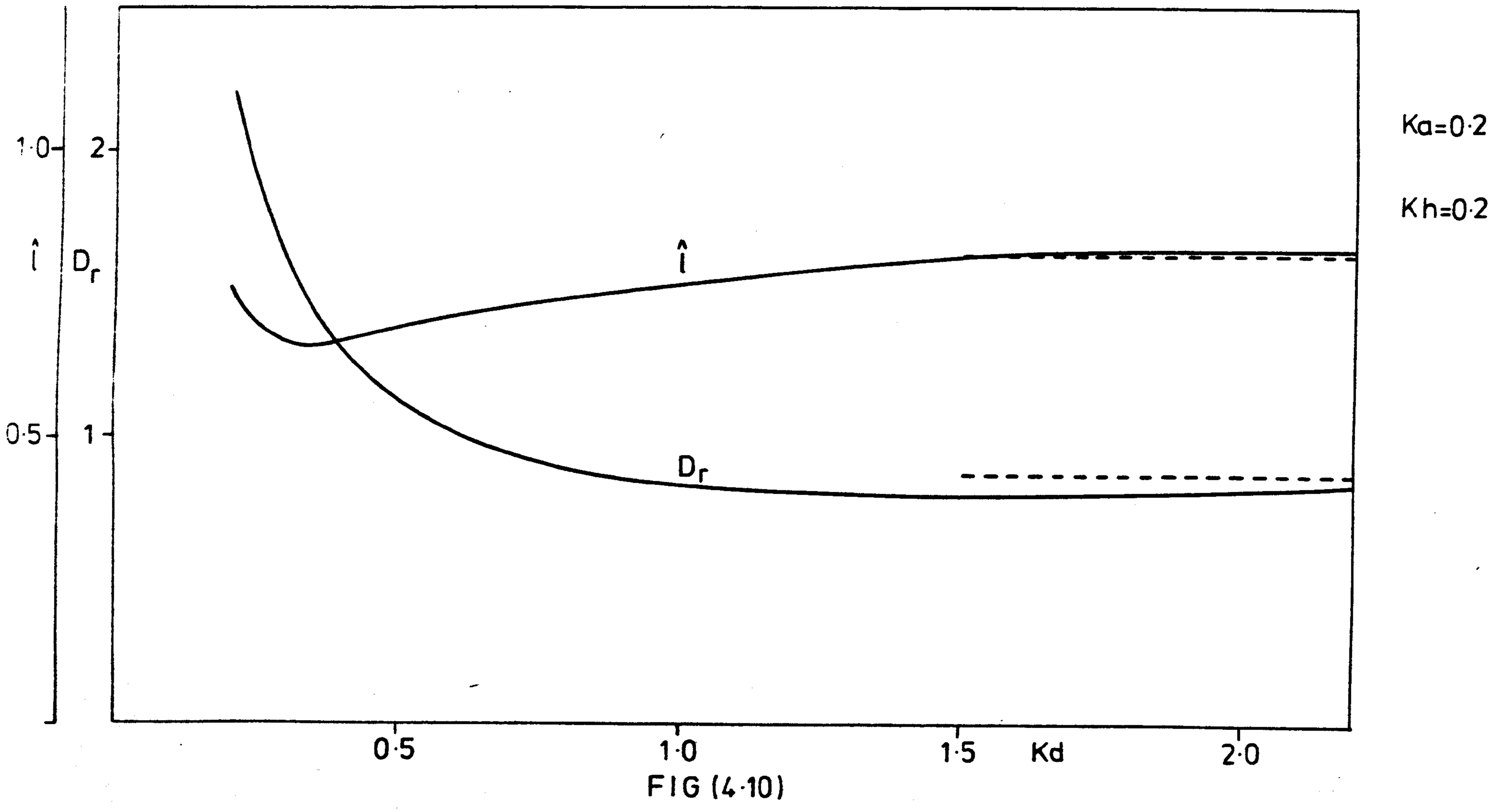

FIG (4·10)

off as rapidly as that of the disc as υ increases.

Before examining the capture width and amplitude ratio variation with wavenumber, the behaviour of the coefficients is studied as the water depth increases. By fixing $\omega^2 a/g$, $\omega^2 h/g$ and plotting the added-mass and damping coefficients as functions of $\omega^2 d/g$ the infinite depth results of Simon (1981a) should be recovered as $\omega^2 d/g$ However, it is first necessary to relate the added-mass and damping coefficient defined here to the effective added-length term, $\hat{l}$ and the damping coefficient, D_r used by Simon. This can be done by examining the respective radiation problems. In the model used here, a piston displacement $\mathrm{Re}\{\xi e^{-i\omega t}\}$ radiates energy away at a rate $\frac{1}{2}\omega^2 B|\xi|^2$ while, in the radiation problem set up by Simon, a volume flow $\mathrm{Re}\{Qe^{i\omega t}\}$ in the duct radiates energy away at a rate $\frac{1}{4}\rho\omega K D_r |Q|^2$ (Simon, 1981a). If D_r, $\hat{l}$ are defined in finite depth such that they correspond to D_r, $\hat{l}$ defined in infinite depth by Simon, then after some algebra it is found

$$\Lambda = \frac{\pi}{2}\left(\frac{a}{d}\right)\left(\frac{\omega^2 a}{g}\right)D_r \quad , \quad \mu = \left(\frac{a}{d}\right)\left(\frac{l}{a} + \hat{l}\right)$$

Figure (4.10) gives the variation of D_r and $\hat{l}$ with $\omega^2 d/g$, when $\omega^2 a/g = \omega^2 h/g = 0.2$. In all cases, the values seem to converge to the infinite depth values of Simon (1981a). The accuracy of the results decreases as $\omega^2 d/g$ increases and so, for $\omega^2 a/g = 0.2$, it is not possible to be confident about results for $\omega^2 d/g > 2.5$ say. Note that D_r approaches its infinite depth value from below although, for $\omega^2 d/g < 0.8$, D_r is greater than its infinite depth value.

Figure (4.11) shows the capture width variation for fixed $l/d = 0.8$, with tuning wavenumber $\upsilon_o = 1.0$. It can be seen that widening the duct diameter broadens the curve. The same criterion as for the disc applies in determining whether the device is a 'good' absorber, i.e. as a guide $kd < \frac{1}{2}(d/a)$ should be satisfied at the tuning wavenumber.

So, although the duct could be better tuned, in the case a/d = 0.1 say, Figure (4.12) indicates that the duct diameter should perhaps be too large in order that the assumptions of linear theory be satisfied.

If the capture width is studied at fixed a/d while ℓ/d is varied, the results are not quite so straightforward. As one might expect, Figure (4.13) shows that a wider bandwidth is achieved for ℓ/d = 0.9 rather than 0.6, when the duct mouth is closer to the surface. But when ℓ/d = 0.1 the bandwidth is wider than in the two previous cases, although the curve does decrease more rapidly than the curve corresponding to ℓ/d = 0.9, as ν increases. On the other hand, the amplitude ratios shown in Figure (4.14) indicate a progressive decrease in $|\xi/A|$ as ℓ/d increases, over practically the whole range, and certainly near the tuned wavenumber. To understand further what is happening, attention is focused on a fixed value of ν and the variation of capture width with ℓ/d is studied (Figure (4.15)).

Surprisingly, as ℓ/d increases from zero, the bandwidth of the capture width curve decreases before reaching a minimum and then increases as the duct mouth gets closer to the free-surface. From Figure (4.16) it can be seen that the amplitude ratio falls off rapidly at first, before levelling off to some extent, until the mouth becomes close to the free-surface when it begins to fall again. Apparently, the advantage of the duct is to decrease the amplitude ratio considerably but the duct, in some sense, shields the piston from the incident wavetrain, although this may be offset by having the duct mouth near the free-surface.

The effect of tuning to different wavenumbers may be seen in Figure (4.17). The maximum value of $C_w/2a$, given by the curve $C_{w_{max}} = (2ka)^{-1}$, is shown as a dotted line. Figure (4.18) shows how the piston oscillations are reduced as ν_o increases.

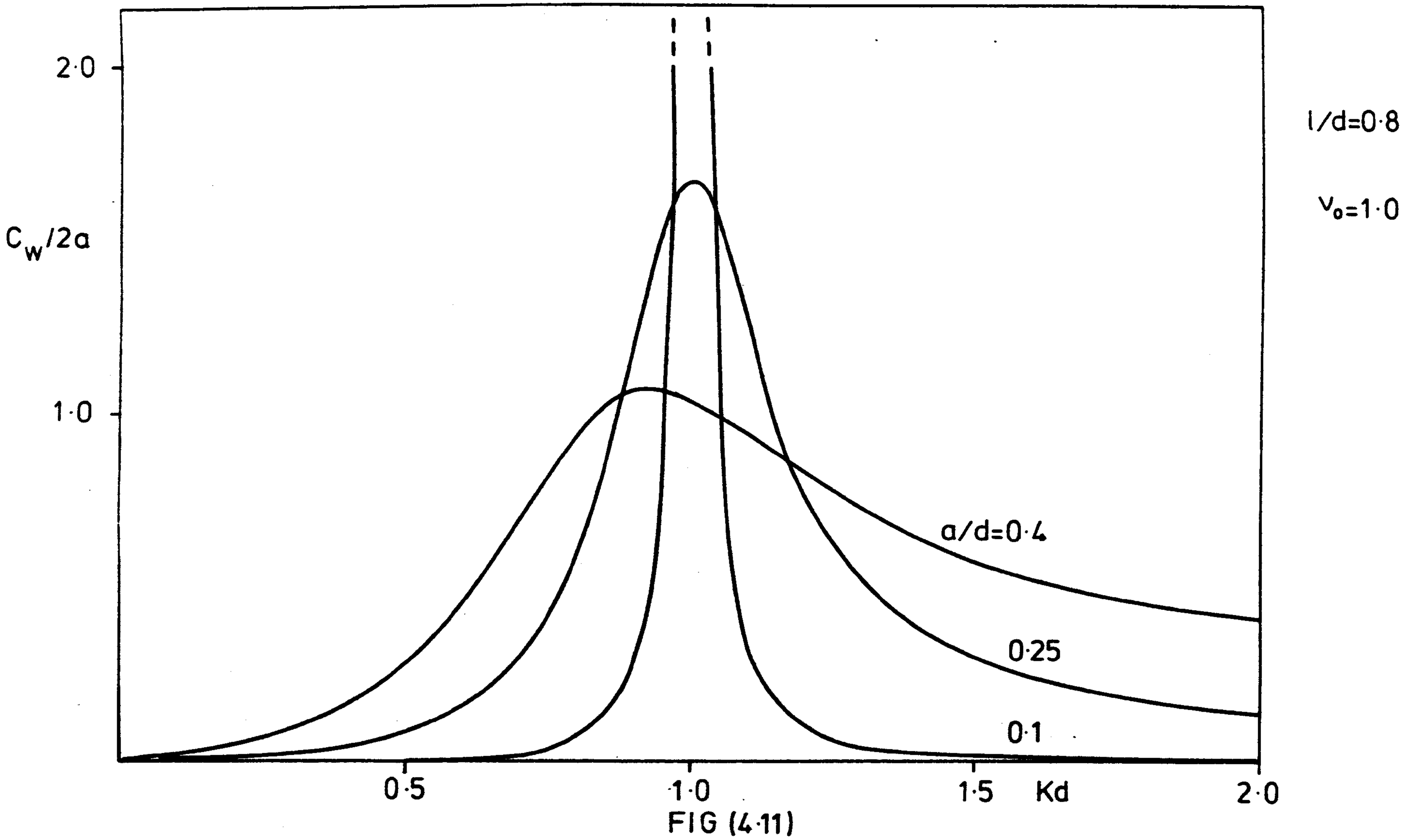

FIG (4·11)

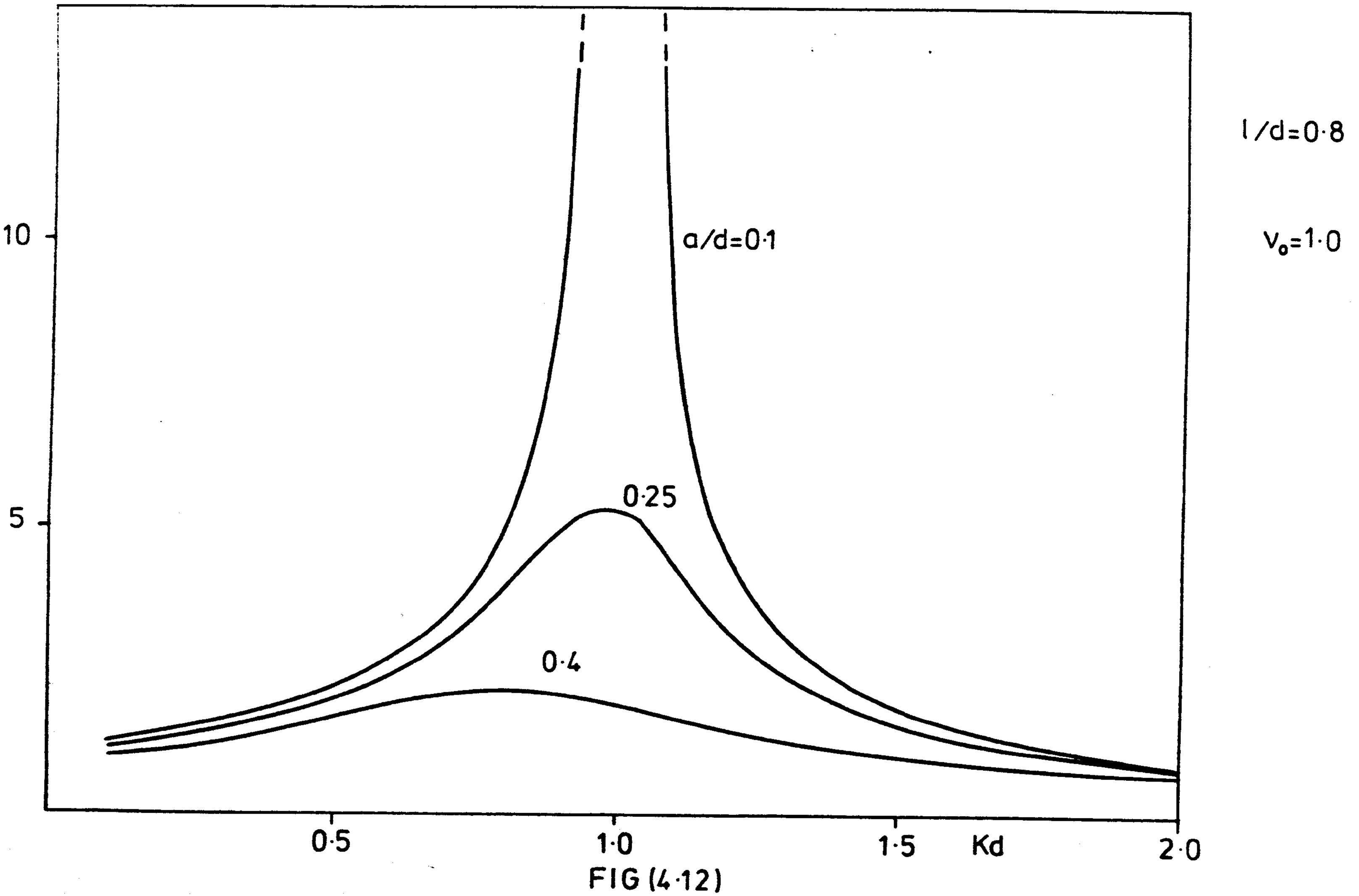

FIG (4·12)

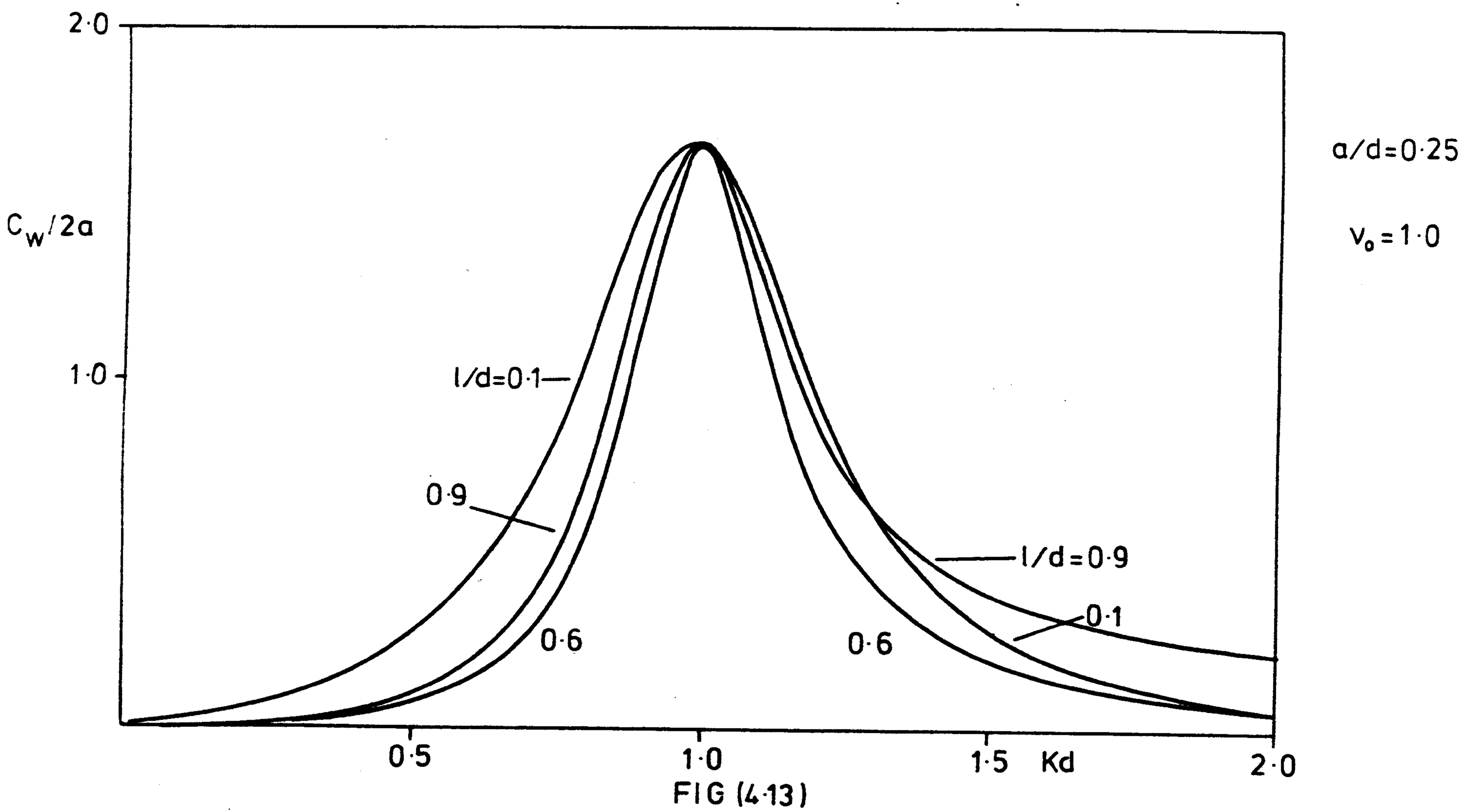

FIG (4·13)

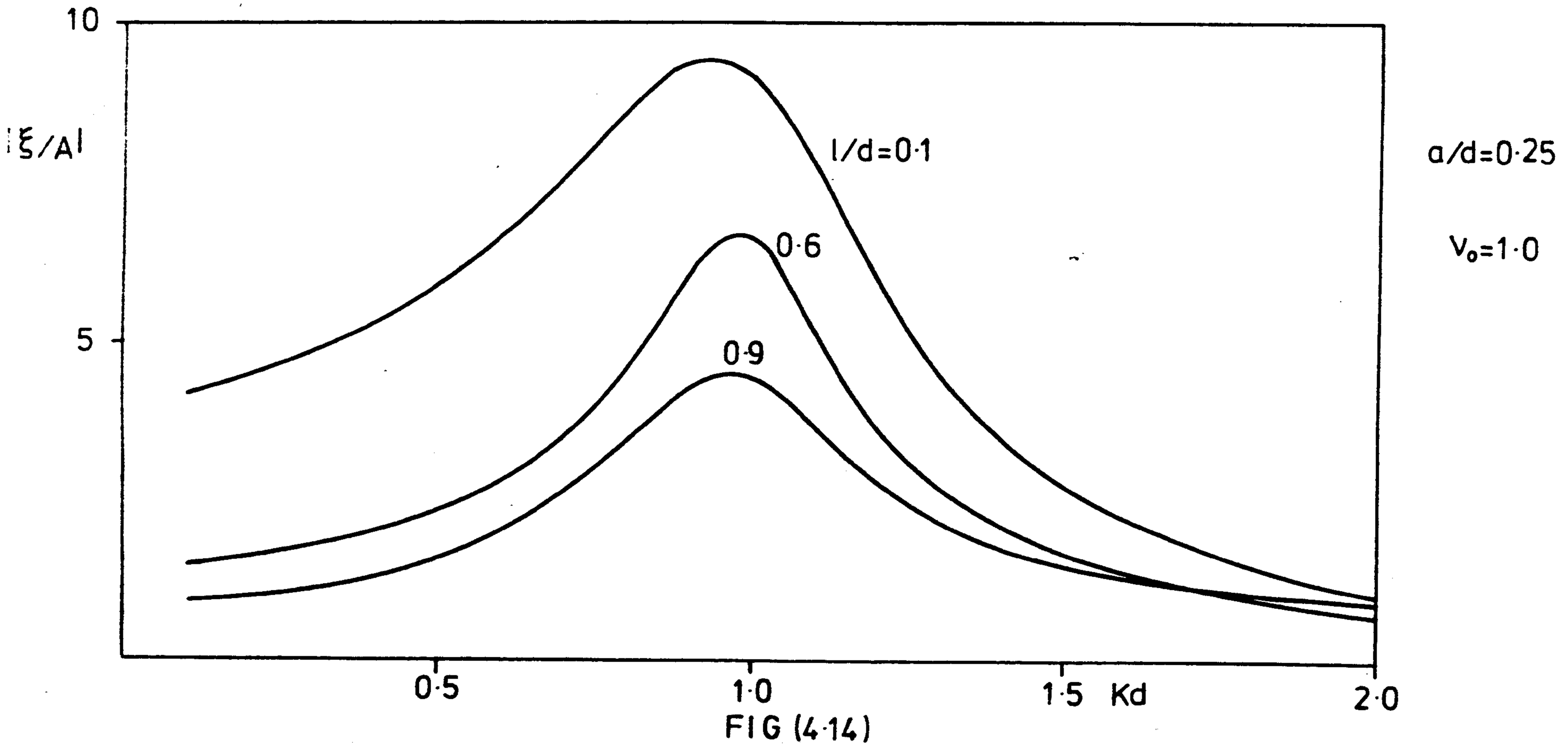

FIG (4·14)

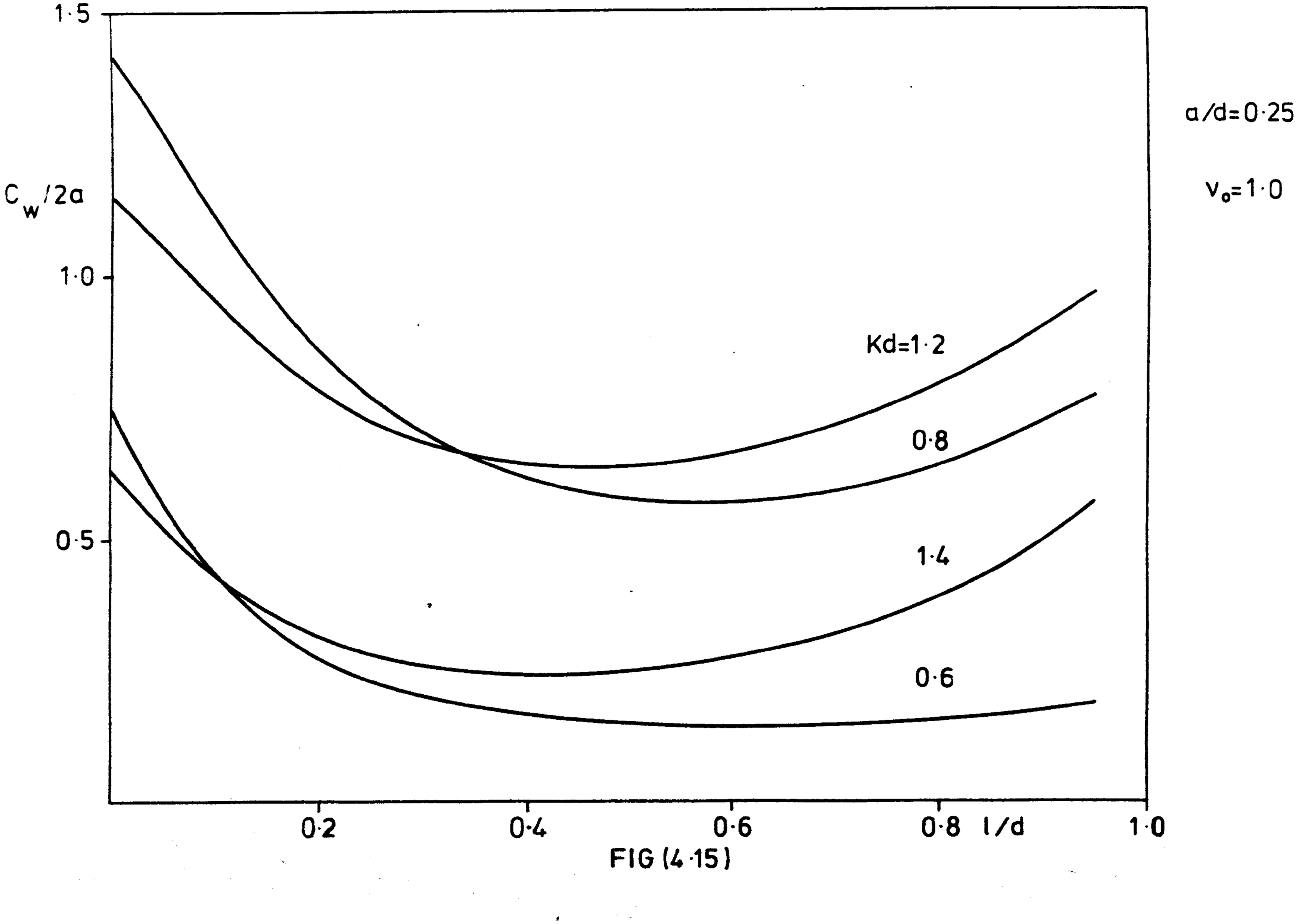

FIG (4·15)

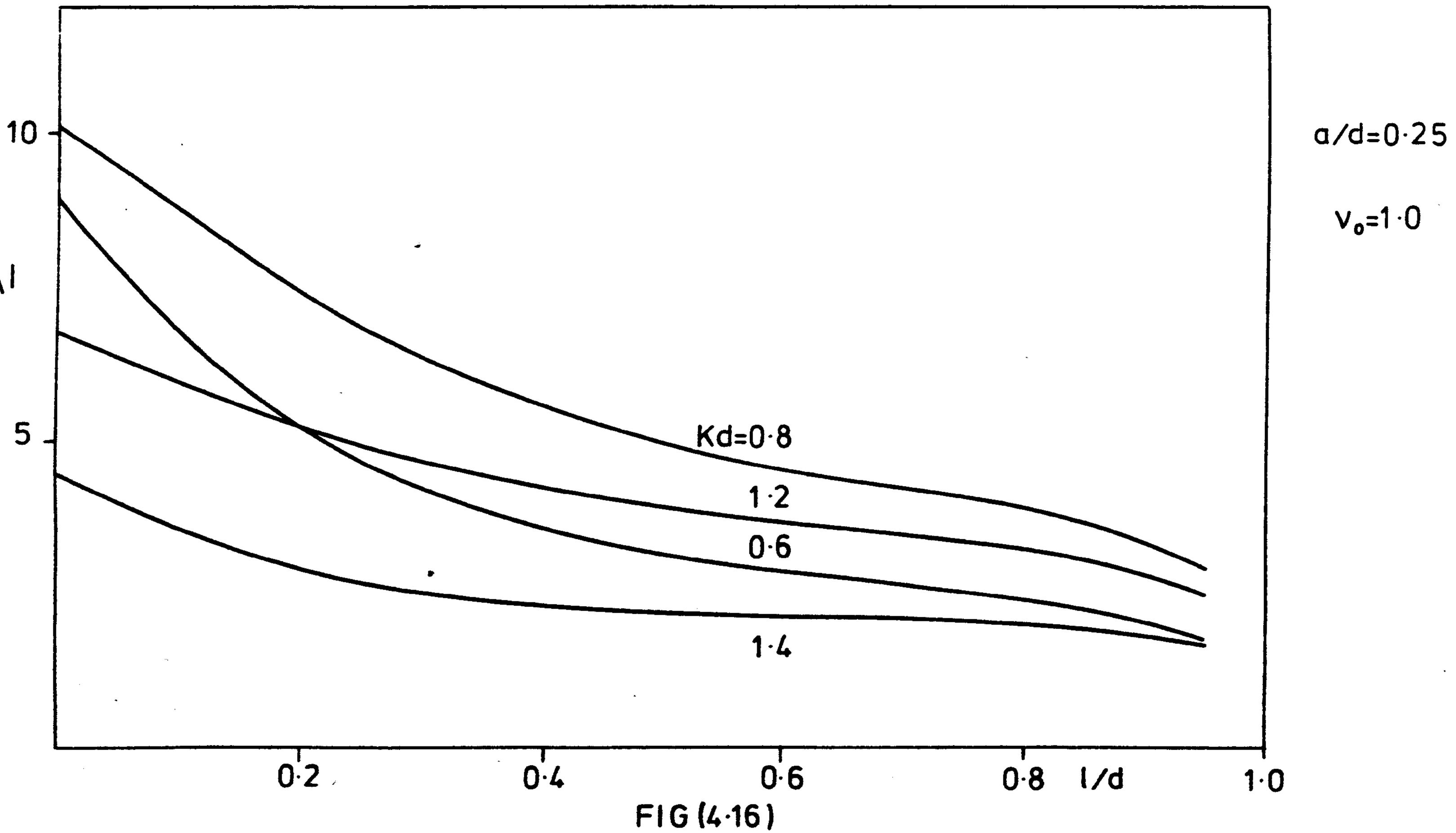

FIG (4·16)

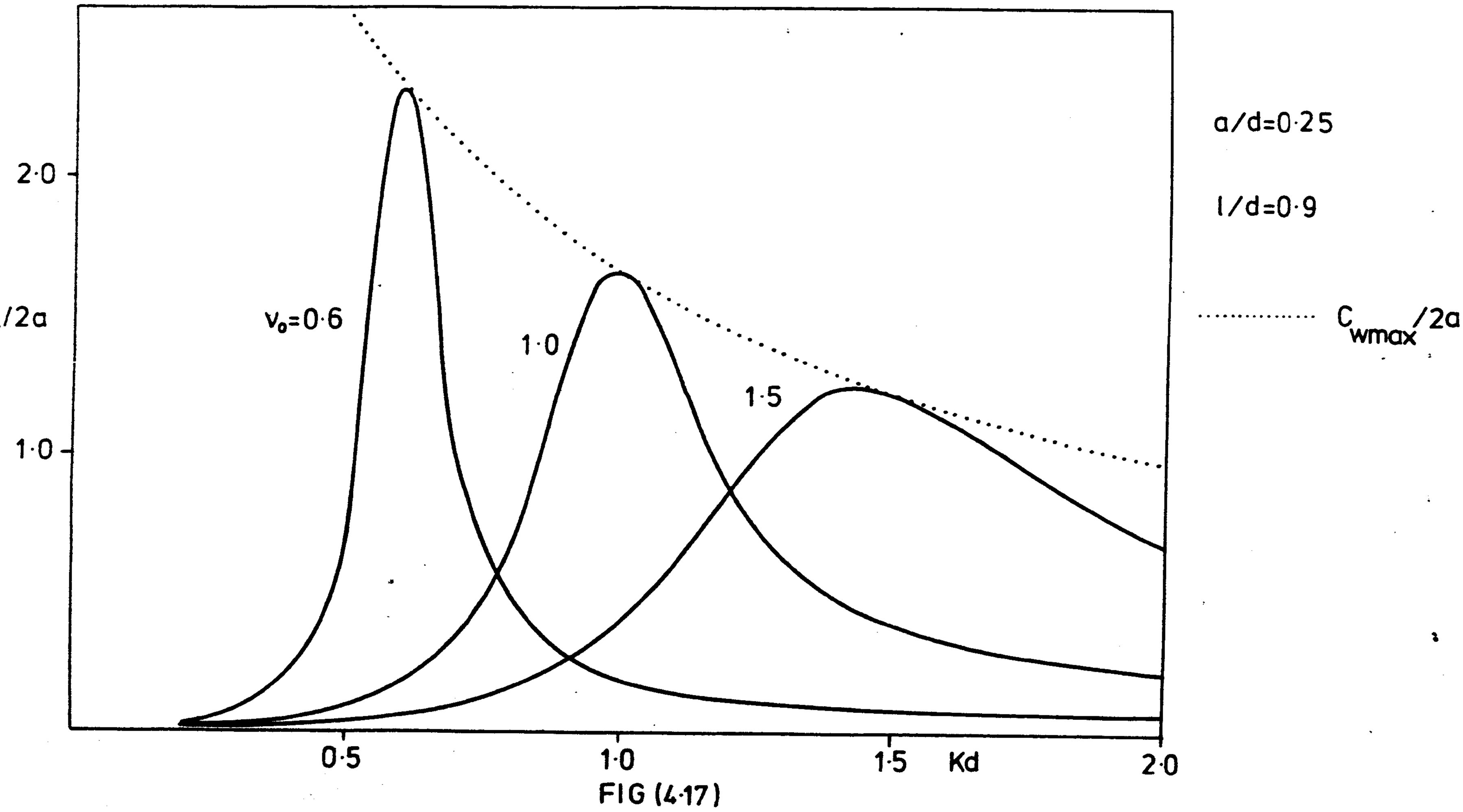

FIG (4·17)

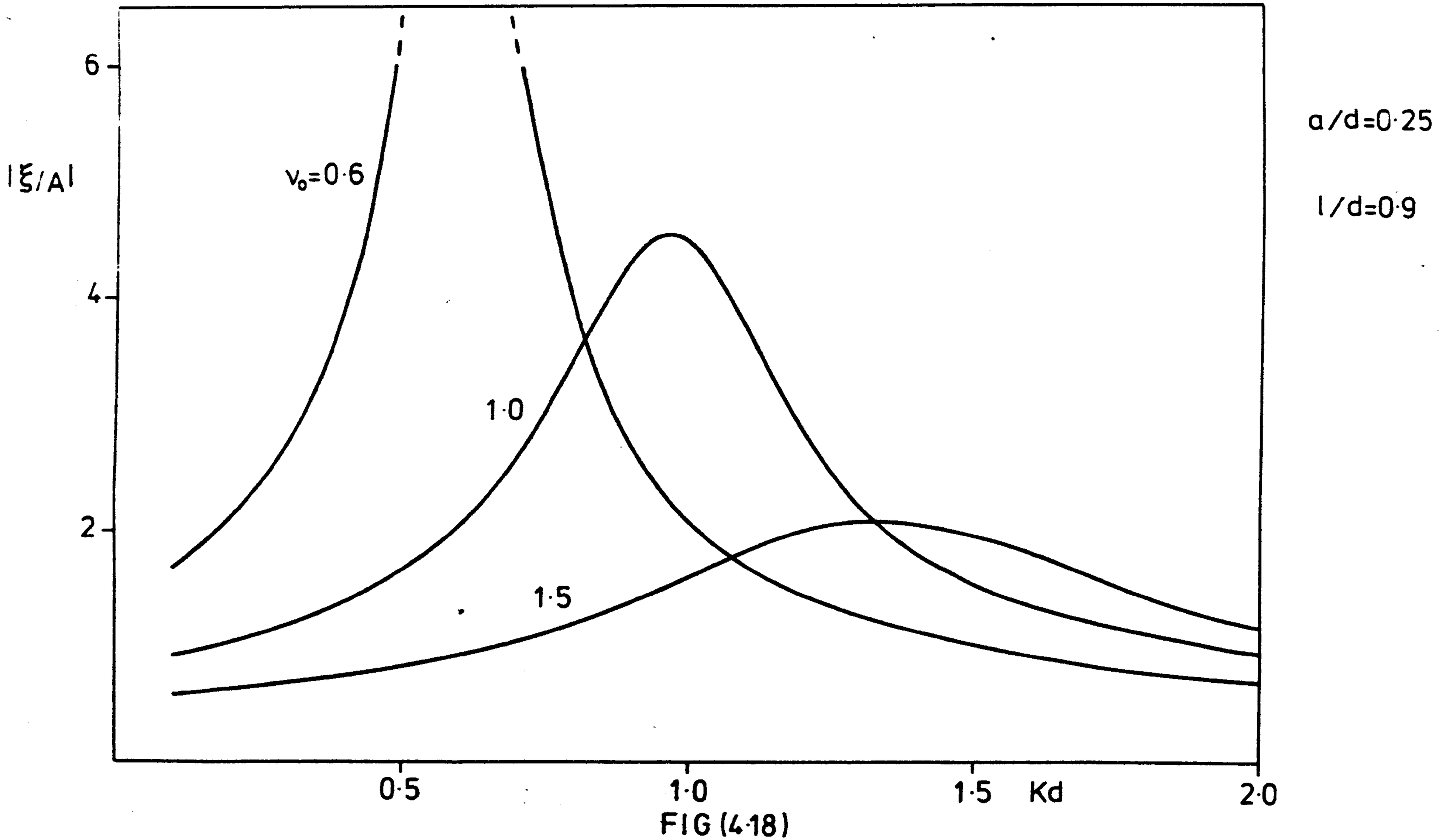

FIG (4·18)

When $\upsilon_o = 0.6$ the capture width bandwidth is very narrow and the amplitude ratio rises markedly above the values where linear theory is applicable; for linear theory to apply, it is required that $|\xi/A| = O(1)$. But, when $\upsilon_o = 1.5$, the amplitude ratio is greatly reduced, as noted in § 7(a), linear theory is valid, and the capture width curve exhibits a broad bandwidth.

(c) A note on numerical methods

The solution of two infinite systems of real equations is required. This is obtained by truncating the system after N terms and solving the finite system using a standard numerical procedure. Both systems have the same left-hand sides so the matrix of coefficients of r_n, s_n need only be inverted once numerically. Then, regarding the solutions obtained as functions of N, the limit as $N \longrightarrow \infty$ is required. By plotting the results against N^{-1} and extrapolating to zero, the convergence of the solutions may be studied.

The convergence is slow and, as Garrett (1970) noted, is almost linearly dependent on N^{-1} for large N. The equations were solved for N = 10, in steps of 10, up to N = 80 terms. Although Garrett found his results to be inaccurate by 15% for N = 40, the solution for N = 40 was accurate to within 1% and a linear extrapolation using N = 40,50 compared well with a smooth extrapolation through all values of N. Using this linear extrapolation, agreement was found to three or four significant figures in general. For smaller values of a/d, and larger values of υ , N needs to be larger to maintain accuracy.

4.8 Conclusion

In this chapter a simplified model of a mouth-upward oscillating water column wave-energy absorber has been used to study the behaviour of the added-mass and damping coefficients and, hence, the capture width.

Expressions for the capture width and amplitude ratio corresponding to those of Evans (1976) were derived for finite depth, and these hold for any axisymmetric heaving body. The limiting case of an oscillating disc on the sea-bed was also analysed, and while this is perhaps not a practical device, it provided some insight into the behaviour of the added-mass and damping coefficients as well as being a useful check on the numerical methods used in the duct problem.

The results indicate that, unless a/d is large, the added-mass shows relatively little change over the range of ν , while the damping coefficient still retains the zeros found in the disc problem, although the presence of the duct can greatly modify the curves. The added-mass and damping coefficient behaviour with increasing depth is presented, showing how these coefficients approach the infinite depth values of Simon (1981a).

The variation of capture width with wavenumber has been illustrated for both fixed a/d and fixed ℓ/d. An unexpected result was that increasing the duct length can actually narrow the bandwidth of the capture width. For moderate values of ℓ/d and 2a/d the linear theory is not really applicable and,although the amplitude ratio may be reduced to some extent by choosing more appropriate tuning wave-numbers, for the device to be a 'good' absorber it is necessary for ℓ/d and 2a/d to be quite large, ℓ/d = 0.8, a/d = 0.4,say; Simon (1981a). noted that h/a needs to be less than 1 in order to achieve reasonable capture widths.

Thus, such a device situated on the sea-bed does not seem to have particularly good wave-energy absorbing characteristics and better results may be obtained by bringing the device closer to the free-surface. However, it must be pointed out that devices of this type will not be isolated but will appear in arrays where interaction effects can occur which may result in an increase in capture width.

An approximate study of such effects can be found in Simon (1981b).

The work in this chapter has been published in Thomas (1981). I should like to acknowledge a referee of that paper for suggesting the Hankel transform method of §6 (b) which has been more fully described in this chapter.

CHAPTER 5

SURFACE PRESSURE DISTRIBUTIONS AND THE THREE-DIMENSIONAL MOUTH-DOWNWARD DUCT

5.1 Introduction

This is the third and final chapter on oscillating water-column devices and it examines the mouth-downward duct. Such a device essentially consists of a hollow, partially immersed structure which encloses a volume of air above the free-surface. With the downward-facing mouth of the duct situated below the free surface, the water column so formed oscillates in response to the incident waves. This, in turn, forces the enclosed air above the free surface back and forth through a constricted opening in the structure in which an air-turbine is housed.

Systems which operate on this principle are the C.E.G.B. device which consists of a forward rectangular duct and a rigid rear portion, the Queen's University, Belfast buoy which is axisymmetric and also the Japanese Kaimei device which is a ship incorporating oscillating water-columns in its hull, (see Chapter 1). Such a system has also been successfully developed by Masuda in Japan to operate navigation buoys.

To analyse these systems Evans (1981b) has recently developed the theory of wave-power absorption by pressure distributions on the free surface. There is a close analogy with the corresponding theory for rigid oscillating bodies and many of the general results are the same. A brief outline of the theory for three-dimensional pressure distributions is given in §2; further details may be found in Evans (1981b). In §§3,4 the theory is applied to rectangular and circular pressure distributions to investigate their maximum capture widths. The surrounding structure determines only the shape and size of the pressure

distribution and plays no part in the hydrodynamics since the ducts are assumed to be of shallow draft.

The hydrodynamic performance of a vertical, mouth-downward duct of circular cross-section is studied in the second part of this Chapter. This system has previously been examined by Evans (1978) when the duct encloses a float and it is assumed that the duct is narrow. A spring-damper system attached to the float models the power extraction mechanism while the narrow duct assumption enables an approximate solution to be constructed in a similar manner to that for the horizontal duct in Chapter 2. Evans' work has been extended to a narrow duct in a channel by Srokosz (1979) which equivalently represents an infinite row of oscillating water-column devices. Studies of the C.E.G.B. device have been carried out by Count et al. (1981) but, as in all previous work, the internal free surface is replaced by a weightless piston or float so that a rigid body problem may be formulated.

The present analysis makes no assumptions about the draft of the duct or its width and uses Evans' pressure-distribution theory rather than introducing a piston, so that a more appropriate formulation is given. The problem is solved using the same method which was applied to the mouth-upward duct in Chapter 4.

Results for the maximum capture width are presented in §8. For this particular system it is possible to compare these results with approximate results derived in two limiting cases. The shallow draft approximation is given in §3 while a narrow duct approximation may easily be constructed following Evans (1978). The modified narrow duct model, incorporating the pressure distribution theory and finite depth of fluid, can be found in Appendix C.

(a) Pressure Distributions - Simple Examples

5.2 Formulation

Consider a duct intersecting the free surface, fixed in position with its mouth submerged and enclosing a volume of air above the free surface. This air volume is connected to the external atmosphere via a turbine which constitutes the power take-off mechanism of the system. The turbine characteristics are assumed to be linear, (that is, the pressure drop across the turbine is proportional to the volume flow rate through it) and hence the mean power absorbed by the system is the time average of this pressure drop and volume flux. Assuming the compressibility effects of the air to be neglibible, the pressure at the turbine is the same as the uniformly distributed pressure over the internal free surface, while the volume flux through the turbine is just the product of the spatial average of the vertical velocity of the internal free surface and its area.

The governing equations for pressure distributions are as given in Chapter 2, equations (2.2.1) - (2.2.7a) where the linearised free-surface condition (2.2.4) is now applied on the external free-surface while the internal free-surface condition is given by

$$K\Phi - \partial\Phi/\partial z = \frac{1}{\rho g}\frac{dP}{dt}\ , \text{on } S_{int}\ , \qquad (5.2.1)$$

where S_{int} is the internal free-surface and P(t) is the uniformly distributed pressure over S_{int}. This replaces the corresponding rigid body condition (2.2.7b). As the problem is linear, the pressure P may be written

$$P(t) = Re\{ p e^{-i\omega t} \}.$$

and (5.2.1) becomes

$$K\phi - \partial\phi/\partial z = -\frac{i\omega}{\rho g} p\ . \qquad (5.2.2)$$

As in the rigid body case, the potential ϕ may be decomposed into a scattering and a radiation potential

$$\Phi = \Phi_s - \frac{i\omega\rho}{\rho g}\Psi . \qquad (5.2.3)$$

The complex potential ϕ_s is the solution of the scattering problem in which P(t) = 0, i.e. the usual free-surface boundary condition is applied to S_{int}. The complex potential Ψ is the solution of the radiation problem when $P(t) = \rho g \cos\omega t$, i.e. a pressure of constant magnitude is applied to S_{int} in the absence of incoming waves. Thus the boundary condition (5.2.2) becomes

$$K\phi_s - \partial\phi_s/\partial z = 0 \ , \ K\Psi - \partial\Psi/\partial z = 1 \ , \ on \ S_{int}. \qquad (5.2.4)$$

The volume flow rate across S_{int}, denoted by $Q(t) = Re\{q e^{-i\omega t}\}$ is given by

$$q = q_s + q_r \ , \qquad (5.2.5)$$

where

$$q_s = \int_{S_{int}} \partial\phi_s/\partial z \, dS \ , \ q_r = -\frac{i\omega\rho}{\rho g}\int_{S_{int}} \partial\Psi/\partial z \, dS . \qquad (5.2.6)$$

Corresponding to the decomposition of the radiation force in the rigid body problem into added-mass and damping components, the volume flow rate $Q_r = Re\{q_r e^{-i\omega t}\}$ is decomposed into components in phase with the pressure and in phase with the rate of change of pressure

$$Q_r = -\underline{A}\dot{P} - \underline{B}P , \qquad (5.2.7)$$

where A and B are real, so that

$$q_r = -ZP \ , \ where \ Z = \underline{B} - i\omega\underline{A} . \qquad (5.2.8)$$

The mean power, W absorbed by the turbine is equal to the time average over a period of the pressure P(t) and the volume flow rate Q(t), thus

$$W = \tfrac{1}{2}\,\mathrm{Re}\,\bar{P} q_s - \tfrac{1}{2} B |P|^2, \qquad (5.2.9)$$

where the overbar denotes the complex conjugate.

This may be rewritten in the form

$$W = \tfrac{1}{8} B^{-1} |q_s|^2 - \tfrac{1}{2}\overline{(P - \tfrac{1}{2}B^{-1}q_s)}\,B\,(P - \tfrac{1}{2}B^{-1}q_s)\ , B \neq 0, \qquad (5.2.10)$$

yielding

$$W_{max} = \tfrac{1}{8} B^{-1} |q_s|^2, \qquad (5.2.11)$$

when

$$P = \tfrac{1}{2} B^{-1} q_s . \qquad (5.2.12)$$

In three-dimensions, Evans (1981b) has shown that

$$B = \frac{1}{8\lambda P_w} \int_0^{2\pi} q_s(\theta)\,\overline{q_s(\theta)}\,d\theta, \qquad (5.2.13)$$

where $q_s(\Theta)$ is the induced volume flux across S_{int} due to waves incident upon the duct travelling in a direction making an angle Θ with the positive x-axis, and P_w is the mean power per unit width of the incident waves given by (2.2.22). Thus the maximum capture width $C_{Wmax} = W_{max}/P_w$ is given by

$$C_{Wmax} = \lambda |q_s(\Theta)|^2 \Big/ \int_0^{2\pi} |q_s(\theta)|^2 d\theta . \qquad (5.2.14)$$

Note that for an axisymmetric device, where there is no angular dependence

$$C_{Wmax} = \lambda/2\pi, \qquad (5.2.15)$$

which is the result obtained for a single heaving, axisymmetric, rigid body (Evans, 1976). Further, for an axisymmetric device, if B = 0 at some frequency then, from (5.2.13), this implies $q_s = 0$ and hence, from (5.2.9), W = 0 i.e. $C_w = 0$ when B = 0.

To achieve the maximum capture width the turning condition (5.2.12) must be satisfied, that is, the pressure over S_{int} must be in phase with and some real multiple of, the induced volume flux of the scattering problem. This condition is somewhat artificial and in practice it will probably be easier to control the volume flow rate through the turbine rather than the pressure drop across it. Thus it is assumed that

$$q = \Gamma p, \tag{5.2.16}$$

where Γ is some constant. It may then be shown (Evans, 1981b) that (5.2.10) becomes

$$W = \frac{1}{8} B^{-1} |q_s|^2 \left\{ 1 - \frac{|\Gamma - \bar{Z}|^2}{|\Gamma + Z|^2} \right\}, \tag{5.2.17}$$

and hence the tuning condition is

$$\Gamma = \bar{Z}. \tag{5.2.18}$$

Unless the turbine characteristics enable a phase lag to exist between the volume flux and pressure drop, Γ will be real and positive, in which case

$$W = \frac{1}{8} B^{-1} |q_s|^2 \left\{ 1 - \frac{(\Gamma - B)^2 + \omega^2 A^2}{(\Gamma + B)^2 + \omega^2 A^2} \right\}. \tag{5.2.19}$$

This yields an optimal value

$$W_{max} = \frac{1}{8} B^{-1} |q_s|^2 \left\{ 1 - \frac{\Gamma_{opt} - B}{\Gamma_{opt} + B} \right\}, \tag{5.2.20}$$

where

$$\Gamma_{opt} = (B^2 + \omega^2 A^2)^{\frac{1}{2}}. \tag{5.2.21}$$

In the next two sections the expressions for C_{wmax} above are examined for different configurations under the simplification that the fixed immersed part of the system is of shallow draft, that is, the only effect of the structure is to determine the boundary of the internal free-surface. Alternatively the configurations may be

thought of as pressure 'patches'.

5.3 The Maximum Capture Width of a Rectangular Pressure Patch

The theoretical maximum capture width is given by (5.2.14) assuming the tuning condition (5.2.18) can be satisfied. The assumption of shallow draft enables the volume flux q_s to be easily determined by integrating the incident wave potential over S_{int}, as the disturbance to the incident wave may be neglected. This provides a method of deriving simple expressions for q_s which can, in turn, be used to examine the effect of size and shape of pressure distributions upon the maximum capture width.

As an example, consider a rectangular pressure patch such that the internal free surface is given by $S_{int}: |x| \le a, |y| \le b$. The incident wave potential is given by (2.2.8) and thus, from (5.2.6), q_s is given by

$$q_{vs} = g\frac{A}{\omega} k \tanh kd \int_{-a}^{a} dx \int_{-b}^{b} dy\, e^{ik(x\cos\Theta + y\sin\Theta)},$$

$$= 4\omega A k^{-2} f(\Theta), \qquad (5.3.1)$$

where

$$f(\Theta) = \sin(ka\cos\Theta)\sin(kb\sin\Theta)/\sin\Theta\cos\Theta, \qquad (5.3.2)$$

and use has been made of (2.2.9). Thus the maximum capture width is given by

$$C_{Wmax} = \lambda |f(\Theta)|^2 / \int_0^{2\pi} |f(\theta)|^2 d\theta. \qquad (5.3.3)$$

Note that

$$C_{Wmax}(\Theta_1)/C_{Wmax}(\Theta_2) = |f(\Theta_1)|^2/|f(\Theta_2)|^2, \qquad (5.3.4)$$

and in particular

$$C_{Wmax}(\pi/2)/C_{Wmax}(0) = a^2\sin^2 kb / b^2 \sin^2 ka, \qquad (5.3.5)$$

which reveals the relative effectiveness of the pressure patch in beam and head seas.

Figures (5.1), (5.2) show how the maximum capture width varies with Θ for different values of ka, for the case b/a = 2. The dashed lines indicate the corresponding result for an axisymmetric pressure distribution of radius b, (equation (5.2.15)).

As one might expect the variation in C_{Wmax} is greater for larger ka since the shape of the patch has more influence on the shorter waves. When ka is small the variation is almost sinusoidal in appearance and the increase in C_{Wmax} over the axisymmetric case is about 10% for $\Theta = 0$. Between $\Theta = \pi/4$ and $5\pi/4$ approximately, the regular distribution is less efficient than the axisymmetric distribution however. As ka increases the appearance of the curves change; the 'troughs' fill out while the 'crests' become sharper. The fluctuations in C_{Wmax} become much larger resulting in considerable increases in the maximum capture width for small Θ. This behaviour continues until ka $\simeq$ 1.6 when secondary maxima appear at $\Theta = \pi/2, 3\pi/2$. This is clearly shown for the case ka = 2 and is also present when ka = 1.6 although not visible on the graph due to the scale.

Notice that $2b/\lambda = (b/a)ka/\pi$, and so when $ka = \pi/2$ (for the case $b/a = 2$) the length of the patch is equal to the wavelength of the incident waves. Consequently a secondary resonance seems to occur which produces a local maximum of C_{Wmax}. In all cases it was found that, provided the wavelength was greater than the length of the patch, the curves were of the shape shown in Figure (5.1). Once the wavelength is shorter than the patch length the situation became more complicated. At first the behaviour is as in Figure (5.2) but as ka was increased further the peaks of the curves became sharper and further local maxima appeared. For large ka, the maximum capture

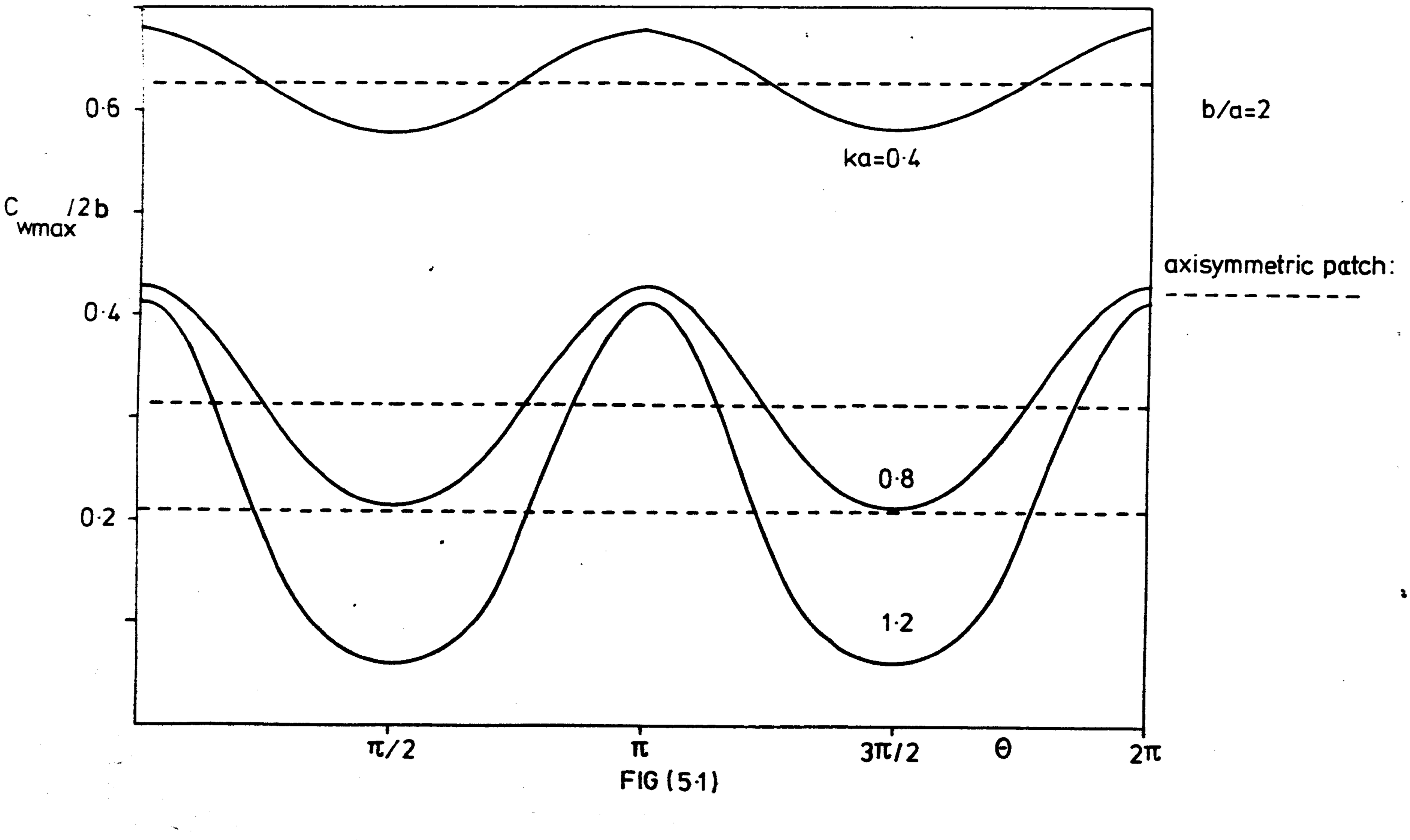
0·6
0·4
0·2
C wmax /2b
ka=0·4
b/a=2
axisymmetric patch:
0·8
1·2
π/2
π
3π/2
Θ
2π

FIG (5·1)

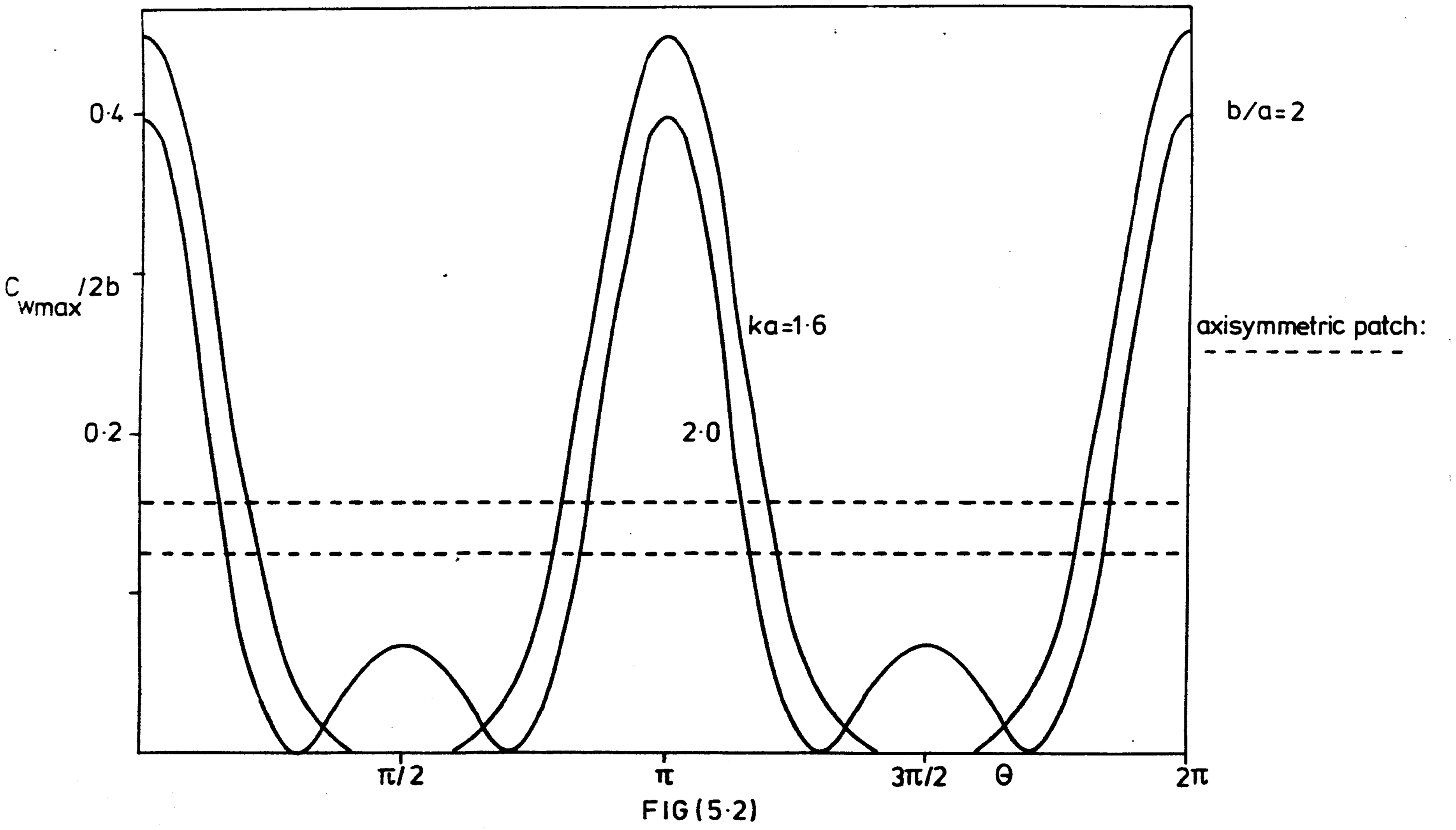

FIG (5·2)

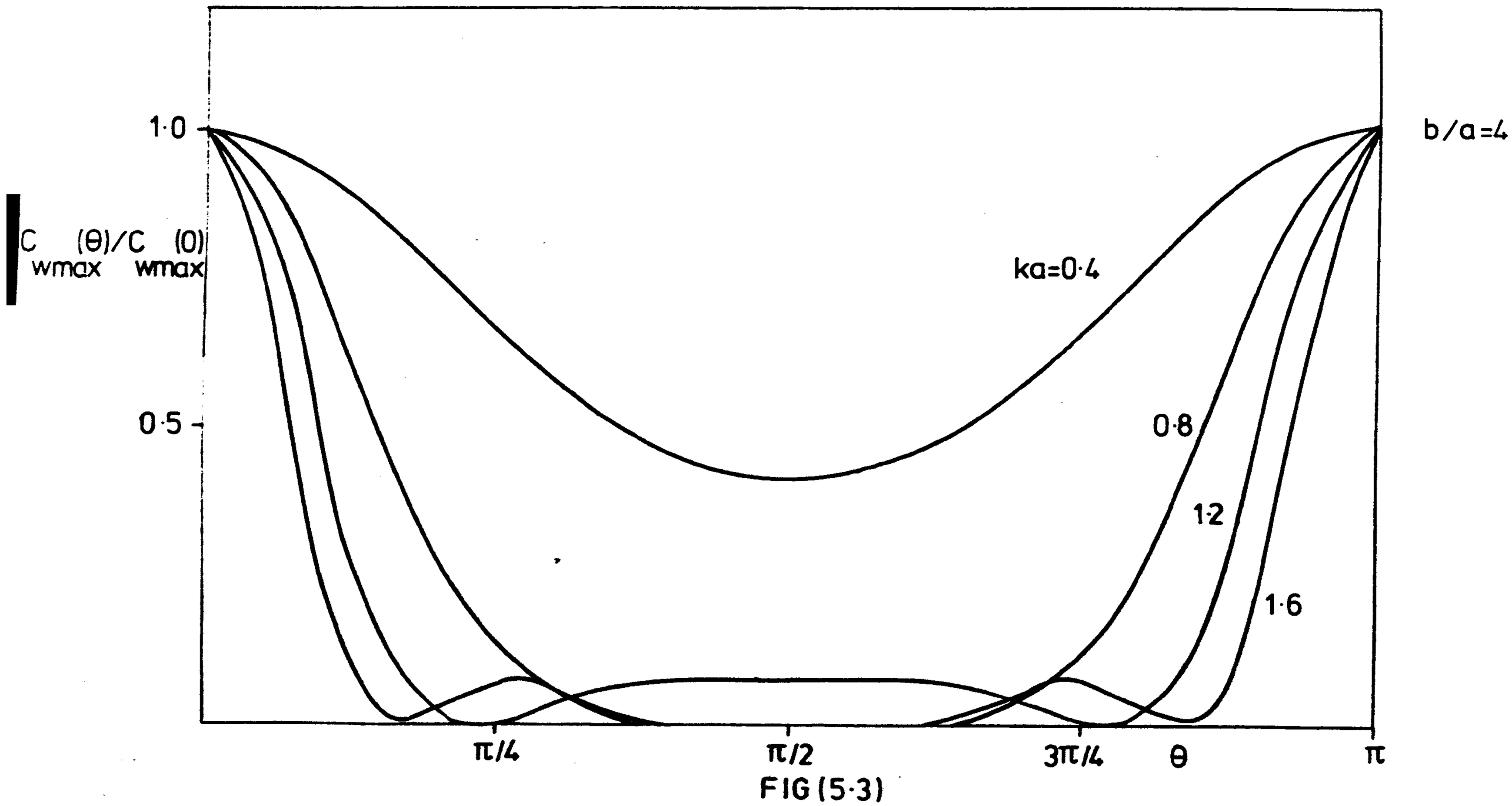

FIG (5·3)

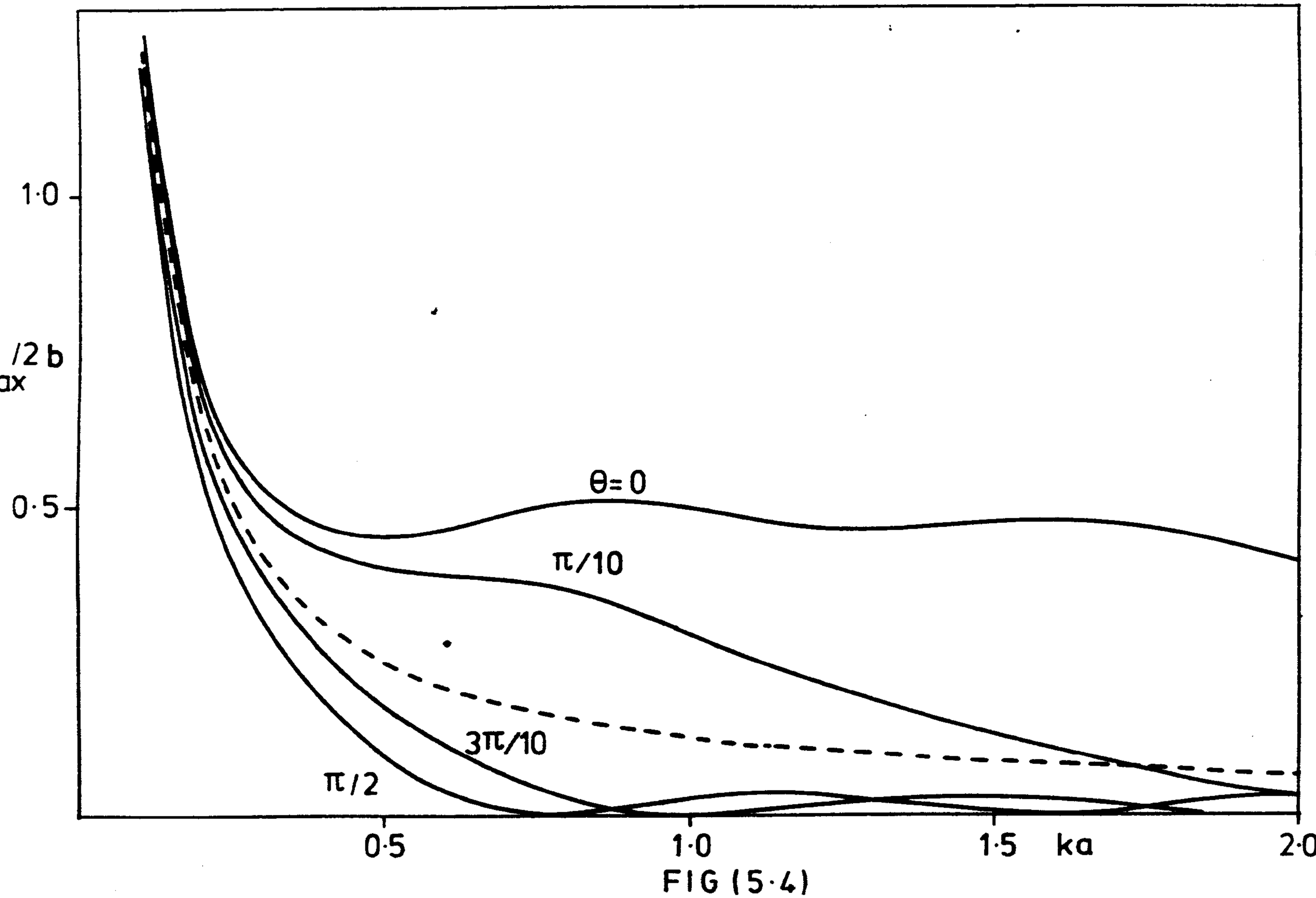
b/a=4
axisymmetric patch:
C wmax /2 b
1·0
0·5
θ=0
π/10
3π/10
π/2
0·5
1·0
1·5
ka
2·0

FIG (5·4)

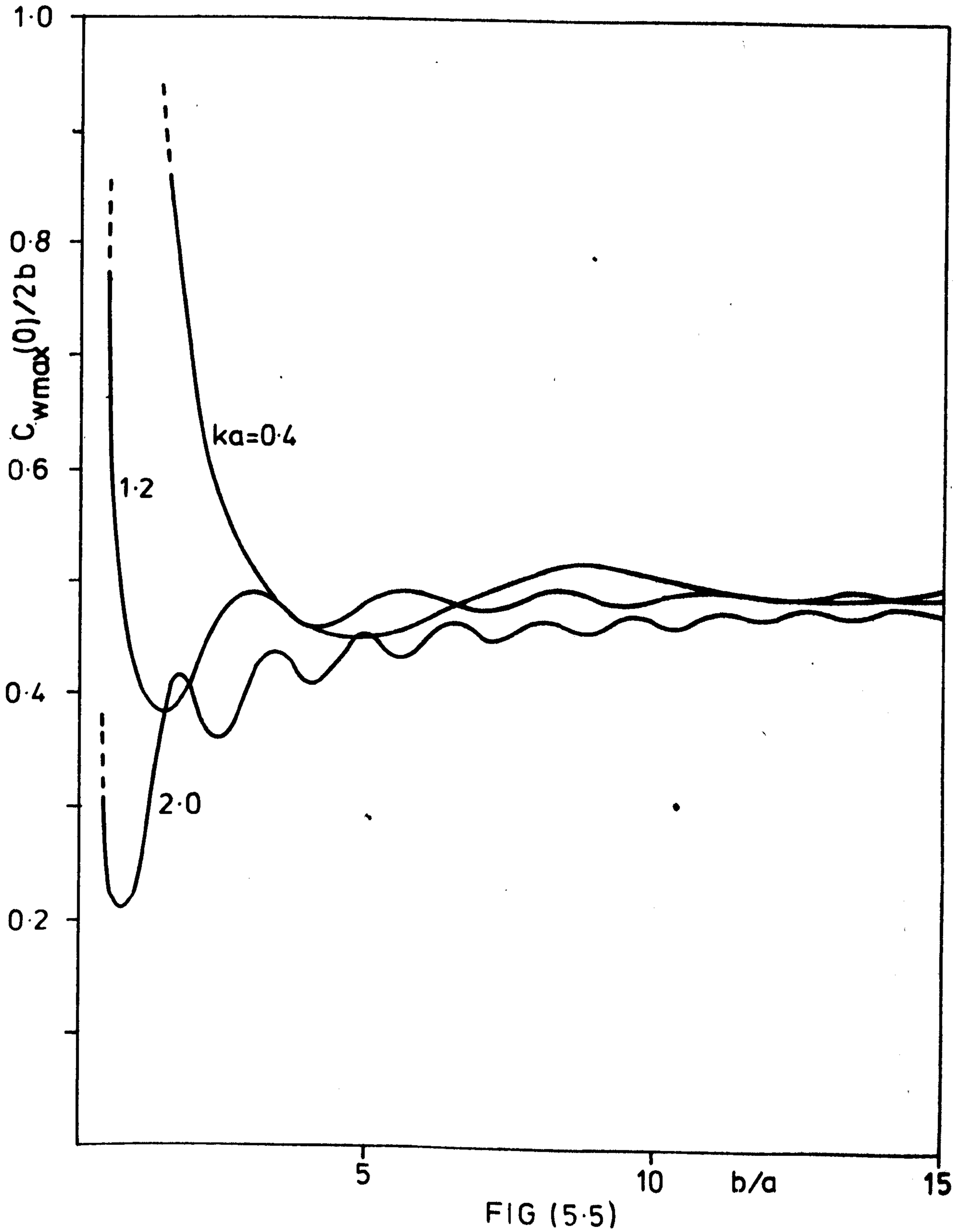

FIG (5·5)

width is very sensitive to changes in wave direction, for example, when $b/a = 10$, $ka = 2$, normal incidence upon the side of length 2b gives $C_{wmax}/2b$ as 0.47 but a change in wave direction of 18^{o} gives $C_{wmax}/2b$ as 8.3×10^{-6}, quite a dramatic decrease.

To study how C_{wmax} changes compared to its value at normal wave incidence, Figure (5.3) illustrates the variation of $C_{wmax}(\Theta)/C_{wmax}(0)$ with Θ. The behaviour has been explained above but the results demonstrate how sensitive the maximum capture width is to changes in wave direction for different values of ka.

Figure (5.4) shows the behaviour of C_{wmax} as a function of ka. Also included is the corresponding result for the axisymmetric pressure distribution. This clearly confirms the increasing sensitivity of C_{wmax} to wave direction as ka increases. Note the zeros of the maximum capture width occur when $ka \cos\Theta = n\pi$ or $kb \sin\Theta = n\pi, (n=1,2,\ldots)$ (see equation (5.3.2)).

The dependence of the maximum capture width upon b/a for normally incident waves can be seen in Figure (5.5). In the limit as $b/a \rightarrow \infty$, the rectangular patch becomes an infinitely long strip. For such a pressure distribution, Evans (1981b) has shown that the maximum efficiency is 50% and hence it is expected that as $b/a \rightarrow \infty$, $C_{wmax}/2b \rightarrow \frac{1}{2}$. This is confirmed by Figure (5.5) and may also be shown analytically as follows.

From (5.3.3) it is clear that

$$\frac{C_{wmax}(0)}{2b} = \frac{\pi k b \sin^2 ka}{I} \qquad (5.3.6)$$

where

$$I = \int_0^{2\pi} |f(\theta)|^2 \, d\theta . \qquad (5.3.7)$$

Now

$$I = 4\int_0^{\pi/2} \frac{\sin^2(b/a\, ka\sin\theta)\sin^2(ka\cos\theta)}{\sin^2\theta\cos^2\theta}\, d\theta , \qquad (5.3.8)$$

and substituting $x = \sin\Theta$ this becomes

$$I = 4\int_0^1 \frac{\sin^2\left(\frac{b}{a}kax\right)\sin^2\left(ka(1-x^2)^{\frac{1}{2}}\right)}{x^2(1-x^2)^{3/2}}\,dx, \qquad (5.3.9)$$

$$= 2\int_0^1 \frac{\left[1-\cos\left(2\frac{b}{a}kax\right)\right]\sin^2\left[ka(1-x^2)^{\frac{1}{2}}\right]}{x^2(1-x^2)^{3/2}}\,dx,$$

$$= \lim_{\varepsilon\to 0}\int_\varepsilon^1 \left(2-e^{2ib/a\,kax}-e^{-2ib/a\,kax}\right)\frac{\sin^2\left[ka(1-x^2)^{\frac{1}{2}}\right]}{x^2(1-x^2)^{3/2}}\,dx,$$

$$= \lim_{\varepsilon\to 0}\left\{\int_{-1}^{-\varepsilon} + \int_\varepsilon^1\right\}\left(1-e^{2ib/a\,kax}\right)\frac{\sin^2\left[ka(1-x^2)^{\frac{1}{2}}\right]}{x^2(1-x^2)^{3/2}}\,dx,$$

$$= \left\{\int_C - \int_{\mathcal{L}}\right\}\left(1-e^{2ib/a\,kax}\right)\frac{\sin^2\left[ka(1-x^2)^{\frac{1}{2}}\right]}{x^2(1-x^2)^{3/2}}\,dx,$$

where C is a contour from x=-1 to x=+1 passing above the singularity at x=0. Thus

$$I = \left\{\int_C dx + \pi i \operatorname*{Res}_{x=0}\right\}\left(1-e^{2ib/a\,kax}\right)\frac{\sin^2\left[ka(1-x^2)^{\frac{1}{2}}\right]}{x^2(1-x^2)^{3/2}},$$

$$= 2\pi\left(\frac{b}{a}\right)ka\sin^2 ka + \int_C \left(1-e^{2ib/a\,kax}\right)\frac{\sin^2\left[ka(1-x^2)^{\frac{1}{2}}\right]}{x^2(1-x^2)^{3/2}}\,dx. \qquad (5.3.10)$$

The integrand is bounded except near $x=\pm 1$ where it is $O\left((1-x^2)^{-\frac{1}{2}}\right)$. Hence, as $b/a \longrightarrow \infty$

$$I \sim 2\pi kb\sin^2 ka + O(1), \qquad (5.3.11)$$

and from (5.3.6) it can be seen that

$$\frac{C_{wmax}(0)}{2b} \longrightarrow \frac{1}{2} \quad , \text{as } b/a \longrightarrow \infty. \qquad (5.3.12)$$

The results presented above are also valid for a heaving rectangular plate on the sea-bed. For rigid bodies, Evans (1980b) has derived the result corresponding to (5.2.14), where q_s is now replaced by the exciting force, X_s. As noted in Chapter 4, § 6(a) the exciting force may easily be evaluated as there are again no diffracted waves, and the expression for the maximum capture width is again given by (5.3.2), (5.3.3). The plate may be considered to be a simple first approximation to a membrane on the sea-bed which has been suggested as a possible type of wave energy absorber.

5.4 The Maximum Capture Width of a Circular Pressure Patch

The theoretical maximum capture width for a circular pressure patch is simply $\lambda/2\pi$, as given by (5.2.15), which is valid provided (5.2.18) can be satisfied. In this section the maximum capture width is examined when there is no mechanism for introducing a phase difference between the volume flux across and pressure drop through a turbine. From (5.2.20) it can be seen that in this case

$$C_{wmax} = \frac{\lambda}{2\pi}\left(1 - \frac{\Gamma_{opt} - \underline{B}}{\Gamma_{opt} + \underline{B}}\right), \qquad (5.4.1)$$

where Γ_{opt} is given by (5.2.21). Alternatively, to compare this result with the theoretical maximum capture width result, (5.4.1) may be written as

$$C_{wmax} = \frac{\lambda}{2\pi} Q_{max}, \qquad (5.4.2)$$

where

$$Q_{max} = \frac{2\underline{B}}{\underline{B} + (\underline{B}^2 + \omega^2 \underline{A}^2)^{\frac{1}{2}}}. \qquad (5.4.3)$$

To evaluate Q_{max}, C_{Wmax} it is sufficient to consider the radiation problem only, as $\underline{A}$ and $\underline{B}$ can be determined from (5.2.6), (5.2.8). The solution of the radiation problem can be found using

a Hankel transformation of order zero in a similar manner as for the radiation problem for an oscillating disc on the sea-bed in Chapter 4, § 6(b).

Cylindrical polar coordinates (r, Θ, z) are chosen with z positive upwards and the origin on the sea-bed such that r = 0, z = d corresponds to the centre of the circular pressure patch. The free-surface boundary condition is given by

$$K\psi - \partial\psi/\partial z = 1 \quad , \quad r \le a, z = d, \tag{5.4.4}$$

$$K\psi - \partial\psi/\partial z = 0 \quad , \quad r > a, z = d, \tag{5.4.5}$$

where a is the radius of the circular pressure distribution. The Hankel transform of ψ is given by (4.6.4), with ϕ replaced by ψ. The transformed potential $\tilde{\psi}$ then satisfies

$$(\partial^2/\partial z^2 - \xi^2)\tilde{\psi}(\xi, z) = 0, \tag{5.4.6}$$

$$K\tilde{\psi} - \partial\tilde{\psi}/\partial z = \frac{a}{\xi} J_1(\xi a) \quad , \text{on } z = d, \tag{5.4.7}$$

$$\partial\tilde{\psi}/\partial z = 0 \quad , \text{on } z = 0. \tag{5.4.8}$$

As in Chapter 4, there is no Θ-dependence in the problem by symmetry, i.e. $\psi = \psi(r,z)$ and, from (4.6.4) - (4.6.7), it is clear that (5.4.6) - (5.4.8) are the required governing equations. The potential ψ, although different from ϕ_r, is still a radiation potential and thus the radiation condition for ψ is of the form given by (4.2.3).

The solution of (5.4.6) with the boundary conditions (5.4.7), (5.4.8) is found to be

$$\tilde{\psi}(\xi, z) = \frac{a J_1(\xi a) \cosh \xi z}{\xi (K \cosh \xi d - \xi \sinh \xi d)}, \tag{5.4.9}$$

Hence, applying the inverse transform as defined by (4.6.9)

and $\underline{A}$ is found to be

$$\underline{A} = -\frac{2\pi a^2}{\rho g}\left[\frac{\pi \sinh^2 kd\, N_0^{-1} J_1(ka)Y_1(ka)}{2Kd} + \sum_{n=1}^{\infty} \frac{N_n^{-1}\sin^2 k_n d\, I_1(k_n a)K_1(k_n a)}{Kd}\right] \quad (5.4.16)$$

The corresponding infinite water-depth results may be deduced from (5.4.15), (5.4.16). As $d \longrightarrow \infty$, then from (2.2.9) $k \to K$ and hence

$$\underline{B} \longrightarrow \frac{2\pi a^2 \omega}{\rho g} J_1^2(Ka), \text{ as } d \to \infty. \quad (5.4.17)$$

Similarly

$$\frac{\pi \sinh^2 kd\, N_0^{-1} J_1(ka)Y_1(ka)}{2kd} \longrightarrow \pi J_1(Ka)Y_1(Ka), \text{ as } d \to \infty.$$

The n th. term of the infinite sum in $\underline{A}$ may be rewritten

$$\frac{N_n^{-1}\sin^2 k_n d\, I_1(k_n a)K_1(k_n a)}{Kd} = \frac{2K\, I_1(k_n a)K_1(k_n a)}{d(k_n^2 + K^2 - K/d)},$$

where (2.2.10), (2.2.12) have been used. Also, from (2.2.10) it can be seen that

$$k_{n+1} - k_n = \pi/d + O(1/d^2).$$

Thus, if A_1, A_2 $(A_1 < A_2)$ are two positive numbers, then the sum over all k_n such that $A_1 < k_n < A_2$ can be written

$$\sum_{A_1 < k_n < A_2} \frac{N_n^{-1}\sin^2 k_n d\, I_1(k_n a)K_1(k_n a)}{Kd} = \frac{2K}{\pi} \sum_{A_1 < k_n < A_2} \frac{I_1(k_n a)K_1(k_n a)(k_{n+1} - k_n)}{(k_n^2 + K^2 - K/d)} + O(1/d^2),$$

$$\longrightarrow \frac{2K}{\pi}\int_{A_1}^{A_2} \frac{I_1(ua)K_1(ua)\,du}{u^2 + K^2}, \text{ as } d \to \infty.$$

Letting $A_1 \longrightarrow 0$ and $A_2 \longrightarrow \infty$ gives

$$\sum_{n=1}^{\infty} \frac{N_n^{-1}\sin^2 k_n d\, I_1(k_n a)K_1(k_n a)}{Kd} \longrightarrow \frac{2K}{\pi}\int_0^{\infty} \frac{I_1(ua)K_1(ua)\,du}{u^2 + K^2}, \text{ as } d \to \infty,$$

and, from (5.4.16)

$$\underline{A} \longrightarrow -\frac{2\pi a^2}{\rho g}\left[\pi J_1(Ka)Y_1(Ka) + \frac{2Ka}{\pi}\int_0^\infty \frac{I_1(u)K_1(u)}{u^2+K^2a^2}du\right], \text{ as } d\to\infty \quad (5.4.18)$$

The expressions for $\underline{A}$ and $\underline{B}$ in infinitely deep fluid can also be found by solving the infinite depth problem directly using the Hankel transform. The results obtained by this method agree with (5.4.17), (5.4.18).

From (5.4.3), it can be seen that Q_{max} attains its maximum value of unity if $\underline{A} = 0$ when, from (5.2.7), the induced volume flux downwards across the internal free-surface is exactly in phase with the applied pressure on the surface. The computation of $\underline{A}$ as a function of ka is given in Figure (5.6), for $a/d = \frac{1}{2}$, 1 and infinitely deep fluid. Although finite depth produces some change in the value of $\underline{A}$ from its infinite depth value, the difference is surprisingly small (even for the $a/d = 1$ case). It has been found numerically that $\underline{A}$ has just seven zeros, (a greater number may possibly exist if a/d is large although this has not been pursued). The finite number of zeros is due to the integral term in (5.4.18) which is always positive and dominates the oscillatory J_1 Y_1 term for large ka. In infinite depth the first zero of $\underline{A}$ occurs at ka = 1.96 corresponding to a disc radius of about three-tenths the wavelength of the incident waves. For finite depth it is found that the first zero occurs at a greater value of ka but the change is small for $a/d \lesssim 1$; the first zero is at ka $\simeq$ 2.05 for $a/d = \frac{1}{2}$, ka $\simeq$ 2.12 for $a/d = 1$.

The damping term $\underline{B}$ shown in Figure (5.7) vanishes at the zeros of J_1, just as for the oscillating disc on the sea-bed (see equation (4.5.8)) so again there exist particular frequencies at which no outward propagating waves are produced. The asymptotic behaviour of $\underline{B}$ is however different in the two cases. As ka $\to$ 0, the damping coefficient for the disc behaves as O(ka) while, for the pressure

distribution, $\underline{B}=O((ka)^3)$, (or $O((ka)^{5/2})$ in infinite depth). As $ka \longrightarrow \infty$, the modulation amplitude of the pressure distribution damping term is $O((ka)^{-\frac{1}{2}})$ while the damping coefficient of the disc decays exponentially because it is submerged beneath the free surface.

Note that as $ka \longrightarrow 0$, $\underline{A}$ tends to a finite value whereas B tends to zero; the limiting value of $\underline{A}$ can be found. From (5.2.6), (5.4.4) it can be seen that

$$q_r \longrightarrow \frac{i\omega P}{\rho g}\pi a^2 \quad , as \ ka \rightarrow 0,$$

and, thus from (5.2.8)

$$\underline{A} \longrightarrow -\frac{2\pi a^2}{\rho g}\left(-\frac{1}{2}\right), \ \underline{B} \rightarrow 0 \quad , as \ ka \rightarrow 0. \qquad (5.4.19)$$

This behaviour may be deduced from (5.4.16), (5.4.17).

Figure (5.8) shows the variation of Q_{max} with ka. It attains its first maximum at $ka \simeq 2$ (depending on the fluid depth) before decreasing to zero at $ka \simeq$ 3.8 when the coefficient B is first zero. It then increases rapidly, rising to a second maximum and maintains a relatively high value until $ka \simeq 5$ before diminishing once more; as ka increases, this behaviour is repeated, accompanied by a gradual decrease in the maximum value of Q_{max} once ka is greater than the value at which the seventh zero of A occurs. The maximum capture width ratio, $C_{wmax}/2a$, illustrated in Figure (5.9), gives directly the maximum amount of power the device is capable of absorbing. Here it can be seen that an absolute maximum of about 0.4 is reached at $ka \simeq$ 0.7 in infinitely deep fluid; in finite depth the maximum value is slightly smaller and occurs at a marginally larger value of ka. The theoretical maximum capture width (from equation (5.4.2)), is also shown as a long-dashed curve.

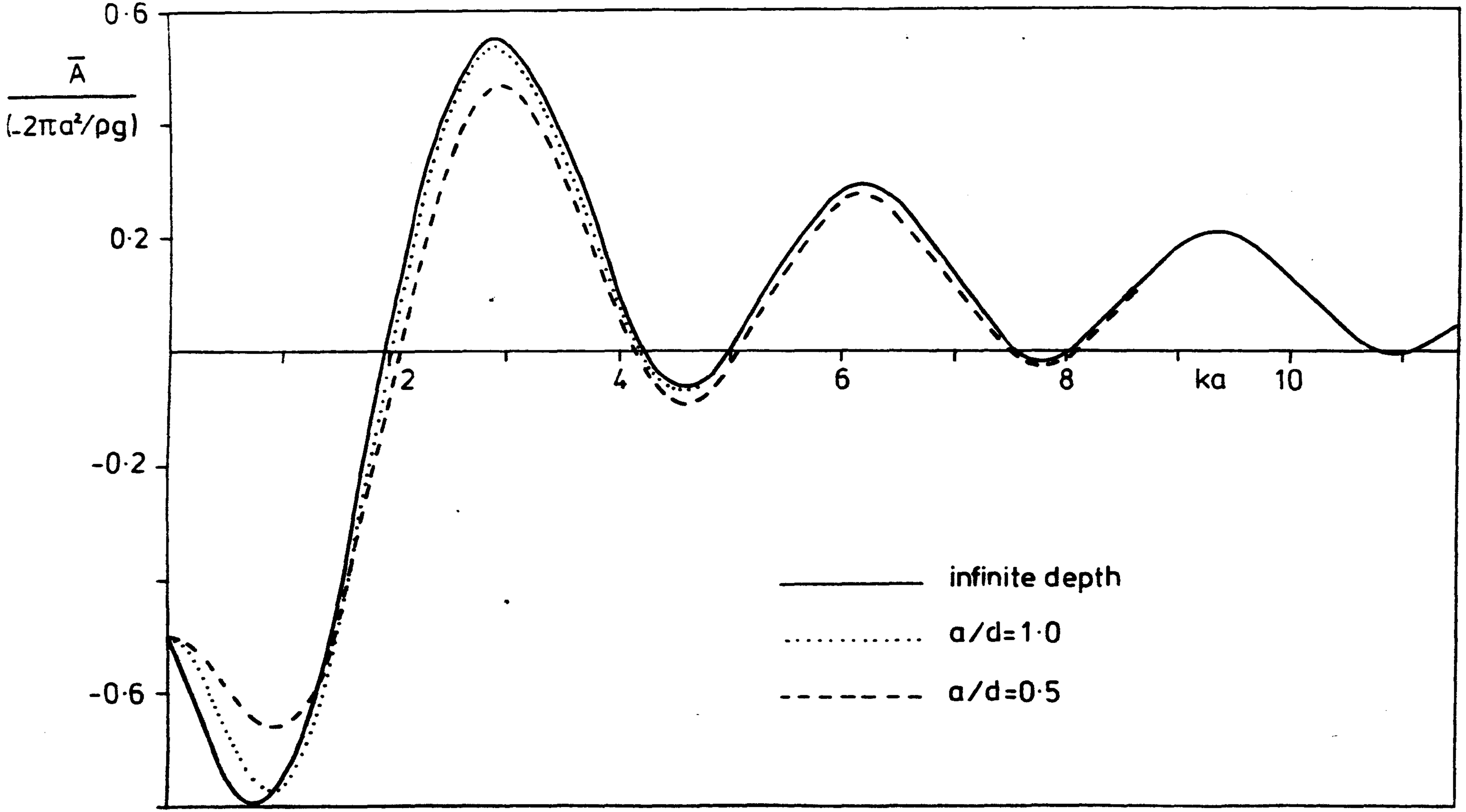
0·6
$\frac{\bar{A}}{(-2\pi a^2/\rho g)}$
0·2
-0·2
-0·6
2
4
6
8
ka
10
infinite depth
a/d=1·0
a/d=0·5

FIG (5·6)

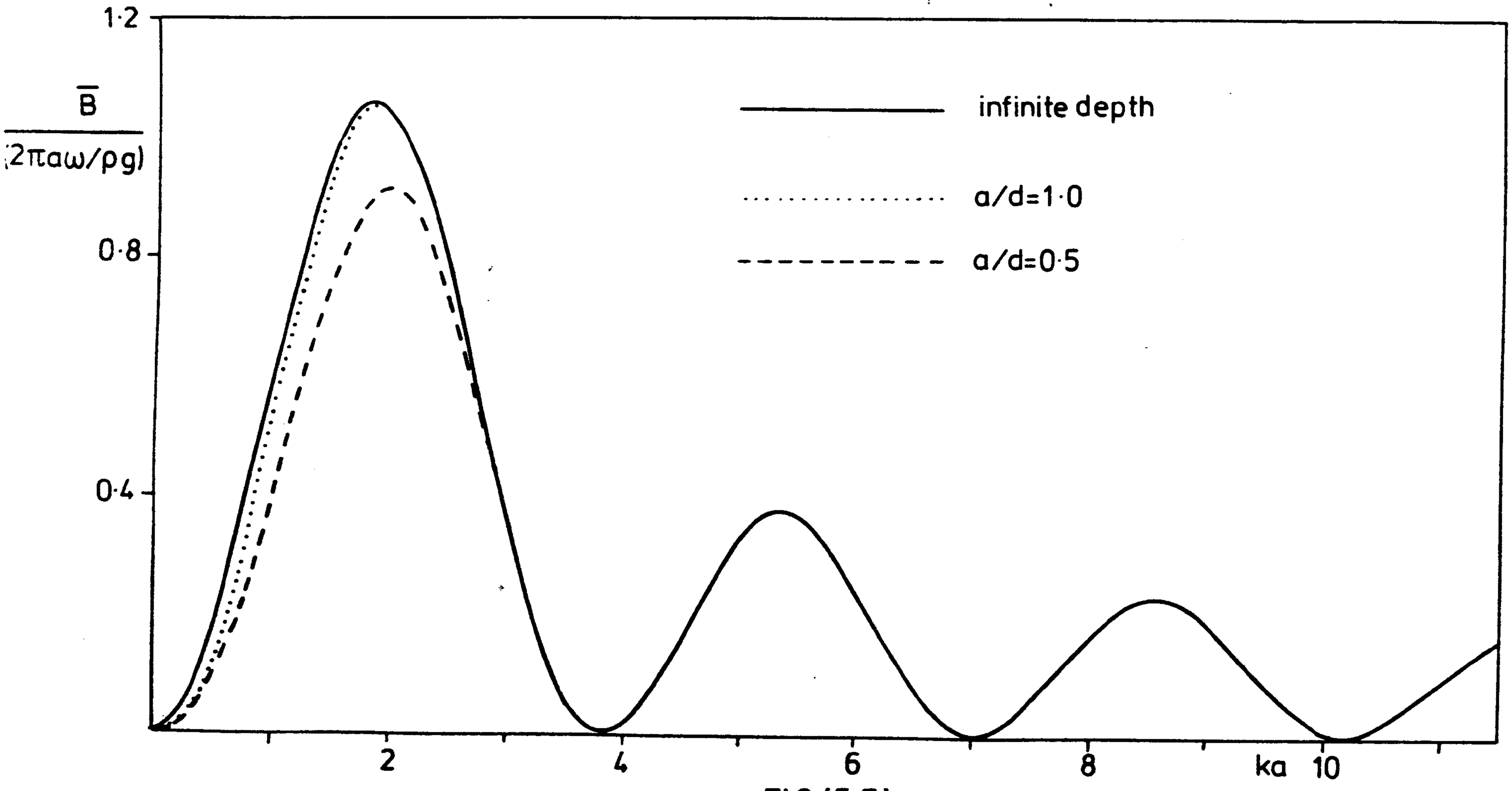
1·2
$\frac{\overline{B}}{(2\pi a\omega/\rho g)}$
0·8
0·4
infinite depth
a/d=1·0
a/d=0·5
2
4
6
8
ka
10

FIG (5·7)

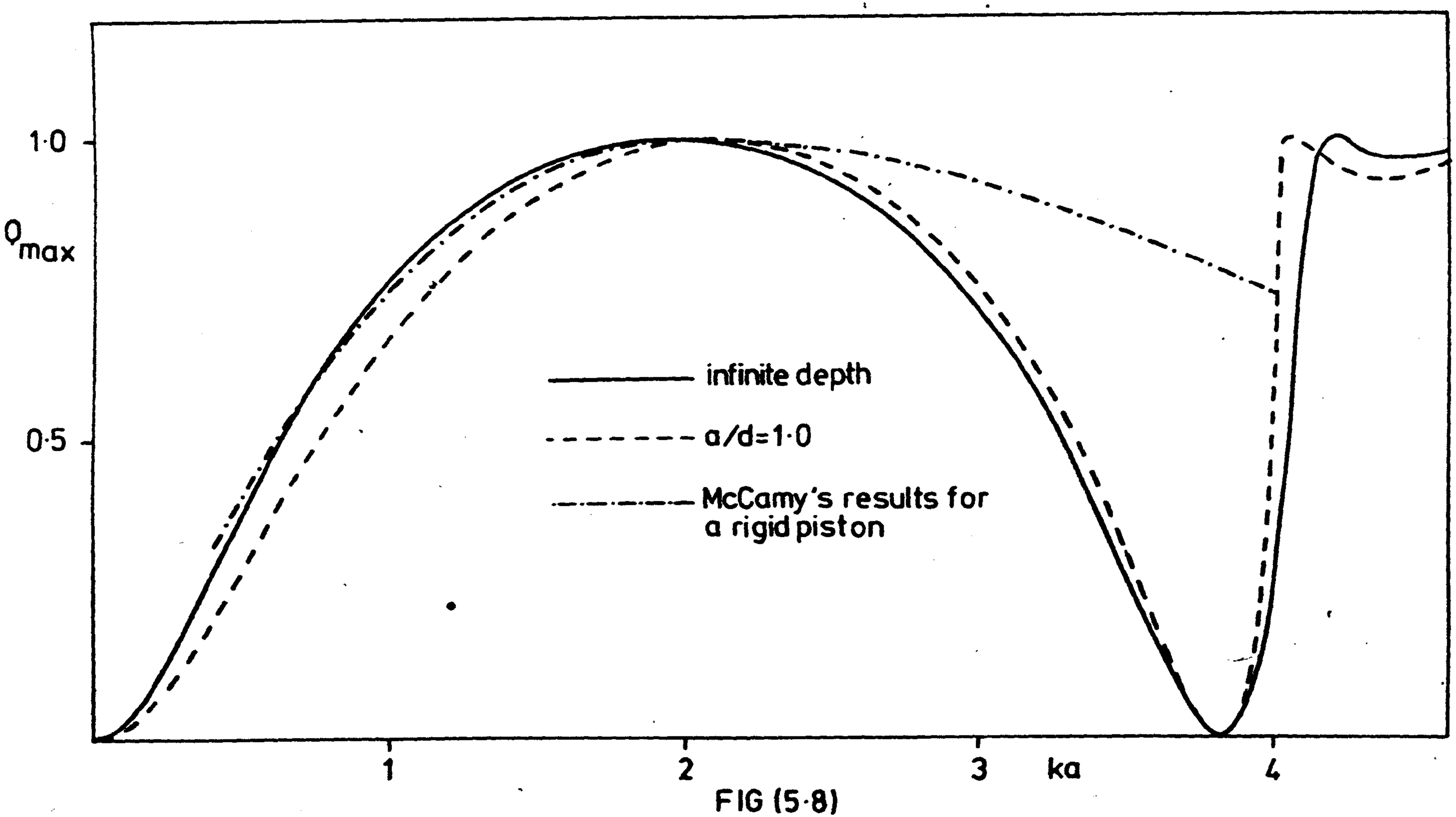
1·0
0_{max}
0·5
infinite depth
a/d=1·0
McCamy's results for a rigid piston
1
2
3
ka
4

FIG (5·8)

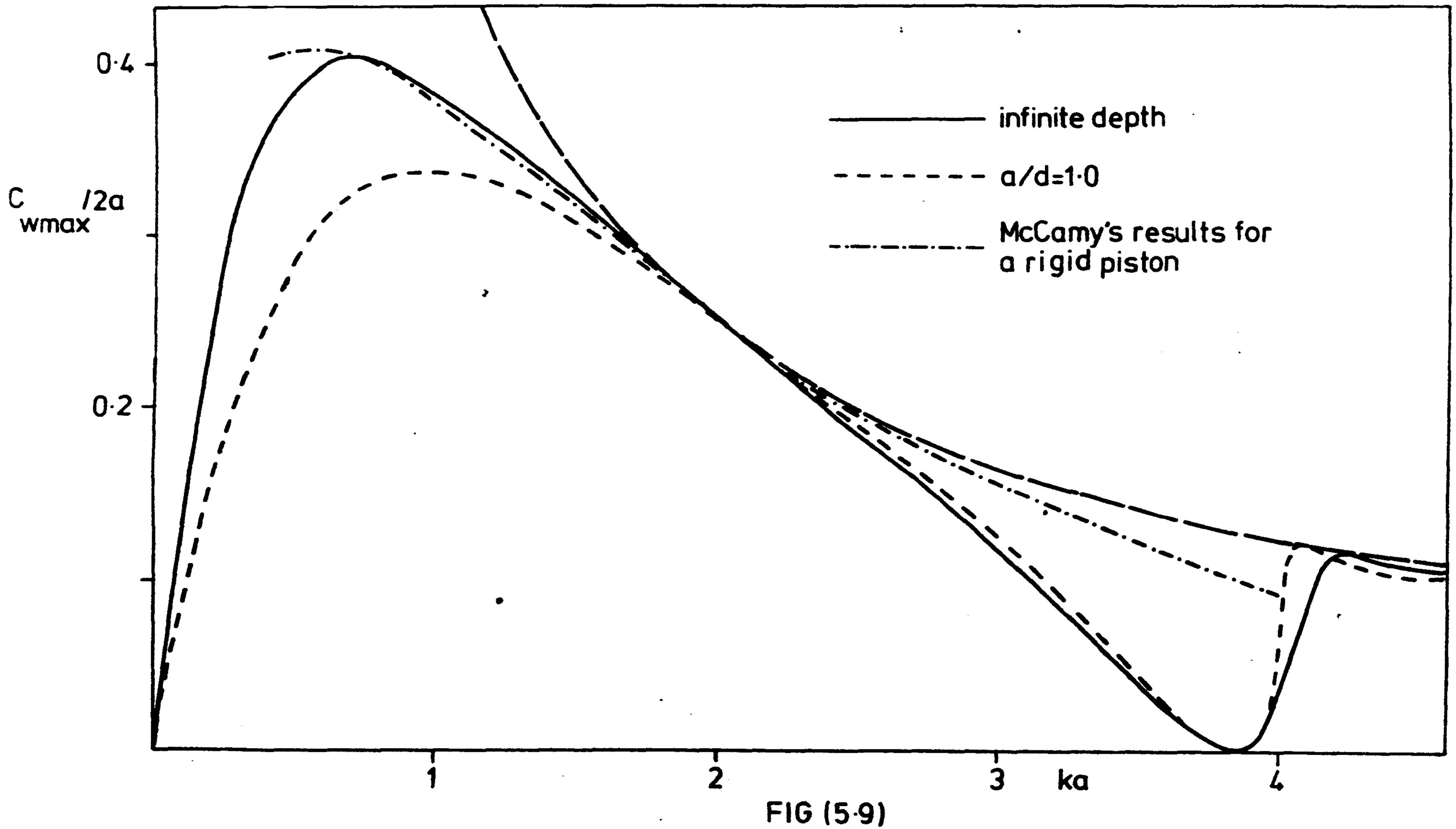
0·4
0·2
C wmax /2a
infinite depth
a/d=1·0
McCamy's results for a rigid piston
1
2
3
ka
4

FIG (5·9)

Figures (5.8), (5.9) include the corresponding Q_{max}, $C_{Wmax}/2a$ results when the pressure patch is replaced by a rigid, light piston in infinitely deep fluid. Replacing the internal free-surface by such a piston has been the previous method of treating a free-surface intersecting duct and it is of interest to study the difference between the results of the two approaches.

As given by Evans (1981b), the capture width for the rigid piston (see equation (4.4.11)) may be written in an analogous form to (5.4.1). In this case the 'A coefficient' for the piston is given by

$$\underline{A}(\omega) = m_0 + M(\omega) - c\omega^{-2},$$

where m_0, M are the mass and added-mass of the piston respectively, and $c = \pi a^2 \rho g$ is the buoyancy restoring coefficient (the spring restoring force on the piston is provided by the buoyancy only). The corresponding 'B coefficient' for the piston is the usual damping coefficient. Thus, for a weightless piston, $\underline{A}$ and $\underline{B}$ are given by

$$\underline{A}(\omega) = \rho a^3 \{ \mu(\omega) - \pi/Ka \},$$

$$\underline{B}(\omega) = \rho a^3 \omega \Lambda(\omega),$$

where μ and Λ are non-dimensionalised added-mass and damping coefficients respectively. These coefficients have been determined by McCamy (1961) although an error appears in the non-dimensionalisation of his coefficients. It can be shown that $\mu \longrightarrow 4/3$ as $Ka \to \infty$, $\mu \to 8/3$ as $Ka \to 0$ using Hankel transform methods and these asymptotics suggest that the extra 2π appearing in his non-dimensionalisation should not be present. Subsequent work by Hulme, approximating the disc by a shallow spheroid of aspect ratio 0.05 and using a ring source method (Hulme, 1981), supports this view.

Using McCamy's corrected results it is found that $\underline{A}(\omega)$ has only one zero which occurs at ka $\simeq$ 2.1, while $\underline{B}(\omega)$ is always positive for ka > 0. From Figure (5.8) it can be seen that, for ka ≤ 2, there is very little difference between the pressure patch and rigid disc values of Q_{max}. This is expected for small ka by consideration of the boundary conditions over the pressure patch and rigid disc. Only for ka >2 when Q_{max} for the pressure patch begins falling to zero is there then appreciable difference. A similar conclusion holds for the capture width (see Figure (5.9)). The apparent divergence of the two curves as ka $\rightarrow$ 0 may be due to errors in McCamy's depicted results or numerical errors in his computations, which are magnified by the extended scale (compare with Figure (5.8), when the difference for small ka appears slight).

(b) The Three-Dimensional Mouth Downward Duct

5.5 Formulation and Solution

The theory of wave-power absorption by a pressure distribution is now applied to a surface-piercing duct. The method of solution follows the method used for the mouth-upward duct in Chapter 4.

Consider a vertical duct submerged to a depth ℓ and of circular cross-section a, in fluid of depth d($d > \ell$), as shown in Figure (5.10). The co-ordinate system chosen is cylindrical polars as defined for the circular pressure patch of the previous section.

The free surface condition to be satisfied by the radiation potential Ψ is again given by (5.4.4), (5.4.5). In addition, Ψ is required to satisfy Laplace's equation (2.2.3) and the boundary condition on the sea-bed (2.2.5) with $z_f = d$ while, from (2.2.7a), the boundary condition on the side of the duct is given by

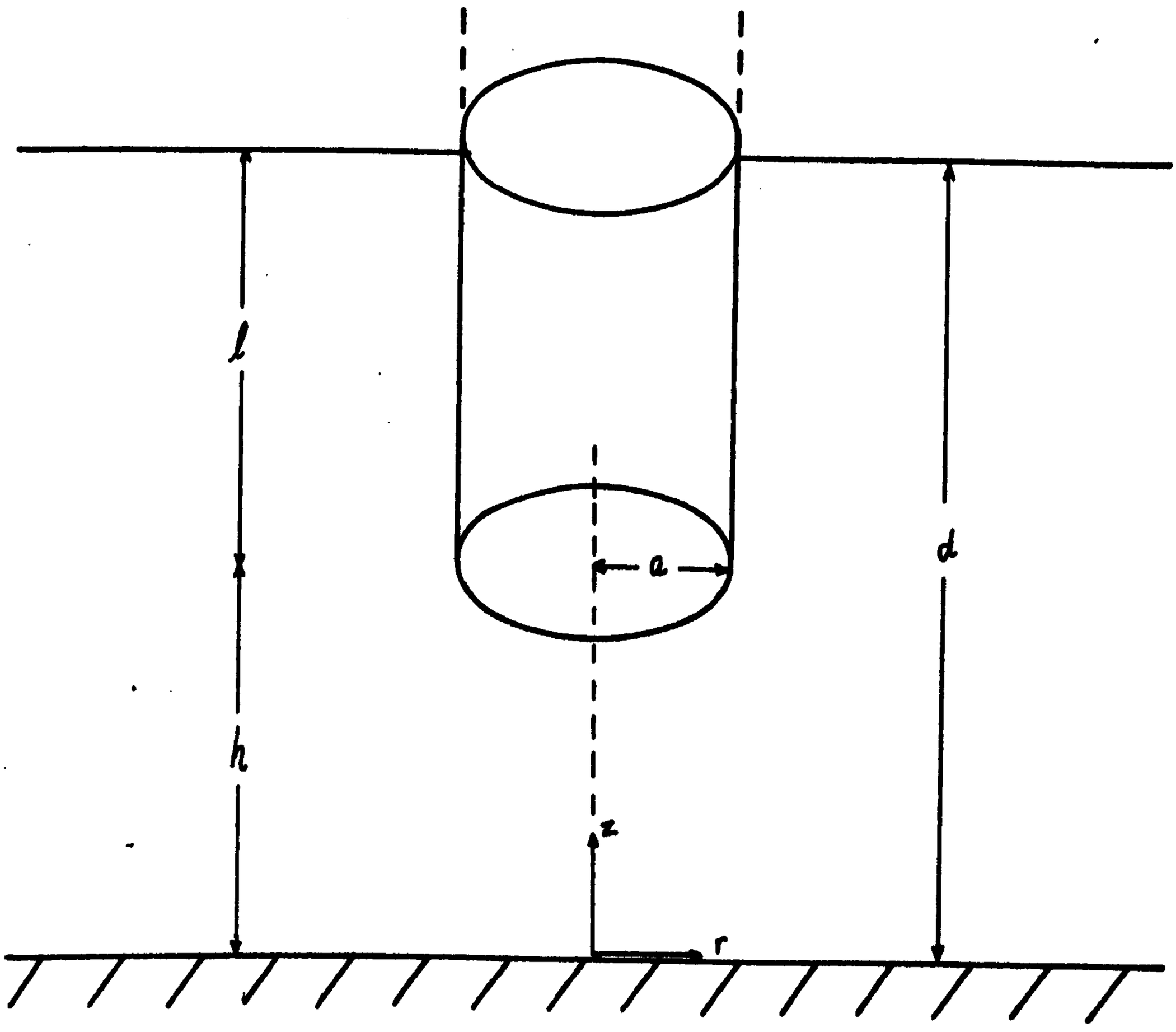

FIGURE (5.10)

$$\partial\psi/\partial r = 0 \quad , \text{on } r = a, \; l \le z \le d. \tag{5.5.1}$$

As for the circular pressure patch in § 4, the radiation condition for ψ is of the form defined by (4.2.3).

By symmetry, there is no θ-dependence in the problem and hence the solution of Laplace's equation by separation of variables

in the inner ($r \leq a$) and outer ($r \geq a$) regions yields

$$\psi = \sum_{n=0}^{\infty} A_n I_0(k_n r) Z_n(z) + K^{-1} , \quad (r \leq a), \tag{5.5.2}$$

$$\psi = \sum_{n=0}^{\infty} B_n K_0(k_n r) Z_n(z) , \quad (r \geq a), \tag{5.5.3}$$

where the A_n, B_n are unknown constants; the definition of the Z_n is given in Chapter 4, § 2. The particular solution included in the inner region to satisfy (5.4.4) is clearly harmonic and also satisfies the sea-bed boundary condition (2.2.5).

As in Chapter 4, § 2 the radial velocity at the cylindrical interface, r=a is expanded in terms of the vertical eigenfunctions, $Z_n(Z)$, i.e.

$$\frac{\partial \psi}{\partial r} = \begin{cases} f(z) , \text{at } r=a, 0 \leq z < h , \\ 0 , \text{at } r=a, h \leq z \leq d. \end{cases} \tag{5.5.4}$$

and

$$\left.\frac{\partial \psi}{\partial r}\right|_{r=a} = \sum_{n=0}^{\infty} \mathcal{F}_n Z_n(z) , \quad 0 \leq z \leq d, \tag{5.5.5}$$

where

$$\mathcal{F}_n = \frac{1}{d} \int_0^h f(z) Z_n(z) dz . \tag{5.5.6}$$

After (5.5.5) has been employed to substitute for A_n, B_n in terms of the unknown $\mathcal{F}_n$ in (5.5.2), (5.5.3), the expressions for ψ in the inner and outer regions can be matched at $r=a$, $0 \leq z < h$, as the pressure is continuous over this interval. Hence

$$\sum_{n=0}^{\infty} \frac{\mathcal{F}_n K_0(k_n a)}{k_n K_0'(k_n a)} Z_n(z) = K^{-1} + \sum_{n=0}^{\infty} \frac{\mathcal{F}_n I_0(k_n a)}{k_n I_0'(k_n a)} Z_n(z) \text{ , for } 0 \le z < h,$$

and, with R_n defined as in (4.2.14), this becomes

$$\sum_{n=0}^{\infty} \mathcal{F}_n R_n Z_n(z) = -(Ka)^{-1} \quad , 0 \le z < h. \tag{5.5.7}$$

The boundary condition (5.5.1) gives

$$\sum_{n=0}^{\infty} \mathcal{F}_n Z_n(z) = 0 \quad , h \le z \le d, \tag{5.5.8}$$

and, by multiplying (5.5.7) (5.5.8) by $(1/d)\, Z_m(z)$, integrating over the region of validity and adding, it is found that

$$\sum_{n=0}^{\infty} E_{mn} \mathcal{F}_n = C_m , \tag{5.5.9}$$

where in this case

$$E_{mn} = (R_n - 1) D_{mn} + \delta_{mn} , \tag{5.5.10}$$

$$D_{mn} = \frac{1}{d} \int_0^h Z_m(z) Z_n(z) dz, \tag{5.5.11}$$

$$C_m = -\frac{1}{Kad} \int_0^h Z_M(z) dz . \tag{5.5.12}$$

(Expressions for D_{mn}, C_m are given in Appendix B).

The complex matrix equation (5.5.9) can be reduced to two real matrix equations by performing the decompositions (4.3.6), (4.3.7). The decomposition (4.3.7) given by (B.11)-(B.13) is the same as for the mouth-upward duct with the term D_{m0} now given by (B.17), and thus the solution follows that given in Chapter 4, § 3. This yields an identical expression (4.3.14) for the unknown $\mathcal{F}_n$, with the r_n, s_n defined as the solution of (4.3.10), (4.3.11) when C_m is defined by (5.5.12) and p_m, q_m by (B.12), (B.13) respectively.

5.6 Wave Energy Absorption

The volume flux q_r across the internal free-surface is given by (5.4.11) where, in this case

$$\frac{\partial \Psi}{\partial z}(r,d) = -\sum_{n=0}^{\infty} \frac{N_n^{-\frac{1}{2}} \mathcal{F}_n I_0(k_n r)}{I_0'(k_n a)} \sin k_n d ,$$

and use has been made of (5.5.2), (5.5.5) with (4.2.6), (4.2.7).

Thus, from (5.4.11) it is found that

$$q_r = \frac{2\pi i \omega \rho}{\rho g} \sum_{n=0}^{\infty} \frac{N_n^{-\frac{1}{2}} \sin k_n d \, \mathcal{F}_n}{I_0'(k_n a)} \int_0^a I_0(k_n r) r \, dr,$$

$$= \frac{2\pi i a \omega \rho}{\rho g} \sum_{n=0}^{\infty} \frac{N_n^{-\frac{1}{2}} \sin k_n d \, \mathcal{F}_n}{k_n} . \qquad (5.6.1)$$

The coefficients $\underline{A}$ and $\underline{B}$ are given by (5.2.8) and substitution in (5.6.1) gives

$$\underline{A} = \frac{2\pi a^2}{\rho g} \sum_{n=0}^{\infty} \frac{Re(\mathcal{F}_n) N_n^{-\frac{1}{2}} \sin k_n d}{k_n a} , \qquad (5.6.2)$$

$$\underline{B} = \frac{2\pi a^2 \omega}{\rho g} \sum_{n=0}^{\infty} \frac{Im(\mathcal{F}_n) N_n^{-\frac{1}{2}} \sin k_n d}{k_n a} . \qquad (5.6.3)$$

The maximum capture width may now be examined using (5.4.2), (5.4.3) once $\underline{A}$ and $\underline{B}$ are evaluated, and the results are presented in §8.

It is clearly possible to use the methods of §§ 5,6 to determine $\underline{A}$ and $\underline{B}$ for the limiting case of a zero length duct, that is, a circular pressure patch, just as the oscillating disc results were found in Chapter 4. The results in this limiting case agree with those found using the Hankel transform method in § 4.

5.7 The Scattering Problem

The complementary scattering problem for the duct has been investigated by Garrett (1970). In this case, waves are incident upon the duct in the absence of an applied pressure on the internal free-surface, and thus the duct is equivalent to Garrett's 'bottomless harbour'. The relation of the induced volume flux q_s across the internal free-surface to the coefficient $\underline{B}$ is given by (5.2.13) as

$$\underline{B} = \frac{2\pi}{8\lambda P_w} |q_s|^2 . \qquad (5.7.1)$$

Hence (5.7.1) may be used to derive $\underline{B}$ from the scattering problem and this will provide a check on the value of $\underline{B}$ calculated via the radiation problem, given by (5.6.3).

The scattering potential, ϕ_s satisfies the same governing equations as the radiation potential, Ψ except for the internal free-surface condition which is now given by (5.2.4), that is the usual free-surface condition, and the radiation condition which must now also account for the incident wavetrain. The solution for the potential is given by Garrett (1970) and this is applied to this pressure distribution problem.

The incident wave potential ϕ_0, included in ϕ_s, may be written as a cylindrical wave expansion as in Chapter 4, §4(b). Similarly the free-surface displacement, $\chi(r,\theta)$ and the displacement potential, $\Psi_d(r,\theta,z)$, $[=(1/-i\omega)\phi_s]$, can be written as

$$\chi(r,\theta) = A \sum_{m=0}^{\infty} \varepsilon_m i^m \chi_m(r) \cos m\theta, \qquad (5.7.2)$$

$$\Psi_d(r,\theta,z) = A \sum_{m=0}^{\infty} \varepsilon_m i^m \Psi_m(r,z) \cos m\theta, \qquad (5.7.3)$$

where A is the incident wave amplitude and $\varepsilon_0=1, \varepsilon_n=2\ (n\gg 1)$.

The volume flux q_{vs} across the internal free-surface is given by

$$q_{vs} = -i\omega\int_0^a dr\int_0^{2\pi} d\theta\, \chi(r,\theta),$$

$$= -2\pi i\omega A\int_0^a \chi_0(r)\, r\, dr, \qquad (5.7.4)$$

and from (5.7.2), (5.7.3)

$$\chi_0(r) = \left.\frac{\partial\psi_0}{\partial z}\right|_{z=d}.$$

Hence

$$q_{vs} = -2\pi i\omega A\int_0^a \left.\frac{\partial\psi_0}{\partial z}\right|_{z=d} r\, dr. \qquad (5.7.5)$$

Only the potential $\psi_0(r,z)$ is necessary to determine the induced volume flux q_{vs}. This potential can be found by separation of variables and writing the radial displacement due to ψ_0 at $r=a$ as an expansion in terms of the vertical eigenfunctions, exactly as for the radiation problem in §5. If $f, \mathcal{F}_n$ are replaced by $g, \mathcal{G}_n$ respectively in (5.5.4), (5.5.5) it is found that

$$\psi_0(r,z) = \left\{J_0(kr) - \frac{J_0'(ka)}{H_0^{(1)\prime}(ka)} H_0^{(1)}(kr)\right\}\frac{Z_0(z)}{Z_0'(d)} + \sum_{n=0}^{\infty}\frac{g_n K_0(k_n r) Z_n(z)}{k_n K_0'(k_n a)}, \quad (r\geq a), \qquad (5.7.6)$$

$$\psi_0(r,z) = \sum_{n=0}^{\infty}\frac{g_n I_0(k_n r)}{k_n I_0'(k_n a)} Z_n(z), \quad (r\leq a), \qquad (5.7.7)$$

(see Garrett 1970, equations (2.20),(2.22))

and matching the pressure at $r=a, 0\leq z\leq h$ as for the radiation potential Ψ, gives

$$\sum_{n=0}^{\infty} g_n R_n Z_n(z) = F_o Z_o(z) \quad , 0 \le z \le h, \tag{5.7.8}$$

and

$$\sum_{n=0}^{\infty} g_n Z_n(z) = 0 \quad , h \le z \le d, \tag{5.7.9}$$

(Garrett 1970, equations (2.29),(3.1)), where R_n is as defined in (4.2.14) and F_o is given by

$$F_o = 2i \left[\pi k^2 a^2 H_o^{(1)\prime}(ka) Z_o'(d) \right]^{-1}.$$

Multiplying (5.7.8), (5.7.9) by $(1/d)\ Z_m(z)$, integrating and adding yields

$$\sum_{n=0}^{\infty} E_{mn} g_n = C_m' \quad , (m = 0,1,2,\ldots), \tag{5.7.10}$$

where E_{mn} is the same as for the corresponding radiation problem (equation (5.5.10)) while

$$C_m' = F_o D_{om},$$

$$= (C_r + iC_i) q_m, \tag{5.7.11}$$

where q_m is given by (B.13) and

$$C_r = -\frac{Y_1(ka)}{Z_o(d)} \quad , C_i = -\frac{J_1(ka)}{Z_o(d)}. \tag{5.7.12}$$

The decomposition process used in Chapter 4, § 3 is now applied to the complex matrix equation (5.7.10). The coefficients g_n may be written

$$g_n = c_n + i d_n \quad , (c_n, d_n \text{ real}), \tag{5.7.13}$$

and, with E_{mo} decomposed as in (4.3.7), equation (5. 7.10) becomes

$$c_o p_m + \sum_{n=1}^{\infty} E_{mn} c_n = (C_r + d_o) q_m \qquad (5.7.14a)$$

$$d_o p_m + \sum_{n=1}^{\infty} E_{mn} d_n = (C_i - C_o) q_m \qquad (5.7.14b)$$

where both systems are real. If S_n is the solution of (4.3.11) as defined in § 5 then clearly

$$c_n = (C_r + d_o) S_n , \qquad (5.7.15a)$$

$$(n = 0, 1, 2, \ldots)$$

$$d_n = (C_i - C_o) S_n , \qquad (5.7.15b)$$

which, using (5.7.13), finally yields

$$g_n = \left\{ (C_r + S_o C_i) + i(C_i - S_o C_r) \right\} \frac{S_n}{1 + S_o^2} , (n = 0, 1, 2, \ldots). \qquad (5.7.16)$$

Returning to the expression (5.7.5) for the induced flux, with ψ_o given by (5.7.7), q_s is

$$q_s = -2\pi i \omega A \sum_{n=0}^{\infty} \frac{a g_n Z_n'(d)}{k_n^2} ,$$

$$= 2\pi i \omega a^2 A \sum_{n=0}^{\infty} \frac{N_n^{-\frac{1}{2}} g_n \sin k_n d}{k_n a} . \qquad (5.7.17)$$

Substituting for q_s in (5.7.1) enables the coefficient $\underline{B}$ to be evaluated. In all subsequent computations, the value of $\underline{B}$ found by this method agrees with that found via the radiation problem.

As noted by Garrett (1970), when $J_o'(ka) = J_1(ka) = 0$ no scattered wave or local transient field is required to satisfy the boundary conditions and the matching for ψ_o (see equations (5.7.6),

(5.7.7); hence inside the duct

$$\chi_0(r) = J_0(kr) \quad , (r \le a),$$

and from (5.7.4), the induced volume flux is zero. Consequently, from (5.7.1), the coefficient $\underline{B}$ is also zero when $J_1(ka)=0$. Thus, exactly as for the circular pressure patch, the damping term $\underline{B}$ vanishes at an infinite number of frequencies.

Clearly for the mouth-upward duct of Chapter 4, since the damping coefficient is proportional to the square of the exciting force (see equations (4.4.8), (4.4.9)),a similar argument to that given above will hold to show that the exciting force is zero whenever $J_1(ka)=0$ Hence the damping coefficient for the mouth-upward duct must also vanish at $J_1(ka)=0$ as confirmed by the numerical results.

5.8 Results and Discussion

In the following results the performance factor, Ω_{max} of the duct is not presented in order to limit the number of Figures. The coefficients $\underline{A}$ and $\underline{B}$ are presented in non-dimensionalised form as

$$\underline{A} = -\frac{2\pi a^2}{\rho g}\mathcal{A} \quad , \quad \underline{B} = \frac{2\pi a^2 \omega}{\rho g}\mathcal{B}$$

It is useful to begin by examining the mouth-downward duct using a 'narrow-duct' approximation (see Appendix C) before proceeding with the computation of the results of § 6. Figure (5.11a) illustrates the variation of $\underline{A}$ as a function of $k\ell$ for $a/\ell = \frac{1}{4}$, $\ell/d = \frac{1}{2}$ and infinite depth. This contrasts sharply with the behaviour of $\underline{A}$ for the circular pressure patch of § 4. In this case there is just one zero of $\underline{A}$ which occurs near $k\ell = 1$ and, for $k\ell > 1$, $\underline{A}$ decreases monotonically to zero. There is a slight difference between the values of $\underline{A}$ for infinite depth and $\ell/d = \frac{1}{2}$; when $\ell/d = \frac{1}{4}$ the difference from the infinite depth value cannot be detected on the scale

used in Figure (5.11a). The damping term B has an extremely sharp resonance which reaches a maximum value when A=0, and is not shown here. It is noted, however, that the finite depth coefficient B has a slightly smaller maximum value at a slightly larger value of kl.

Figure (5.11b) shows the maximum capture width variation with when $a/l = \frac{1}{4}$. Both curves have narrow bandwidths which are found to become even narrower as the non-dimensional duct width a/l decreases. The curve for infinitely deep fluid shown in Figure (5.11b) agrees exactly with Evans' (1978) results for a duct enclosing a weightless float attached to a spring-damper system as a means of modelling the power take-off system, (when the external spring restoring force is zero). This is expected since the narrow duct approximation assumes uniform flow in the depths of the duct in which case both mechanisms of power extraction must produce the same results.

To examine the accuracy of the approximate solution, the full solutions for the various wave-power absorption quantities given in §6 are computed for $a/l = \frac{1}{4}$, $l/d = \frac{1}{2}$. It is found that the approximate solution for the coefficient A agrees very closely with the full solution for all values of $Kd \in [0,2]$. The coefficient B shows a greater discrepancy between the two solutions and this discrepancy increases as Kd increases. The approximate solution over predicts the value of B, (by 7% at $Kd = 0.8$, rising to 40% at $Kd = 2$), but the shapes of the two curves are very similar. A comparison of the maximum capture widths in the two cases is shown in Figure (5.12). Although the approximate solution indicates a larger bandwidth, the agreement between the results is reasonably good especially when is less than its value at resonance, and it must be remembered that the duct length is only twice its diameter; for narrower ducts the agreement is even better. For larger Kd, it is expected that the approximate solution will not be so good when the wavelength of the

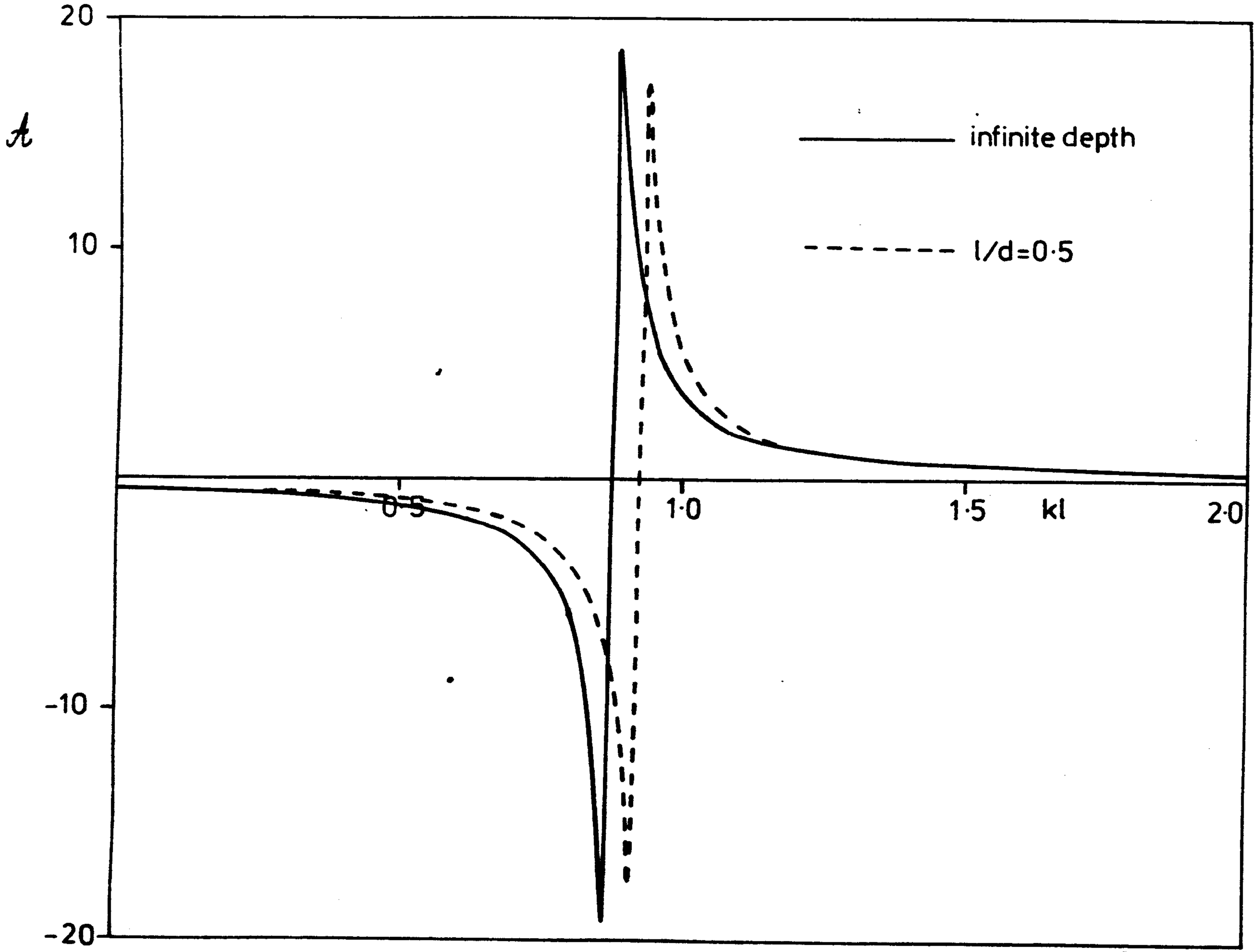

FIG (5·11a)

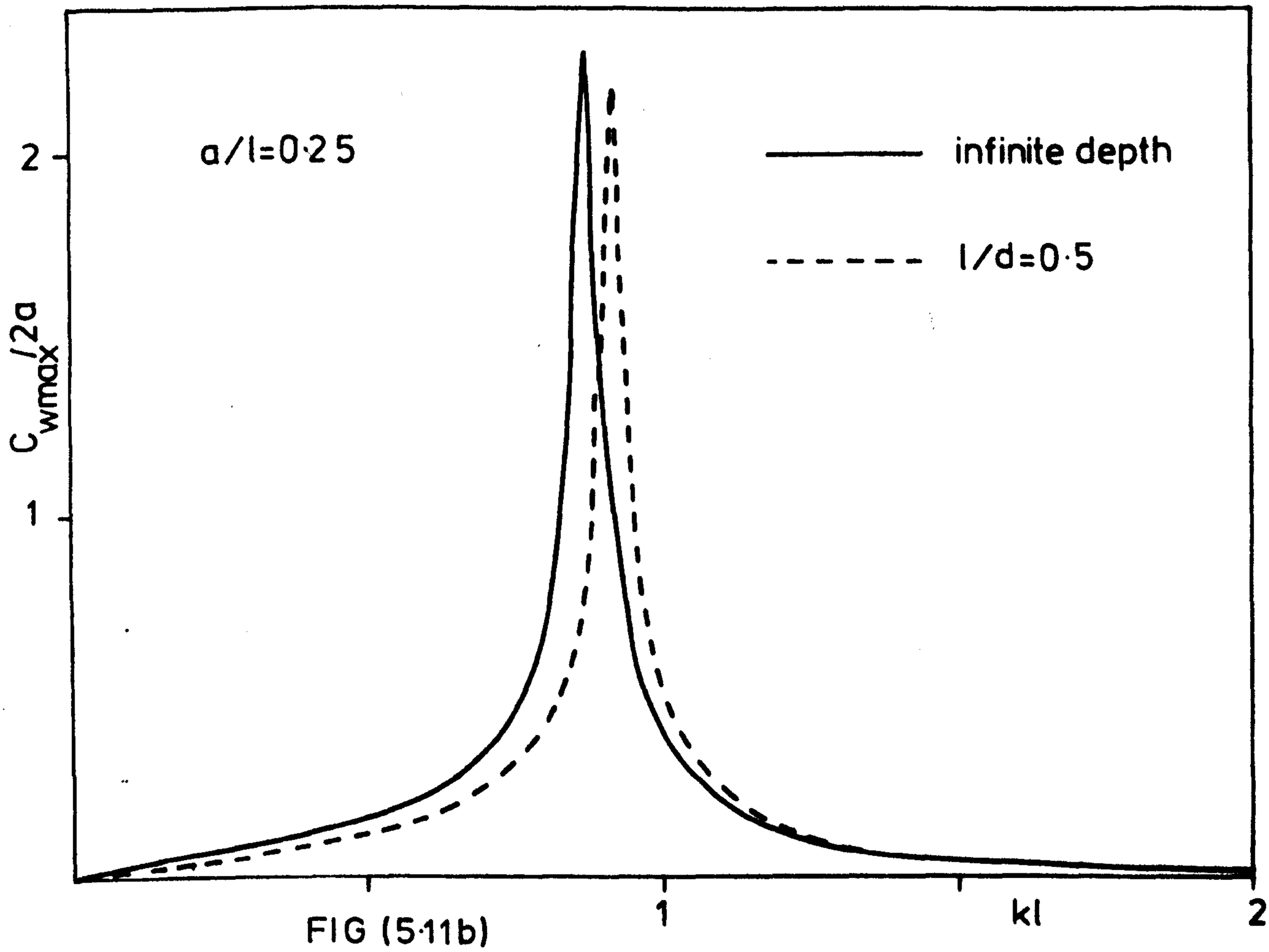

FIG (5·11b)

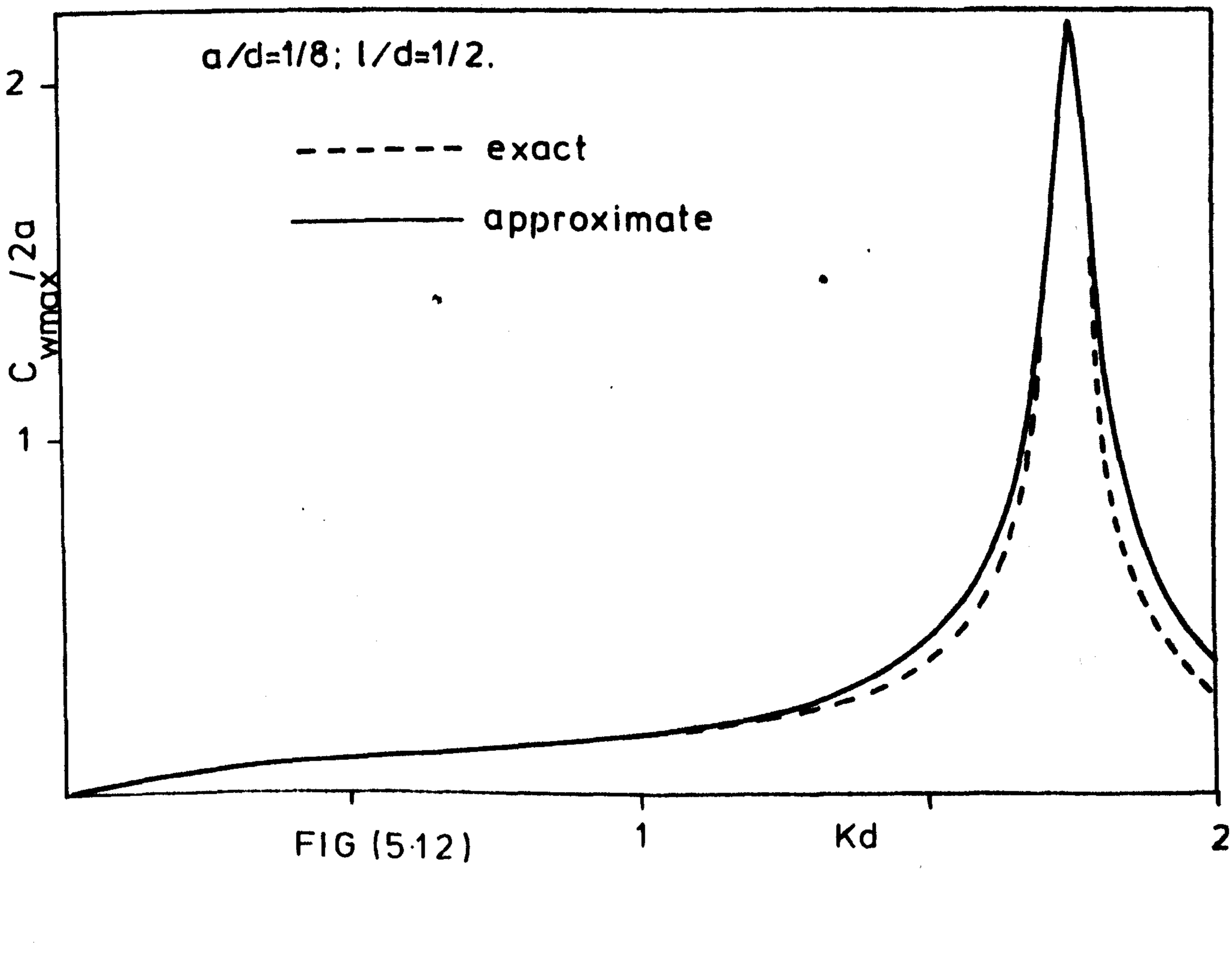

FIG (5·12)

incident waves is no longer large compared to the duct diameter.

For a narrow duct resonance occurs near $k\ell = 1$ when $\underline{A}$ is zero; Figure (5.13a) shows how the parameter a/d affects the coefficient $\underline{A}$ and the position of its first zero. As the radius of the duct is increased, so the peak values of $\underline{A}$ decrease and the value of Kd at which $\underline{A}$ is zero decreases. The maximum value of the damping term similarly decreases as a/d increases while the bandwidth of its curve increases; in each case its maximum value occurs when $\underline{A}=0$ (see Figure (5.13b)). Curves of the maximum capture width are given in Figure (5.13c). When a/d is greater than some value between $\frac{1}{4}$ and $\frac{1}{2}$ it can be seen that the maximum capture width will always be less than the duct diameter although a better bandwidth is achieved for larger a/d .

Figure (5.14a) illustrates the effect of the duct length upon the coefficient $\underline{A}$, when $a/d = 1$. As the duct length increases the first zero of $\underline{A}$ occurs at progressively smaller values of Kd . In addition, the first maxima and minima of $\underline{A}$ move closer together and increase in magnitude. The maximum value of $\underline{B}$ increases as increases and is attained at a smaller value of Kd, (when $\underline{A}=0$). Its behaviour can be seen in Figure (5.14b). It appears that the non-dimensional duct width a/ℓ is an important factor in determining the shape of the curves. For instance, when $a/d = 3$, $\ell/d = \frac{1}{2}$ the difference in appearance from the corresponding pressure patch curves is not so great as for $a/d = 1$, $\ell/d = \frac{1}{2}$ and its corresponding pressure patch results. The position of the first zero of $\underline{A}$ is similarly dependent upon a/ℓ . The capture width results are given in Figure (5.14c) for various ℓ/d . It is noticeable that for small ℓ/d there is very little variation in $C_{Wmax}/2a$ over the range $Kd = [0.3, 1.5]$. The theoretical maximum capture width $\lambda/2\pi$ is also shown on Figure (5.14c) as a dashed line, together with the results for the circular

pressure patch (shown as crosses). The results for the pressure patch, (which are also shown on Figures (5.14a,b)), clearly justify the assertion that it is a shallow draft approximation.

The maximum capture width is now examined using more realistic parameter values. For the Queen's University Belfast buoy (Long, 1979) it has been suggested that the duct diameter is of order 20-25m. while the duct length is a quarter of this value. Thus, in water of depth 40-50m., the parameter values are typically $a/d = \frac{1}{4}, l/d = \frac{1}{4}$. The maximum capture width variation is shown in Figure (5.15) for $a/d = \frac{1}{4}$ and different values of l/d. It can be seen that for $l/d = \frac{1}{4}$, its value never rises above 0.4 when $Kd \leq 2$, whereas for $l/d \geq \frac{1}{2}$ values of greater than unity are attained. A longer duct brings the first zero of $\underline{A}$ into the range $Kd \in [0,2]$ enabling the theoretical maximum, (shown as a dashed line), to be reached within this range. The narrow-duct approximation is shown in Figure (5.15) for $l/d = \frac{1}{2}, \frac{3}{4}$ (indicated by x and o respectively). The approximation overpredicts the maximum capture width as previously noted, and, as expected, is better for the narrower duct, i.e. $l/d = \frac{3}{4}$.

The behaviour of the maximum capture width for fixed $l/d = \frac{1}{8}$ and various values of a/d is shown in Figure (5.16). For $a/d \geq \frac{1}{2}$, $C_{Wmax}/2a$ reaches its maximum value within the range $Kd \in [0,2]$ but, for all values of a/d shown, the maximum capture width ratio is less than 0.4.

The capture width results so far presented in this section indicate the maximum possible capture width when the volume flow rate across the turbine is proportional to the pressure drop through it and the constant of proportionality is real and positive. The actual capture width curves when the system is 'tuned' to a particular wavenumber are contained in the envelope defined by the appropriate maximum capture width curve. If Γ_{opt}, given by (5.2.21), is chosen to

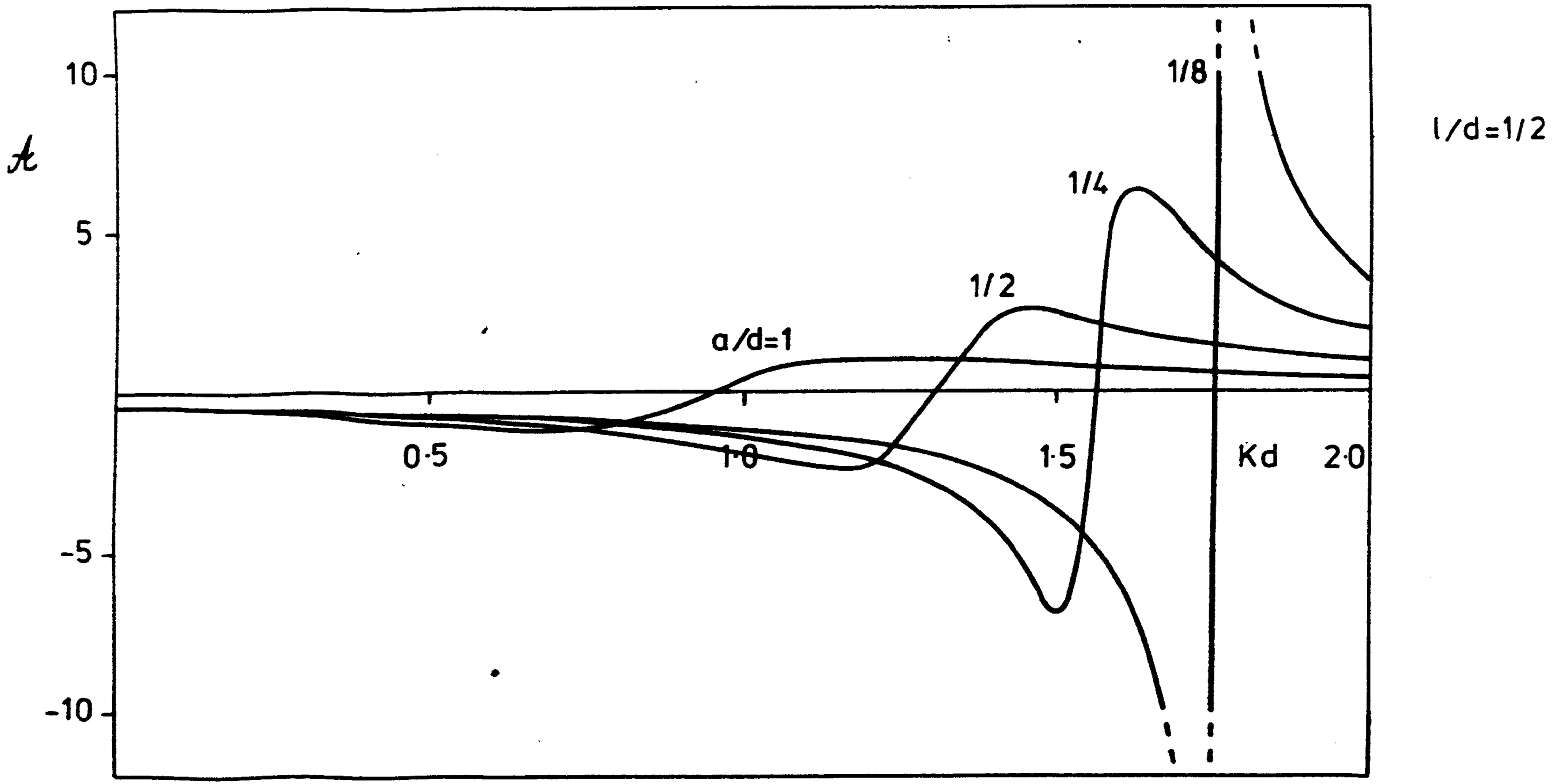

FIG (5·13a)

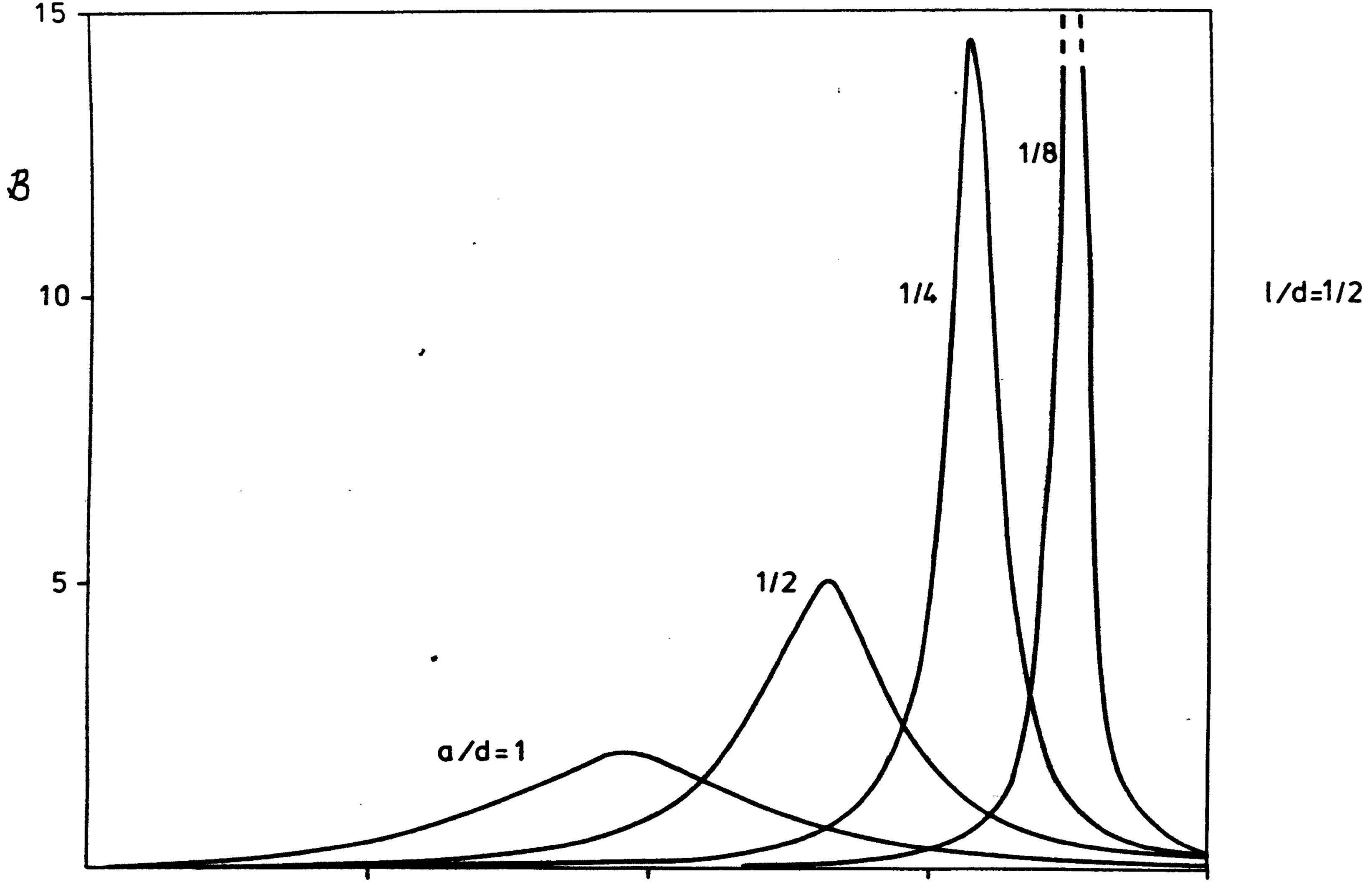

FIG (5·13b)

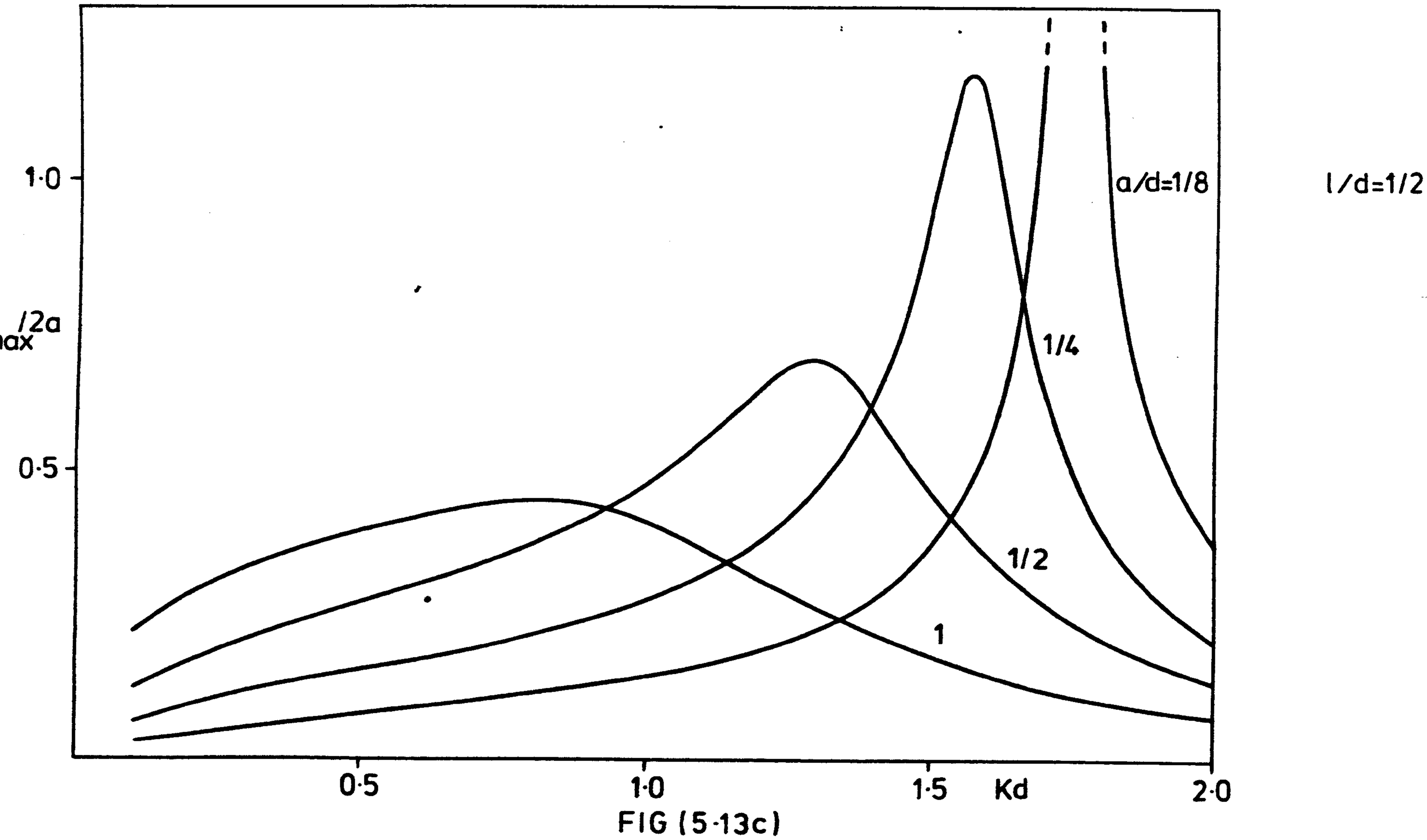

FIG (5·13c)

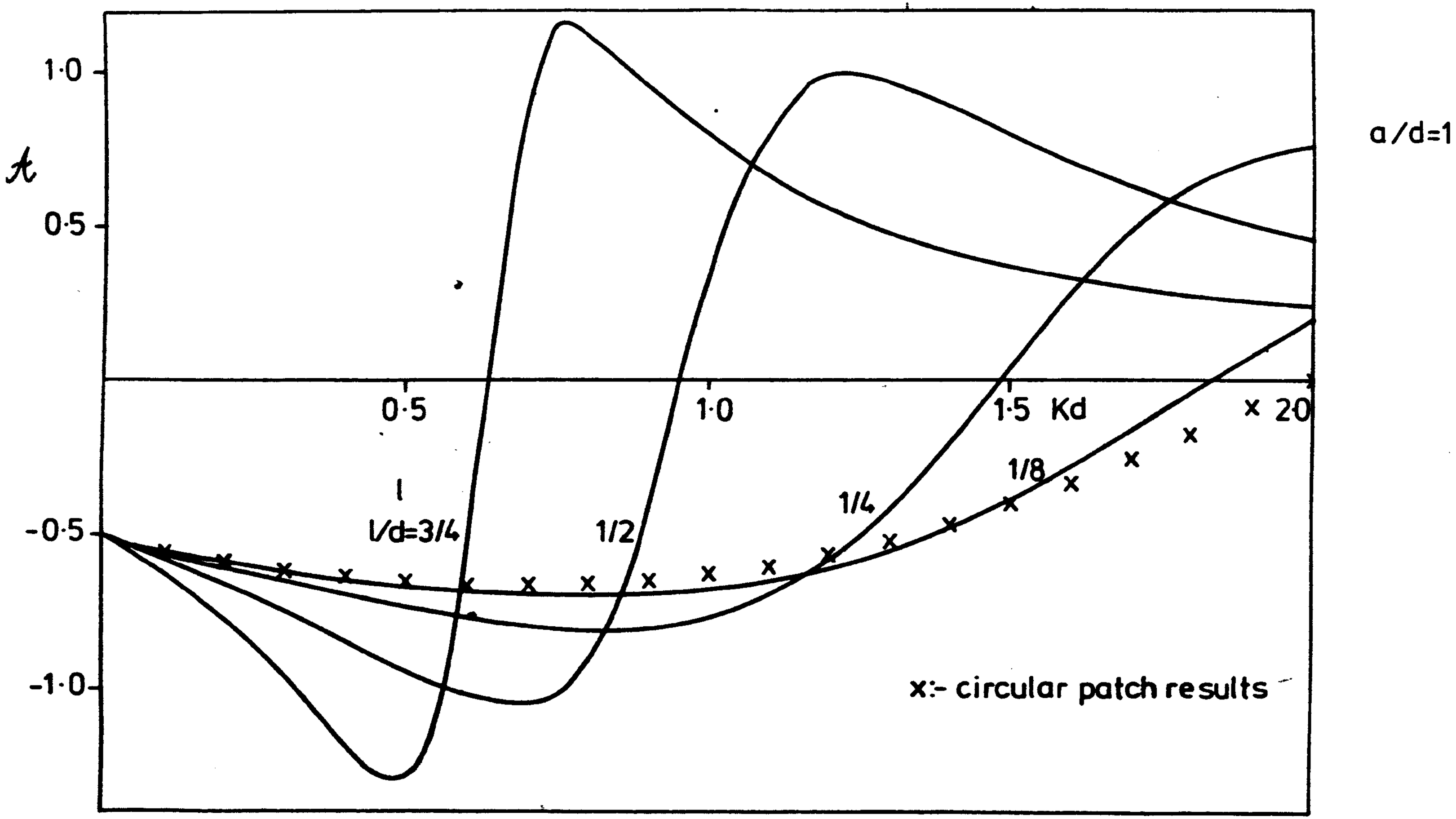
1·0
0·5
-0·5
-1·0
0·5
1·0
1·5 Kd
x 20
l/d=3/4
1/2
1/4
1/8
a/d=1
x:- circular patch results

FIG (5·14a)

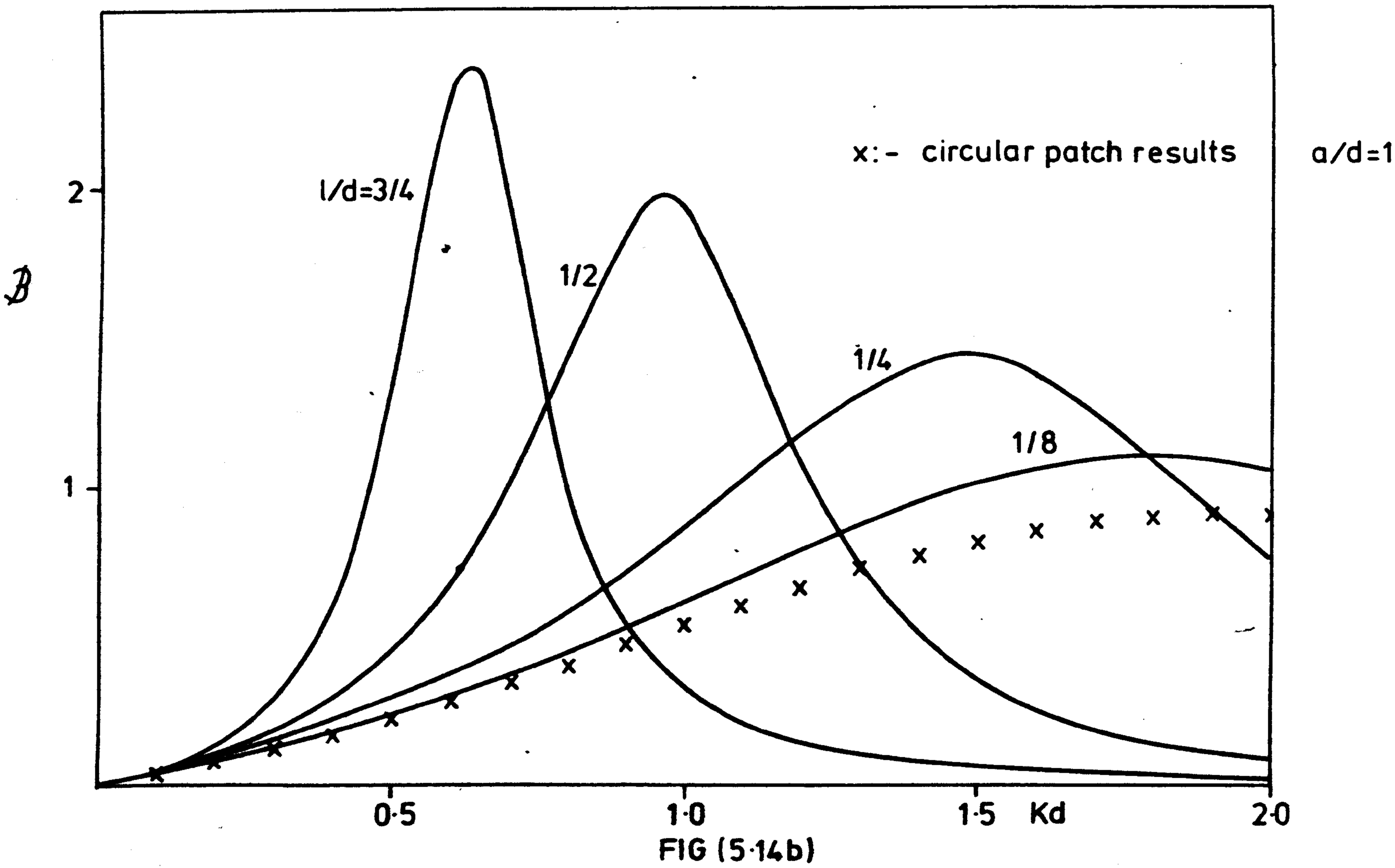

FIG (5·14b)

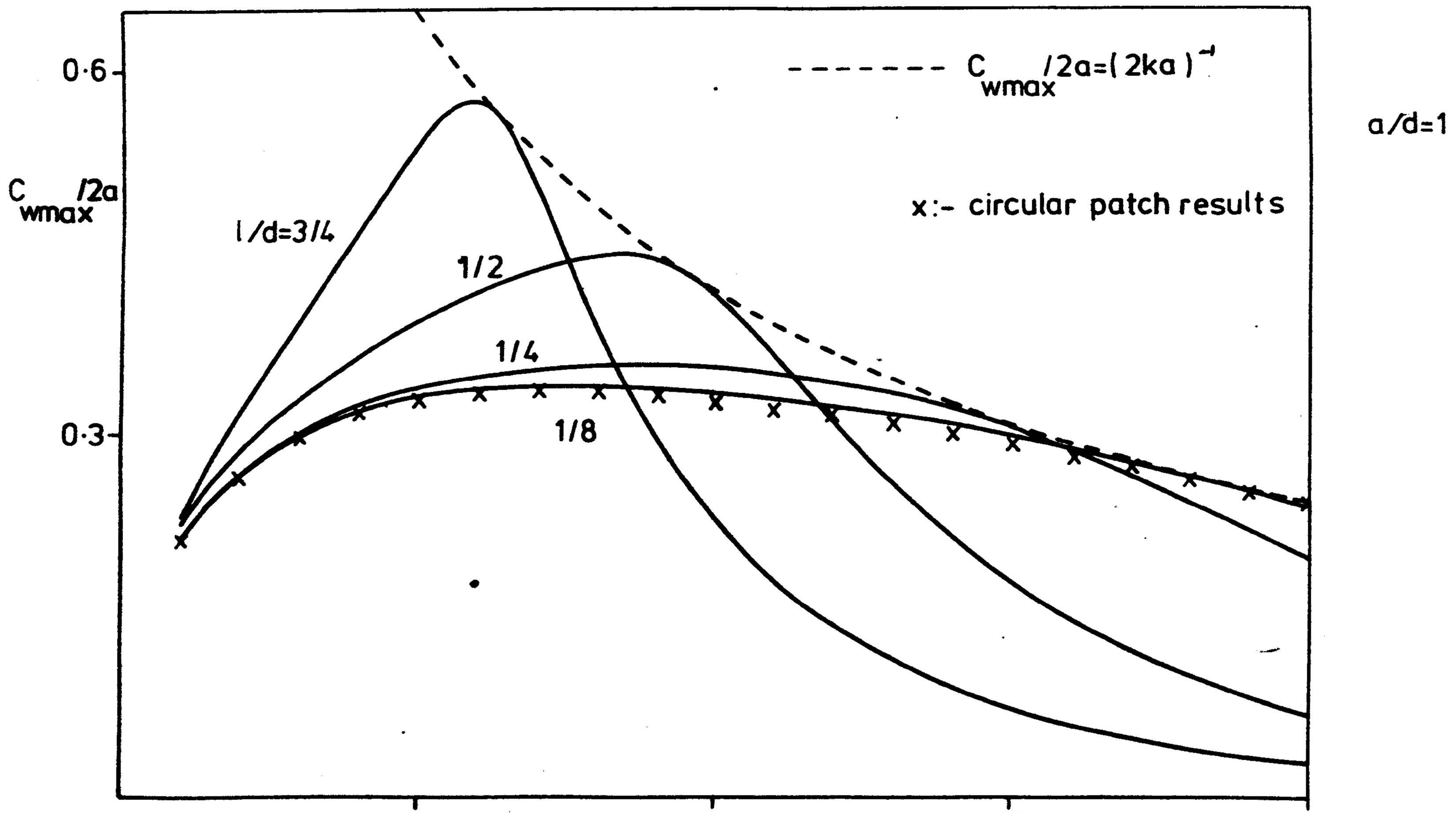
0·6
0·3
$C_{wmax}/2a$
$C_{wmax}/2a=(2ka)^{-1}$
a/d=1
x:- circular patch results
l/d=3/4
1/2
1/4
1/8
0·5
1·0
1·5
Kd
2·0

FIG (5·14c)

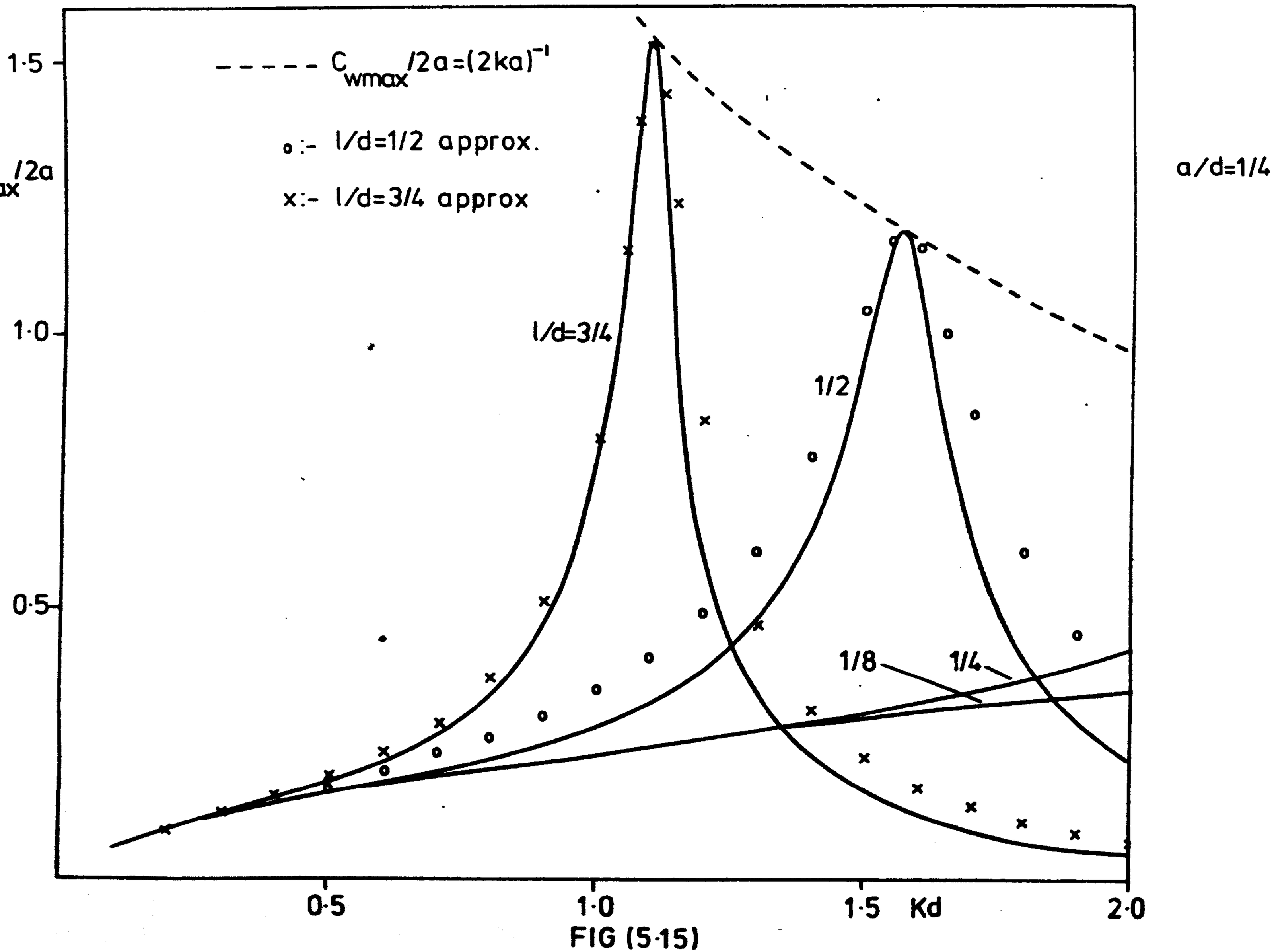
$C_{wmax}/2a$
1·5
1·0
0·5
$C_{wmax}/2a=(2ka)^{-1}$
o :- l/d=1/2 approx.
x :- l/d=3/4 approx
a/d=1/4
l/d=3/4
1/2
1/8
1/4
0·5
1·0
1·5
Kd
2·0

FIG (5·15)

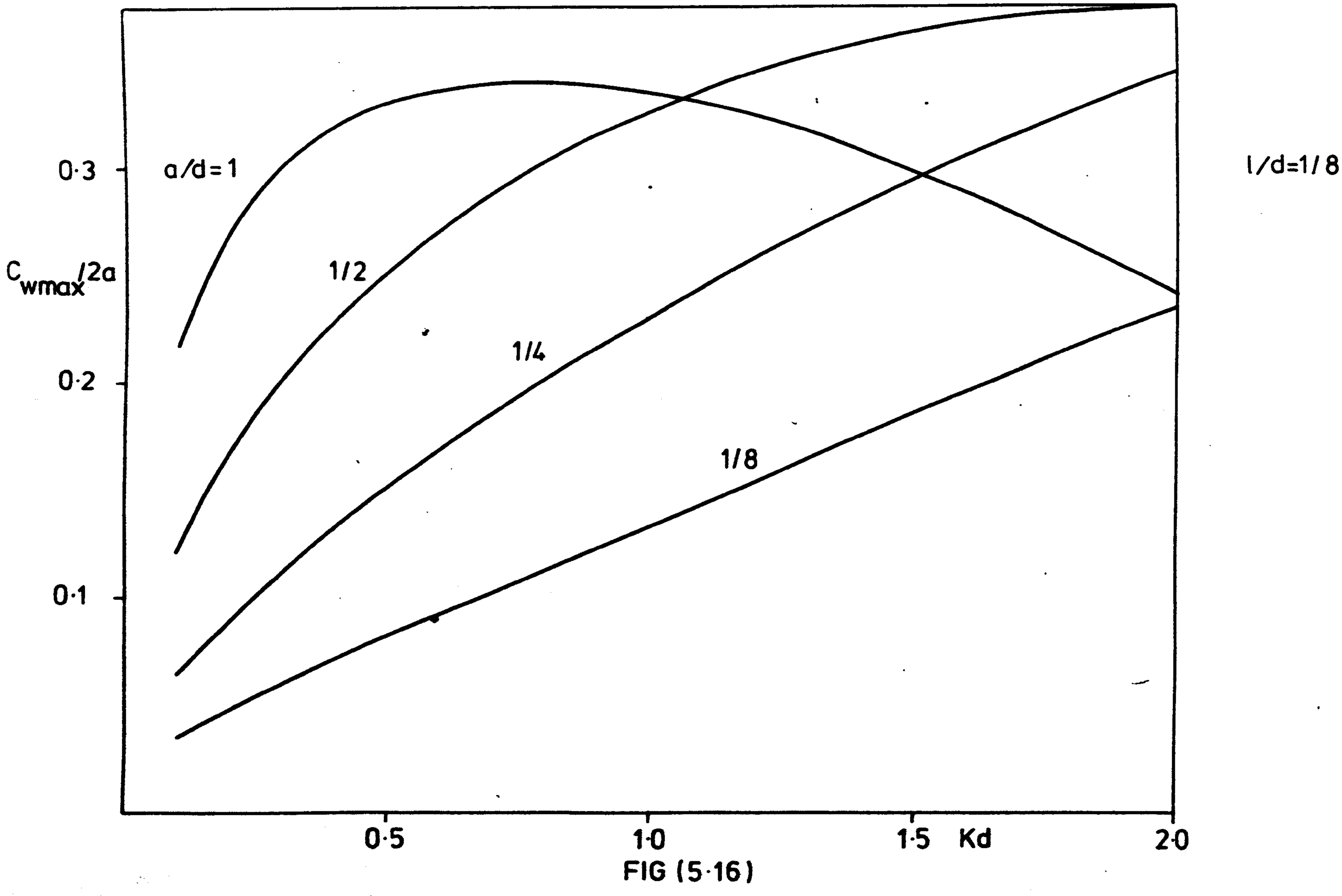

FIG (5·16)

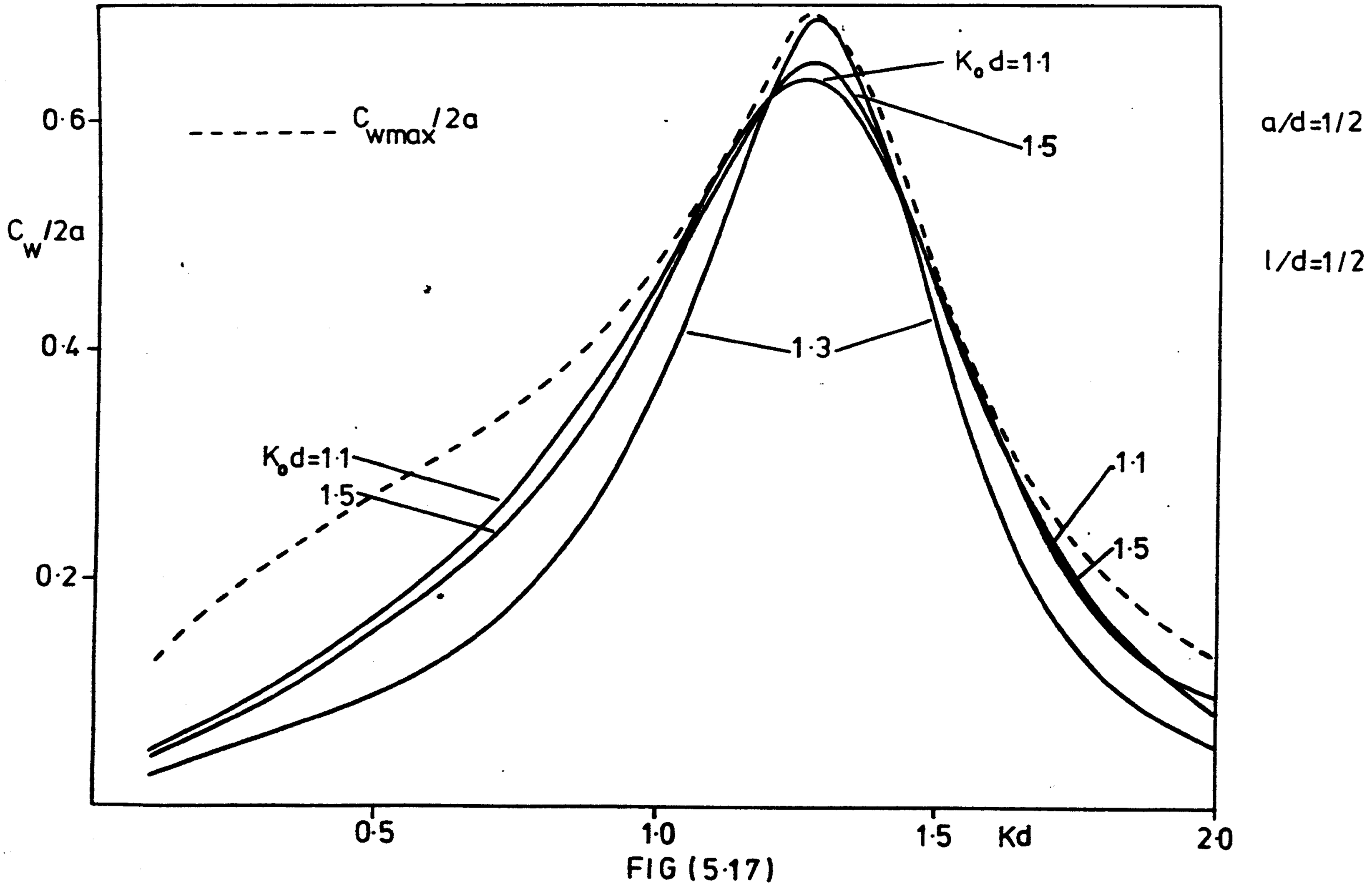
$C_{wmax}/2a$
$K_0 d=1{\cdot}1$
1·5
1·3
$K_0 d=1{\cdot}1$
1·5
1·1
1·5
a/d=1/2
l/d=1/2
$C_w/2a$
0·6
0·4
0·2
0·5
1·0
1·5
Kd
2·0

FIG (5·17)

give a maximum capture width value at a particular wavenumber then the capture width may be found from (5.2.19). Figure (5.17) illustrates the actual capture width behaviour when the tuned wavenumber, $K_0 d = 1.1, 1.3, 1.5$ and $a/d = \frac{1}{2}, l/d = \frac{1}{2}$.

As in Chapter 4, the solution of two infinite systems of real equations, defined in §5, is required in computing the capture widths and coefficients, $\underline{A}$ and $\underline{B}$. For the mouth-upward and mouth-downward duct these systems are very similar and the comments made concerning the mouth-upward duct in Chapter 4, §6 (c) apply in this case also. It was found however, that when the duct is narrow, the values of the coefficients $\underline{A}$ and $\underline{B}$ are very large near resonance and the number of terms, N retained in the systems needs to be larger in this region in order to maintain accuracy; a linear extrapolation of results for $1/N$ to zero using T=80,90 rather than 40,50 produced better results here.

5.9 Conclusion

The theory of wave-power absorption by surface pressure distributions derived by Evans (1981b) has been applied to mouth-downward ducts of different configurations. In the first part of this Chapter the shallow draft approximation has been used to analyse ducts of rectangular and circular cross-section. The study of the theoretical maximum capture width for the rectangular duct provides a useful example of the influence of wave direction upon device performance. The maximum capture width of a circular duct is examined in the more realistic situation when it is not possible to introduce a phase difference between the volume flow rate through and pressure drop across the air-turbine. As for the mouth-upward duct and corresponding oscillating disc problem, this simplified model is very helpful in understanding the behaviour of a mouth-downward duct which is not of shallow draft.

The second part of this Chapter is concerned with the mouth-downward duct of circular cross-section when no restriction is placed upon its draft. The maximum capture width attains its theoretical maximum $\lambda/2\pi$ when $\underline{A}$ is zero and $\underline{B}$ reaches a local maximum value. For a narrow duct, when a/ℓ is small, this occurs near $k\ell = 1$ whereas for a duct of shallow draft, when ℓ/a is small, it initially happens near $ka=2$. For ducts of an intermediate configuration the theoretical maximum is achieved at a wavenumber between these two extremes.

The high capture widths obtainable near $k\ell=1$ for a narrow duct are related to the manometric resonance which occurs in open tubes, discussed by Isaacs & Wiegel (1949). Maximum capture width ratios ($C_{Wmax}/2a$) of greater than unity are possible in this case but the bandwidth of the maximum capture width curves is very narrow. A wide or shallow draft duct does produce curves with much better bandwidths but their maximum capture width ratios are almost invariably less than a half.

A better overall performance (in the sense of a reasonably high maximum capture width ratio coupled with a broad bandwidth) can be achieved by ducts which are neither narrow nor of shallow draft but these ducts might have excessively large structures. An example of a duct with a reasonable performance is the one with parameters $a/d=\frac{1}{4}$, $\ell/d=\frac{1}{2}$ which would have a diameter and length of 20m in water of depth 40m. The results clearly show that the choice of duct parameters influences the range of wavenumbers over which the duct can achieve high capture width ratios. For example, it is pointless to choose $a/d=\frac{1}{4}$, $\ell/d=\frac{3}{4}$ when a good performance is required in the region of $Kd=1.7$, say. This factor, together with structural costs, is important in determining the shape of the duct.

It has been found experimentally that the performance of the duct can be significantly improved by introducing a flat horizontal circular plate, of slightly larger diameter than the duct, a short distance below the duct mouth (Whittaker & Murray, 1981). There may be other ways of achieving better results, such as choosing a different cross-sectional shape or, as Lighthill (1979) suggests, using a tapered duct. Finally, as noted in Chapter 4, the possible favourable interaction of devices in arrays could result in an improved performance.

I should like to thank Dr. W.G. Boyd for his helpful suggestions concerning the limit analysis in § 3.

CHAPTER 6

MEAN FORCES ON CYLINDERS

6.1 Introduction

The previous three chapters have been concerned with the energy absorbing characteristics of different types of oscillating water-column devices. In this chapter a different hydrodynamic aspect of bodies in waves is examined : the mean force.

Before defining the term 'mean force', it is first necessary to understand the approximations involved in linearised water-wave problems. To study such problems the velocity potential and other functions inherent in the problem are expanded as perturbation series in terms of some dimensionless parameter ε (usually taken to be the wave slope). These series are substituted into the equations of fluid motion and the boundary conditions. When the terms are grouped according to the power of ε, a sequence of equations and boundary conditions is created. The system corresponding to the coefficient of ε is known as the first-order or linearised problem and this is described in Chapter 2. In addition to this, a sequence of higher-order problems exists corresponding to higher orders of ε . The first-order problem is hence an approximation which becomes increasingly accurate as the perturbation parameter $\varepsilon \rightarrow 0$ and for this reason is also known as the infinitesimal wave approximation. A more detailed explanation of the perturbation procedure can be found in Wehausen & Laitone (1960).

When waves are incident upon a body which is floating or submerged in a fluid, the body experiences a hydrodynamic force due to the waves. To first-order the force is oscillatory in time, having the same frequency as the incident wave and so, when a time-average over a cycle is taken, there is no net or mean first-order force. Although

the second-order force is smaller in magnitude than the first-order oscillatory force, it does in general have a non-zero time-averaged or mean value and this Chapter is concerned with this mean second-order force.

The mean-force can be important in situations where the restoring force is weak. This arises in ship hydrodynamics when the mean horizontal or drift force can result in a significant displacement of an unanchored ship over a large period of time. The drift force and moment on ships in waves has been investigated by Newman (1967). The mean vertical force can cause large vertical motions of submerged, neutrally buoyant bodies and its effect on such bodies which are also slender has been examined by Lee & Newman (1971). Mean forces and moments are also thought to be the cause of the instability of semi-submersible offshore platforms (Martin & Kuo, 1979).

The mean horizontal force on floating or submerged bodies with application to sand bars and wave power devices has been studied by Longuet-Higgins (1977). This problem has practical significance in that the force can present mooring problems for wave power devices. The first part of this Chapter is concerned with the mean vertical force on the Bristol Cylinder when it is absorbing power. Preliminary experiments suggest that this force can be appreciable and an understanding of its behaviour is clearly desirable.

The analysis presented is a generalisation of the method of Ogilvie (1963) who noted that the mean second-order force could be found from knowledge of the first-order problem only. Ogilvie then proceeded on a comprehensive investigation of the first-order and mean second-order forces on submerged circular cylinders which are either fixed, freely-floating and neutrally buoyant, or undergoing forced oscillation. The method of solution presented in this Chapter

enables Ogilvie's results for the fixed and the freely-floating, neutrally buoyant cylinder to be recovered as special cases. It is shown that the expression for the mean horizontal force agrees with that due to Longuet-Higgins. Results are presented to illustrate the variation of the mean vertical force with wavenumber, depth of submergence and tuning frequency. A comparison is made of the mean vertical force with the corresponding force on fixed and freely floating cylinders together with the mean horizontal force on the Bristol cylinder. The behaviour of the first-order forces is examined and also the effect of fluid depth.

A study of the mean force on submerged cylinders of arbitrary cross-section is undertaken in the second part of this Chapter. As in Newman (1967) and Lee & Newman (1971), momentum arguments may be used to express the mean vertical force as an integral over the free surface, while the mean horizontal force reduces to Longuet-Higgins' (1977) result. The surface integral is examined and it appears that the mean vertical force can be approximated by a simple expression when the cylinder is deeply submerged and either fixed or freely-floating. A comparison is made between this approximation, an approximation due to Ogilvie (1963) and the exact results for circular cylinders.

The formulation in this Chapter is slightly different from that given in Chapter 2. Cartesian co-ordinates (x,y) are chosen instead of (x,z) and z will be used to represent the complex number $z=x+iy$ in the analysis of the first part of this Chapter; this is consistent with Ogilvie's (1963) notation. Secondly, the time-dependence of the velocity potential is not immediately removed but is retained during the formulation in order that the time average may be taken.

(a) Mean Forces on the Bristol Cylinder

6.2 Formulation

Consider a circular cylinder of radius a submerged in infinitely deep fluid with its centre at a depth h below the undisturbed free surface, such that $a<h$. Cartesian coordinates (x,y) are chosen such that y=0 is the undisturbed free surface and y= -h is the position of the cylinder centre, as shown in Figure (6.1).

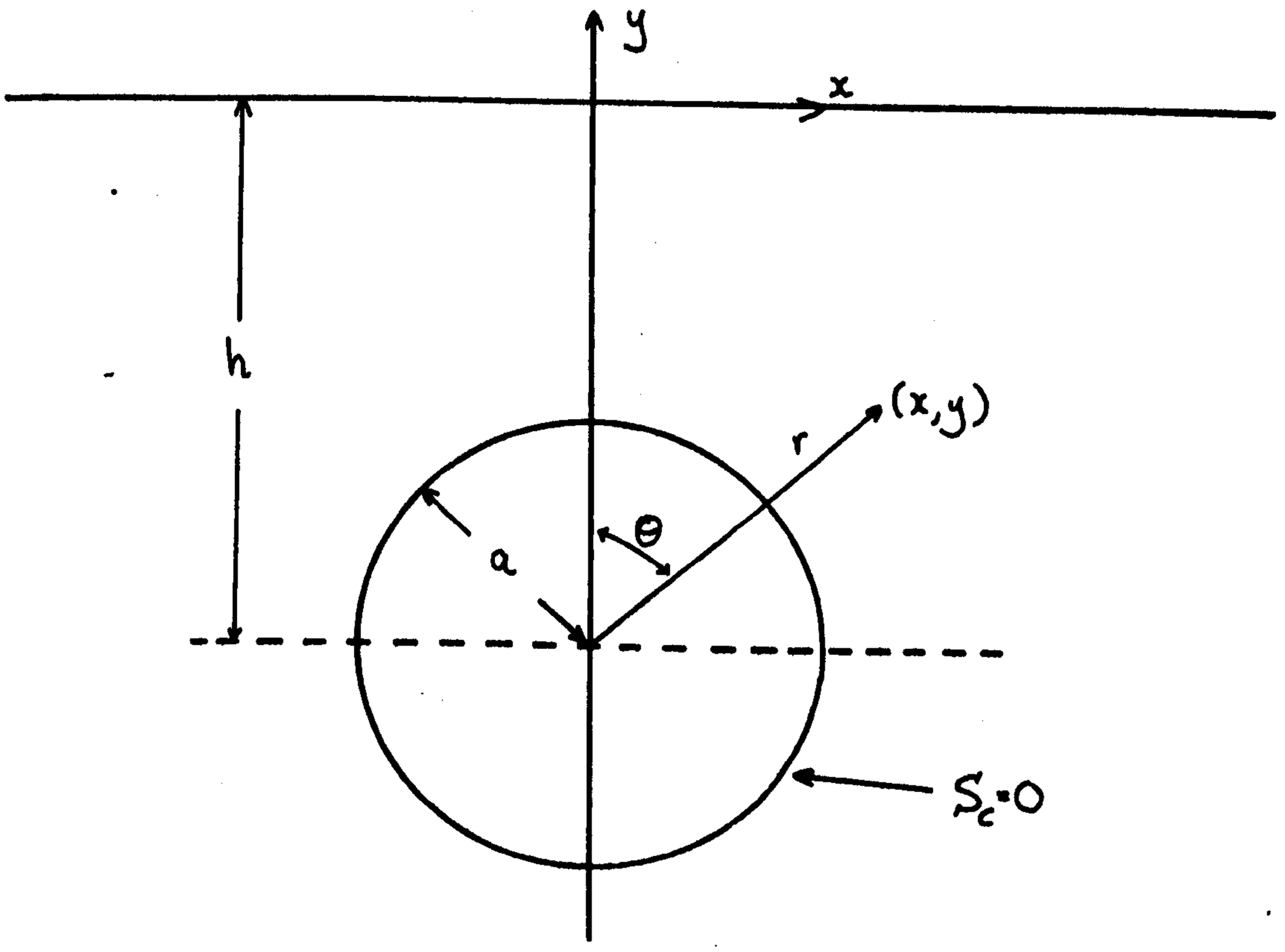

FIGURE (6.1)

When a regular wavetrain of frequency ω is incident upon the cylinder, the cylinder responds under the constraints of the power take-off mechanism. Its resultant motion is a linear combination of its motions parallel to the x and y axes, i.e. its motion in sway and heave respectively.

The linearised first-order velocity potential $\bar{\Phi}(x,y,t)$ satisfies the two-dimensional Laplace equation

$$\partial^2\bar{\Phi}/\partial x^2 + \partial^2\bar{\Phi}/\partial y^2 = 0, \qquad (6.2.1)$$

the linearised free surface condition

$$\partial^2\bar{\Phi}/\partial t^2 + g\,\partial\bar{\Phi}/\partial y = 0 \ , \ \text{on } y=0, \qquad (6.2.2)$$

and, assuming the fluid to be infinitely deep,

$$\nabla\bar{\Phi} \longrightarrow 0 \quad \text{as } y \longrightarrow -\infty. \qquad (6.2.3)$$

Equations (6.2.1)-(6.2.3) correspond to equations (2.2.2),(2.2.4) and (2.2.6) but, in this case, the time-dependence of the velocity potential has been retained.

Let $\xi(t), \eta(t)$ be the displacements of the cylinder in the x,y directions respectively, that is, at time t, the cylinder centre is at $x = \xi(t), y = -h + \eta(t)$. Then the linearised boundary condition on the cylinder surface, that the component of the body velocity normal to the surface is equal to the normal velocity of the fluid at that point, is given by

$$\partial\bar{\Phi}/\partial n = \dot{\xi} n_1 + \dot{\eta} n_2 \ , \ \text{on } S_c, \qquad (6.2.4)$$

where $\underline{n} = (n_1, n_2)$ is the normal vector from the cylinder into the fluid at the point (x,z) and S_c is the undisturbed position of the cylinder surface, defined by $S_c(x,y) = x^2 + (y+h)^2 - a^2 = 0$.

The first-order linear oscillatory force on the cylinder is found by integrating the fluid pressure over the surface S_c , as explained in Chapter 2, thus

$$F_i(t) = \rho \int_S \partial\bar{\Phi}/\partial t \; n_i \, dS, \qquad (6.2.5)$$

where $F_i(t)$ is the force in the i-th. direction. Here $i=1,2$ corresponds to the x,y directions respectively. Ogilvie (1963) obtained an expression for the second-order force on the cylinder and, upon taking the time-average, noted that the mean second-order force did not depend upon the second-order velocity potential; it could be determined solely from the linearised first-order problem. Further details can be found in Ogilvie (1963), only his result is given here; the mean second-order force can be expressed as

$$\mathbb{F}_i = \rho \int_{S_c} \left\{ \frac{1}{2}\overline{\left(\frac{\partial\Phi}{\partial x}\right)^2}^t + \frac{1}{2}\overline{\left(\frac{\partial\Phi}{\partial y}\right)^2}^t + \xi \overline{\frac{\partial^2\Phi}{\partial x \partial t}}^t + \eta \overline{\frac{\partial^2\Phi}{\partial y \partial t}}^t \right\} n_i \, dS \qquad (6.2.6)$$

where $\mathbb{F}_i$ denotes the mean second-order force in the ith. direction, and the overbar followed by a t indicates the time-averaged quantity.

6.3 Equations of Motion of the Cylinder

In this section, a non-rigorous analysis is undertaken to determine the effect of the power take-off mechanism of the Bristol cylinder on its equations of motion. To begin with, consider a cylinder of finite length in fluid of finite depth.

Suppose the cylinder is of length L $(L \gg a)$ and is held down by a pair of cables at each end attached to the cylinder and anchored to the sea-bed via hydraulic pumps, as shown in Figure (6.2). The characteristics of the pumps are assumed to be linear so that they can be replaced by springs and dampers which have a resistance to motion proportional to the extension and rate of extension of the cables respectively.

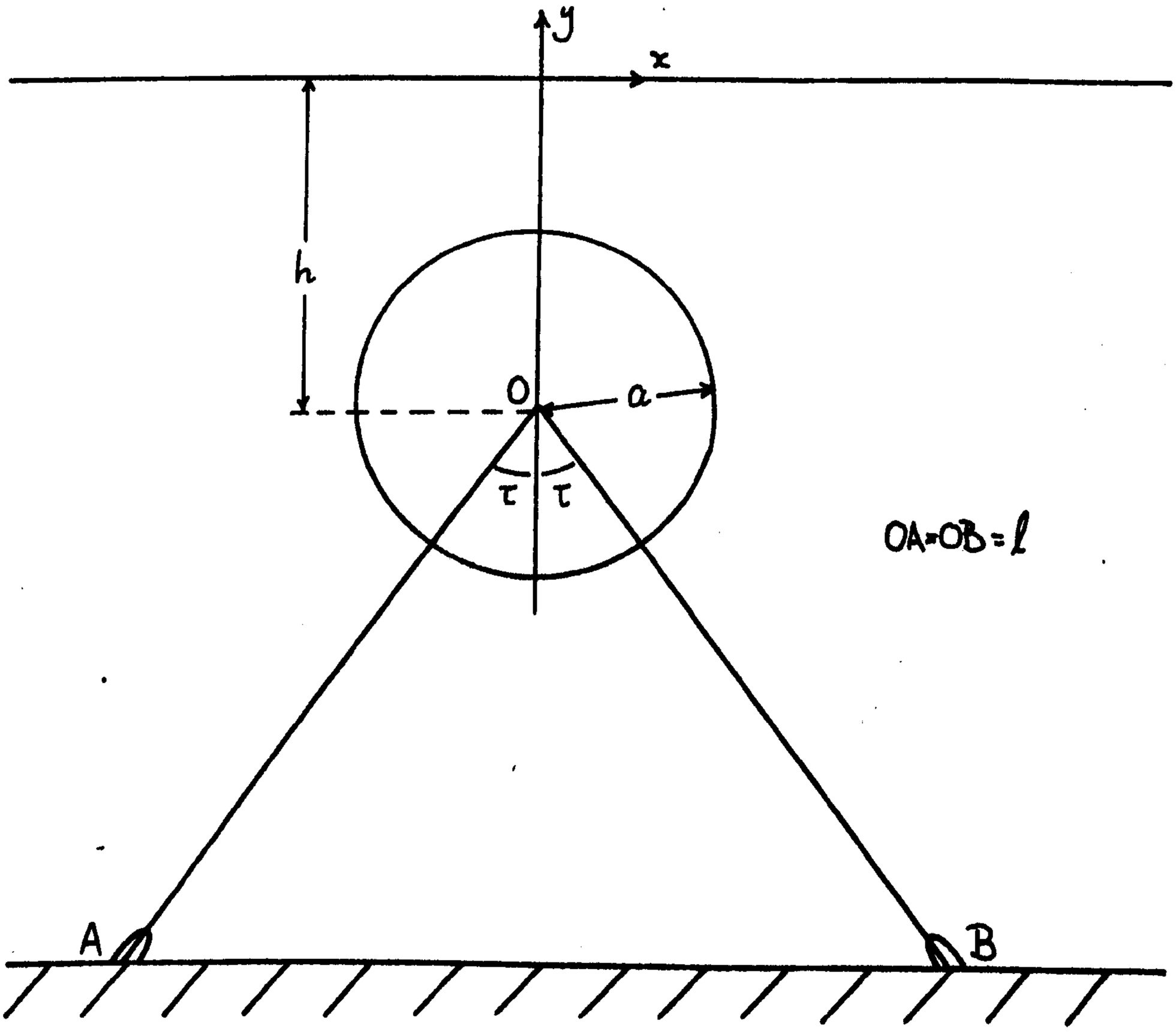

FIGURE (6.2)

Let the cables be of length l and inclined at an angle τ to the vertical. The cylinder is designed to be positively buoyant so that, when the fluid is undisturbed and the cylinder is at rest, the cable tension, $T_0 > 0$ is given by

$$4T_0 \cos\tau = (M_0 - m_0)gL = M_0 gL(1-m') \quad , (m' < 1), \qquad (6.3.1)$$

where M_0, m_0 and m' are the mass of fluid displaced, the cylinder mass and the relative cylinder mass $(= m_0/M_0)$ respectively, all measured per unit cylinder length.

If the cylinder centre is displaced by (ξ, η) then,

under the assumptions of linear theory, it is required that

$$|\xi(t)/\ell| \ll 1 \ , \ |\eta(t)/\ell| \ll 1,$$

and the extensions of OA,OB, denoted by $\delta A, \delta B$ respectively, can easily be shown to be

$$\delta A \simeq \xi \sin\tau + \eta\cos\tau, \qquad (6.3.2)$$

$$\delta B \simeq -\xi \sin\tau + \eta\cos\tau . \qquad (6.3.3)$$

When the cylinder is in motion the cable tensions in OA,OB are determined by

$$T_{OA} = T_0 + \frac{\hat{\alpha}}{2}\delta A + \frac{\hat{\beta}}{2}\dot{\delta A},$$

$$T_{OB} = T_0 + \frac{\hat{\alpha}}{2}\delta B + \frac{\hat{\beta}}{2}\dot{\delta B},$$

where $\hat{\alpha}/2$, $\hat{\beta}/2$ are the spring and damper constants of each cable. The force on the cylinder in the x - direction due to all the cables is hence found to be

$$\hat{C}_1 \simeq -\frac{4T_0}{\ell}\xi\cos^2\tau - 2\hat{\alpha}\xi\sin^2\theta - 2\hat{\beta}\dot{\xi}\sin^2\tau,$$

$$= \left(-\frac{4T_0}{\ell}\cos^2\tau - 2\hat{\alpha}\sin^2\tau\right)\xi - 2\hat{\beta}\sin^2\tau\,\dot{\xi} . \qquad (6.3.4)$$

This result has been derived for finite length cables; in the following mathematical analysis the cylinder is considered to be in infinitely deep fluid, thus the limit $\ell \to \infty$ should be taken for consistency. Hence

$$\hat{C}_1 \simeq -2\hat{\alpha}\sin^2\tau\,\xi - 2\hat{\beta}\sin^2\tau\,\dot{\xi} . \qquad (6.3.5)$$

A comparison of the terms comprising the coefficent of ξ in (6.3.4) gives

$$\frac{(2\tau_0/\ell)}{\hat{\alpha}} \simeq 0{\cdot}05,$$

using realistic values of the Bristol cylinder design parameters, so that (6.3.5) represents a reasonable approximation of (6.3.4) without considering a limit argument.

Similarly it can be shown that the force on the cylinder in the y - direction due to the cables can be written as

$$\hat{C}_2 \simeq -2\hat{\alpha}\cos^2\tau\ \eta - 2\hat{\beta}\cos^2\tau\ \dot{\eta} \qquad (6.3.6)$$

Note that, when the cables are splayed symmetrically, the cable forces in each direction depend only upon the displacement in that direction.

These forces can be written as forces per unit length by dividing by L and writing $C_1 = \hat{C}_1/L$, $C_2 = \hat{C}_2/L$ and thus

$$C_1 = -2\alpha\sin^2\tau\ \xi - 2\beta\sin^2\tau\ \dot{\xi},$$

$$C_2 = -2\alpha\cos^2\tau\ \eta - 2\beta\cos^2\tau\ \dot{\eta},$$

where $\alpha = \hat{\alpha}/L$, $\beta = \hat{\beta}/L$.

These equations give the hydrodynamic cable forces per unit length on a cylinder of finite length in deep fluid. In the following analysis, when the cylinder is idealised as being of infinite length, the same forces per unit length are assumed to be acting. It has also been implicitly assumed throughout that the cables themselves have negligible effect upon the fluid motion.

Hence the equations of motion of the idealised two-dimensional cylinder may be written as

$$m_0\ddot{\xi} + 2\beta\sin^2\tau\ \dot{\xi} + 2\alpha\sin^2\tau\ \xi = F_1(t), \qquad (6.3.7)$$

$$M_0\ddot{\eta} + 2\beta\cos^2\tau\,\dot{\eta} + 2\alpha\cos^2\tau\,\eta = F_2(t). \qquad (6.3.8)$$

Evans (1976) has shown that in order to attain an efficiency of 100% in power aborption at a particular frequency, ω_0 the following tuning conditions must be satisfied

$$2\alpha\sin^2\tau = (m_0 + M_{11})\omega_0^2, \; 2\beta\sin^2\tau = B_{11}, \qquad (6.3.9)$$

$$2\alpha\cos^2\tau = (m_0 + M_{22})\omega_0^2, \; 2\beta\cos^2\tau = B_{22}, \qquad (6.3.10)$$

where $M_{11}, B_{11}, (M_{22}, B_{22})$ are the added-mass and damping coefficients in sway (heave) respectively. For the cylinder in fluid of infinite depth, the sway and heave added-mass and damping coefficients are identical (Ogilvie, 1963), i.e. $M_{11} = M_{22} = M$, $B_{11} = B_{22} = B$ say. Hence from (6.3.9),(6.3.10) it is required that $\tau = 45^\circ$ and (6.3.7), (6.3.8) become

$$M_0\ddot{\xi} + \beta\dot{\xi} + \alpha\xi = F_1(t), \qquad (6.3.11)$$

$$M_0\ddot{\eta} + \beta\dot{\eta} + \alpha\eta = F_2(t), \qquad (6.3.12)$$

while the tuning conditions (6.3.9), (6.3.10) reduce to

$$\alpha = \{m_0 + M(\omega_0)\}\omega_0^2, \; \beta = B(\omega_0), \qquad (6.3.13)$$

giving total wave power absorption at $\omega = \omega_0$.

6.4 Solution of the Linear Problem

The mean second-order force is non-linear and thus, unlike the first-order force, it cannot be written as the sum of radiation forces and an exciting force. Hence the decomposition of the velocity

potential into a scattering potential and radiation potentials (see equation (2.2.15)) is not performed and a solution in terms of the total potential $\Phi(x,y,t)$ is sought.

The general solution of the linear problem has been determined by Ursell (1950). Only an outline of the method of solution is given here, together with results necessary in the later analysis. The following results can be found in Ogilvie (1963), who gives a more detailed precis of Ursell's method.

The velocity potential $\Phi(x,y,t)$ may be written as

$$\Phi(x,y,t) = Re\{f(z,t)\}, \text{ where } z = x+iy. \tag{6.4.1}$$

The potential of a wavetrain incident from $x = +\infty$ is then given by (see equation (2.2.14))

$$f_o(z,t) = g\frac{A}{\omega} e^{-iKz-i\omega t}, \tag{6.4.2}$$

and the total potential $f(z,t)$ may be expressed as

$$f(z,t) = f_o(z,t) + \sum_{n=1}^{\infty} \{\alpha_n f_{n1}(z,t) + \beta_n f_{n2}(z,t) + \gamma_n g_{n1}(z,t) + \delta_n g_{n2}(z,t)\}, \tag{6.4.3}$$

where f_{n1}, f_{n2}, g_{n1} and g_{n2} are a set of singularity potentials (see Appendix D), each of which satisfies (6.2.1)-(6.2.3) and represents outgoing waves only as $x \to \pm\infty$; they also form a complete set on r=a in terms of which the normal velocity of the fluid can be expanded. The unknown constants $\alpha_n, \beta_n, \gamma_n$ and δ_n are determined by applying the boundary condition on the cylinder given by (6.2.4). If the displacements ξ, η are decomposed as

$$\xi(t) = \xi_1 \sin\omega t + \xi_2 \cos\omega t, \tag{6.4.4a}$$

$$\eta(t) = \eta_1 \sin\omega t + \eta_2 \cos\omega t, \tag{6.4.4b}$$

then (6.2.4) becomes

$$\frac{\partial}{\partial r}\left\{Re\,f(z,t)\right\} = \omega\cos\theta\left(\eta_1\cos\omega t - \eta_2\sin\omega t\right) + \omega\sin\theta\left(\xi_1\cos\omega t - \xi_2\sin\omega t\right), \quad (6.4.5)$$

on $r=a$,

where (r,θ) are polar coordinates with origin at the cylinder centre such that $\theta=0$ corresponds to the positive y-axis, i.e. $x=r\sin\theta$, $y=-h+r\cos\theta$.

Substitution of (6.4.3) into (6.4.5) yields four sets of equations involving the unknown coefficients and the as yet undetermined displacements. As shown by Ursell, these equations may be uncoupled to give expressions for α_n, β_n, γ_n and δ_n in terms of the displacements and the solutions ξ_n, η_n of two infinite systems of equations (see Appendix D, equations (D.3)-(D.4)).

6.5 Evaluation of the Forces

The velocity potential may now be expressed in terms of the unknown displacements. The next step is to use the equations of motion of the cylinder to determine the displacements which, in turn, enables the first-order and mean second-order forces to be evaluated.

The first-order forces can be found from (6.2.5) and are given by (Ogilvie, 1963, equation (37))

$$F_1(t) = \pi\rho\omega a\left\{\left(\frac{2\delta_1}{ka} - \omega a\xi_1\right)\sin\omega t - \left(\frac{2\gamma_1}{ka} + \omega a\xi_2\right)\cos\omega t\right\}, \quad (6.5.1a)$$

$$F_2(t) = \pi\rho\omega a\left\{\left(\frac{2\beta_1}{ka} + \omega a\eta_1\right)\sin\omega t - \left(\frac{2\alpha_1}{ka} - \omega a\eta_2\right)\cos\omega t\right\}. \quad (6.5.1b)$$

Using the equations of motion (6.3.11),(6.3.12) together with (6.4.4a,b) it is found that

$$-\frac{m_0\omega^2}{M_0}(\xi_1\sin\omega t+\xi_2\cos\omega t)+\frac{\beta\omega}{M_0}(\xi_1\cos\omega t-\xi_2\sin\omega t)+\frac{\alpha}{M_0}(\xi_1\sin\omega t+\xi_2\cos\omega t)$$

$$=\frac{\omega}{a}\left\{\left(\frac{2\delta_1}{Ka}-\omega a\xi_1\right)\sin\omega t-\left(\frac{2\gamma_1}{Ka}+\omega a\xi_2\right)\cos\omega t\right\}, \qquad (6.5.2a)$$

$$-\frac{m_0\omega^2}{M_0}(\eta_1\sin\omega t+\eta_2\cos\omega t)+\frac{\beta\omega}{M_0}(\eta_1\cos\omega t-\eta_2\sin\omega t)+\frac{\alpha}{M_0}(\eta_1\sin\omega t+\eta_2\cos\omega t)$$

$$=\frac{\omega}{a}\left\{\left(\frac{2\beta_1}{Ka}+\omega a\eta_1\right)\sin\omega t-\left(\frac{2\alpha_1}{Ka}-\omega a\eta_2\right)\cos\omega t\right\}, \qquad (6.5.2b)$$

where $M_0=\pi a^2\rho$ is the mass of fluid displaced by the cylinder per unit length.

Substituting from (D.3) for $\alpha_1,\beta_1,\gamma_1$ and δ_1 yields four equations for the four unknowns ξ_i and η_i, $(i=1,2)$. These equations may be simplified by writing

$$\tilde{\alpha}=\frac{\alpha}{M_0\omega^2}-\left(\frac{m_0}{M_0}-1\right), \qquad (6.5.3)$$

$$\tilde{\beta}=\frac{\beta}{M_0\omega}, \qquad (6.5.4)$$

and, after some algebra (see Appendix D), it can be shown that

$$\xi_1=-\eta_2=\frac{-gAe^{-kh}\varepsilon_1(S_3\varepsilon_1-S_2\beta_1+\tilde{\beta}/2+S_2\tilde{\alpha}/2)}{\omega^2a(Ka)\{(\beta_1+S_2\tilde{\beta}/2-\tilde{\alpha}/2)^2+(S_3\varepsilon_1-S_2\beta_1+S_2\tilde{\alpha}/2+\tilde{\beta}/2)^2\}}, \qquad (6.5.5a)$$

$$\xi_2=\eta_1=\frac{gAe^{-kh}\varepsilon_1(\beta_1+S_2\tilde{\beta}/2-\tilde{\alpha}/2)}{\omega^2a(Ka)\{(\beta_1+S_2\tilde{\beta}/2-\tilde{\alpha}/2)^2+(S_3\varepsilon_1-S_2\beta_1+S_2\tilde{\alpha}/2+\tilde{\beta}/2)^2\}} \qquad (6.5.5b)$$

From (6.4.4a,b) it can be seen that $\beta(t)=\eta(t+\pi/2\omega)$ and so the cylinder follows a circular path as expected (see Evans, 1976). It is also possible to recover Ogilvie's results for a neutrally buoyant, freely floating cylinder and for a fixed cylinder. From (6.5.3),(6.5.4)

$$\tilde{\alpha} = \tilde{\beta} = 0 \Longrightarrow \alpha = \beta = 0 \text{ and } m_0 = M_0 , \qquad (6.5.6)$$

since the first term on the right-hand-side of (6.5.3) is frequency dependent whereas the second term is not. Thus $\tilde{\alpha} = \tilde{\beta} = 0$ corresponds to a neutrally buoyant, freely floating cylinder. The fixed cylinder is essentially an 'infinitely damped' cylinder and so taking the limit $\tilde{\beta} \longrightarrow \infty$ should recover the fixed cylinder results. These special cases form useful checks on the analysis throughout and it is indeed found that (6.5.5a,b) reduce to Ogilvie's results.

Now that the cylinder displacement has been found, it is possible to determine the mean second-order force. The expression (6.2.6) for the mean force may be rewritten in terms of the complex potential

$$F_i = \rho \int_{S_c} \left\{ \tfrac{1}{2} \overline{f' \bar{f}'}^{t} + \mathrm{Re} \left(\overline{(\xi + i\eta) \partial f' / \partial t}^{t} \right) \right\} n_i \, ds . \qquad (6.5.7)$$

Using (6.4.3) and (6.5.5a,b) the mean force may be evaluated, and it can be shown (see Appendix D) that

$$F_1 = \frac{2\pi \rho g A^2 \; \tfrac{1}{2} \varepsilon_1 \tilde{\beta} e^{-2kh}}{\left\{ (\beta_1 - \tilde{\alpha}/2 + S_2 \tilde{\beta}/2)^2 + (S_3 \varepsilon_1 - S_2 \beta_1 + S_2 \tilde{\alpha}/2 + \tilde{\beta}/2)^2 \right\}} \times$$

$$\times \sum_{m=1}^{\infty} \frac{m(m+1)}{(ka)^{2m+2}} \left(\beta_{m+1} \varepsilon_m - \varepsilon_{m+1} \beta_m \right) , \qquad (6.5.8)$$

$$F_2 = \frac{2\pi \rho g A^2 \; e^{-2kh}}{\left\{ (\beta_1 - \tilde{\alpha}/2 + S_2 \tilde{\beta}/2)^2 + (S_3 \varepsilon_1 - S_2 \beta_1 + S_2 \tilde{\alpha}/2 + \tilde{\beta}/2)^2 \right\}} \times$$

$$\times \sum_{m=1}^{\infty} \frac{m(m+1)}{(ka)^{2m+2}} \left[\frac{\tilde{\beta}^2 \varepsilon_m \varepsilon_{m+1}}{4} + \left\{ (\beta_1 - \tilde{\alpha}/2) \varepsilon_m - \varepsilon_1 \beta_m \right\} \left\{ (\beta_1 - \tilde{\alpha}/2) \varepsilon_{m+1} - \varepsilon_1 \beta_{m+1} \right\} \right] \qquad (6.5.9)$$

Note that for $\tilde{\alpha} = \tilde{\beta} = 0$ and for $\lim \tilde{\beta} \longrightarrow \infty$, the mean horizontal force F_1 is zero. This and the non-zero values of the mean vertical

force F_2 agree with Ogilvie's results in both limiting cases.

Longuet-Higgins (1977) has shown that for two-dimensional floating or submerged bodies the mean horizontal force may be calculated once the incident, reflected and transmitted wave amplitudes are known, and this force may be written as

$$F_1 = \tfrac{1}{4}\rho g A^2 (1 + |R_1|^2 - |T_1|^2), \qquad (6.5.10)$$

where R_1 and T_1 are the reflection and transmission for the body respectively, and the force acts in the direction of travel of the incident waves. For the cylinder it is known (Ogilvie, 1963) that there are no reflected waves, thus

$$F_1 = \tfrac{1}{4}\rho g A^2 (1 - |T_1|^2) = \tfrac{1}{4}\rho g A^2 E, \qquad (6.5.11)$$

where E is the efficiency of the system in power absorption. This is because $|R_1|^2, |T_1|^2$ are measures of the power in the reflected and transmitted wave respectively, and hence

$$E = 1 - |R_1|^2 - |T_1|^2,$$
$$= 1 - |T_1|^2 \text{ , for the cylinder.}$$

Evans (1976) has derived an expression for the efficiency of such a cylinder; substitution of his expression in (6.5.11) yields

$$F_1 = \tfrac{1}{4}\rho g A^2 \left\{ \frac{4\omega^2 \beta B}{[\alpha - (m_0 + M)\omega^2]^2 + \omega^2 [\beta + B]^2} \right\}, \qquad (6.5.12)$$

or, introducing a non-dimensional wavenumber, $\upsilon = ka$ and non-dimensionalising the added-mass and damping coefficients as $M = M_0\mu$, $B = M_0\omega\Lambda$

$$F_1 = \tfrac{1}{4}\rho g A^2 \left\{ \frac{4\upsilon(\upsilon_0^{\frac{1}{2}}\Lambda_0)(\upsilon^{\frac{1}{2}}\Lambda)}{[(m' + \mu_0)\upsilon_0 - (m' + \mu)\upsilon]^2 + \upsilon[\upsilon_0^{\frac{1}{2}}\Lambda_0 + \upsilon^{\frac{1}{2}}\Lambda]^2} \right\}, \qquad (6.5.13)$$

where

$$\nu_0=\omega_0^2 a/g\ ,\ \mu_0=\mu(\nu_0),\ \Lambda_0=\Lambda(\nu_0),$$

so that, from (6.3.13), the cylinder is tuned to $\omega=\omega_0$, i.e. $\nu=\nu_0$.

Clearly it must be possible to rearrange (6.5.8) into the form (6.5.12). To accomplish this, it is first noted that in a rederivation of Ogilvie's results for forced oscillations of a cylinder, Evans *et al.* (1979) have shown that

$$\mu=2\beta_1-\left(1+\frac{2S_\beta S_\varepsilon \varepsilon_1}{1+S_\varepsilon^2}\right), \qquad (6.5.14)$$

$$\Lambda=\frac{2S_\beta\varepsilon_1}{1+S_\varepsilon^2}\ . \qquad (6.5.15)$$

Rearranging the terms in the denominator of (6.5.8) and using (6.5.3), (6.5.4) together with (6.5.14), (6.5.15) it can be shown that

$$F_1=-\tfrac{1}{4}\rho g A^2\left\{\frac{4\omega^2\beta B}{[\alpha-(m_0+M)\omega^2]^2+\omega^2[\beta+B]^2}\right\}\times$$

$$\times\left(\frac{S_\beta}{2\pi e^{-2Kh}}\right)^{-1}\sum_{m=1}^{\infty}\frac{m(m+1)}{(Ka)^{2m+2}}\left(\beta_m\varepsilon_{m+1}-\beta_{m+1}\varepsilon_m\right). \qquad (6.5.16)$$

Hence, for (6.5.8) to be correct, the following identity must be satisfied

$$\frac{S_\beta}{2\pi e^{-2Kh}}=\sum_{m=1}^{\infty}\frac{\beta_m}{(m-1)!}=\sum_{m=1}^{\infty}\frac{m(m+1)}{(Ka)^{2m+2}}\left(\beta_m\varepsilon_{m+1}-\beta_{m+1}\varepsilon_m\right), \qquad (6.5.17)$$

where (D.5) has been used. A numerical check has shown that this identity holds exactly for all values of Ka and h/a considered.

The negative sign preceding the expression for the mean force in (6.5.16) reflects the fact that waves are incident from $x=+\infty$ and so the force is directed in the negative x- direction.

Returning to the mean vertical force, this can also be rewritten in a form similar to (6.5.13). In this case, (6.5.9) becomes

$$F_2 = 2\pi\rho g A^2 \frac{4\nu^2 e^{-2kh}}{(1+S_\varepsilon^2)\left[\{(m'+\mu_0)v_0-(m'+\mu)v\}^2+v\{v_0\Lambda_0+v\Lambda\}^2\right]} \times$$

$$\times \sum_{m=1}^{\infty} \frac{m(m+1)}{(Ka)^{2m+2}} \left\{ \frac{v_0\Lambda_0^2}{4v} \varepsilon_m\varepsilon_{m+1} - (\delta\varepsilon_m - \varepsilon_1 \beta_m)(\delta\varepsilon_{m+1} - \varepsilon_1\beta_{m+1}) \right\}, \qquad (6.5.18)$$

where

$$\delta = (2v)^{-1}\{(m'+\mu)v - (m'+\mu_0)v_0 + S_\varepsilon v\Lambda\}. \qquad (6.5.19)$$

Unlike the expression for the mean horizontal force, there is no obvious simplification of this expression for the mean vertical force. It is noticeable, however, that the expression (6.5.18) does include a 'resonant-type' denominator and so one might expect the mean vertical force to reach some peak value near the tuning point of the system.

The first-order oscillatory forces may also be calculated from (6.5.1a,b), using (D.6) together with the expressions for the displacements given by (6.5.5a,b). In the notation of Ogilvie, it is found that

$$F_1(t) - i F_2(t) = -\frac{\pi\rho g A}{K} e^{-i(\omega t-\psi)} \times$$

$$\times \frac{\varepsilon_1 e^{-kh}\{(\tilde\alpha-1)^2+\tilde\beta^2\}^{\frac12}}{\{(\beta_1+S_\varepsilon\tilde\beta/2-\tilde\alpha/2)^2+(S_g\varepsilon_1-S_\varepsilon\beta_1+S_\varepsilon\tilde\alpha/2+\tilde\beta/2)^2\}^{\frac12}}, \qquad (6.5.20)$$

where

$$\psi = \tan^{-1}\frac{\tilde\beta(S_\varepsilon\tilde\beta/2+\beta_1-\frac12)+(\tilde\alpha-1)(S_g\varepsilon_1-S_\varepsilon\beta_1+S_\varepsilon\tilde\alpha/2)}{\tilde\beta(\tilde\beta/2+S_g\varepsilon_1-S_\varepsilon\beta_1+S_\varepsilon/2)-(\tilde\alpha-1)(\beta_1-\tilde\alpha/2)}, \qquad (6.5.21)$$

and this may be rewritten as

$$F_1(t) - i F_2(t) = -\frac{2\pi\rho g A}{K}\left[\frac{\varepsilon_1^2 e^{-2kh}(E_0^2+\nu v_0\Lambda_0^2)}{(1+S_\varepsilon)^2\left[(E_0-\mu\nu)^2+\nu E_1^2\right]}\right]^{\frac12} e^{-i(\omega t-\psi)}, \qquad (6.5.22)$$

where

$$\psi = \tan^{-1}\frac{S_\varepsilon\{\upsilon\nu_o^{\frac{1}{2}}\Lambda_o E_1 + E_o(E_o-\mu\upsilon)\} + \upsilon\{\Lambda E_o + \mu\upsilon\nu_o^{\frac{1}{2}}\Lambda_o\}}{\upsilon\nu_o^{\frac{1}{2}}\Lambda_o E_1 + E_o(E_o-\mu\upsilon) - S_\varepsilon\upsilon(\Lambda E_o + \mu\upsilon\nu_o^{\frac{1}{2}}\Lambda_o)}, \qquad (6.5.23)$$

and

$$E_o = (m'+\mu_o)\nu_o - m'\upsilon \quad , \quad E_1 = \nu_o^{\frac{1}{2}}\Lambda_o + \upsilon^{\frac{1}{2}}\Lambda .$$

6.6 Results and Discussion

The behaviour of the mean vertical force is illustrated in Figure (6.3) for a cylinder of relative mass, $m' = 0.6$ submerged to a depth such that $h/a = 2.0$ and tuned to $K_o a = \omega_o^2 a/g = 0.25$ (that is, tuned to waves of wavelength approximately 150m for a cylinder of radius 6m). These parameter values roughly correspond to the current design values of the Bristol cylinder. It can immediately be seen that the behaviour of the mean vertical force on the cylinder when it is absorbing power is completely different from the corresponding fixed and neutrally buoyant, freely-floating cases also shown. As Ka increases, the force rises rapidly reaching a maximum at $Ka \simeq 0.2$ and then decreases to become negative over a range of wavenumbers before finally asymptoting to the fixed and freely-floating cylinder curves. Its maximum value is almost three times the maximum value of the mean force for the corresponding fixed cylinder case and it is found that this maximum value ratio increases as h/a increases (at $h/a = 1.5$, this ratio is approximately 1.9). Increasing the relative mass results in a larger maximum value (approximately a 5.6% increase when $m' = 0.7$, at $h/a = 1.5$) and a slight shift towards the origin of the wavenumber range over which the mean vertical force is negative. As h/a increases however these changes become less noticeable.

The mean horizontal force on the power-absorbing cylinder is also

shown as a dashed line in Figure (6.3). It reaches its maximum value at $K_0 = 0.25$ when the efficiency is a maximum, $E = 1$ (see equation (6.5.11)), and this maximum value is much smaller than that of the mean vertical force. The maximum value of the mean horizontal force is, however, independent of the depth of submergence (and, from (6.5.11), equals $\frac{1}{4}\rho g A^2$) whereas the mean vertical force is not. This is because the cylinder can be tuned to absorb all the wave energy (and hence momentum) no matter what its depth of submergence is.

Figure (6.4) displays the behaviour of the mean vertical force for various values of h/a, when $m' = 0.6$ and $K_0 a = 0.25$. The maximum value of the force is clearly dependent upon the submergence of the cylinder; this value decreases by 40% in going from $h/a = 1.5$ to 2.0. It can also be seen that, when the cylinder is sufficiently near the free surface, the mean vertical force always remains positive although there is still a prominent local minimum.

The effect of tuning upon the mean vertical force is illustrated in Figure (6.5). Tuning the cylinder to $K_0 a = 0.3$ instead of 0.25 produces a curve with a smaller maximum value and a smaller 'negative force effect', together with a shift of the curve away from the origin. There is however, very little difference between the two cases for $Ka > 1$. The dotted curve gives the optionally tuned cylinder results, that is, the value which the mean vertical force would have at a particular wavenumber if the cylinder were tuned to that wavenumber. It is not an envelope curve and is therefore of limited value here but it does provide some indication of the likely behaviour of the mean vertical force for various tunings.

The amplitude of the first-order oscillatory forces for fixed, freely-floating and tuned cylinders is shown in Figure (6.6). Near the tuning wavenumber the amplitude is much larger when the cylinder is absorbing power but, for larger Ka it falls below both the fixed

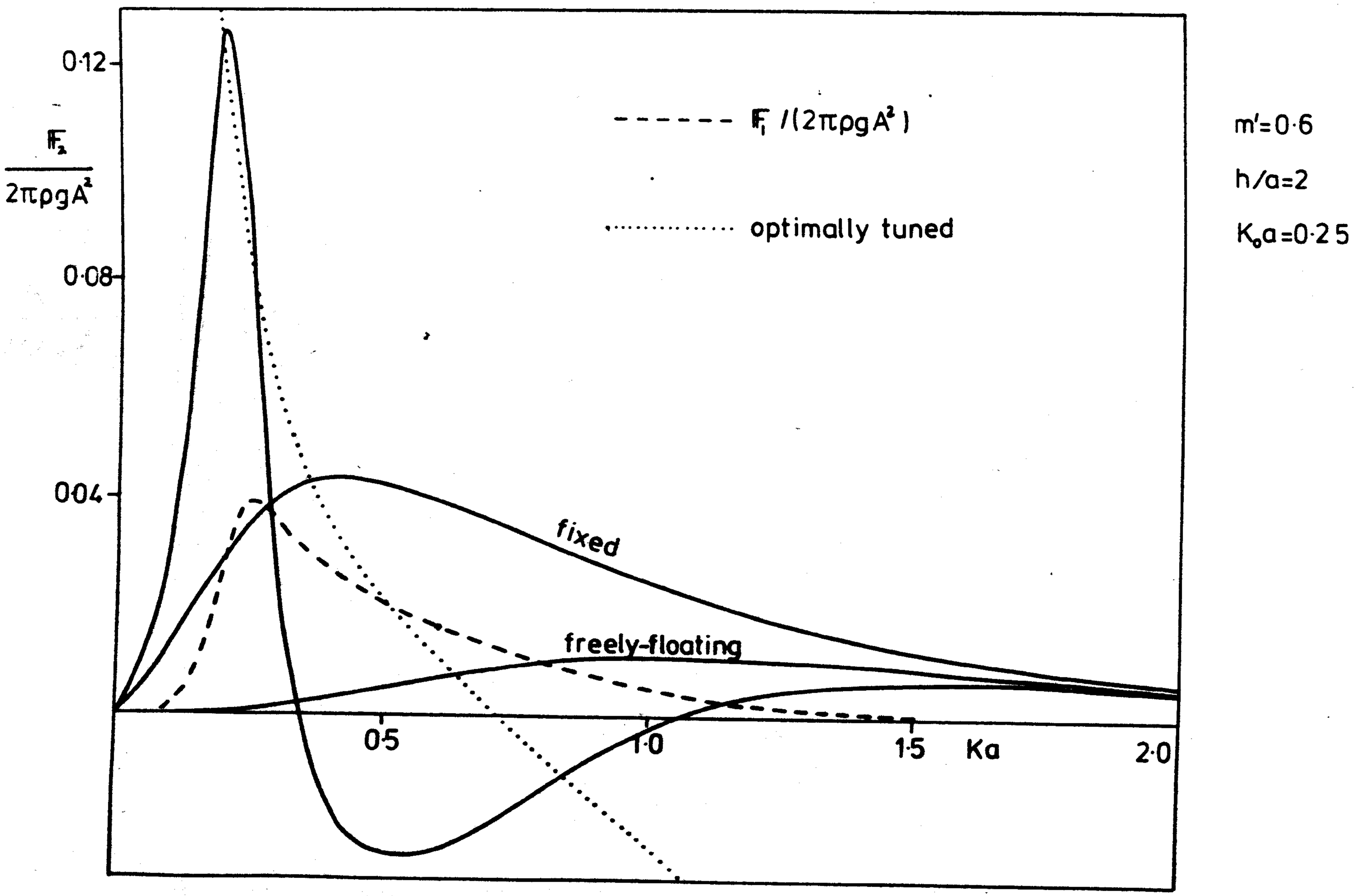
0·12
0·08
0·04
$\frac{F_2}{2\pi\rho g A^2}$
$F_1/(2\pi\rho g A^2)$
optimally tuned
m'=0·6
h/a=2
K_0a=0·25
fixed
freely-floating
0·5
1·0
1·5
Ka
2·0

FIG (6·3)

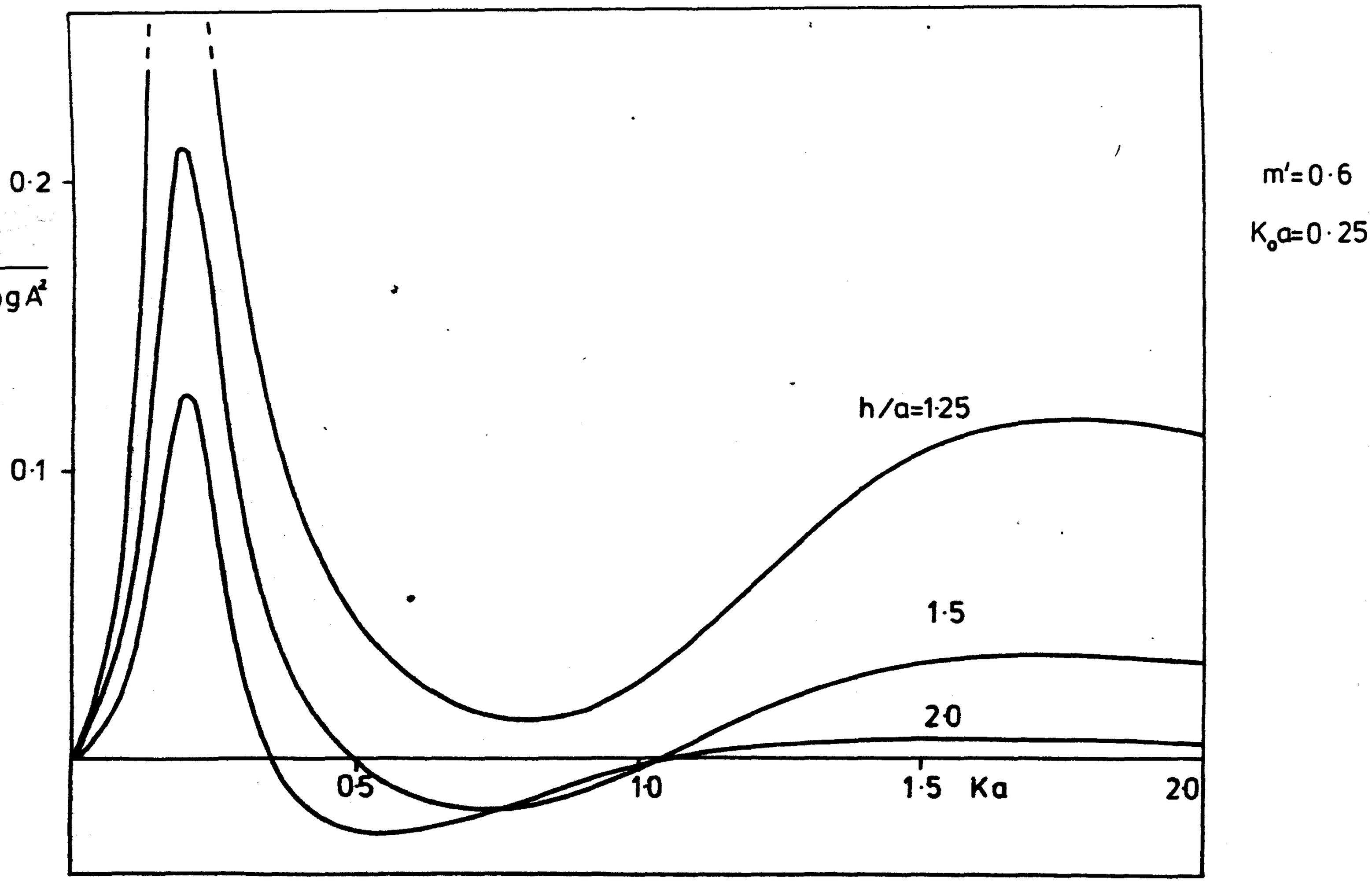

FIG (6·4)

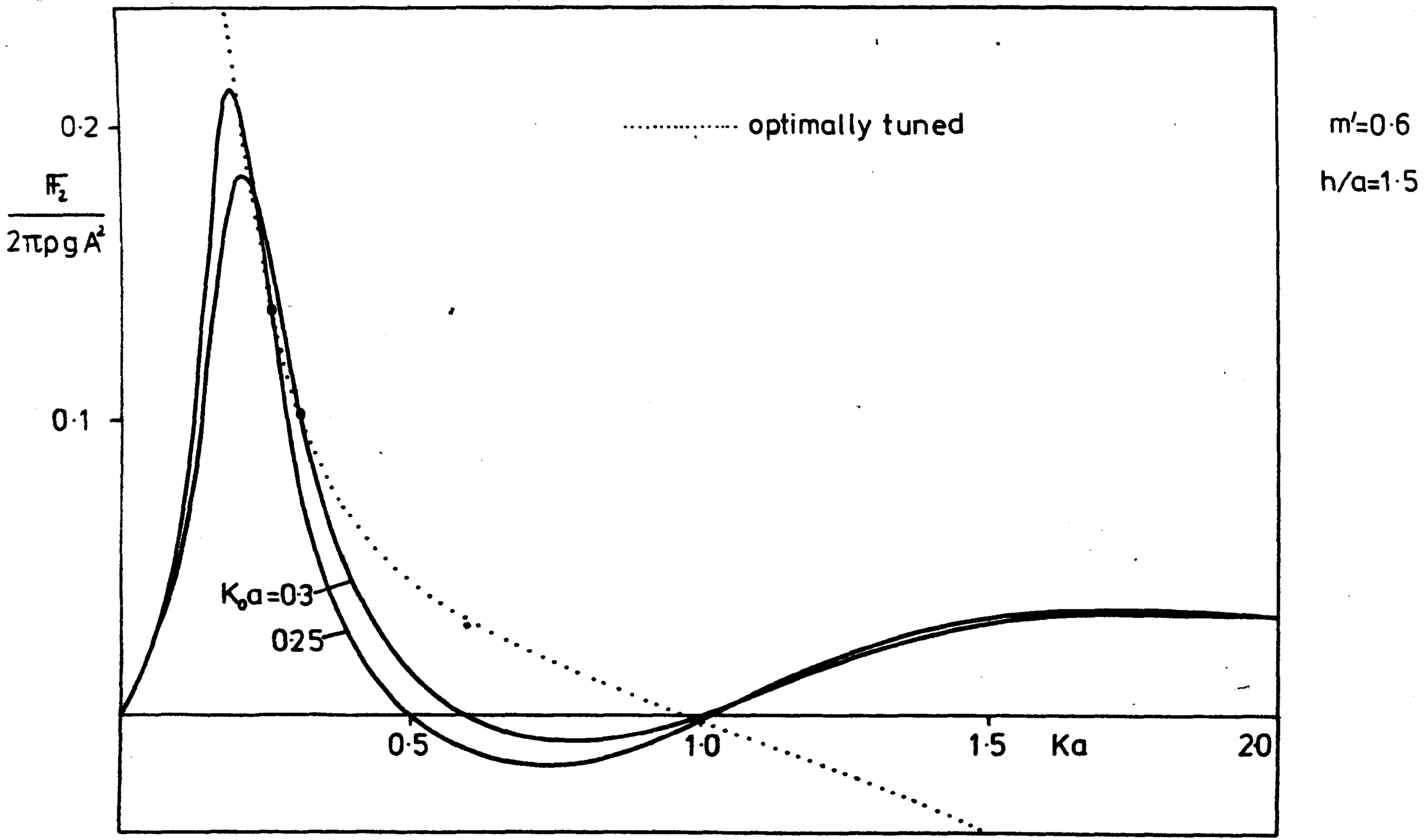
0·2
0·1
$\frac{F_z}{2\pi\rho g A^2}$
optimally tuned
m'=0·6
h/a=1·5
K_0a=0·3
0·25
0·5
1·0
1·5
Ka
20

FIG (6·5)

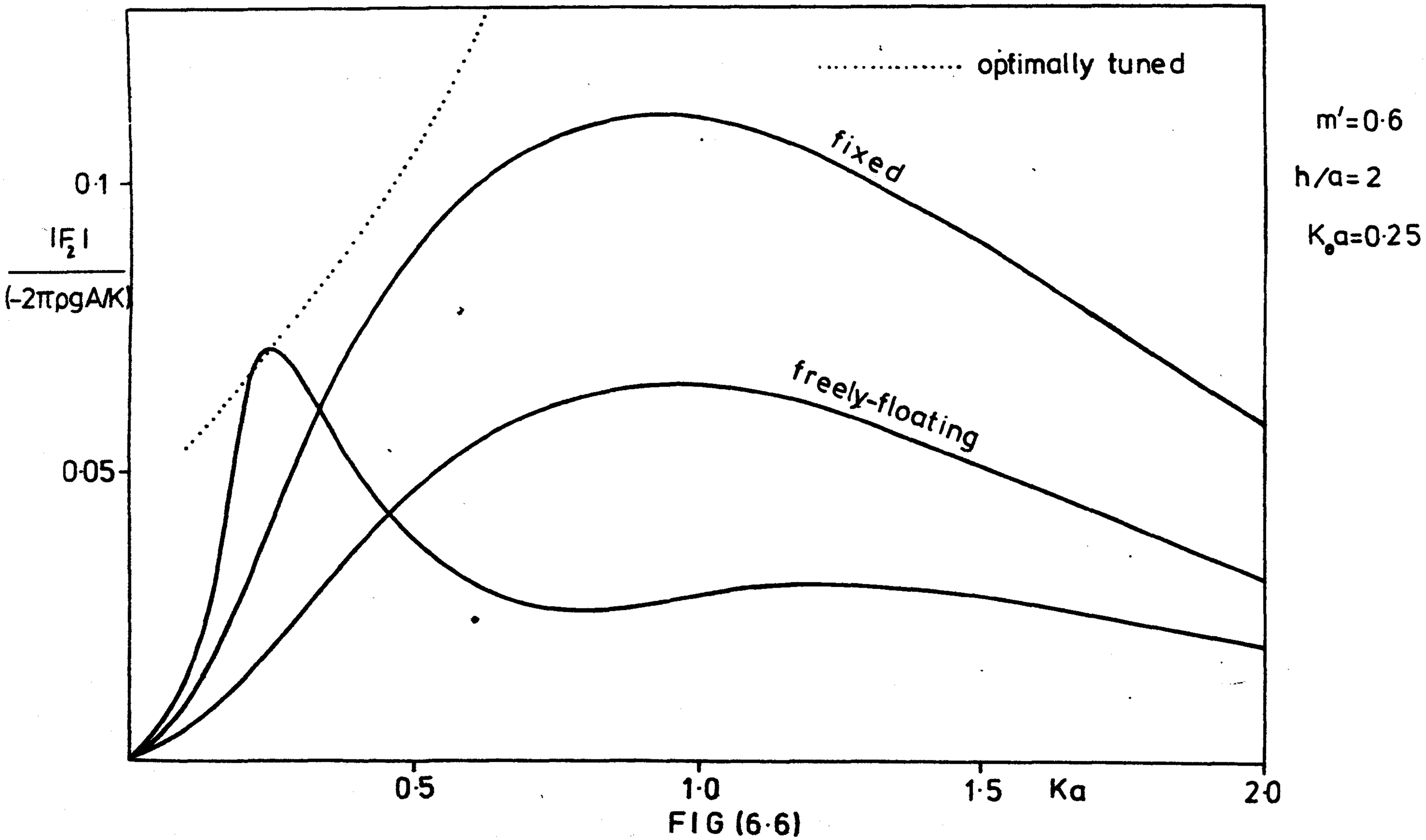
optimally tuned
fixed
freely-floating
m'=0·6
h/a=2
K₀a=0·25
0·1
|F₂|
(-2πρgA/K)
0·05
0·5
1·0
1·5
Ka
2·0

FIG (6·6)

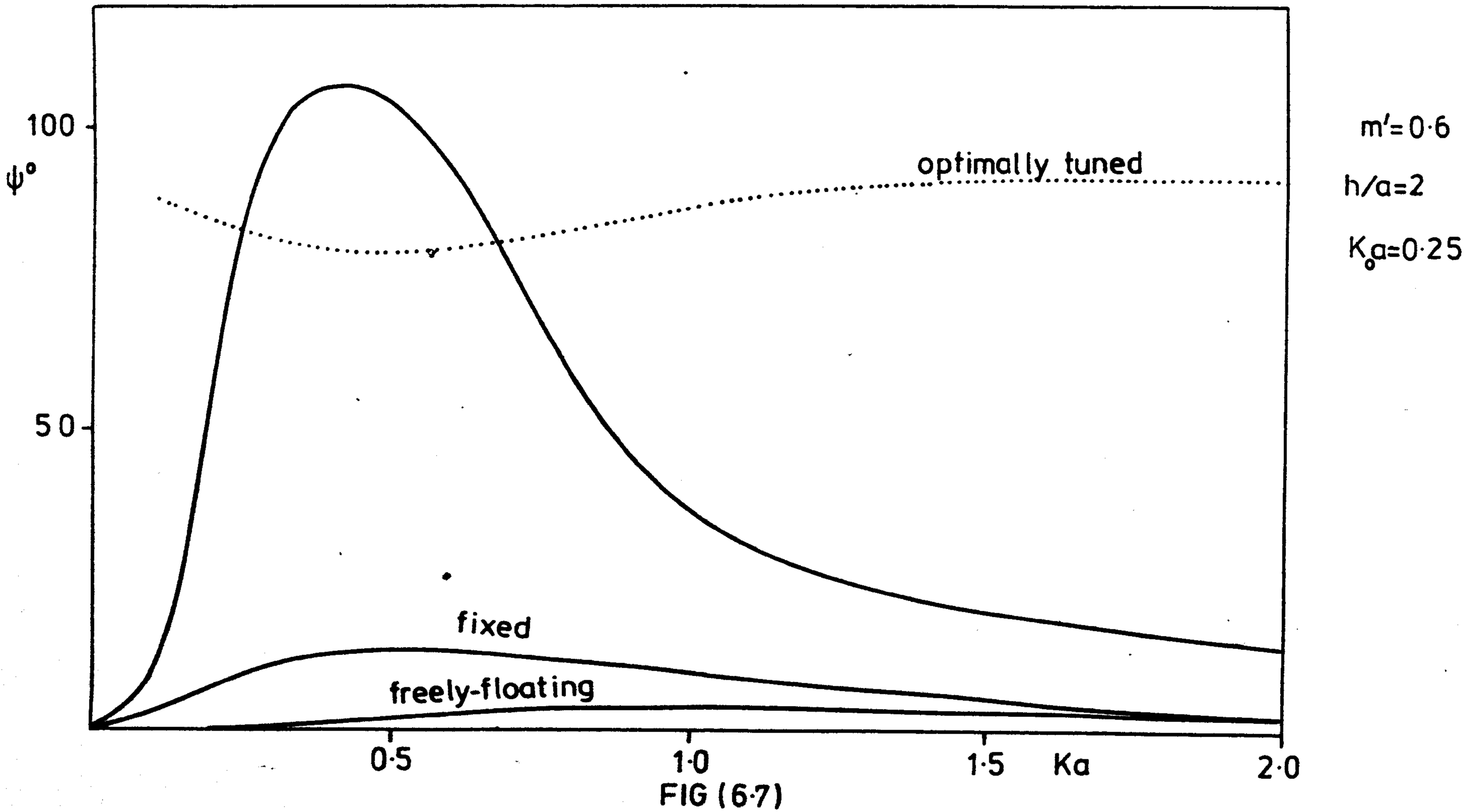
100
ψ°
50
optimally tuned
fixed
freely-floating
0·5
1·0
1·5
Ka
2·0
m'=0·6
h/a=2
K₀a=0·25

FIG (6·7)

h/a=2. FIXED CYLINDER

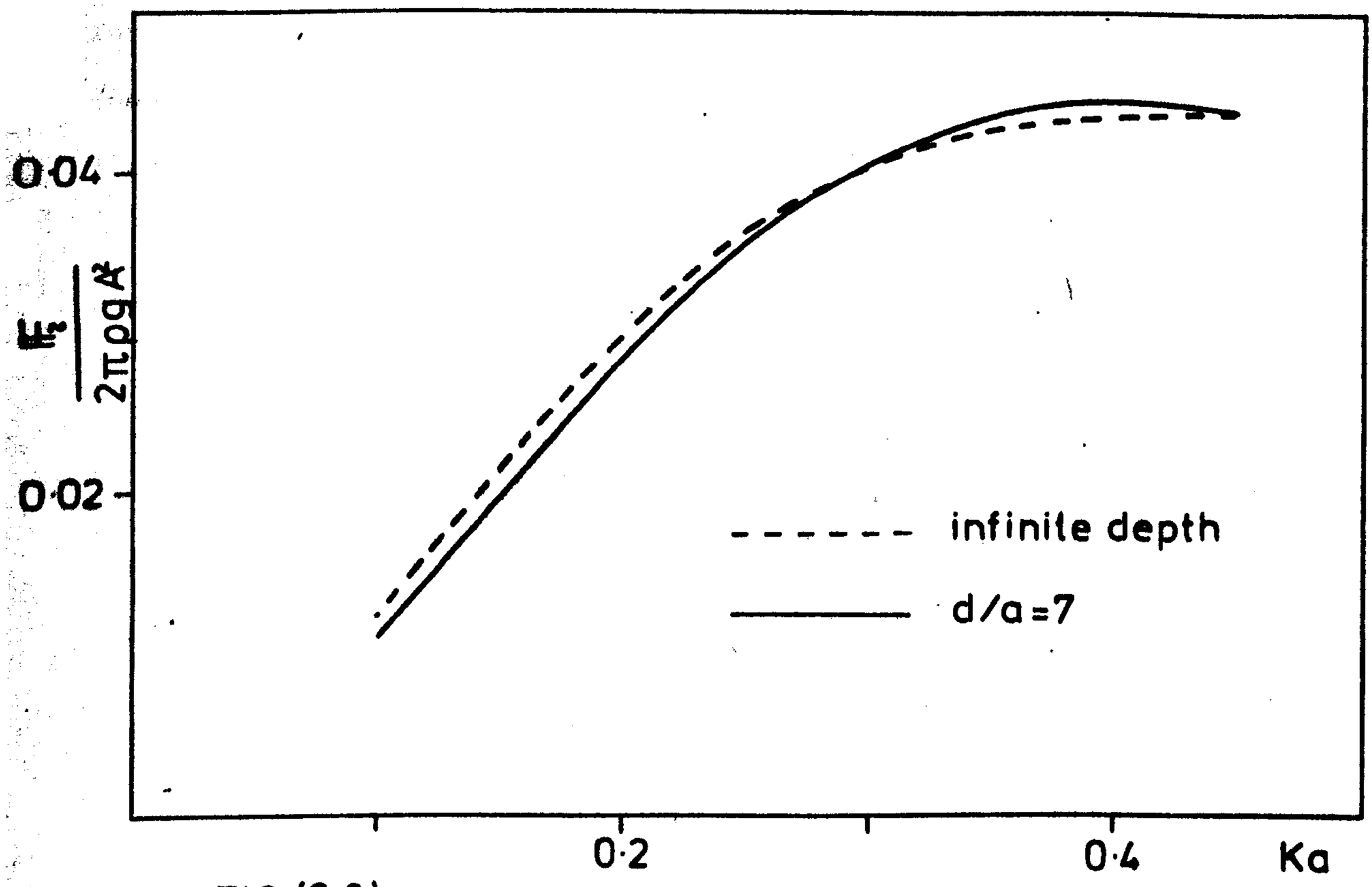

FIG (6·8)

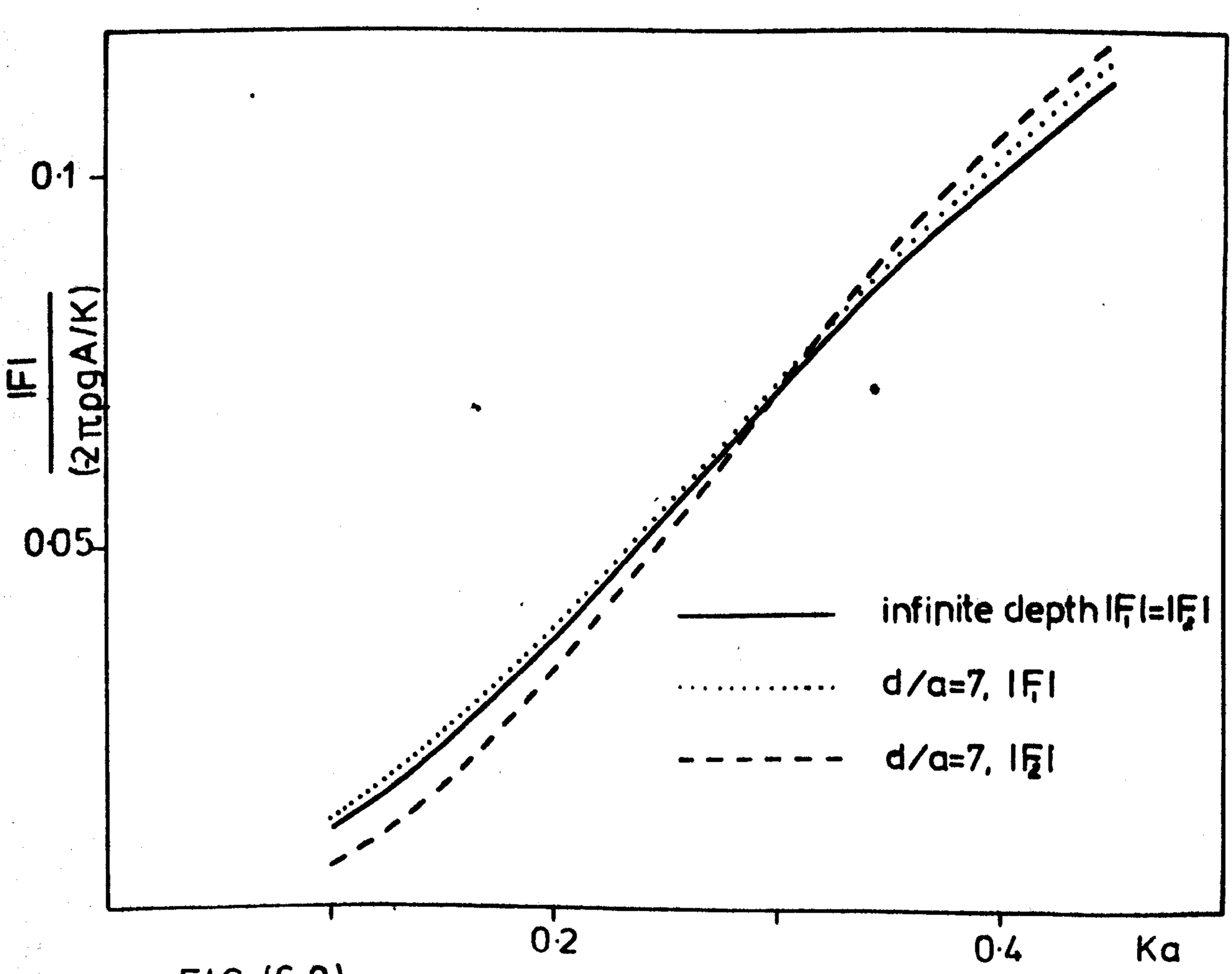

FIG (6·9)

and freely-floating results. The corresponding phase-lag ψ of these forces (see equation (6.5.22)) has also been calculated (Figure (6.7)), showing a marked difference in value between the tuned and fixed or freely-floating cases.

It is of interest to compare the magnitudes of various forces on the tuned cylinder. For this purpose the parameters are set as follows:

$m' = 0.6$, $K_0 a = 0.25$, cylinder radius, a = 6m.

		$\|F_2\|/\|F_2\|$	F_2/F_B	F_1/F_2
Maximum values	h/a=1.5	–	$2.9A^2$ %	19 %
	h/a=2.0	–	$1.8A^2$ %	30 %
h/a=1.5	Ka=0.2	10.6A %	-	17 %
	Ka=0.25	8.9A %	-	27 %
h/a=2.0	Ka=0.2	6.7A %	-	22 %
	Ka=0.25	4.7A %	-	48 %

TABLE 1

N.B. Maximum value $F_2/F_1 = \max_{Ka} F_2 / \max_{Ka} F_1$, etc.

The table above compares the mean vertical force, F_2 with the amplitude of the first-order oscillatory vertical force, $|F_2|$, the buoyancy force, F_B and the mean horizontal force. The amplitude A of the incident waves is measured in metres.

It can be seen from Table 1 that the largest upward force is the buoyancy force and, for waves of amplitude 1m say, the mean vertical force is a small fraction of this force. However, for larger amplitude waves the mean vertical force becomes more significant; care must be taken here to ensure that the wave amplitude and the cylinder displacement are sufficiently small so that the cylinder does not break the free surface if linear theory is to apply. The mean vertical

force can be quite a substantial fraction of the amplitude of the oscillatory vertical force although this ratio decreases as h/a increases.

Returning to Figure (6.3), it has been noted that the mean vertical force is negative, that is, it acts downwards over a range of wavenumbers. However, the maximum value of the downward mean vertical force is only $0.36A^2\%$ of the buoyancy force for $h/a = 2.0$ and so this effect is very unlikely to be important.

The two-dimensional, infinitely-deep fluid model of the Bristol cylinder was chosen to enable Ogilvie's work to be generalised and so that Ogilvie's results could provide checks on the analysis by considering limiting cases. This model has also been used by Evans (1976, 1979) in developing the mathematical theory for energy-absorption by the cylinder and so the results derived here are relevant to Evans' model.

It can be argued that the water depth of 42m, in which the cylinder is envisaged as operating, is certainly not deep water for the range of wavelengths which are of interest, and finite-depth models are perhaps the next step. It is, however, possible to compare the mean vertical force and the amplitude of the first-order oscillatory forces on a fixed cylinder when in infinitely deep fluid and when in finite depth of fluid. The comparisons are shown in Figures (6.8),(6.9). Note that in finite depth the amplitudes of the horizontal and vertical oscillatory forces are not equal. Clearly, with the exception of the vertical oscillatory force for small Ka, the deep water model provides a reasonable approximation of the forces in finite depth.

The finite-depth forces on a fixed cylinder were derived by Dr. G.P. Thomas (private communication). The numerical computation necessary to calculate all the results given in this Chapter was carried

out using an adaptation of a programme originally written by Dr. G.P. Thomas, to determine the added-mass and damping coefficients for a two-dimensional cylinder in deep water. It was found that the infinite systems of equations defined by (D.4a,b) have excellent convergence properties and truncating them after only 20 terms gave results of at least six-figure accuracy except for h/a very close to unity.

(b) Mean Forces on Cylinders of Arbitrary Cross-Section

6.7 The Mean Forces

Consider now a cylinder of arbitrary cross-section submerged in fluid and subjected to incident waves of frequency ω. Let (x,y) be Cartesian co-ordinates as defined in part (a), § 6.2 of this Chapter. Then the linearised velocity potential $\Phi(x,y,t)$ describing the fluid motion satisfies (6.2.1)-(6.2.3) together with a boundary condition on the cylinder and a radiation condition. If the time-dependence of the velocity potential is removed as in (2.2.1) then the complex potential $\phi(x,y)$ also satisfies Laplace's equation while (6.2.2), (6.2.3) become

$$K\phi - \partial\phi/\partial y = 0 \quad , \text{on } y=0, \tag{6.7.1}$$

$$\nabla\phi \to 0 \quad , \text{as } y \to \infty, \tag{6.7.2}$$

c.f. equations (2.2.4), (2.2.6).

The boundary condition on the cylinder is given by

$$\partial\phi/\partial n = V_n, \tag{6.7.3}$$

where $V_n = Re\{v_n e^{-i\omega t}\}$ is the normal velocity component of the

cylinder surface. (As in part (a), the normal is taken as being directed into the fluid). The radiation condition to be satisfied is

$$\phi \sim \frac{gA}{\omega} e^{ky}\left(e^{-ikx} + R_1 e^{ikx}\right), \text{ as } x \longrightarrow +\infty, \qquad (6.7.4)$$

$$\phi \sim \frac{gA}{\omega} T_1 e^{-ikx+ky} \text{ , as } x \longrightarrow -\infty, \qquad (6.7.5)$$

where A is the amplitude of the incident waves, R_1 and T_1 are the reflection and transmission coefficients respectively, and waves are taken as being incident from $x = +\infty$.

The linear wave-induced momentum $\underset{\sim}{M}$ of fluid in a volume V enclosed by a surface S is given by

$$\underset{\sim}{M} = \rho \int_V \underset{\sim}{V}\, dV, \qquad (6.7.6)$$

where $\underset{\sim}{V}$ is the fluid velocity, giving the rate of change of momentum as

$$\frac{d\underset{\sim}{M}}{dt} = \rho \int_V \partial \underset{\sim}{V}/\partial t \, dV - \rho \int_S \underset{\sim}{V}\, U_n \, dS, \qquad (6.7.7)$$

where U_n is the normal velocity component of the surface S. Using Euler's equation of motion and the equation of continuity, it can be shown (Newman, 1967 and Lee & Newman 1971) that the volume integral can be reduced to a surface integral. If $\underset{\sim}{M} = (M_1, M_2)$ and $\underset{\sim}{n} = (n_1, n_2)$ it is found that

$$\frac{dM_1}{dt} = \rho \int_S \left\{ \frac{P}{\rho} n_1 + \frac{\partial \Phi^I}{\partial x}\left(\frac{\partial \Psi}{\partial n} - U_n\right)\right\} dS, \qquad (6.7.8)$$

$$\frac{dM_2}{dt} = \rho \int_S \left\{ \frac{P}{\rho} n_2 + \frac{\partial \Psi}{\partial y}\left(\frac{\partial \Phi^I}{\partial n} - U_n\right)\right\} dS, \qquad (6.7.9)$$

correct to second order, where p is the hydrodynamic pressure

given by Bernoulli's equation as $p=-\rho\partial\Phi/\partial t-\frac{1}{2}\rho(\nabla\Phi)^2$. The closed surface, S is taken to be $S=S_c+S_f+S_{V+}+S_{V-}+S_\infty$ where S_c is the cylinder surface, S_{V+} and S_{V-} are vertical planes at $x=+X_0, -X_0, (X_0>0)$ respectively, S_∞ is the horizontal closure at $y=-\infty$ and S_f is the undisturbed free surface (y=0). The error introduced into (6.7.8), (6.7.9) in taking the undisturbed position of the free surface instead of the actual position is of higher than second order and is neglected.

Note that on the cylinder surface, S_c the normal velocity of the surface is equal to the normal fluid velocity and hence, $\partial\Phi/\partial n-U_n=0$ on S_c. Further, the hydrodynamic force $F(t)$ on the cylinder is given by

$$F_i(t)=-\int_{S_c} p n_i \, dS, \quad (i=1,2), \tag{6.7.10}$$

The horizontal force component is first considered. If the time average of (6.7.8) is taken then, as the motion is periodic, there is no net increase in momentum in the volume V over a wave cycle. Thus $\overline{dM_1/dt}^t=0$ and using (6.7.10) it can be seen that

$$\overline{F_1(t)}^t=-\rho\int_{S-S_c}\overline{\left\{\frac{p}{\rho}n_1+\frac{\partial\Phi}{\partial x}\left(\frac{\partial\Phi}{\partial n}-U_n\right)\right\}}^t dS, \tag{6.7.11}$$

$$=-\rho\int_{S_f}\overline{\frac{\partial\Phi}{\partial x}\frac{\partial\Phi}{\partial y}}^t dS-\rho\int_{S_{V+}}\overline{\left\{\frac{p}{\rho}+\left(\frac{\partial\Phi}{\partial x}\right)^2\right\}}^t dS$$

$$+\rho\int_{S_{V-}}\overline{\left\{\frac{p}{\rho}+\left(\frac{\partial\Phi}{\partial x}\right)^2\right\}}^t dS,$$

Using Bernoulli's equation this becomes

$$\overline{F_1(t)}^t = -\frac{\rho}{2}\int_{S_f} \frac{\partial\phi}{\partial x}\frac{\partial\bar{\phi}}{\partial y}\,dS - \rho/4\int_{S_{V+}}\left\{\left|\frac{\partial\phi}{\partial x}\right|^2-\left|\frac{\partial\phi}{\partial y}\right|^2\right\}dS$$

$$+\rho/4\int_{S_{V-}}\left\{\left|\frac{\partial\phi}{\partial x}\right|^2-\left|\frac{\partial\phi}{\partial y}\right|^2\right\}dS,$$

using (2.2.1). Letting $X_e \longrightarrow \infty$ and substituting for $\partial\phi/\partial y$ from (6.7.1) it is found that

$$\overline{F_1(t)}^t = -\frac{\rho K}{4}\int_{-\infty}^{\infty}\frac{\partial}{\partial x}\left(|\phi|^2\right)\Big|_{y=0}dx - \rho/4\int_{-\infty}^{0}\left\{\left|\frac{\partial\phi}{\partial x}\right|^2-\left|\frac{\partial\phi}{\partial y}\right|^2\right\}\Big|_{x=+\infty}dy$$

$$+\rho/4\int_{-\infty}^{0}\left\{\left|\frac{\partial\phi}{\partial x}\right|^2-\left|\frac{\partial\phi}{\partial y}\right|^2\right\}\Big|_{x=-\infty}dy,$$

$$= -\frac{\rho K}{4}\left[\phi\bar{\phi}\right]_{\substack{x=-\infty\\y=0}}^{x=+\infty} - \rho/4\int_{-\infty}^{0}dy\left[\frac{\partial\phi}{\partial x}\frac{\partial\bar{\phi}}{\partial x}-\frac{\partial\phi}{\partial y}\frac{\partial\bar{\phi}}{\partial y}\right]_{x=-\infty}^{x=+\infty}. \qquad (6.7.12)$$

Applying the radiation conditions(6.7.4), (6.7.5) yields

$$\overline{F_1(t)}^t = -\frac{1}{4}\rho g A^2\left(1+|R_1|^2-|T_1|^2\right). \qquad (6.7.13)$$

As expected, this is Longuet-Higgins' result for the mean second-order horizontal force. The minus sign reflects the fact that the force is in the negative x-direction as waves are incident from $x=+\infty$.

If the time average of (6.7.9) is taken, then it is found that

$$\overline{F_2}^t(t) = -\rho\int_{S_f}\left\{\overline{\frac{P}{\rho}+\left(\frac{\partial\Phi}{\partial y}\right)^2}^t\right\}dS - \rho\int_{S_{V+}}\overline{\frac{\partial\Phi}{\partial y}\frac{\partial\Phi}{\partial x}}^t dS + \rho\int_{S_{V-}}\overline{\frac{\partial\Phi}{\partial y}\frac{\partial\Phi}{\partial x}}^t dS, \qquad (6.7.14)$$

and in exactly the same way as before

$$\overline{F_2(t)}^t = \rho/4 \int_{S_f} \left(\frac{\partial\phi}{\partial x}\frac{\partial\bar{\phi}}{\partial x} - \frac{\partial\phi}{\partial y}\frac{\partial\bar{\phi}}{\partial y} \right) ds - \rho/2 \int_{S_{H}} \frac{\partial\bar{\phi}}{\partial y}\frac{\partial\phi}{\partial x}\, ds + \rho/2 \int_{S_{V-}} \frac{\partial\bar{\phi}}{\partial y}\frac{\partial\phi}{\partial x}\, ds .$$

Using the free surface condition (6.7.1) gives

$$\overline{F_2(t)}^t = \rho/4 \int_{S_f} \left\{ \frac{\partial}{\partial x}\left(\bar{\phi}\frac{\partial\phi}{\partial x}\right) - \bar{\phi}\frac{\partial^2\phi}{\partial x^2} - K^2\phi\bar{\phi} \right\} ds$$

$$- \rho/2 \int_{S_{V+}} \frac{\partial\bar{\phi}}{\partial y}\frac{\partial\phi}{\partial x}\, ds + \rho/2 \int_{S_{V+}} \frac{\partial\bar{\phi}}{\partial y}\frac{\partial\phi}{\partial x}\, ds .$$

This may be rewritten as

$$\overline{F_2(t)}^t = -\rho/4 \int_{S_f} \bar{\phi}\left(\partial^2/\partial x^2 + K^2\right)\phi\, ds + \rho/4 \int_{S_f} \frac{\partial}{\partial x}\left(\bar{\phi}\,\partial\phi/\partial x\right) ds$$

$$- \rho/2 \int_{S_{V+}} \frac{\partial\bar{\phi}}{\partial y}\frac{\partial\phi}{\partial x}\, ds + \rho/2 \int_{S_{V-}} \frac{\partial\bar{\phi}}{\partial y}\frac{\partial\phi}{\partial x}\, ds .$$

By letting $X_0 \rightarrow \infty$ and applying the radiation conditions (6.7.4), (6.7.5) it may easily be shown that the contributions from the last two integrals cancel with the contribution from the second integral and hence

$$\overline{F_2(t)}^t = -\rho/4 \int_{S_f} \bar{\phi}\left(\partial^2/\partial x^2 + K^2\right)\phi\, ds . \qquad (6.7.15)$$

The mean second-order vertical force can thus be expressed as an integral along the free-surface. The corresponding three-dimensional result found by Lee and Newman (1971) is similar to (6.7.15) with $\partial^2/\partial x^2$ replaced by $\left(\partial^2/\partial x^2 + \partial^2/\partial z^2\right)$ if (x,z) are Cartesian co-ordinates in the plane of the free surface.

6.8 Interpretation of the Surface Integral

Equation (6.7.15) does not yield a simple expression for the mean vertical force in terms of the wave amplitude and reflection and transmission coefficients as was found for the mean horizontal force. However, it is possible to gain some further insight into the expression for the mean vertical force.

The potential ϕ may be decomposed as

$$\phi = \phi_0 + \phi_c \,, \tag{6.8.1}$$

where ϕ_0 is the incident wave potential and ϕ_c is a 'disturbance' potential due to the presence of the cylinder. From (6.4.1), (6.4.2) the potential ϕ_0 may be written as

$$\phi_0 = \frac{gA}{\omega} e^{-iKx+ky} \,, \tag{6.8.2}$$

which clearly satisfies

$$(\partial^2/\partial x^2 + K^2)\phi_0 = 0 \,. \tag{6.8.3}$$

Thus, from (6.7.15), the mean vertical force, $\overline{F_2(t)}^t = F_2$ can be expressed in the form

$$F_2 = -\rho/4 \int_{S_f} \bar{\phi}_0 (\partial^2/\partial x^2 + K^2)\phi_c \, dS - \rho/4 \int_{S_f} \bar{\phi}_c (\partial^2/\partial x^2 + K^2)\phi_c \, dS, \tag{6.8.4}$$

where the real part of the right-hand side is understood.

Consider the first integral in (6.8.4), denoted by I_1. Since $\bar{\phi}_0$ also satisfies (6.8.3), the integral becomes

$$I_1 = -\rho/4 \int_{S_f} \{ \bar{\phi}_0 \partial^2\phi_c/\partial x^2 - \phi_c \partial^2\bar{\phi}_0/\partial x^2 \} dS,$$

$$I_1 = -\rho/4 \int_{-\infty}^{\infty} \frac{\partial}{\partial x}\left\{\bar{\phi}_0 \partial\phi_c/\partial x - \phi_c \partial\bar{\phi}_0/\partial x\right\}\Big|_{y=0} dx,$$

$$= -\rho/4 \left[\bar{\phi}_0 \partial\phi_c/\partial x - \phi_c \partial\bar{\phi}_0/\partial x\right]_{x=-\infty}^{x=+\infty}_{y=0}. \qquad (6.8.5)$$

From (6.8.1) and (6.7.4), (6.7.5) the radiation condition for the potential ϕ_c is

$$\phi_c \sim \frac{gA}{\omega} R_1 e^{iKx+Ky}, \quad \text{as } x \longrightarrow +\infty, \qquad (6.8.6)$$

$$\phi_c \sim \frac{gA}{\omega}(T_1 - 1) e^{-ikx+Ky}, \quad \text{as } x \longrightarrow -\infty. \qquad (6.8.7)$$

Application of the radiation condition for ϕ_c together with (6.8.2) in (6.8.5) yields

$$I_1 = \tfrac{1}{2}\rho g A^2 q_m(T_1). \qquad (6.8.8)$$

The first integral depends only upon the incident wave amplitude and the amplitude and phase of the transmitted wave.

The second integral, I_2 involves only the disturbance potential and, using (6.7.1), it may be written as

$$I_2 = -\rho/4 \int_{S_f}\left\{\left|\frac{\partial\phi_t}{\partial y}\right|^2 - \left|\frac{\partial\phi_c}{\partial x}\right|^2\right\} ds - \rho/4 \left[\bar{\phi}_c \partial\phi_t/\partial x\right]_{x=-\infty}^{x=+\infty}_{y=0},$$

$$= -\rho/4 \int_{S_f}\left\{\left|\frac{\partial\phi_c}{\partial y}\right|^2 - \left|\frac{\partial\phi_t}{\partial x}\right|^2\right\} ds, \qquad (6.8.9)$$

as the real part only is understood. Clearly the progressive wave components of ϕ_c , given by (6.8.6), (6.8.7), do not contribute to this integral; only the local disturbance above the cylinder which decays exponentially as $|x| \longrightarrow \infty$ will contribute. Alternatively the integral (6.8.9) can be thought of as a measure of the local distortion of the surface fluid particle orbits due to the presence of the cylinder.

6.9 Approximation of the Mean Vertical Force

Ogilvie (1963) derived an approximate solution for the mean vertical force by neglecting the free surface and using Milne-Thomson's (1960) 'circle theorem'. He found that the approximations were valid for $Ka \ll 1$ or $2Kh \gg 1$ for fixed and freely-floating cylinders; the approximate results are just the first terms in an expansion of the exact results in powers of Ka . The approximations are

$$F_2(\text{fixed}) = 2\pi\rho g A^2 \; Ka e^{-2Kh} I_1(2Ka), \tag{6.9.1}$$

$$F_2(\text{free}) = 2\pi\rho g A^2 \; Ka e^{-2Kh} [I_1(2Ka) - Ka]. \tag{6.9.2}$$

For a fixed or a freely-floating, neutrally buoyant cylinder it may be anticipated that, when the cylinder is deeply submerged, the second integral I_2 given above, being of second-order with respect to the disturbance potential, will be small compared to I_1. The disturbance due to the presence of the cylinder will not be negligible near the tuned wavenumber if the cylinder is absorbing power. At the tuned wavenumber, the cylinder is capable of absorbing all the incident wave power no matter how deeply submerged it is but, in order to cancel out the transmitted wave, it undergoes

extremely large oscillations if deeply submerged as the pressure field decays exponentially with depth.

The transmission coefficients for fixed and freely-floating circular cylinders can be found in Ogilvie (1963) and, upon substitution of their expressions in (6.8.8), it is found

$$I_1(\text{fixed}) = 2\pi\rho g A^2 \frac{S_\varepsilon}{2\pi(1+S_\varepsilon^2)}, \tag{6.9.3}$$

$$I_1(\text{free}) = 2\pi\rho g A^2 \frac{(S_\varepsilon\gamma_1 - S_\gamma\varepsilon_1)\gamma_1}{2\pi[\gamma_1^2 + (S_\varepsilon\gamma_1 - S_\gamma\varepsilon_1)^2]}, \tag{6.9.4}$$

where $\varepsilon_1, \gamma_1, S_\varepsilon$ and S_γ are defined in Appendix D.

The use of (6.9.3), (6.9.4) as approximations to the exact values of the mean vertical force is illustrated in Figures (6.10), (6.11) for the fixed and freely-floating cases respectively; also included are Ogilvie's approximations (6.9.1), (6.9.2), (shown as dotted curves). In both cases it can be seen that the approximation becomes increasingly accurate as h/a increases. Indeed, for the freely-floating case, the approximation is extremely good even for h/a=2 when the top of the cylinder is only one radius away from the free-surface. (It might be expected that the approximation will be better for a freely-floating cylinder than a fixed one since it is able to respond to the waves and hence the contribution due to I_2 will be smaller). Ogilvie's approximation is not as good as that using (6.8.8) although, as h/a increases, the difference between the two approximations decreases.

Leppington & Siew (1980) have produced approximations for the transmission and reflection coeeficients when fixed circular or elliptic cylinders are deeply submerged and suggested approximations in the case of cylinders of arbitrary cross-sections. Their analysis proceeds under the constraint $K(h-a)^2/h \gg 1$ for the circular cylinder

FIXED CYLINDER

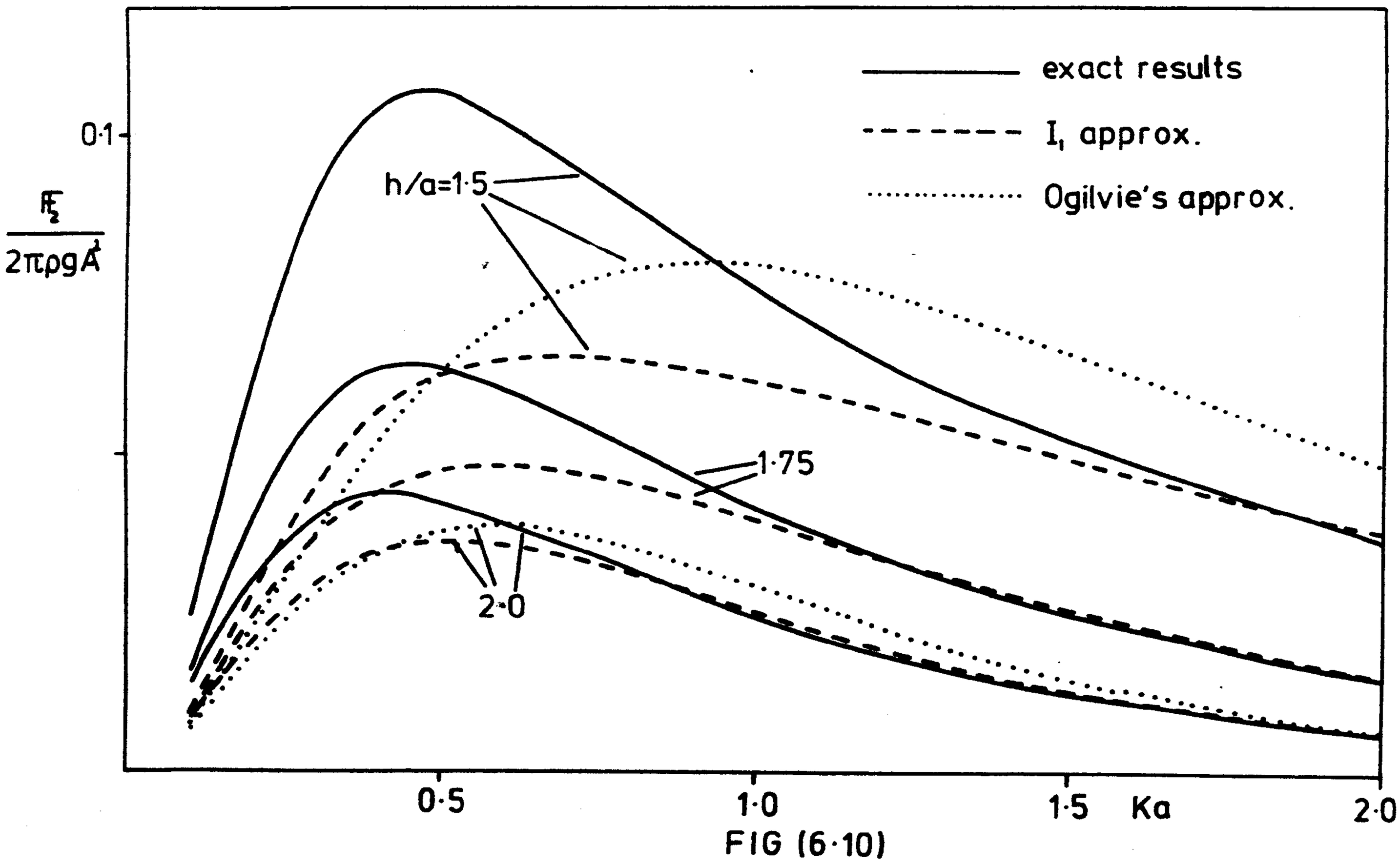

FIG (6·10)

FREELY-FLOATING CYLINDER

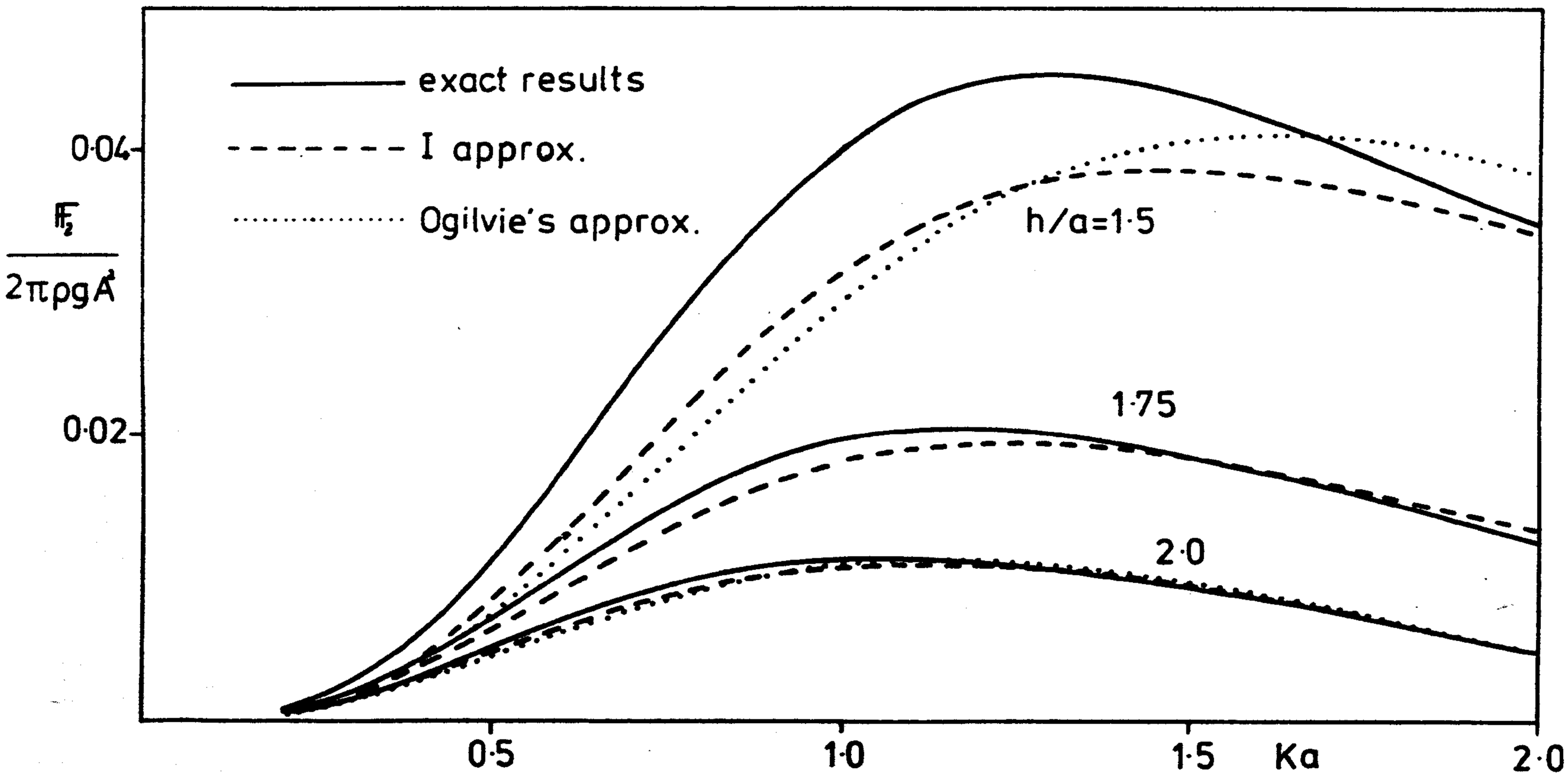

FIG (6·11)

which necessarily implies Kh is large and includes the three cases : (i) $Ka \gg 1$, (ii) $h \to \infty$ (with K and a fixed), (iii) $Ka \ll 1, Kh \gg 1$. The diffraction potential is then approximated by neglecting the free-surface as done by Ogilvie (1963). Correction potentials are then included to ensure that all the boundary conditions are satisfied and it is shown that, under the constraint above, contributions to the reflection and transmission coefficients from these correction potentials are of smaller order than that from the first approximations. It is found that for the circular cylinder

$$T_1 \sim 1 + 4\pi i Ka\, e^{-2Kh} I_1(2Ka), \qquad (6.9.5)$$

and substitution of this in (6.8.8) yields

$$I_1(\text{fixed}) = 2\pi \rho g A^2 Ka\, e^{-2Kh} I_1(2Ka), \qquad (6.9.6)$$

which is exactly Ogilvie's approximation (6.9.1). Thus, for the circular cylinder, when $K(h-a)^2/h \gg 1$, the approximation (6.8.8) and Ogilvie's approximation are the same although from Figure (6.10) it appears that (6.8.8) is a much better approximation when this constraint is relaxed.

For an elliptic cylinder, Leppington & Siew have shown

$$T \sim 1 + 4\pi i e^{-2Kh} \left\{ \left(\frac{Kab}{d_0}\right) I_1(2Kd_0) + \sum_{n=1}^{\infty} n \left(\frac{\beta_0}{\alpha_0}\right)^n |J_n(Kc e^{i\theta_0})|^2 \right\}, \qquad (6.9.7)$$

when

$$K(h-d_0)^2/h \gg 1,$$

where as shown in Figure (6.12), 2a, 2b are the lengths of the major and minor axes respectively, h is the depth of submergence of the ellipse centre, d_0 is the vertical distance of the highest point of the ellipse above its centre, θ_0 is the inclination of the major-

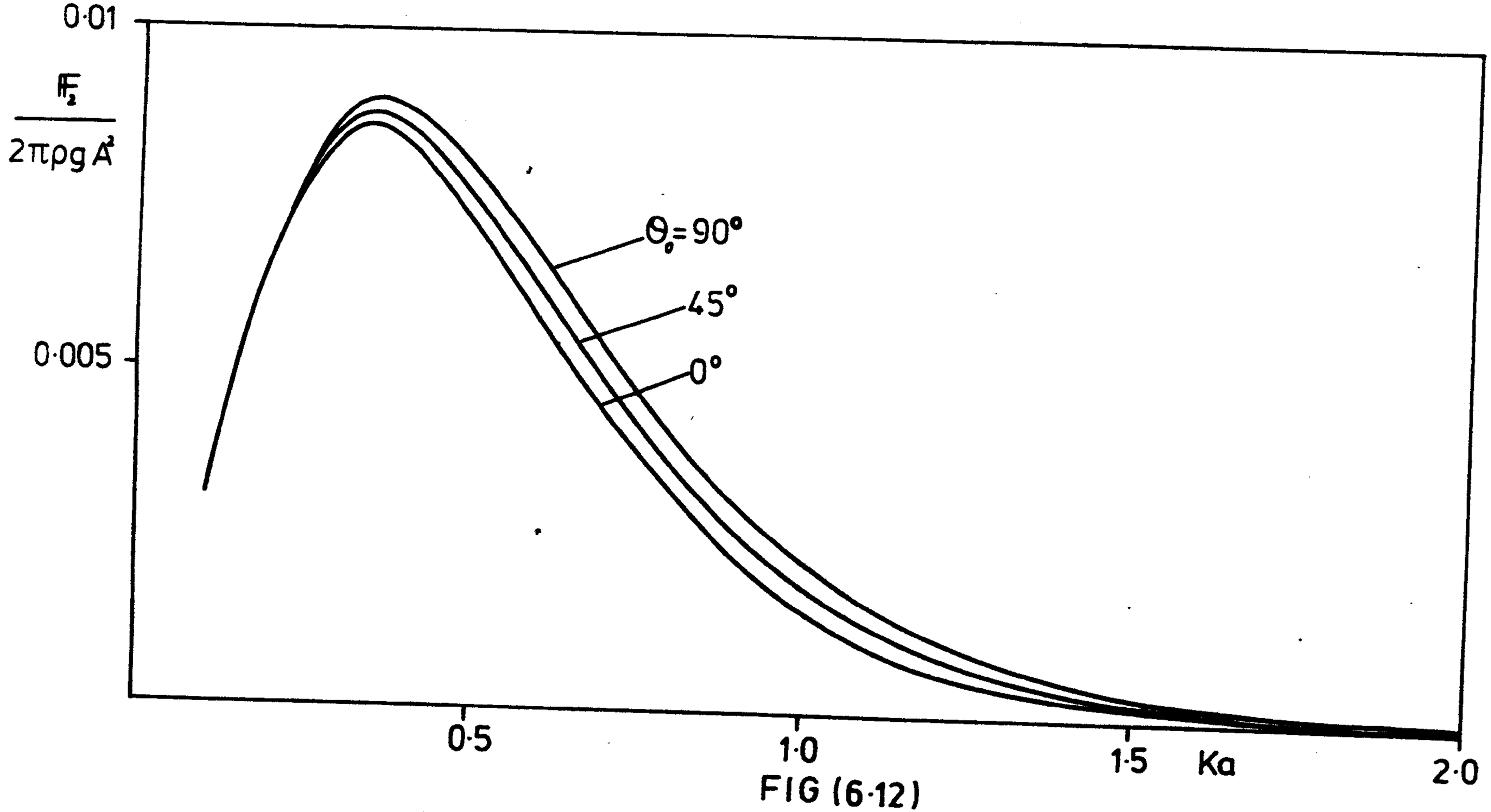

h/a=3

b/a=0·5

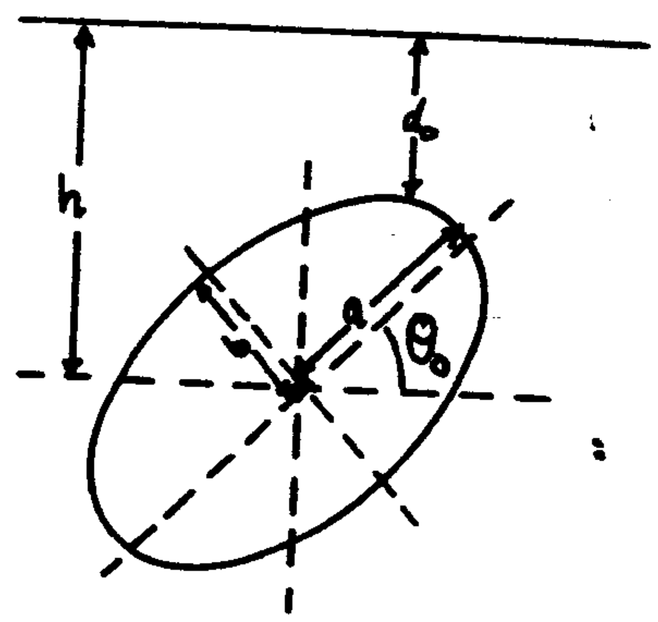

FIG (6·12)

axis to the horizontal and

$$\alpha_0 = \tfrac{1}{2}(a+b)\,,\ \beta_0 = \tfrac{1}{2}(a-b)\,,\ c = (a^2-b^2)^{\frac{1}{2}}$$

Substitution of (6.9.7) into (6.8.8) gives

$$\mathbb{I}_1(\text{fixed}) = 2\pi\rho g A^2 e^{-2Kh}\left\{\left(\frac{Kab}{d_0}\right)I_1(2Kd_0) + \sum_{n=1}^{\infty} n\left(\frac{\beta_0}{\alpha_0}\right)^n \left|J_n(Kce^{i\theta_0})\right|^2\right\}, \quad (6.9.8)$$

Thus assuming $\mathbb{I}_2$ to be negligible once more when $K(h-d_0)/h \gg 1$, the mean vertical force on a fixed elliptic cylinder is approximated by (6.9.8). Figure (6.12) illustrates the variation of this approximation for different inclinations of the cylinder when $h/a = 3$, $b/a = \frac{1}{2}$. It can be seen that the mean vertical force is greatest when the major-axis is vertical and that for $Ka \ll 1$ the inclination is of no consequence to the mean vertical force.

6.10 Conclusion

The first part of this Chapter examines the mean forces on the Bristol cylinder. It is shown that when the cylinder is absorbing power the mean vertical force is quite different from the corresponding force in the fixed and freely-floating cases. It is much larger near the tuning wavenumber and there even exist a range of wavenumbers when this mean vertical force is acting downwards against the buoyancy. The mean horizontal force is shown to agree with Longuet-Higgins' (1977) result and, for the Bristol cylinder, it is simply a constant multiple of the efficiency of the device. Comparison of the mean vertical force with the amplitude of the first-order vertical oscillatory force indicates that it can be appreciable near tuning when the cylinder is absorbing power. Although it is a small fraction of the buoyancy force its effect does increase as the wave slope increases and the extra upward force due to this mean

vertical force should not be neglected.

The mean forces on cylinders of arbitrary cross-section is investigated in part (b). Following Lee & Newman (1971), the mean vertical force is expressed as an integral over the free surface. It is conjectured that, when the cylinder is deeply submerged or more exactly when $k\bar{h}^2/h \gg 1$ where $\bar{h}$ is the vertical distance from the top of the cylinder to the free surface and h is the submergence of the cylinder centre; the mean vertical force may be approximated by a simple quantity $[\frac{1}{2}\rho g A^2 \eta_m(T_1)$. It is shown that this approximation agrees with Ogilvie's (1963) approximation for a fixed circular cylinder and both approximations are compared with the exact results for fixed and freely-floating circular cylinders. The mean vertical force on an elliptic cylinder is also examined using the above approximation. For other cross-sections estimates of the mean vertical force may be made if T_1 can be found either analytically or empirically.

APPENDIX A

The following results are required in Chapter 3. The majority can be found in Evans (1972) and are given here for completeness. The function $L(\gamma)$ arising in the Wiener-Hopf problem is decomposed into two functions regular and non-zero in D+ ($\tau \succ -$ d) and D- ($\tau \prec$ d), $L_+(\gamma)$ and $L_-(\gamma)$ respectively. This decomposition was originally found by Heins (1950).

$$L(\gamma) = \frac{\gamma \sinh \gamma f (\gamma \sinh \gamma h - K \cosh \gamma h)}{\gamma \sinh \gamma d - K \cosh \gamma d} = \frac{L_-(\gamma)}{L_+(\gamma)}, \tag{A.1}$$

and

$$L_-(\gamma) = \frac{i\gamma f (m-\gamma) k}{(k-\gamma) m} \frac{\prod_{n=1}^{\infty} (1 + i\gamma/a_n)(1 + i\gamma/m_n) e^{-\frac{i\gamma(f+h)}{n\pi}}}{\prod_{n=1}^{\infty} (1 + i\gamma/k_n) e^{-\frac{i\gamma d}{n\pi}}} \cdot \exp \chi(\gamma), \tag{A.2}$$

$$L_+(\gamma) = \frac{im(k+\gamma)}{\gamma(m+\gamma)k} \frac{\prod_{n=1}^{\infty} (1 - i\gamma/k_n) e^{i\gamma d/n\pi}}{\prod_{n=1}^{\infty} (1 - i\gamma/a_n)(1 - i\gamma/m_n) e^{i\gamma(f+h)/n\pi}} \cdot \exp \chi(\gamma), \tag{A.3}$$

where

$$a_n = n\pi/f \quad \text{and} \quad \chi(\gamma) = (i\gamma/\pi)(f \log f + h \log h - d \log d).$$

The functions $L_{\pm}^{+}(\gamma)$ have the following properties:

$$L_+(\gamma) \sim (2if/\gamma)^{\frac{1}{2}}, \quad L_-(\gamma) \sim (i\gamma f/2)^{\frac{1}{2}} \quad , \text{ as } \gamma \to \infty, \tag{A.4}$$

in D+, D- respectively,

$$L_-(-\gamma) L_+(\gamma) = f, \tag{A.5}$$

and for real γ

$$\left| \frac{L_-(\gamma)}{L_-(-\gamma)} \right| = \left| \frac{(\gamma - m)(\gamma + k)}{(\gamma + m)(\gamma - k)} \right|. \tag{A.6}$$

Using (A.1), (A.5) and (A.6) it can be shown

$$\frac{L_+(k)}{L_-(k)} = \frac{m-k}{m+k} \cdot \frac{4dN_0}{\sinh^2 kd} e^{2i\theta_1}, \qquad (A.7)$$

where

$$\theta_1 = \arg L_+(k), \qquad (A.8)$$

and

$$\frac{L_-(-m)}{L_+(m)} = \frac{m-k}{m+k} 4m^2 h M_0 e^{-2i\theta_2}, \qquad (A.9)$$

where

$$\theta_2 = \arg L_+(m). \qquad (A.10)$$

Application of the Wiener-Hopf method also requires the decomposition

$$L_+ \frac{\partial F_d}{\partial z}(\gamma, 0) = N_+(\gamma) + N_-(\gamma), \qquad (A.11)$$

where $N_-^+(\gamma)$ are regular in D_-^+, and $F_d(\gamma, z)$ is the Fourier transform of the source potential $G_d(x,z)$ given by (3.4.5). The transform is given by

$$F_d(\gamma,z) = \frac{K\sinh\gamma(h-z) - \gamma\sinh\gamma(h-z)}{\gamma(\gamma\sinh\gamma d - K\cosh\gamma d)}\cosh\gamma f \quad , (z>0),$$

$$= \frac{K\sinh\gamma h - \gamma\cosh\gamma h}{\gamma(\gamma\sinh\gamma d - K\cosh\gamma d)}\cosh\gamma(z+f), \ (z<0),$$

Thus

$$\frac{\partial F_d}{\partial z}(\gamma, 0^+) = \frac{\gamma\sinh\gamma h - K\cosh\gamma h}{\gamma\sinh\gamma d - K\cosh\gamma d}\cosh\gamma f \quad , (z \longrightarrow 0^+), \qquad (A.12)$$

$$\frac{\partial F_d}{\partial z}(\gamma, 0^-) = \frac{K\sinh\gamma h - \gamma\cosh\gamma h}{\gamma\sinh\gamma d - K\cosh\gamma d}\sinh\gamma f \quad , (z \longrightarrow 0^-), \qquad (A.13)$$

For $-d < b_1 < \tau < b_2 < d$ it can be shown that (see Noble, 1958, p.13)

$$N_-(\alpha) = -\frac{1}{2\pi i}\int_{-\infty+ib_2}^{+\infty+ib_2} L_+(\beta)\frac{\partial F_d}{\partial z}(\beta,0)\frac{1}{(\beta-\gamma)}d\beta,$$

$$N_+(\alpha) = \frac{1}{2\pi i}\int_{-\infty+ib_1}^{+\infty+ib_1} L_+(\beta)\frac{\partial F_d}{\partial z}(\beta,0)\frac{1}{(\beta-\gamma)}d\beta.$$

As in Evans (1972), the paths of integration may be closed by large semicircles in D+,D- respectively and the integrals reduce to sums of residues. Thus

$$N_-(\delta) = \frac{\sinh kf \cosh kf\, L_+(k)\, N_0^{-1}}{2d(k-\delta)} + \sum_{n=1}^{\infty} \frac{\sin 2k_n f\, L_+(ik_n)\, N_n^{-1}}{2d(k+i\delta)}, \qquad \text{(A.14)}$$

and using (A.1) to replace $L_+(\jmath)$ in the expression for $N_+(\delta)$,

$$N_+(\delta) = \frac{L_-(-m)\, M_0^{-1}}{2hm(m+\delta)} - \sum_{n=1}^{\infty} \frac{L_-(-im_n)\, M_n^{-1}}{2hm_n(m_n - i\delta)}. \qquad \text{(A.15)}$$

To arrive at (A.14), (A.15) it does not matter which of the expressions (A.12), (A13) is used to represent $\partial F_d/\partial z$.

Finally, from Evans (1972), equation (4.1), the correction potential $\phi_c(x,z)$ is given by

$$\phi_c(x,z) = -\frac{i\mathcal{D}^2 e^{ikx} \cosh k(z+f) \cosh kf}{2kf}$$

$$-\mathcal{D}\cosh kf \sum_{n=1}^{\infty} \frac{\mathcal{D}_n e^{-k_n x} \cos k_n(z+f)}{(k_n - ik)f} - \mathcal{D}e^{ikx}\cosh k(z+f) \sum_{n=1}^{\infty} \frac{\mathcal{D}_n \cos k_n f}{(k_n - ik)f}$$

$$+ \sum_{n=1}^{\infty}\sum_{m=1}^{\infty} \frac{\mathcal{D}_n \mathcal{D}_m e^{-k_n x} \cos k_n(z+f) \cos k_m f}{(k_n + k_m)f}, \quad \text{for } x \geq 0, \qquad \text{(A.16)}$$

where

$$\mathcal{D} = \frac{2k \sinh kf\, L_+(k)}{2kd + \sinh 2kd},$$

$$\mathcal{D}_n = \frac{2k_n \sin k_n f\, L_+(ik_n)}{2k_n d + \sin 2k_n d}, \quad \text{for } n \geq 1.$$

APPENDIX B

In this appendix various expressions required in Chapters 4 and 5 are evaluated. The expressions for D_{mn}, C_m for the mouth-upward and mouth-downward ducts are given in parts (a) and (b) respectively. The decomposition of E_{mo} and resulting expressions for p_m and q_m (equations (B.11) - (B.13)) are identical in both cases.

(a) The Mouth-Upward Duct

$$D_{mn} = \frac{1}{d}\int_l^d Z_m(z) Z_n(z)\, dz \qquad \text{(B.1)}$$

gives

$$D_{mn} = (N_m N_n)^{-\frac{1}{2}}\left(k_n d \sin k_m l \cos k_m l - k_m d \sin k_m l \cos k_n l\right)/\left(k_m^2 d^2 - k_n^2 d^2\right), \qquad \text{(B.2)}$$

for $m \neq n$, and $m, n \geq 1$;

$$D_{mm} = \frac{1}{2} N_m^{-1}\left(\frac{h}{d}\right)\left\{1 + \frac{\sin k_m h \cos k_m (l+d)}{k_m h}\right\}, \qquad \text{(B.3)}$$

for $m \geq 1$;

$$D_{0m} = D_{m0} = -(N_0 N_n)^{-\frac{1}{2}}\left(k d \sinh k l \cos k_m l + k_m d \cosh k l \sin k_m l\right)/\left(k_m^2 d^2 + k^2 d^2\right), \qquad \text{(B.4)}$$

for $m \geq 1$;

$$D_{00} = \frac{1}{2}\left(\frac{h}{d}\right) N_0^{-1}\left\{1 + \frac{\sinh kh \cosh k(l+d)}{kh}\right\}. \qquad \text{(B.5)}$$

$$C_m = \frac{1}{ad}\int_l^d \left\{(d-z) - K^{-1}\right\} Z_m(z)\, dz \qquad \text{(B.6)}$$

gives

$$C_m = \frac{N_m^{-\frac{1}{2}}}{k_m a}\left\{\frac{\sin k_m h}{k_m d \sin k_m d} - \left(\frac{h}{d}\right)\sin k_m l\right\}, \qquad \text{(B.7)}$$

for $m \geq 1$;

$$C_o = -\frac{N_o^{-\frac{1}{2}}}{ka}\left\{\frac{\sinh kh}{kd\sinh kd}+\left(\frac{h}{d}\right)\sinh kl\right\}. \qquad \text{(B.8)}$$

Note: for the disc case, $l = 0$ and hence

$$C_m = \frac{N_m^{-\frac{1}{2}}}{k_m^2 ad}, \qquad \text{(B.9)}$$

for $m \geq 1$;

$$C_o = \frac{-N_o^{-\frac{1}{2}}}{k^2 ad}. \qquad \text{(B.10)}$$

In equation (4.3.7) the decomposition

$$E_{mo} = p_m + iq_m, \quad (m \geq 0)$$

is performed and, from (4.3.3)

$$E_{mo} = (R_o - 1)\, D_{mo} + \delta_{mo}. \qquad \text{(B.11)}$$

Thus

$$p_m = \left\{ \frac{(J_1^2(ka)+Y_1^2(ka))^{-1} Y_1(ka)}{\frac{1}{2}\pi k^2 a^2 J_1(ka)} - 1 \right\} D_{mo} + \delta_{mo}, \qquad \text{(B.12)}$$

$$q_m = (J_1^2(ka)+Y_1^2(ka))^{-1} \frac{D_{mo}}{\frac{1}{2}\pi k^2 a^2}. \qquad \text{(B.13)}$$

(b) **The Mouth-Downward Duct**

$$D_{mn} = \frac{1}{d}\int_0^h Z_m(z) Z_n(z)\, dz \qquad \text{(B.14)}$$

gives

$$D_{mn} = (N_m N_n)^{-\frac{1}{2}}(k_n d \sin k_n h \cos k_m h - k_m d \cos k_n h \sin k_m h)/(k_n^2 d^2 - k_m^2 d^2), \qquad \text{(B.15)}$$

for $m \neq n$, and $m, n \geq 1$;

$$D_{mm} = \frac{1}{2}\left(\frac{h}{d}\right) N_m^{-1}\left(1 + \frac{\sin 2k_m h}{2k_m h}\right), \qquad \text{(B.16)}$$

for $m \geq 1$;

$$D_{om} = D_{mo} = (N_o N_m)^{-\frac{1}{2}}(kd\sinh kh \cos k_m h - k_m d \cosh kh \sin k_m h)/(k^2 d^2 + k_m^2 d^2), \qquad \text{(B.17)}$$

$$D_{oo} = \frac{1}{2}\left(\frac{h}{d}\right) N_o^{-1}\left(1 + \frac{\sinh 2kh}{2kh}\right) . \qquad \text{(B.18)}$$

$$C_m = -\frac{1}{Kad}\int_0^h Z_m(z)\,dz \qquad \text{(B.19)}$$

gives

$$C_m = -\frac{N_m^{-\frac{1}{2}} \sin k_m h}{Ka(k_m d)} , \qquad \text{(B.20)}$$

for $m \geq 1$;

$$C_o = -\frac{N_o^{-\frac{1}{2}} \sinh kh}{Ka(kd)} . \qquad \text{(B.21)}$$

APPENDIX C

Analysis of the Mouth-Downward Duct using the Narrow-Duct Approximation

An approximate solution of the mouth-downward duct problem, described in Chapter 5(b), can be derived when the duct is narrow, that is, $a \ll \ell$, $K\ell = O(1)$. This approximate method was used by Evans (1978) to study the mouth-downward duct when the power extraction mechanism consisted of a linear spring-damper system attached to a weightless float enclosed by the duct. The same method may be used with minor alterations when the problem is formulated in terms of a pressure distribution as in Chapter 5, § 5. There are only three changes; the radiation problem is considered, the boundary condition on the internal free-surface is now given by (5.4.4) and the fluid is taken to be of finite depth.

Further details of the method may be found in Evans (1978) or in the similar two-dimensional problem studied in Chapter 3.

In the far-field, the oscillatory flow into and out of the duct mouth appears as an oscillatory point source. Hence the outer solution is

$$\psi = q\, G(r,z) \quad , KR = O(1), Ka \ll 1, \tag{C.1}$$

where $R^2 = r^2 + (z-h)^2$, q is the unknown source strength and $G(r,z)$ is the potential of a three-dimensional oscillatory point source at $(0,0,h)$. This potential may be written as

$$G(r,z) = \frac{1}{R} + \frac{1}{R'} + \int_0^\infty \frac{2(K+s)e^{-sd}\cosh sz \cosh sh\, J_0(sr)}{s\sinh sd - K\cosh sd}\, ds$$

$$+ \frac{4\pi i (K+k) e^{-kd} \cosh kd \cosh kh \cosh kz\, J_0(kr)}{2kd + \sinh 2kd},$$

$$G(r,z) = \frac{1}{R} + G_0(r,z),$$

where $R'^2 = r^2 + (z+h)^2$. The inner limit of the outer solution is then

$$\psi \sim \frac{q}{R} + q\, G_0(0,h) \quad , r \ll l, \tag{C.2}$$

and

$$G_0(0,h) = \frac{1}{2h} + \int_0^\infty \frac{2(K+s)e^{-sd}\cosh^2 sh}{s\sinh sd - K\cosh sd}\,ds + \frac{4\pi i(K+k)e^{-kd}\cosh kd\cosh^2 kh}{4kd\,N_0} \tag{C.3}$$

using the expression (2.2.11) for N_0.

In the region of the duct mouth the flow appears as an oscillatory flow out of a semi-infinite pipe. The appropriate expansionsof the inner solution are given by Noble (1958) as

$$\psi \sim \frac{q}{R} + T \quad , r \gg a, \tag{C.4}$$

$$\psi \sim \frac{4q}{a^2}(z-h+l') + T \;, \quad (z-h)/a \ll 1, \tag{C.5}$$

where $l' = 0.6133a$ is the 'end correction' for an open pipe. Matching the inner limit of the outer solution, (C.2) with the outer limit of the inner solution, (C.4) in the region of overlap given by $a \ll r \ll l$ yields

$$T = q\, G_0(0,h) . \tag{C.6}$$

The source strength q can be found by applying the boundary condition (5.4.4) to the expansion (C.5) which describes the flow in the depths of the duct. Thus

$$\frac{4K}{a^2}q(\ell+\ell') + kT - \frac{4q}{a^2}q = 1,$$

or

$$q^{-1} = \frac{1}{a^2}\left[Ka^2 G_0(0,h) + 4(K\ell + K\ell' - 1)\right], \qquad (C.7)$$

using (C.6).

The coefficients, $\underline{A}$ and $\underline{B}$ may be determined from (5.4.11) and hence it is found that

$$\underline{A} = -\frac{4\pi}{\rho g}\,\mathrm{Re}\,q \quad , \quad \underline{B} = -\frac{4\pi\omega}{\rho g}\,\mathrm{Im}\,q\,. \qquad (C.8)$$

In non-dimensional form these quantities are given by

$$\mathcal{A} = \mathrm{Re}\left(\frac{-2q}{a^2}\right) \quad , \quad \mathcal{B} = \mathrm{Im}\left(\frac{-2q}{a^2}\right), \qquad (C.9)$$

where

$$\frac{2q}{a^2} = 2\left[Ka^2 G_0(0,h) + 4\{K(\ell+\ell') - 1\}\right]^{-1}. \qquad (C.10)$$

When the fluid is infinitely deep, the same expressions (C.9), (C.10) hold with $G_0(0,h)$ now given as

$$G_0(0,h) = \frac{1}{2\ell} - 2K\, e^{-2K\ell}\, Ei(2K\ell) + 2\pi i K e^{-2K\ell},$$

and $Ei(x)$ denotes the exponential integral.

Note that in terms of the added-mass and damping coefficients derived by Evans (1978), the coefficients $\mathcal{A}$ and $\mathcal{B}$ are given by

$$\mathcal{A} = \frac{1}{2K\ell}\,\frac{(\mu - 1/K\ell)}{(\mu - 1/K\ell)^2 + \Lambda^2},$$

$$\mathcal{B} = \frac{1}{2K\ell}\,\frac{\Lambda}{(\mu - 1/K\ell)^2 + \Lambda^2}.$$

Equations (5.4.2), (5.4.3) may now be used to examine the maximum capture width of the duct using this narrow-duct approximation.

APPENDIX D

Only the results and expressions required in Chapter 6, part (a) are given here; further details may be found in Ogilvie (1963).

The velocity potential is expanded as a linear combination of the following sets of basic singularity potentials

$$f_{n1}(z,t) = \left\{ \frac{e^{in\theta}}{(kr)^n} - \sum_{m=0}^{\infty} A_{m+n} \frac{(m+n)!}{m!(n-1)!} (kr)^m e^{-im\theta} \right\} \sin\omega t$$

$$- \left\{ \sum_{m=0}^{\infty} B_{m+n} \frac{(m+n)!}{m!(n-1)!} (kr)^m e^{-im\theta} \right\} \cos\omega t , \qquad \text{(D.1a)}$$

$$f_{n2}(z,t) = \left\{ \frac{e^{in\theta}}{(kr)^n} - \sum_{m=0}^{\infty} A_{m+n} \frac{(m+n)!}{m!(n-1)!} (kr)^m e^{-im\theta} \right\} \cos\omega t$$

$$+ \left\{ \sum_{m=0}^{\infty} B_{m+n} \frac{(m+n)!}{m!(n-1)!} (kr)^m e^{-im\theta} \right\} \sin\omega t , \qquad \text{(D.1b)}$$

$$g_{n1}(z,t) = \left\{ \frac{i e^{in\theta}}{(kr)^n} + i \sum_{m=0}^{\infty} A_{m+n} \frac{(m+n)!}{m!(n-1)!} (kr)^m e^{-im\theta} \right\} \sin\omega t$$

$$+ \left\{ \sum_{m=0}^{\infty} B_{m+n} \frac{(m+n)!}{m!(n-1)!} (kr)^m e^{-im\theta} \right\} \cos\omega t , \qquad \text{(D.1c)}$$

$$g_{n2}(z,t) = \left\{ \frac{i e^{in\theta}}{(kr)^n} + i \sum_{m=0}^{\infty} A_{m+n} \frac{(m+n)!}{m!(n-1)!} (kr)^m e^{-im\theta} \right\} \cos\omega t$$

$$+ \left\{ \sum_{m=0}^{\infty} B_{m+n} \frac{(m+n)!}{m!(n-1)!} (kr)^m e^{-im\theta} \right\} \sin\omega t , \qquad \text{(D.1d)}$$

where

$$A_m = \frac{1}{m(2Kh)^m} + \frac{2}{m!}\left\{e^{-2Kh}Ei(2Kh) - \sum_{j=1}^{m}\frac{(j-1)!}{(2Kh)^j}\right\}, (m\geq 1), \quad \text{(D.2a)}$$

$$A_0 = -\log(-2iKh) + 2e^{-2Kh}Ei(2Kh), \quad \text{(D.2b)}$$

$$B_m = \frac{2\pi e^{-2Kh}}{m!}, (m\geq 0), \quad \text{(D.2c)}$$

and $Ei(x)$ is the exponential integral.

Application of the boundary condition (6.4.5) on the cylinder finally yields the following sets of equations for the unknown constants $\alpha_m, \beta_m, \gamma_m, \delta_m$:

$$\alpha_m = \frac{-\omega a S_3(Ka)(\eta_1+\eta_2 S_\varepsilon) - (g\frac{A}{\omega})e^{-Kh}S_\varepsilon}{1+S_\varepsilon^2}\varepsilon_m + \eta_2(Ka)\omega a \zeta_m, \quad \text{(D.3a)}$$

$$\beta_m = \frac{\omega a S_3(Ka)(-\eta_2+\eta_1 S_\varepsilon) + (g\frac{A}{\omega})e^{-Kh}}{1+S_\varepsilon^2}\varepsilon_m - \eta_1(Ka)\omega a \zeta_m, \quad \text{(D.3b)}$$

$$\gamma_m = \frac{\omega a S_3(Ka)(\xi_1+\xi_2 S_\varepsilon) + (g\frac{A}{\omega})e^{-Kh}}{1+S_\varepsilon^2}\varepsilon_m - \xi_2(Ka)\omega a \zeta_m, \quad \text{(D.3c)}$$

$$\delta_m = \frac{\omega a S_3(Ka)(\xi_2-\xi_1 S_\varepsilon) - (g\frac{A}{\omega})e^{-Kh}S_\varepsilon}{1+S_\varepsilon^2}\varepsilon_m + \xi_1(Ka)\omega a \zeta_m, \quad \text{(D.3d)}$$

where ε_m and ζ_m are defined by

$$\varepsilon_m + \frac{(Ka)^{2m}}{m!}\sum_{n=1}^{M}\gamma_{mn}\varepsilon_n = \frac{(Ka)^{2m}}{m!}, \quad \text{(D.4a)}$$

$$\beta_m + \frac{(Ka)^{2m}}{m!}\sum_{n=1}^{\infty}\gamma_{mn}\beta_n = \delta_{m1}\,, \qquad \text{(D.4b)}$$

and

$$S_x = 2\pi e^{-2Kh}\sum_{n=1}^{\infty} x_n/(n-1)!\,, \qquad \text{(D.5)}$$

$$\gamma_{mn} = \frac{(m+n)!}{(n-1)!}A_{m+n}\,,$$

$$\delta_{mn} = \begin{cases} 1\,, & \text{if } m = n, \\ 0\,, & \text{if } m \neq n. \end{cases}$$

Thus $\alpha_m, \beta_m, \gamma_m, \delta_m$ are expressed in terms of the displacements $\xi_1, \xi_2, \eta_1, \eta_2$ and the solutions ε_m, β_m of (D.4a,b).

The displacements may be found from (6.5.2a,b) and using (6.5.3), (6.5.4). Equating coefficients of $\cos\omega t, \sin\omega t$ yields

$$\tilde{\alpha}\xi_1 - \tilde{\beta}\xi_2 = 2\delta_1/\omega a(Ka), \qquad \text{(D.6a)}$$

$$\tilde{\alpha}\xi_2 + \tilde{\beta}\xi_1 = -2\gamma_1/\omega a(Ka), \qquad \text{(D.6b)}$$

$$\tilde{\alpha}\eta_1 - \tilde{\beta}\eta_2 = -2\beta_1/\omega a(Ka)\,, \qquad \text{(D.6c)}$$

$$\tilde{\alpha}\eta_2 + \tilde{\beta}\eta_1 = 2\alpha_1/\omega a(Ka)\,. \qquad \text{(D.6d)}$$

Sustituting for $\alpha_1, \beta_1, \gamma_1, \delta_1$ from (D.3) and rearranging

$$\xi_1\left\{\tilde{\beta}/2 + S_\beta\varepsilon_1/(1+S_\varepsilon^2)\right\} + \xi_2\left\{\tilde{\alpha}/2 + S_\beta S_\varepsilon\varepsilon_1/(1+S_\varepsilon^2) - \beta_1\right\} = \frac{-gAe^{-kh}\varepsilon_1}{\omega^2 a(Ka)(1+S_\varepsilon^2)},$$

$$\xi_1\left\{\tilde{\alpha}/2 + S_\beta S_\varepsilon\varepsilon_1/(1+S_\varepsilon^2) - \beta_1\right\} - \xi_2\left\{\tilde{\beta}/2 + S_\beta\varepsilon_1/(1+S_\varepsilon^2)\right\} = \frac{-gAe^{-kh}S_\varepsilon\varepsilon_1}{\omega^2 a(Ka)(1+S_\varepsilon^2)},$$

$$\eta_1\{\tilde{\beta}/2 + S_3\varepsilon_1/(1+S_\varepsilon^2)\} + \eta_2\{\tilde{\alpha}/2 + S_3 S_\varepsilon \varepsilon_1/(1+S_\varepsilon^2) - \beta_1\} = \frac{gAe^{-kh} S_\varepsilon \varepsilon_1}{\omega^2 a(ka)(1+S_\varepsilon^2)},$$

$$\eta_1\{\tilde{\alpha}/2 + S_3 S_\varepsilon \varepsilon_1/(1+S_\varepsilon^2) - \beta_1\} - \eta_2\{\tilde{\beta}/2 + S_3\varepsilon_1/(1+S_\varepsilon^2)\} = \frac{-gAe^{-kh}\varepsilon_1}{\omega^2 a(ka)(1+S_\varepsilon^2)}.$$

These two pairs of simultaneous equations may be solved to give expressions for $\xi_1, \xi_2, \eta_1, \eta_2$ (see equations (6.5.5a,b)). It may be noted that $\xi_1 = -\eta_2$, $\xi_2 = \eta_1$.

Using (6.5.5a,b), equations (D.3) for $\alpha_m, \beta_m, \gamma_m$ and δ_m may be rewritten as

$$\alpha_m = -\delta_m = \frac{-gAe^{-kh}\left[\left[S_3\varepsilon_1(\beta_1 - \tilde{\alpha}/2) - S_\varepsilon\left((\beta_1 - \tilde{\alpha}/2)^2 + \tilde{\beta}^2/4\right)\right]\varepsilon_m - \varepsilon_1\left(S_3\varepsilon_1 - S_\varepsilon\beta_1 + S_\varepsilon\tilde{\alpha}/2 + \tilde{\beta}/2\right)\beta_m\right]}{\omega\left[\left(\beta_1 + S_\varepsilon\tilde{\beta}/2 - \tilde{\alpha}/2\right)^2 + \left(S_3\varepsilon_1 - S_\varepsilon\beta_1 + S_\varepsilon\tilde{\alpha}/2 + \tilde{\beta}/2\right)^2\right]}, \quad \text{(D.7a)}$$

$$\beta_m = \gamma_m = \frac{gAe^{-kh}\left[\left[S_3\varepsilon_1\tilde{\beta}/2 + \tilde{\beta}^2/4 + (\beta_1 - \tilde{\alpha}/2)^2\right]\varepsilon_m - \varepsilon_1\left(\beta_1 + S_\varepsilon\tilde{\beta}/2 - \tilde{\alpha}/2\right)\beta_m\right]}{\omega\left[\left(\beta_1 + S_\varepsilon\tilde{\beta}/2 - \tilde{\alpha}/2\right)^2 + \left(S_3\varepsilon_1 - S_\varepsilon\beta_1 + S_\varepsilon\tilde{\alpha}/2 + \tilde{\beta}/2\right)^2\right]}. \quad \text{(D.7b)}$$

To evaluate the mean force on the cylinder it can first be seen that (6.5.7) can be written as

$$F_1 - iF_2 = -ia\rho\int_{-\pi}^{\pi} e^{i\theta}\left[\frac{1}{2}\overline{f'\bar{f}'}^t + \mathrm{Re}\left(\overline{(\xi+i\eta)\partial f'/\partial t}^t\right)\right]_{r=a} d\theta \quad \text{(D.8)}$$

since $\underline{n} = (\sin\theta, \cos\theta)$.

The complex potential $f(z,t)$ is given by (6.4.3) and substituting for $\alpha_m, \beta_m, \gamma_m$ and δ_m from (D.3) it can be shown that

(Ogilvie, 1963, equation(19′))

$$f(z,t) = \cos\omega t\left[\sum_{m=1}^{\infty}{}'\frac{(\beta_m - i\alpha_m)e^{im\theta}}{(Kr)^m} + \sum_{m=1}^{\infty}{}'(\beta_m + i\alpha_m)\frac{(Kr)^m}{(Ka)^{2m}}e^{-im\theta}\right.$$
$$\left. + \omega r e^{-i\theta}(\xi_2 + i\xi_1) - \sum_{m=1}^{\infty}{}' m\{A_m(\beta_m + i\alpha_m) + B_m(\alpha_m - i\beta_m)\}\right]$$
$$+ \sin\omega t\left[\sum_{m=1}^{\infty}{}'\frac{(\alpha_m + i\beta_m)}{(Kr)^m}e^{im\theta} + \sum_{m=1}^{\infty}{}'(\alpha_m - i\beta_m)\frac{(Kr)^m}{(Ka)^{2m}}e^{-im\theta}\right.$$
$$\left. - \omega r e^{-i\theta}(-\xi_1 + i\xi_2) - \sum_{m=1}^{\infty}{}' m\{A_m(\alpha_m - i\beta_m) - B_m(\beta_m + i\alpha_m)\}\right], \qquad (D.9)$$

where (D.7a,b) and the relations between $\xi_i, \eta_i, (i=1,2)$ have been used. The derivative of f with respect to z becomes

$$f'(z,t) = \cos\omega t\left[iK\sum_{m=1}^{\infty}{}' m(\beta_m - i\alpha_m)\frac{e^{i(m+1)\theta}}{(Kr)^{m+1}} - iK\sum_{m=1}^{\infty}{}' m(\beta_m + i\alpha_m)\frac{(Kr)^{m-1}}{(Ka)^{2m}}e^{-i(m-1)\theta}\right.$$
$$\left. - i\omega(\xi_2 + i\xi_1)\right] + \sin\omega t\left[iK\sum_{m=1}^{\infty}{}' m(\alpha_m + i\beta_m)\frac{e^{i(m+1)\theta}}{(Kr)^{m+1}}\right.$$
$$\left. - iK\sum_{m=1}^{\infty}{}' m(\alpha_m - i\beta_m)\frac{(Kr)^{m-1}}{(Ka)^{2m}}e^{-i(m-1)\theta} + i\omega(-\xi_1 + i\xi_2)\right], \qquad (D.10)$$

$$= R_1\cos\omega t + R_2\sin\omega t.$$

Thus

$$\frac{1}{2}\overline{f\bar{f}'}^{t} = \frac{1}{4}(R_1\bar{R}_1 + R_2\bar{R}_2), \qquad (D.11)$$

and

$$\overline{(\xi + i\eta)\partial f'/\partial t}^{t} = \frac{\omega R_2}{2}(\xi_2 - i\xi_1) - \frac{\omega R_1}{2}(\xi_1 + i\xi_2), \qquad (D.12)$$

where (6.4.4a,b) has been used.

From (D.8) it can be seen that only the coefficient of $e^{-i\theta}$ in $[\quad]_{r=a}$ will contribute to the integral and so, picking out this and using (D.11), (D.12), it is found that

$$\int_{-\pi}^{\pi} \frac{1}{2}\overline{f'\bar{f}'}\Big|_{r=a}^{t} e^{i\theta}d\theta = \frac{2\pi K}{a}\sum_{m=1}^{\infty}\frac{m(m+1)}{(Ka)^{2m+2}}(\alpha_m+i\beta_m)(\alpha_{m+1}-i\beta_{m+1})$$

$$+\frac{2\pi K\omega}{(Ka)^3}(\alpha_2-i\beta_2)(\xi_1+i\xi_2), \qquad \text{(D.13)}$$

$$\int_{-\pi}^{\pi} \overline{\mathrm{Re}(\xi+i\eta)\partial f'/\partial t}\Big|_{r=a}^{t} e^{i\theta}d\theta = -\frac{2\pi K\omega}{(Ka)^3}(\alpha_2-i\beta_2)(\xi_1+i\xi_2). \qquad \text{(D.14)}$$

Thus, from (D.8)

$$F_1 - iF_2 = -2\pi i\rho K\sum_{m=1}^{\infty}\frac{(\alpha_m+i\beta_m)(\alpha_{m+1}-i\beta_{m+1})m(m+1)}{(Ka)^{2m+2}}, \qquad \text{(D.15)}$$

i.e.

$$F_1 = 2\pi\rho K\sum_{m=1}^{\infty}\frac{m(m+1)}{(Ka)^{2m+2}}(\beta_m\alpha_{m+1}-\alpha_m\beta_{m+1}), \qquad \text{(D.16)}$$

$$F_2 = 2\pi\rho K\sum_{m=1}^{\infty}\frac{m(m+1)}{(Ka)^{2m+2}}(\alpha_m\alpha_{m+1}+\beta_m\beta_{m+1}). \qquad \text{(D.17)}$$

Substituting for α_m, β_m from (D.7a,b) finally yields expressions for F_1, F_2 given by (6.5.8), (6.5.9)

As shown by Ogilvie (1963), the first-order force defined by (6.2.5) can also be found. Expressions (6.5.1a,b) may be derived

and, using (D.6), these may be rewritten as

$$F_1(t) = \pi\rho\omega^2 a^2 \left[\sin\omega t \left\{ (\tilde{\alpha}-1)\xi_1 - \tilde{\beta}\xi_2 \right\} + \cos\omega t \left\{ (\tilde{\alpha}-1)\xi_2 + \tilde{\beta}\xi_1 \right\} \right],$$

$$F_2(t) = \pi\rho\omega^2 a^2 \left[\sin\omega t \left\{ (\tilde{\alpha}-1)\xi_2 + \tilde{\beta}\xi_1 \right\} \cos\omega t \left\{ (\tilde{\alpha}-1)\xi_1 - \tilde{\beta}\xi_2 \right\} \right],$$

or

$$F_1(t) - i F_2(t) = \pi\rho(\omega a)^2 \left\{ (\tilde{\alpha}-1)^2 + \tilde{\beta}^2 \right\}^{\frac{1}{2}} \left\{ \xi_1^2 + \xi_2^2 \right\}^{\frac{1}{2}} e^{-i(\omega t - \psi)},$$

where

$$\psi = \tan^{-1} \frac{(\tilde{\alpha}-1)\xi_1 - \tilde{\beta}\xi_2}{(\tilde{\alpha}-1)\xi_2 + \tilde{\beta}\xi_1}.$$

Substituting for the displacements ξ_1, ξ_2 defined by (6.5.5a,b) gives the required results, (6.5.20) and (6.5.21).

REFERENCES

Abramowitz, M. & Stegun, I. 1970 Handbook of Mathematical Functions. 9th edn. Dover Publications.

Black, J.L., Mei, C.C. & Bray, M.C.G. 1971 Radiation and scattering of water waves by rigid bodies. J. Fluid Mech. 46, pp 151-164.

Brevig, P., Greenhow, M. & Vinje, T. 1981 Extreme wave forces on submerged cylinders. See Stephens & Stapleton 1981, pp 143-166.

Budal, K. & Falnes, J. 1975 A resonant point absorber of ocean-wave power. Nature 256, pp 478-9 (corrigendum 257, p 626).

Chester-Browne, C.V. 1978 The Vickers device. See Quareell 1978, pp 55-57.

Clark, P.J., Dawson, J.M. & Stansfield, H.B. 1978 Full-scale wave-power stations. See Quarrell 1978, pp 65-77.

Count, B.M. 1978a The theoretical analysis of wave power devices with non-linear mechanical conditioning. C.E.G.B. Marchwood Rep. No. R/M/N1008.

Count, B.M. 1978b On the dynamics of wave-power devices. Proc. Roy. Soc. London, Ser. A 363, pp 559-579.

Count, B.M., ed. 1980 Power from Sea Waves - Proc. I.M.A. Conf., Edinburgh, 1979. London/NY : Academic Press.

Count, B.M., Fry, R., Haskell, J. & Jackson, N. 1981 The M.E.L. oscillating water column. C.E.G.B. Marchwood Rep. No. RD/M/1157N81

Crabb, J.A. 1980 Synthesis of a directional wave climate. See Count 1980.

Drew, S.D. 1981 Progress towards a submerged oscillating water column device. See Stephens & Stapleton 1981, pp 385-396.

Elliot, G. & Roxburgh, G. 1981 Wave energy studies at the UK National Engineering Laboratory. See Stephens & Stapleton 1981, pp 269-282.

Evans, D.V. 1972 The application of a new source potential to the problem of the transmission of water waves over a shelf of arbitrary

profile. Proc. Camb. Phil. Soc. 71, pp 391-410.

Evans, D.V. 1976 A theory for wave-power absorption by oscillating bodies. J. Fluid Mech. 77, pp 1-25.

Evans, D.V. 1978 The oscillating water column wave-energy device. J. Inst. Maths. Applics. 22, pp 423-433.

Evans, D.V. 1980a Some theoretical aspects of three-dimensional wave-energy absorbers. Proc. 1st Symp. Wave Energy Utilization, Gothenburg, 1979 eds. Jansson, Lunde & Rindby. Chalmers Tech. Univ., 1980.

Evans, D.V. 1980b Some analytic results for two and three dimensional wave energy absorbers. See Count 1980.

Evans, D.V. 1981a Power from Water Waves. Ann. Rev. Fluid Mech. 13, pp 157-187.

Evans, D.V. 1981b Wave-power absorption by systems of oscillating surface pressure distributions. Univ. of Bristol, Maths Dept. Int. Rep. No. AM-81-01 & J. Fluid Mech. (to appear).

Evans, D.V. & Morris, C.A.N. 1972a The effect of a fixed vertical barrier in obliquely incident surface waves in deep water. J. Inst. Maths. Applics. 9, pp 198-204.

Evans, D.V. & Morris, C.A.N. 1972b Complementary approximations to the solution of a problem in water waves. J. Inst. Maths. Applics. 10, pp 1-9.

Evans, D.V., Jeffrey, D.C., Salter, S.H. & Taylor, J.R.M. 1979 Submerged cylinder wave-energy device : theory and experiment. Appl. Ocean Res. 1, pp 3-12.

Falnes, J. 1978 Radiation impedance matrix and optimum power absorption for interacting oscillators in surface waves. Norges Tekniske Høgskole, Int. Rep. May 1978 (reissued Sept. 1979).

French, M.J. 1978 The flexible bag wave power device. See Quarrell 1978, pp 59-60.

Fry, R. & Jeffreys, E.R. 1979 Tank trials of a model Kaimei. C.E.G.B. Marchwood Rep. No. R/M/N1072.

Garrett, C.J.R. 1970 Bottomless harbours. J. Fluid Mech. 43, pp 433-449.

Garrett, C.J.R. 1971 Wave forces on a circular dock. J. Fluid Mech. 46, PP 129-139.

Garrison, C.J. 1978 Hydrodynamic loading of large offshore structures. Three-dimensional source distribution methods. Ch. 3 of Numerical Methods in Offshore Engineering,eds. Zienkiewicz, Lewis & Staggs. Wiley.

Haskind, M.D. 1957 The exciting forces and wetting of ships in waves. Izv. Akad. Nauk S.S.S.R., Otd. Tekh. Nauk 7, pp 65-79 (Eng. trans. David Taylor, Model Basin Trans. no. 307).

Heins, A.E. 1950 Water waves over a channel of finite depth with submerged plane barrier. Can. J. Math. 2, pp 210-222.

Hulme, A. 1981 The potential of a horizontal ring of wave sources in a fluid with a free surface. Proc. Roy. Soc. London, Ser. A 375, pp 295-305.

Isaacs, J.D. & Wiegel, R.L. 1949 The measurement of wave heights by means of a float in an open-end pipe. Trans. Am. Geophys. Union 30, pp 501-506.

Kenward, M. 1976 Waves a million. New Scientist, 6th May, pp 309-310.

Knott, G.F. & Flower, J.O. 1979 Wave tank experiments on an immersed parallell-plate duct. J. Fluid Mech. 90, pp 327-336.

Knott, G.F. & Flower, J.O. 1980a Wave tank experiments on an immersed vertical circular duct. J. Fluid Mech. 100, pp 225-236.

Knott, G.F. & Flower, J.O. 1980b Measurement of energy losses in oscillatory flow through a pipe exit. Appl. Ocean Res. 2, pp155-164.

Kotik, J. & Mangulis, V. 1962 On the Kramers-Kronig relations for

ship motions. Int. Shipbuilding Prog. 9 .

Lamb, H. 1932 Hydrodynamics. C.U.P.

Lee, C.M. & Newman, J.N. 1971 The vertical mean force and moment of submerged bodies under waves. J. Ship Res. 15, pp 231-245.

Leppington, F.G. & Siew, P.F. 1980 Scattering of surface waves by submerged cylinders. Appl. Ocean Res. 2, pp 129-137.

Lighthill, M.J. 1979 Two dimensional analyses related to wave energy extraction by submerged resonant ducts. J. Fluid Mech. 91, pp 253-318.

Long, A.E. 1979 A summary of progress on the Belfast device. Technical note issued at Wave Energy Conf. Maidenhead 1979.

Longuet-Higgins, M.S. 1977 The mean force exerted by waves on floating or submerged bodies with applications to sand bars and wave power machines. Proc. Roy. Soc. Lond., Ser. A 352, pp 463-480.

Martin, J. & Kuo, C. 1978 Calculations for the steady tilt of semi submersibles in regular waves. Trans. R.I.N.A. 121, pp 87-102.

McCamy, R.C. 1961 On the heaving motion of cylinders of shallow draft. J. Ship Res. 5, pp 34-43.

McCormick, M.E. 1974 Analysis of a wave energy conversion buoy. J. Hydronaut. 8, pp 77-82.

Mei, C.C. 1976 Power extraction from water waves. J. Ship. Res. 20, pp 63-66.

Meir, R. 1978 The development of the oscillating water column. See Quarrell 1978, pp 35-43.

Miles, J.W. & Gilbert, F. 1968 Scattering of gravity waves by a circular dock. J. Fluid Mech. 34, pp 783-793.

Milne-Thomson, L.M. 1960 Theoretical Hydrodynamics, 4th ed. NY : Mac-Millan.

Newman, J.N. 1962 The exciting forces on fixed bodies in waves. J. Ship Res. 6, pp 10-17.

Newman, J.N. 1967 The drift force and moment on ships in waves. J. Ship Res. 11, pp 51-60.

Newman, J.N. 1974 Interaction of water waves with two closely spaced vertical obstacles. J. Fluid Mech. 66, pp 97-106.

Newman, J.N. 1975 Interaction of waves with two-dimensional obstacles : a relation between the radiation and scattering problems. J. Fluid Mech. 71, pp 273-282.

Newman, J.N. 1976 The interaction of stationary vessels with regular waves. Proc. Symp. Naval Hydrodyn., 11th, London, pp 491-501.

Newman, J.N. 1977 Marine Hydrodynamics. Cambridge : M.I.T. Press.

Nóble, B. 1958 Methods based on the Wiener-Hopf technique for the solution of partial differential equations. Pergammon Press.

Ogilvie, T.F. 1963 First and second-order forces on a cylinder submerged under a free surface. J. Fluid Mech. 16, pp 451-472.

Quarrell, P. ed. 1978 Proc. Wave Energy Conf. London-Heathrow. London : Publ. H.M.S.O.

Rainey, R.C.T. 1977 The dynamics of tethered platforms. Trans. R. I.N.A. 107, pp 1-13.

Robinson, R.W. & Murray, M.A. 1981 Geometric wavefield influence on the behaviour of an oscillating water column. Int. Symp on Hydrodyn. in Ocean Eng. Trondheim 1981. The Norwegian Inst. Tech.

Salter, S.H. 1974 Wave power. Nature 249, pp 720-724.

Simon, M.J. 1981a Wave-energy extraction by a submerged cylindrical resonant duct. J. Fluid Mech. 104, pp 159-187.

Simon, M.J. 1981b Ph.D. thesis. Univ. Cambridge.

Srokosz, M.A. 1979 Some theoretcial aspects of wave power absorption. PhD thesis. Univ. Bristol.

Stahl, A.W. 1892 The utilization of the power of ocean waves. Trans. A.S.M.E. 13, pp 438-506.

Standing, R.G. 1980 Use of potential flow theory in evaluating wave

forces on offshore structures. See Count 1980, pp 175-210.

Stephens, H.S. & Stapleton, C.A. eds. 1981 Proc. 2nd Int. Symp. Wave and Tidal Energy. BHRA Fluid Engrg., Cranfield, Bedford, England.

Thomas, J.R. 1981 The absorption of wave energy by a three-dimensional submerged duct. J. Fluid Mech. 104, pp 189-215.

Thomas, G.P. & Evans, D.V. 1981 Arrays of three-dimensional wave energy absorbers. J. Fluid Mech. 108, pp 67-88.

Thorne, R.C. 1953 Multipole expansions in the theory of surface waves. Proc. Camb. Phil. Soc. 49, pp 707-716.

Ursell, F. 1950 Surface waves on deep water in the presence of a submerged circular cylinder I. Proc. Camb. Phil. Soc. 46, pp 141-152.

Wehausen, J.V. 1971 The motion of floating bodies. An.. Rev. Fluid Mech. 3, pp 237-268.

Wehausen, J.V. & Laitone, E.V. 1960 Surface Waves. Handbuch der Physik IX, pt. III, pp 446-814. Springer-Verlag.

Whittaker, T.J.T. & Murray, M.A. 1981 Performance characteristics of hydropnematic buoys in line arrays. Int. Symp. on Hydrodyn. in Ocean Eng. Trondheim 1981. The Norwegian Inst. Tech.

Butterworth, J. 1978 The KaiMei project. See Quarrell 1978, pp 45-48.